Dissecting functions of members of β-oxidation multi-gene families in Arabidopsis

This thesis is presented for the degree of Doctor of Philosophy at the University of Western Australia

THE UNIVERSITY OF WESTERN AUSTRALIA

Achieve International Excellence

Andrew Wiszniewski

2011

ARC Centre of Excellence Plant Energy Biology,

School of Biomedical, Biomolecular and Chemical Sciences

Declaration

The work presented in this thesis is my own work unless otherwise stated. This work was carried out in the ARC Centre of Excellence in Plant Energy Biology, Discipline of Biochemistry and Molecular Biology, School of Biomedical and Chemical Sciences in the Faculty of Life and Physical Sciences at the University of Western Australia. The material presented in this thesis has not been submitted for any other degree or diploma in this or any other institutions.

Andrew Aleksander Gerhard Wiszniewski

30th September 2011

Publications

Parts of this thesis have been published in the following journal article:

Wiszniewski A.A.G., Zhou W., Smith S.M., Bussell J.D. (2009). Identification of two Arabidopsis genes encoding a peroxisomal oxidoreductase-like protein and an acyl-CoA synthetase-like protein that are required for responses to pro-auxins. Plant Molecular Biology 69: 503–515.

Acknowledgments

I would like to acknowledge the support and guidance of my supervisors Steve Smith and John Bussell, which has proved invaluable throughout my PhD. Thanks to Steve for providing me the opportunity to study and learn in his lab. I also greatly appreciate John for being the go to person for so many different things over the years of my PhD.

Also appreciated is the support of past and present members of Plant Energy Biology especially the Smith lab. Specifically I would like to thank Wenxu Zhou, Ricarda Fenske, and Matthew Timmins for assistance with GC-MS fatty-acid analysis, and David Nelson with qRT-PCR. It has been a great experience to have so many scientists happy to share their knowledge and teach me how to be a better scientist.

Thanks to friends and family for personal and emotional support over the years.

I also value the time Tegan Armarego-Marriott, John Bussell and Steve Smith have spent proof-reading and providing comments for this thesis.

I wish to acknowledge the Australian Postgraduate Award, UWA graduate research travel award and ARC Centre of Excellence in Plant Energy biology for financial support during my PhD.

List of Abbreviations

2,4-D	2,4-dichlorophenoxyacetic acid
2,4-DB	2,4-dichlorophenoxybutyric acid
4CL	4-courmate:CoA ligase
AACT	acetoacetyl-CoA thiolase
AAE	acyl-activating enzyme
ABA	abscisic acid
ABC	ATP-binding cassette
ABI	ABA insensitive
ABRE	ABA-responsive elements
ACL	ATP-citrate lyase
ACT	actin
ACX	acyl-CoA oxidase
AIM	abnormal inflorescence meristem
ALA	α-linolenic acid
ATS	altered testa shape
BA	benzoic acid
BHT	2,6-di-tert-butyl-4-methylphenol
bZIP	basic leucine zipper
BZO	benzoyloxyglucosinolate
CACS	clathrin adaptor complex subunit
cDNA	complementary DNA
CDS	coding sequence
CFB	clofibrate
CFI	chalcone flavanone isomerase
CHS	chalcone synthase
CHY	β-hydroxyisobutyryl-CoA hydrolase
CoA	coenzyme A
COI	coronatine-insensitive
Col	Colombia
COP	constitutive photomorphogenic
CSHL	Cold Spring Harbor Laboratory
CTA1	catalase (yeast)
C-terminus	carboxy-terminus
CTS	comatose
DAG	diacylglycerol
DCI	$\Delta^{3,5}$, $\Delta^{2,4}$-dienoyl-CoA isomerase

DDE	delayed dehiscence
DECR	2,4-dienoyl-CoA reductase
DET	de-etiolated
DGAT	diacylglycerol acyltransferase
DNA	deoxyribonucleic acid
dNTP	deoxyribonucleotide
ECH	enoyl-CoA hydratase
EDTA	ethylenediaminetetraacetic acid
EMS	ethyl methanesulfonate
F3H	flavanone 3-hydroxylase
FATB	fatty acyl-ACP thioesterase B
FLS	flavonol synthase
FOX2	yeast hydratase-dehydrogenase
FOX3	yeast 3-ketoacyl-CoA thiolase
FTFLP	fluorescent tagging of full-length proteins
GA	gibberellic acid
GABI	Genomanalyse im biologischen System Pflanze
GARE	GA-response element
GC-MS	gas chromatography-mass spectrometry
GFP	green fluorescent protein
GPA	global proliferative arrest
GUS	β-glucuronidase
HPR	hydroxypyruvate reductase
HY5	elongated hypocotyl 5
HYH	HY5 homolog
IAA	indole-3-acetic acid
IBA	indole-3-butyric acid
IBR	IBA-response
ICL	isocitrate lyase
ICS	isochorismate synthase
IPTG	isopropyl β-D-1-thiogalactopyranoside
JA	jasmonic acid
JA-Ile	jasmonyl-isoleucine
JAR	jasmonate resistant
KAT	3-ketoacyl-CoA thiolase
LACS	long-chain acyl-CoA synthetase
LB	lysogeny broth

LCFA	long-chain fatty-acids
LEC	leafy cotyledon
L*er*	Landsberg *erecta*
MAG	monoacylglycerol
MDH	malate dehydrogenase
MES	2-(N-morpholino)ethanesulfonic acid
MFE	multifunctional enzyme
MFP	multifunctional protein
MLS	malate synthase
MS	Murashige and Skoog medium
MVA	mevalonate
Mya	million years ago
NAA	1-naphthaleneacetic acid
NADH	nicotinamide adenine dinucleotide
NCBI	National Center for Biotechnology Information
NOA	nitric oxide associated
NOS	nitric oxide synthase
N-terminus	amino-terminus
OD	optical denisity
OPC:8	3-oxo-2-(2'-pentenyl)-cyclopentane-1-octanoic acid
OPDA	12-oxo-phytodienoic acid
OPR	OPDA-reductase
PAO	pheide *a* oxygenase oxygenase
PCK	phosphoenoylpyruvate carboxykinase
PCR	polymerase chain reaction
PED	peroxisome deficient
PEX	peroxin
PGIP	polygalacturonase inhibiting protein
PhA	pheophorbide (pheide) *a*
PhyA	phytochrome A
PIPES	piperazine-N,N′-bis(2-ethanesulfonic acid)
PMDH	peroxisomal malate dehydrogenase
POX	yeast acyl-CoA oxidase
PTS	peroxisomal targeting signal
PVP	polyvinylpyrrolidone
PXA	peroxisomal ABC-transporter
qRT-PCR	quantitative reverse-transcription polymerase chain reaction

R2R3-MYB	Repeat 2-Repeat 3-Myeloblastosis
RFP	red fluorescent protein
RNA	ribonucleic acid
RNAi	RNA interference
SA	salicylic acid
SDP	sugar dependent
SNP	single nucleotide polymorphism
SOB	super optimal broth
SPS19	2,4-dienoyl-CoA reductase (yeast)
SSE	shrunken seed
TAG	triacylglycerol
TB	terrific broth
T-DNA	transfer DNA
TED	reversal of the *det* phenotype
TT	transparent testa
TTG	transparent testa glabra
UV	ultraviolet
UVR	UV resistance locus
Ws	Wassilewskija
X-Gal	5-bromo-4-chloro-3-indol-β-D-galactoside
YCAT	yeast carnitine acetyltransferase

Abstract

In plants the catabolism of fatty-acids occurs via peroxisomal β-oxidation by the cleavage of acetyl-CoA from an acyl-CoA chain. β-oxidation is responsible for the metabolism of storage lipids during germination and membrane lipids during senescence. Additionally, the synthesis of auxin and jasmonic acid occurs via this pathway. This thesis describes research in which Arabidopsis mutants disrupted in β-oxidation enzymes were screened for classical β-oxidation phenotypes. These phenotypes included sucrose dependence for seedling establishment in the absence of storage lipid breakdown, and resistance to the auxin precursors IBA and 2,4-DB, which are metabolised to their active form by β-oxidation. As a result two enzymes, acyl activating enzyme 18 (AAE18) and short-chain dehydrogenase A (SDRA) were identified as required for response to auxin precursors. The *sdra* mutants were resistant to the auxin precursors 2,4-DB and IBA, while *aae18* mutants were resistant only to 2,4-DB. Neither of the mutants was sucrose-dependent, and the *sdra* mutant had a similar fatty-acid profile to wild-type during germination. GFP-tagged SDRA and AAE18 localised to the peroxisome.

A detailed characterisation of the 3-ketoacyl-thiolase (KAT) family in Arabidopsis was also instigated. In the last-step of the β-oxidation cycle the KAT enzyme catalyses the cleavage of acetyl-CoA. In Arabidopsis KAT2 is the major peroxisomal thiolase involved in the metabolism of many fatty-acid compounds including storage lipids, auxin, jasmonic acid, and membrane lipids. While *KAT1* displays low constitutive expression, *KAT5* is up-regulated in flowers and siliques. Additionally, the *KAT5* gene encodes two isoforms, the cytosolic KAT5.1 and the peroxisomal KAT5.2. In this part of the project, detailed gene expression analysis was conducted using promoter-GUS-reporter and qRT-PCR experiments. The *KAT1* promoter is weak and very rarely displayed activity. The *KAT2* and *KAT5* promoters were active during seed germination, and flower and seed development. qRT-PCR revealed high expression of *KAT2* throughout different Arabidopsis tissue types with up-regulation in senescing leaves, flowers and siliques. *KAT1* transcript was present at constitutively low levels. *KAT5.1* and *KAT5.2* transcript were both low, with up-regulation in flowers and siliques.

Reverse genetics was used to characterise *KAT* gene function. *kat2* homozygous single mutants are sucrose-dependent, resistant to 2,4-DB, and have reduced germination frequency. Homozygous *kat1, kat5* and a *kat1 kat5* double mutant respond like wild-type to these assays. *kat2-1 kat5-2* (Ws-4) double mutants have smaller rosettes, branched inflorescences, and while they produce viable pollen they are unable to set seed. Growth and fertility defects were confirmed in independent homozygous mutants, *kat2-5 kat5-2* (Ws-4) and *kat2-1 kat5-1* (Ws-4/L*er* hybrid). However, no growth defects were observed in *kat2-4 kat5-1* (L*er*) and *kat2-2 kat5-3* (Col) homozygous mutants. *kat2-1/kat2-1 kat5-2/KAT5* (Ws-4) sesquimutants have reduced germination frequency compared to *kat2-1* single mutants, but *kat2-4 kat5-1* (L*er*)

homozygous mutants do not. Progeny of *kat2-1 kat5-2* (Ws-4) sesquimutants segregated in a 1:2:1 ratio when heterozygous at the *kat5-2* locus, but deviated significantly from the expected 1:2:1 ratio when heterozygous at the *kat2-1* locus (with greatly reduced incidence of *kat2-1* homozygotes). *kat2-1* and *kat5-2* (both Ws-4 accession) single homozygous mutants had reduced seed weight, and lower fatty acid content per seed. Development and fertility could be restored in the *kat2-1 kat5-2* (Ws-4) homozygous double mutant by over-expression of peroxisomal KAT5.2 but not cytosolic KAT5.1. It is concluded that the importance of the *KAT5* gene is dependent on accession, and in Ws-4 it plays an important role in peroxisomal β-oxidation, particularly in ovules and seeds.

I have in this thesis described improvements to *in silico* prediction of targeting, and proteomic characterisation of Arabidopsis peroxisomes to focus the reverse genetic analysis of uncharacterised β-oxidation genes involved in processes beyond the previously known core functionalities. This has resulted in several advances including the discovery of the *aae18* mutant, disrupted in the auxin metabolism pathway, that distinguishes between IAA and 2,4-DB, and provided evidence of differential function of β-oxidation genes amongst Arabidopsis accessions.

Table of Contents

Chapter 1: General Introduction

1.1 Overview of plant peroxisomes

Peroxisomes are small, single-membrane organelles that contain oxidative enzymes and occur in eukaryotes. Peroxisomes of higher plants display plasticity of function depending on tissue localisation (reviewed in Olsen and Harada, 1995). Leaf peroxisomes in photosynthetic tissue contribute to the photorespiratory cycle along with chloroplasts and mitochondria. Peroxisomes present in senescing plant tissue catabolise cell lipids and specialised peroxisomes in legume root nodules are the site of urate oxidation. In the fat storage organs of the seed endosperm and cotyledons, peroxisomes degrade fatty acids via fatty acid β-oxidation, which catabolises an acyl-CoA chain to acetyl-CoA. The glyoxylate cycle, through isocitrate lyase (ICL) and malate synthase (MLS), then yields net production of malate for export and synthesis of sucrose by gluconeogenesis. Peroxisomes therefore contribute the supply of carbon that fuels post-germinative growth before photosynthesis is established (reviewed in Baker *et al.*, 2006; Eastmond and Graham, 2001; Graham, 2008).

Whilst many of the core enzymes of the β-oxidation cycle are well characterised both biochemically and genetically, identification of other components in this pathway requires knowledge of the contents of the peroxisomal matrix. *In vivo* localisation of proteins to the peroxisomal matrix primarily utilises either of two alternative peptide signals, peroxisomal targeting signal type 1 (PTS1) or type 2 (PTS2). The PTS1 has classically been described as a non-cleaved tripeptide sequence with the consensus sequence [SA][RK][LM] at the extreme C-terminus of the protein, however amino acids upstream of this tripeptide also influence targeting (Emanuelsson *et al.*, 2003; Gould *et al.*, 1987). The PTS2 is a nonapeptide sequence defined by the consensus sequence R[LI]x_5HL in the cleaved N-terminal domain of the targeted protein (Reumann, 2004; Swinkels *et al.*, 1991). The success of peroxisomal protein identification in plants using mass-spectrometry based proteomic approaches was initially limited. The fragility of the single peroxisome membrane and contamination from other organelles prevented researchers from isolating peroxisomes from Arabidopsis of high yield and purity (Eubel *et al.*, 2008). Fukao *et al.* (2002) identified 29 proteins from leaf peroxisomes of greening cotyledons whilst Fukao *et al*. (2003) succeeded in identifying 19 peroxisomal proteins from etiolated Arabidopsis cotyledons. However, with improvements to methodologies and technology, Reumann *et al.* (2007) identified 78 peroxisomal proteins from mature plant leaves including 42 novel proteins, and Eubel *et al.* (2008) isolated 89 proteins from Arabidopsis cell culture including 36 not previously identified. Using bioinformatics predictions of peroxisomal matrix targeting signals approximately 220 and 60 proteins that carry a putative PTS1 and PTS2, respectively have been identified (Reumann *et al.*, 2004). This information has been used to establish Araperox (http://www.araperox.uni-goettingen.de/), a database of the putative

Arabidopsis peroxisomal proteome. However, for many of these genes, functional analysis is absent or inadequate.

1.2 β-oxidation and energy metabolism

In dry seeds fatty acids are stored as triacylglycerol (TAG) within oil bodies, before they are degraded during germination. Oleosins are the major structural protein, covering the oil body surface and regulating size. TAG consists of mainly long-chain fatty acids such as palmitic acid (C16:0), stearic acid (C18:0), oleic acid (C18:1), linoleic acid (C18:2) and linolenic acid (C18:3) (Trelease and Doman, 1984). During the degradation process TAG is hydrolysed by TAG lipases into its component three fatty acid chains and a glycerol backbone. *SUGAR DEPENDENT1* (*SDP1*) encodes the major TAG lipase, displaying specificity towards TAG with significantly less activity with diacylglycerol (DAG) and monoacylglycerol (MAG) (Eastmond, 2006). Free fatty acids are imported into peroxisomes by COMATOSE (CTS; also known as PEROXISOMAL ABC-TRANSPORTER1 (PXA1) and PEROXISOME DEFICIENT3 (PED3)) and enter β-oxidation (Figure 1.1). There is also evidence for fatty acyl-CoAs as substrates of CTS/PXA1/PED3 (Footitt *et al.*, 2002; Zolman *et al.*, 2001b). The carbon derived from β-oxidation then enters the glyoxylate cycle and finally gluconeogenesis.

Entry of fatty acids into the β-oxidation cycle typically requires CoA esterification by an acyl-activating enzyme (AAE) with CoA synthetase activity specific to that substrate (Groot *et al.*, 1976). The β-oxidation cycle of saturated fatty acids requires four different enzyme activities on three different proteins (Lazarow, 1981; Osmundsen *et al.*, 1991). Acyl-CoA oxidase (ACX) catalyses the initial oxidase step by converting acyl-CoA to 2E-enoyl-CoA. An enoyl-CoA hydratase (ECH) hydrates the 2E-enoyl-CoA to 3-hydroxyacyl-CoA, which is subsequently converted by a 3-hydroxyacyl-CoA dehydrogenase to 3-oxoacyl-CoA. In the final step, a 3-ketoacyl-CoA thiolase (KAT) cleaves an acetyl-CoA from 3-oxoacyl-CoA, leaving the acyl-CoA chain two carbons shorter. Typically the enoyl-CoA hydratase and 3-hydroxyacyl-CoA dehydrogenase activities of β-oxidation are contained on a single protein called a multifunctional enzyme (MFE). Two forms of MFE exist; bacteria, plants and mammals possess type 1 MFE (MFE-1), and yeast and mammals possess type 2 MFE (MFE-2) (Kunau *et al.*, 1995). MFE-1 mediates the conversion of 2E-enoyl-CoA to 3-oxoacyl-CoA via the isomer 3S-hydroxyacyl-CoA whereas MFE-2 catalyses the same reaction via the R isomer.

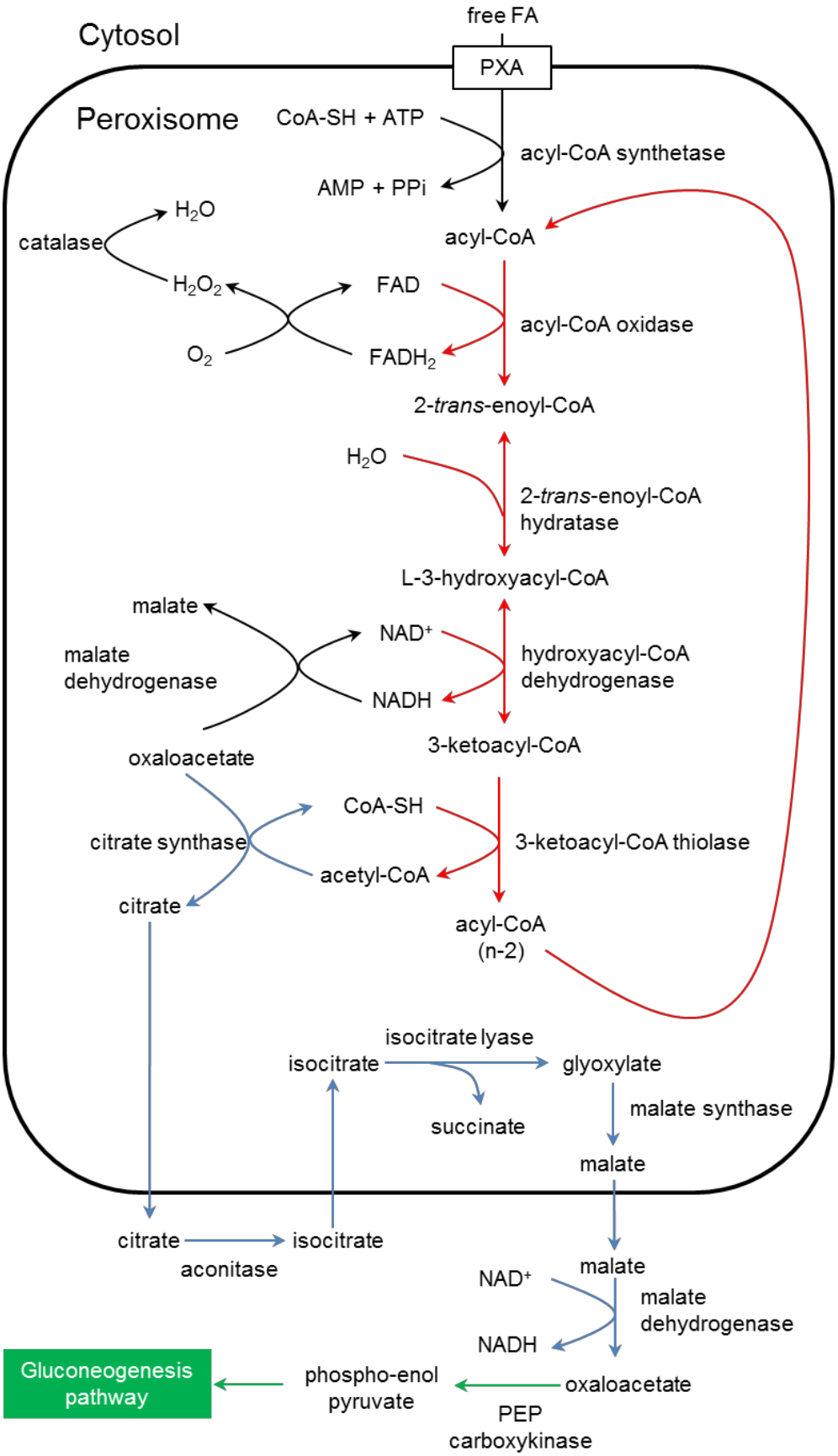
Cytosol
free FA
PXA
Peroxisome
CoA-SH + ATP
acyl-CoA synthetase
AMP + PPi
acyl-CoA
catalase
H_2O
H_2O_2
FAD
O_2
$FADH_2$
acyl-CoA oxidase
2-*trans*-enoyl-CoA
H_2O
2-*trans*-enoyl-CoA hydratase
L-3-hydroxyacyl-CoA
malate
malate dehydrogenase
NAD^+
NADH
hydroxyacyl-CoA dehydrogenase
3-ketoacyl-CoA
oxaloacetate
citrate synthase
CoA-SH
acetyl-CoA
3-ketoacyl-CoA thiolase
citrate
acyl-CoA (n-2)
isocitrate lyase
isocitrate
glyoxylate
succinate
malate synthase
malate
citrate
aconitase
isocitrate
malate
NAD^+
NADH
malate dehydrogenase
Gluconeogenesis pathway
phospho-enol pyruvate
oxaloacetate
PEP carboxykinase

Figure 1.1. Fatty acid β-oxidation and glyoxylate cycle. Free fatty acids are imported from the cytosol by the peroxisomal ABC-transporter (PXA) and activated by an acyl-CoA synthetase. Acyl-CoA is cycled through β-oxidation, each cycle resulting in reduction of the chain length by two carbons. Acetyl-CoA released by β-oxidation enters the glyoxylate cycle as citrate. Malate exported from the peroxisome is metabolised to oxaloacetate that may enter the gluconeogenesis pathway, or can be imported by mitochondria and enter the TCA cycle. H_2O_2 generated by the acyl-CoA oxidase reaction is detoxified by catalase to H_2O. NAD^+ depleted by β-oxidation is regenerated by peroxisomal malate dehydrogenase, which concomitantly metabolises oxaloacetate to malate. To aid legibility of the figure the glyoxylate cycle is not actually depicted as a cycle. Oxaloacetate may be metabolised by citrate synthase to complete the cycle, or succinate may be metabolised to fumarate and then malate. The reactions of fatty acid degradation are colour coded: red (β-oxidation), blue (the glyoxylate cycle), green (gluconeogenesis), and black (other reactions).

Many Arabidopsis mutants disrupted in the import, activation, and β-oxidation of fatty acids accumulate long-chain acyl-CoAs during germination and retain storage lipids in the form of TAG within oil bodies. There is biochemical evidence that lipases can be inhibited by both acyl-CoAs and CoA *in vitro* (Hills *et al.*, 1989). This has led to the proposal that within the plant cell a feedback mechanism is present where acyl-CoA utilisation controls the rate of lipolysis (Baker *et al.*, 2006; Hayashi *et al.*, 2001).

The six Arabidopsis peroxisomal acyl-CoA oxidases (ACX) represent the most well characterised family of β-oxidation enzymes in terms of substrate specificity, with the chain length specificity determined for ACX1 (C14:0), ACX2 (C14:0-C20:0), ACX3 (C8:0-C14:0) and ACX4 (C4:0-C8:0) (Eastmond *et al.*, 2000b; Froman *et al.*, 2000; Hayashi *et al.*, 1999; Hooks *et al.*, 1999). Whilst the *acx1* and *acx2* single mutants display mild phenotypes due to their partial redundancy, an *acx1 acx2* double mutant is unable to catabolise storage lipids, accumulating long-chain acyl-CoA (Pinfield-Wells *et al.*, 2005). Post-germinative seedling growth was severely compromised in the absence of exogenous sucrose. However, a significant sucrose-independent reduction in germination frequency was also observed, suggesting a role for β-oxidation in germination beyond simply the provision of energy (Pinfield-Wells *et al.*, 2005). No sucrose-dependent seedling establishment phenotype was observed for the *acx3* and *acx4* mutants; however ovules abort during the first phase of embryo development in the *acx3 acx4* double mutant implying an essential role for short-chain acyl-CoA oxidase activity (Rylott *et al.*, 2003).

In contrast there is less information on the substrate specificities of the multifunctional enzymes (MFE) or the 3-ketoacyl-CoA thiolases (KAT) in Arabidopsis. The two Arabidopsis MFEs, AIM1 and MFP2, both contain domains with 2E-enoyl-CoA hydratase, and 3S-hydroxyacyl-CoA dehydrogenase activities (Richmond and Bleecker, 1999; Rylott *et al.*, 2006). In cucumber (*Cucumis sativus*), studies of MFE activity included characterisation of four isozymes (Behrends *et al.*, 1988; Gühnemann-Schäfer and Kindl, 1995). The gene encoding a 76.5 kDa isozyme was cloned and the protein was shown to contain, in addition to a 2E-enoyl-CoA hydratase and 3S-hydroxyacyl-CoA dehydrogenase activity, a Δ^3, Δ^2-enoyl-CoA isomerase and 3-hydroxyacyl-CoA epimerase activity (Preisig-Müller *et al.*, 1994). However, it remains unclear if AIM1 and MFP2 in Arabidopsis also possess these auxiliary enzyme activities.

MFP2 expression is significantly up-regulated during early germination and continues to be highly expressed during post-germinative growth (Eastmond and Graham, 2000). Conversely, *AIM1* has low expression during germination and early post-germinative growth, but is up-regulated in siliques and flowers (Richmond and Bleecker, 1999). The *aim1* mutant has

abnormal flower development resulting in reduced fertility, and also displays increased resistance to the synthetic auxin analogue 2,4-DB. The *mfp2* mutant catabolises storage lipids more slowly and accumulates long-chain acyl-CoAs. However, once photosynthesis is established, plants grow like wild-type and produce normal flowers and seeds (Rylott *et al.*, 2006). The *aim1 mfp2* double mutant aborts during the early stages of embryo development, displaying a phenotype comparable to that of the *acx3 acx4* double mutant (Rylott *et al.*, 2003).

Characterisation of the substrate specificity of the three Arabidopsis thiolases, KAT1, KAT2, and KAT5 remains inadequate. In the absence of an exogenous supply of sucrose, *kat2* mutants are severely disrupted in seedling growth following germination, indicating that *KAT2* encodes the major peroxisomal thiolase at this stage of development (Germain *et al.*, 2001; Hayashi *et al.*, 1998). Recombinant KAT2 protein was shown to have acetoacetyl-CoA thiolase activity *in vitro* and long-chain acyl-CoAs accumulated in the *kat2* mutant, suggesting that KAT2 has both short-chain and long-chain 3-ketoacyl-CoA thiolase activity (Germain *et al.*, 2001). As only KAT2 produced a soluble enzyme in an *Escherichia coli* expression system, attempts to characterise the substrate specificity of KAT1 and KAT5 *in vitro* failed (Germain *et al.*, 2001). However, over-expression of the *KAT5* coding sequence in *kat2* mutant resulted in only partial complementation of the seedling arrest phenotype in the absence of exogenous sucrose, indicating differing but overlapping specificities between KAT2 and KAT5 (Germain *et al.*, 2001). Recent analysis of gene co-expression clusters in Arabidopsis is suggestive of a role for KAT5 not in β-oxidation, but instead in flavonoid biosynthesis (Carrie *et al.*, 2007). The *KAT5* gene was also demonstrated to encode two proteins differing at the N-terminus due to alternative transcription starts and RNA splicing that generates either the cytosolic KAT5.1 or the peroxisomal KAT5.2 (Carrie *et al.*, 2007).

The core enzymes of β-oxidation are not capable of completely degrading unsaturated fatty acids with *cis* (Z) double bonds on an even-numbered carbon (Schulz and Kunau, 1987). In MFE-1-possessing organisms, this is due to the fact that hydration of 2Z-enoyl-CoA by the enoyl-CoA hydratase 1 generates 3R-hydroxyacyl-CoA, which is not a substrate of the 3S-hydroxyacyl-CoA dehydrogenase domain present in MFE-1. Additional enzymes are required that contribute to β-oxidation to avoid the metabolic block created by *cis*-unsaturated bonds. Two different pathways (Figure 1.2) have been proposed for the degradation of fatty acids with *cis*-double bonds at even-numbered carbons (Schulz and Kunau, 1987).

In the reductase-isomerase pathway, unsaturated fatty acids are degraded by the core β-oxidation cycle to 2E,4Z-enoyl-CoA which is reduced by 2,4-dienoyl-CoA reductase to 3E-enoyl-CoA (Schulz and Kunau, 1987). A Δ^3, Δ^2-enoyl-CoA isomerase mediates the conversion of 3E-enoyl-CoA to 2E-enoyl-CoA. Both of these auxiliary enzyme activities have been

detected in germinating cucumber seedlings (Behrends *et al.*, 1988). In the hydratase-epimerase pathway unsaturated fatty acids are degraded by the core β-oxidation enzymes instead to 3R-hydroxyacyl-CoA, which can be converted to its S isomer to rejoin the core β-oxidation cycle (Schulz and Kunau, 1987). This conversion may either occur directly by the action of 3-hydroxyacyl-CoA epimerase, or indirectly by the combined action of enoyl-CoA hydratase 2 converting 3R-hydroxyacyl-CoA to 2E-enoyl-CoA, and enoyl-CoA hydratase 1 subsequently converting 2E-enoyl-CoA to 3S-hydroxyacyl-CoA (Engeland and Kindl, 1991; Hiltunen *et al.*, 1989; Preisig-Müller *et al.*, 1994). A MFE-1 from cucumber has been shown to harbour 3-hydroxyacyl-CoA epimerase activity (Preisig-Müller *et al.*, 1994). The novel monofunctional enoyl-CoA hydratase 2 isolated from cucumber cotyledon peroxisomes is responsible for much of the overall epimerase activity, and this activity greatly exceeds that of 2,4-dienoyl-CoA reductase (DECR) (Behrends *et al.*, 1988; Engeland and Kindl, 1991). However, in Arabidopsis, analysis of the *in vivo* flux of unsaturated fatty acids in the β-oxidation cycle indicates a significant contribution to degradation by both the reductase-isomerase and hydratase-epimerase pathway (Allenbach and Poirier, 2000).

In *Saccharomyces cerevisiae* DECR and Δ^3, Δ^2-enoyl-CoA isomerase are essential for the degradation of fatty acids with a *cis* double bond on an even-numbered carbon (Gurvitz *et al.*, 1998; Gurvitz *et al.*, 1997; Robert *et al.*, 2005). The absence of enoyl-CoA hydratase 1 and 3-hydroxyacyl-CoA epimerase activity in *S. cerevisiae* suggests that the reductase-isomerase pathway is the only functional pathway. An Arabidopsis monofunctional peroxisomal $\Delta^{3,5}$, $\Delta^{2,4}$-dienoyl-CoA isomerase (DCI1) has been biochemically characterised and is capable of functionally restoring a yeast mutant disrupted in an orthologous gene (Goepfert *et al.*, 2005). In Arabidopsis a novel peroxisomal enzyme, monofunctional enoyl-CoA hydratase type 2 (ECH2) has been shown *in vivo* to convert the intermediate 3R-hydroxyacyl-CoA, generated by the degradation of fatty acids with Z-unsaturated bonds on an even carbon, to 2E-enoyl-CoA (Goepfert *et al.*, 2006). The Arabidopsis genome also encodes a number of monofunctional enoyl-CoA hydratases and Δ^3, Δ^2-enoyl-CoA isomerases with putative PTSs (Reumann *et al.*, 2004).

Malate functions as a major form of reducing equivalent in the peroxisome, being imported during photorespiration (Cousins *et al.*, 2008; Reumann and Weber, 2006) and exported during fatty acid β-oxidation (Baker *et al.*, 2006; Mettler and Beevers, 1980). Peroxisomal malate dehydrogenase (PMDH) reduces NAD^+ to NADH during the conversion of malate into oxaloacetate (Mettler and Beevers, 1980). In Arabidopsis the *pmdh1 pmdh2* double mutant has a severe disruption to β-oxidation, but not a complete block (Pracharoenwattana *et al.*, 2007). The *S. cerevisiae* peroxisome membrane is impermeable to NAD(H) (van Roermund *et al.*, 1998) and it has been hypothesised that in Arabidopsis NADH levels are unlikely to be maintained by

import (Pracharoenwattana *et al.*, 2010). The photorespiratory enzyme hydroxypyruvate reductase (HPR) is present at low levels in germinating Arabidopsis seedlings (Cornah *et al.*, 2004), and recently a *hpr pmdh1 pmdh2* triple mutant has been generated that is almost completely blocked in the reoxidation of NADH required for β-oxidation (Pracharoenwattana *et al.*, 2010). The absence of an embryo lethal phenotype due to a complete block in β-oxidation as with *aim1 mfp2,* suggests that other mechanisms exist to regenerate or replenish NADH within the peroxisome (Pracharoenwattana *et al.*, 2010; Rylott *et al.*, 2006). Recently a peroxisomal NAD^+ carrier required for optimal fatty acid degradation during oil body mobilisation has been identified (Bernhardt *et al.*, 2012).

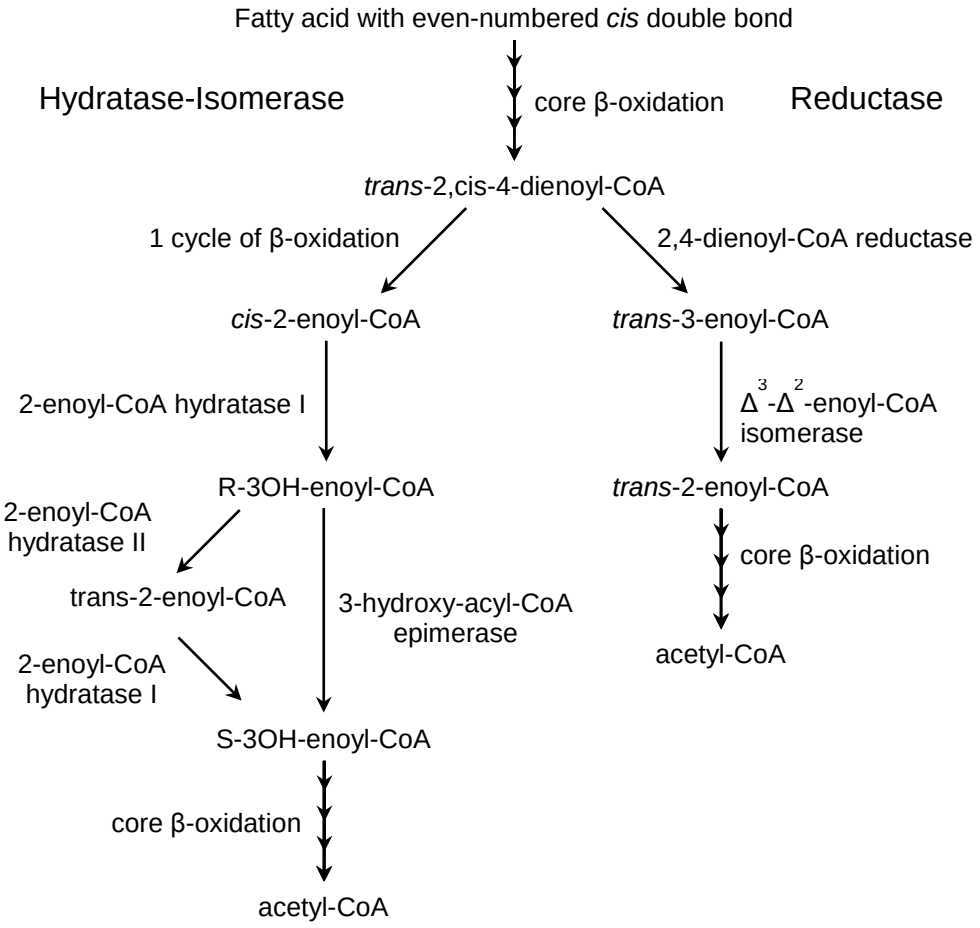

Figure 1.2. Unsaturated fatty acid degradation occurs via two alternate pathways. Two pathways for degradation of fatty acids with an even-numbered *cis* double bond operate in the peroxisome the Hydratase-Isomerase and the Reductase pathways.

1.3 The role of β-oxidation in the synthesis of hormones

1.3.1 Jasmonic acid

Jasmonic acid (JA), auxin and benzoic acid (BA) are hormones (or hormone precursors in the case of BA) synthesised by carbon chain shortening via the β-oxidation pathway (Figure 1.3). JA is an oxylipin signalling molecule derived from linolenic acid (for review see Schaller and Stintzi, 2009; Weber, 2002). Disruption to JA signalling and metabolism has pleiotropic effects on growth, senescence, fertility and plant defence. Biosynthesis of JA begins in plastids with the formation of the JA-precursors 12-oxo-phytodienoic acid (OPDA) and dinor-OPDA. In the peroxisome OPDA and dinor-OPDA are reduced to OPC:8 and OPC:6 respectively before undergoing two or three cycles of β-oxidation, respectively, to generate JA. A mutant disrupted in peroxisomal NADPH-dependent OPDA-reductase, *opr3*, is deficient in JA and has defective pollen production resulting in male sterility (Sanders *et al.*, 2000; Stintzi and Browse, 2000). OPR3 accepts free OPDA *in vitro* suggesting that the reduction of OPDA to OPC:8 precedes CoA esterification of the precursor (Schaller *et al.*, 2000). However, the 4-courmate:CoA ligase-like (4CL-like) enzymes encoded by At4g05160 and At5g63380 activate OPDA and OPC:6 *in vitro*, suggesting that this activation step can occur at various stages of the β-oxidation cycle (Schneider *et al.*, 2005).

ACX1 has an important functional role in JA synthesis, as wound-induced JA levels in the *acx1* mutant are 20% of that found in wild-type (Pinfield-Wells *et al.*, 2005). While *acx5* wound-induced JA levels are similar to wild-type, in an *acx1 acx5* double mutant JA levels are 1% of that observed in wild-type (Schilmiller *et al.*, 2007). The *aim1* mutant has reduced levels of JA and accumulates OPC:4 but not OPC:8 or OPC:6, suggesting overlapping functions with MFP2 (Delker *et al.*, 2007). The *aim1* mutant displays defects in flower development with changes to the floral organ composition effecting fertility (Richmond and Bleecker, 1999). However, JA levels in *aim1* flowers have not been measured nor has exogenous JA been applied to flowers to restore fertility, so a direct link between JA and *aim1* infertility has not be made in the literature. The wide substrate specificity of KAT2 extends to JA intermediates, with both *KAT2* antisense RNA and *ped1* (allelic to *kat2*) mutant lines displaying reduced wound-induced JA synthesis, relative to wild-type (Afitlhile *et al.*, 2005; Castillo *et al.*, 2004). However, even in the *ped1* mutant some accumulation still occurs, implying a compensatory role for other peroxisomal thiolase isoforms (Afitlhile *et al.*, 2005).

Male fertility is reduced in the *acx1 acx5* double mutant with a decrease in pollen viability, while anther elongation and pollen dehiscence remains unaltered (Schilmiller *et al.*, 2007). *ACX1* is highly expressed in floral organs including pollen grains while *ACX5* is highest in stamens and pollen (Schmid *et al.*, 2005). In *acx1 acx5* flowers JA levels remain 25% of wild-

type and *ACX1* expression is more prominent in pollen than anther or filament tissue suggesting other acyl-CoA oxidases may synthesise JA in these floral organs (Schilmiller *et al.*, 2007).

Natural senescence is marked by yellowing of leaves, which corresponds to chlorophyll and chloroplast degradation. The delayed senescence phenotype of the JA-insensitive *coronatine-insensitive1* (*coi1*) mutant and accumulation of JA in senescent leaves, strongly implicates a role for JA in senescence (He *et al.*, 2002). *KAT2* expression is induced in response to the senescence-promoting conditions of dark treatment (Castillo and León, 2008; Charlton *et al.*, 2005a). Transcripts of the other peroxisomal thiolases, *KAT1* and *KAT5*, do not accumulate in senescing leaves (Castillo and León, 2008). *KAT2* antisense lines, expressing approximately 10% of wild-type transcript levels, have delayed senescence as determined by chlorophyll content in dark-treated excised leaves and under natural senescing conditions (Castillo and León, 2008). *KAT2* antisense lines senesce in response to exogenous JA, providing evidence of a dual role for KAT2 in β-oxidation to synthesise JA that then regulates leaf senescence, as well as the general degradation of cellular lipid components by peroxisomes (Castillo and León, 2008).

JA is also required for plant protection against pathogens (Staswick *et al.*, 1998) and insects (Kang *et al.*, 2006). The double mutant *acx1 acx5* is susceptible to larvae of the cabbage looper moth (*Trichoplusia ni*), implying an essential role for β-oxidation and JA in plant defense against insect herbivores (Schilmiller *et al.*, 2007). However, the double mutant maintains resistance to the plant fungal pathogen, *Alternaria brassicola*, accumulating JA in response, suggesting different acyl-CoA oxidases respond to herbivory insects and fungal pathogen attack (Schilmiller *et al.*, 2007).

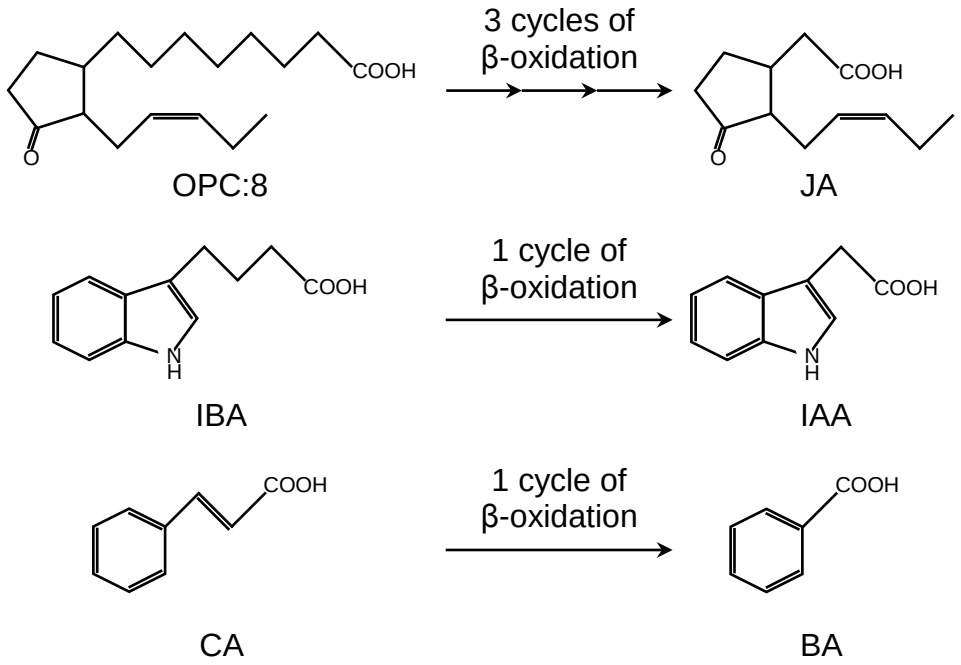

Figure 1.3. Metabolism of hormones via β-oxidation. The chain-shortening of fatty acids by two carbons with each cycle of β-oxidation is used in the synthesis of some plant hormones. Jasmonic acid (JA) is synthesised from 3-oxo-2-(2′-[*Z*]-pentenyl)cyclopentane-1-octanoic acid (OPC:8) via three cycles of β-oxidation. The auxin precursor indole-3-butyric acid (IBA) is metabolised to the active form of indole-3-acetic acid (IAA) by one step of β-oxidation. Benzoic acid (BA) may be synthesised via one cycle of β-oxidation from cinnamic acid (CA).

1.3.2 Auxin

The auxin, indole-3-acetic acid (IAA), is a hormone that plays a role in many aspects of plant growth and development including lateral root initiation, apical dominance, phototropism and geotropism (Woodward and Bartel, 2005). Synthesis of IAA can occur via multiple pathways either dependent or independent of tryptophan, by the hydrolysis of IAA-conjugates, and via one cycle of β-oxidation of the endogenous auxin precursor indole-3-butyric acid (IBA). The proposed mechanism of IBA β-oxidation (Figure 1.3) is analogous to that of fatty acids previously described (Reumann *et al.*, 2004). High concentrations of IBA and the synthetic auxin precursor 2,4-dichlorophenoxybutyric acid (2,4-DB) inhibit root growth when converted to their active forms, IAA and 2,4-dichlorophenoxyacetic acid (2,4-D) respectively. The isolation of mutants resistant to IBA or 2,4-DB but not IAA or 2,4-D, has resulted in the characterisation of many mutants defective in β-oxidation and peroxisome biogenesis (Hayashi *et al.*, 1998; Zolman and Bartel, 2004; Zolman *et al.*, 2000). This has also led to the identification of a novel peroxisomal acyl-CoA dehydrogenase gene, *IBA-response3* (*IBR3*), which apparently acts in an IBA specific β-oxidation pathway (Zolman *et al.*, 2007). Peroxisomal auxin metabolism is discussed in more detail in Chapter 3.

1.3.3 Salicylic and benzoic acids

Salicylic acid (SA) plays a role in thermotolerance, hypersensitivity response and systemic acquired resistance (Durner *et al.*, 1997). SA is derived from benzoic acid (BA) in plants, originating either from phenylalanine or isochorismate. Synthesis from phenylalanine occurs via the chain shortening of *trans*-cinnamic acid either by non-oxidative decarboxylation or β-oxidation (Figure 1.3) yielding BA (Reumann *et al.*, 2004). In the Arabidopsis *isochorismate synthase1* (*ics1*) mutant pathogen-induced SA accumulation is impaired, indicating the majority of SA is synthesised from isochorismate, at least in response to pathogens (Wildermuth *et al.*, 2001).

In the flowers of petunia (*Petunia hybridia* cv. Mitchell) benzoic acid is converted into volatile benzenoids. Silencing of the petunia thiolase gene, *PhKAT1*, results in a decrease in BA and benzenoid while other phenylpropanoid-related volatiles remain unaffected (Moerkercke *et al.*, 2009). *PhKAT1* expression is primarily limited to petal limbs and tubes being scarcely detectable in other tissues, and follows a diurnal rhythm peaking in the dark period that corresponds to the release of volatile benzenoids (Moerkercke *et al.*, 2009). *At*KAT5 has high similarity to *Ph*KAT1 (Moerkercke *et al.*, 2009), and is up-regulated in flowers (Kamada *et al.*, 2003), but it is unknown if *At*KAT5 has a functional role in BA synthesis. β-oxidation may therefore be important for the synthesis of a variety of BA based metabolites and not just limited to SA.

1.4 The role of β-oxidation in plant development

1.4.1 A putative novel signal controlling germination and dormancy

Genetic analysis of some β-oxidation mutants has implicated a role for β-oxidation not just in the supply of carbon for post-germinative seedling growth but also in controlling timing of seed germination and breaking of dormancy (Footitt *et al.*, 2002; Pinfield-Wells *et al.*, 2005; Pracharoenwattana *et al.*, 2005; Russell *et al.*, 2000). Potential novel signalling molecules are generated or degraded by β-oxidation and these are proposed to have a role in controlling onset of germination and breaking of dormancy (Baker *et al.*, 2006).

Germination is divided into three stages: firstly, water uptake during which the seed imbibes; secondly, reinitiation of metabolic processes; and thirdly, radicle elongation as the radicle emerges through the seed endosperm and testa (Bewley and Black, 1994). Following imbibition the seed can enter a non-germinating dormant state controlled by many environmental and genetic factors. Dry seeds require a period of after-ripening for the dormancy to break. Seed dormancy is controlled by a variety of environmental factors such as light, temperature, and water (Koornneef *et al.*, 2002), and regulated by the action of the hormones abscisic acid (ABA) and gibberellin (GA) (Holdsworth *et al.*, 2008; Schwechheimer, 2008).

Free fatty acids are imported into the peroxisome by an ATP-binding cassette transporter disrupted in the *cts* mutant (Footitt *et al.*, 2002; Russell *et al.*, 2000). Severe mutant alleles of *cts* have been described as being in a “forever dormant” state, and have similar protein profiles to dormant wild-type seeds (Russell *et al.*, 2000). In these mutants germination can be induced by removal of the seed coat in combination with exogenous sucrose supply (Footitt *et al.*, 2002). Similarly, mutations that increase seed coat permeability, such as *altered testa shape* (*ats*) and *transparent testa glabra 1* (*ttg1-1*), promote seed germination when present in the *cts* background, implying the seed coat prevents germination in *cts* (Footitt *et al.*, 2002). CTS has broad substrate specificity for the transport of fatty acids and other molecules with different acyl chain lengths, including 2,4-DB, IBA and JA precursors (Footitt *et al.*, 2007b; Footitt *et al.*, 2002; Theodoulou *et al.*, 2005). Transcriptome analysis of the *cts* mutant has revealed that CTS is required late in the second phase of germination following after-ripening (Carrera *et al.*, 2007). CTS is also required for the up-regulation of the flavonoid biosynthesis pathway genes in the epidermis of imbibed after-ripened embryos (Carrera *et al.*, 2007).

Reductions in germination frequency have also been described in the β-oxidation mutants *kat2* (Germain *et al.*, 2001), *acx1 acx2* (Pinfield-Wells *et al.*, 2005), *csy2 csy3* (Pracharoenwattana *et al.*, 2005) and *pmdh1 pmdh2 hpr* (Pracharoenwattana *et al.*, 2010). Changes to organellar morphology have been observed using electron microscopy in some of

these germination mutants. Seedling cotyledon cells of the *cts* mutant retain lipid bodies, have smaller vacuoles, and exhibit chloroplasts with distorted morphology lacking starch granules and granal stacks (Footitt *et al.*, 2002). In the allelic *kat2* and *ped1* mutants, lipid bodies in cotyledons are not degraded, while peroxisomes, mitochondria, and chloroplasts are all decreased in number with a corresponding dramatic increase in size (Germain *et al.*, 2001; Hayashi *et al.*, 1998; Hayashi *et al.*, 2001).

In Arabidopsis two long-chain acyl-CoA synthetase (LACS) isozymes, LACS6 and LACS7, are localised to the peroxisome (Fulda *et al.*, 2002). The *lacs6 lacs7* double mutant is disrupted in peroxisomal LACS activity, unable to mobilise seed lipids, and requires exogenous sucrose for seedling establishment (Fulda *et al.*, 2004). However, unlike many other β-oxidation mutants no reduction in germination frequency was observed, suggesting any potential signal controlling germination is not derived from long-chain fatty-acids (LCFA) or LACS activity. Similarly enlarged peroxisomes have been observed in *kat2*, *mfp2* and *acx1 acx2* (Germain *et al.*, 2001; Hayashi *et al.*, 2001; Pinfield-Wells *et al.*, 2005; Rylott *et al.*, 2006), but not *cts* or *lacs6 lacs7* (Footitt *et al.*, 2002; Fulda *et al.*, 2004). The Arabidopsis genome contains an acyl-activating enzyme (AAE) superfamily of 63 genes, 17 of which encode proteins with putative PTSs (Reumann *et al.*, 2004; Shockey *et al.*, 2003). These include the previously described LACS (Fulda *et al.*, 2004) and 4CL-like enzymes (Schneider *et al.*, 2005), as well as two subfamilies annotated Clade I and Clade VI (Shockey *et al.*, 2003).

Clade I and Clade VI of the AAE superfamily may contain peroxisomal enzymes which are candidates for activating signal precursors. Clade I contains AAE17 and AAE18, which both have limited sequence similarity to a plastidic acetyl-CoA synthetase (Ke *et al.*, 2000). Clade VI contains AAE1, AAE5, AAE7, AAE11, AAE12 and benzoyloxyglucosinolate 1 (BZO1), members of the acid:CoA ligase family that participate in a previously uninvestigated plant-specific branch of CoA dependent acid activation (Shockey *et al.*, 2003). Based on disruptions to the activation of acetate in an *aae7* mutant, AAE7 has been proposed to have a housekeeping role, scavenging free acetate for entry into the glyoxylate cycle, as well as potentially recycling acetate as lipid reserves expire in establishing seedlings (Turner *et al.*, 2005). BZO1 is an enzyme with *in vitro* benzoyl-CoA ligase activity, and *bzo1* mutant seeds do not accumulate benzoyloxyglucosinates, a class of secondary metabolites involved in plant defense (Kliebenstein *et al.*, 2007). The remaining novel peroxisomal AAE isozymes remain uncharacterized, but may act on a range of short chain fatty acids under differing developmental control (Shockey *et al.*, 2003). Intriguingly, the exogenous supply of the short-chain fatty-acids propionate and butyrate promotes germination potential in the absence of sucrose in after-ripened *cts* (Footitt *et al.*, 2002).

The enzymatic breakdown of cell wall components regulates germination and dormancy in Arabidopsis, tobacco, and tomato (*Lycopersicon esculentum*) (Debeaujon *et al.*, 2000; Downie *et al.*, 2003; Leubner-Metzger and Meins, 2000). Similar to *cts*, the allelic *ped3-3* mutant requires removal of the seed coat to germinate (Hayashi *et al.*, 2002). Transcriptomic analysis indicates that *ABA INSENSITIVE 5* (*ABI5)* levels remain high in *ped3-3* after imbibition while levels decrease in wild-type (Kanai *et al.*, 2010). ABI5 is a basic leucine zipper transcription factor that binds to ABA-responsive elements (ABRE) regulating seed maturation and dormancy (Bensmihen *et al.*, 2002; Carles *et al.*, 2002; Nakabayashi *et al.*, 2005; Piskurewicz *et al.*, 2008).

The double mutant *ped3-3 abi5* germinates in the presence of sucrose without removal of the seed coat (Kanai *et al.*, 2010). Polygalacturonase inhibiting proteins (PGIP1 and PGIP2) are up-regulated in *ped3* (as long as ABI5 is present), but are repressed during imbibition in wild-type and *ped3-3 abi5*. Analysis of germinating seeds indicated that while all seed genotypes had a thick mucilage layer at 6 h imbibition, by 24 h this layer was effectively degraded by wild-type, *abi5*, *ped3 abi5*, and *pgip1* seeds, but not by *ped3* and a *PGIP1* over-expresser seeds (Kanai *et al.*, 2010). Disruption to gibberellin 3-oxidase (GA3OX) activity in the *ga3ox1-3 ga3ox2-1* double mutant results in reduced GA levels and seeds cannot germinate without the exogenous supply of GA (Mitchum *et al.*, 2006). However, the seed mucilage layer is degraded in the *ga3ox1-3 ga3ox2-1* double mutant implying the failure to enzymatically degrade pectin in *ped3* is not simply a result of arrested germination (Kanai *et al.*, 2010). Therefore, the up-regulation of PGIP in *ped3* seeds inhibits degradation of pectin in the seed coat during imbibition, preventing germination (Kanai *et al.*, 2010). The pectin mucilage layer of *ped3* seeds can be degraded by exogenous fungal polygalacturonase or low pH media to promote germination (Kanai *et al.*, 2010).

It remains unclear how PED3 regulates the expression of ABI5 (Kanai *et al.*, 2010). It has been hypothesised that in *cts* seeds some product of lipid catabolism may accumulate, signalling the embryo to remain dormant or inhibiting carbohydrate metabolism to prevent germination (Footitt *et al.*, 2002). While β-oxidation may degrade or synthesise some signalling molecules controlling germination and dormancy, IAA has no characterised role in germination (Baker *et al.*, 2006). Recently, the JA precursor OPDA has been shown to accumulate in *cts*, *kat2* and *acx1 acx2* seeds (Dave *et al.*, 2011). When applied exogenously OPDA acts synergistically with ABA to inhibit germination of wild-type seeds, and stabilises ABI5 protein levels in *35S:HA-ABI5* seeds (Dave *et al.*, 2011). While CTS/PED3 negatively regulates ABA signalling (Dave *et al.*, 2011; Kanai *et al.*, 2010), KAT2 appears to positively regulate ABA signalling (Jiang *et al.*, 2011). The *kat2-3* mutant is ABA-insensitive while *KAT2* over-expressing plants are hypersensitive (Jiang *et al.*, 2011). ROS levels are reduced in *kat2-3* leaves, and are not

induced by application of 5 μM ABA as in wild-type leaves (Jiang *et al.*, 2011). The interaction between β-oxidation, ABA signalling and ROS homeostasis evidently requires further investigation.

The peroxisome is a source of reactive oxygen species such as H_2O_2 and nitric oxide that may play a signaling role in germination and dormancy (Corpas *et al.*, 2001; Nyathi and Baker, 2006). H_2O_2 also has a proposed role in the degradation of cell wall components resulting in weakening of the endosperm layer (El-Maarouf-Bouteau and Bailly, 2008; Müller *et al.*, 2007; Müller *et al.*, 2009). Chemical inhibition of catalase in dormant lettuce seeds results in elevated levels of H_2O_2 that promote germination (Hendricks and Taylorson, 1975). Supply of exogenous H_2O_2 has also been demonstrated to break dormancy in barley (Fontaine *et al.*, 1994; Wang *et al.*, 1998) and rice (Naredo *et al.*, 1998). The additional role of H_2O_2 as a signalling molecule is implied by evidence that ABI2, a protein phosphatase that negatively regulates ABA signalling, is highly sensitive to inactivation by micromolar concentrations of H_2O_2 (Meinhard and Grill, 2001).

Imbibition with the NO donor sodium nitroprusside breaks dormancy and promotes germination in Arabidopsis and barley (*Hordeum vulgare*) (Bethke *et al.*, 2004), and purified NO gas has been confirmed to reduce seed dormancy in Arabidopsis (Bethke *et al.*, 2006). NO reduces sensitivity of seeds to ABA, and is required for expression of the GA biosynthetic genes *GA3ox1* and *GA3ox2* (Bethke *et al.*, 2007). Peroxisomes are required for the accumulation of NO. A pea nitric oxide synthase associated with leaf senescence has been identified biochemically in isolated pea leaf peroxisomes, and confirmed by immunolocalisation to localise to peroxisomes and chloroplasts (Barroso *et al.*, 1999; Corpas *et al.*, 2004). Two mutants disrupted in PEROXIN (PEX) proteins regulating peroxisomal matrix protein import, *pex12* and *pex13*, have lower NO content, suggesting peroxisomes are functionally associated with NO synthesis (Corpas *et al.*, 2009). While a putative nitric oxide synthase (AtNOS1) was identified in Arabidopsis mitochondria (Guo and Crawford, 2005; Guo *et al.*, 2003), this protein has since been demonstrated not to have NOS activity *in vitro*, with mutant defects in NO accumulation instead attributed as an indirect consequence of impaired mitochondrial biogenesis (Crawford, 2006; Zemojtel *et al.*, 2006). Currently attempts to identify a plant NOS remain unsuccessful (Hancock *et al.*, 2011; Moreau *et al.*, 2010).

1.4.2 Seed development and fertility

During development seeds accumulate oil in the form of TAG. β-oxidation of lipids assists in supporting metabolism once import of carbon from maternal tissue ceases, following breaking of the trophic connection between seed and mother plant, but before metabolic activity ceases. However, β-oxidation activity is present in Arabidopsis developing seeds even while

there exists a net synthesis of fatty acids (Arai *et al.*, 2002). Peroxisomal β-oxidation plays an essential role in seed development as *pex10*, *acx3 acx4* and *aim1 mfp2* display early embryonic lethality (Rylott *et al.*, 2006; Rylott *et al.*, 2003; Sparkes *et al.*, 2003), while *ped1 ped3* and *aim1* have severe defects in reproductive tissue growth (Hayashi *et al.*, 2002; Richmond and Bleecker, 1999).

Oil turnover during late seed development provides carbon for metabolism during seed desiccation, with the loss of at least 10% of storage lipid from embryo during this period observed in *Brassica napus* (Chia *et al.*, 2005). Furthermore a 28% decrease in the fatty acid content of developing seeds observed in Arabidopsis at 20 d after flowering, during the late maturation stage, suggests an important role for stored lipid at this stage of seed metabolism (Baud *et al.*, 2002). In *B. napus* the activity of enzymes from the glyoxylate cycle, β-oxidation and gluconeogenesis can be detected in developing seed embryos during the period of oil accumulation, with increasing enzyme activity as seeds desiccate and mature (Chia *et al.*, 2005).

A role for KAT2 has been proposed in reproductive success (Footitt *et al.*, 2007a). Detailed morphological analysis of *kat2* reveals increased flower and silique production, combined with a reduction in silique length and seed yield. At maturity a high incidence of aborted seeds and reduced seed weight is also evident. Footitt *et al.* (2007a) proposed that in *kat2* reduced carbon flow through β-oxidation into the glyoxylate cycle results in a decrease in ovule respiration, altering resource allocation from ovules to floral meristems. This evidence implicates peroxisomal thiolases in a range of metabolic and signalling pathways influencing development.

The *shrunken seed 1* (*sse1*) mutant, disrupted in the function of the Arabidopsis PEX16p homolog, has defective peroxisome biogenesis resulting in seeds with low lipid oil and protein bodies content, but accumulated starch granules (Lin *et al.*, 1999). Low seed oil phenotypes have also been observed in *kat2*, *pmdh1 pmdh2* and *csy2 csy3* (Germain *et al.*, 2001; Pracharoenwattana *et al.*, 2005; Pracharoenwattana *et al.*, 2007). Additionally, lower seed weight, but not lower total seed yield per plant, was observed in *acx1*, *acx1 acx2* and *cts* (Pinfield-Wells *et al.*, 2005). Developing seeds in the *sse1* mutant have a reduced fatty acid synthesis rate, resulting in early seed development defects and an impaired greening process during seedling establishment (Lin *et al.*, 2004).

The function of PEX16 in fatty acid synthesis remains unclear: a *pex16i* (RNAi) knockdown is competent in matrix protein import but has peroxisomes of reduced abundance and increased size, containing vesicles speculated to originate via peroxisomal membrane invagination (Nito *et al.*, 2007). Plant development was not impaired and seedlings were not dependent on sucrose for establishment, but were unexpectedly resistant to 2,4-DB.

β-oxidation appears to play a role in catabolising excess fatty acids when synthesis is greater than that demanded by cell metabolism or the TAG synthesis pathway, allowing the fine-tuning of net fatty acid levels as demonstrated in *B. napus* (Eccleston and Ohlrogge, 1998) and Arabidopsis (Poirier *et al.*, 1999). Fatty acid-derived molecules have been proposed to provide a negative feedback, regulating the balance between synthesis and degradation (Lin *et al.*, 2004; Ohlrogge and Jaworski, 1997).

1.4.3 Dark-induced and natural senescence

β-oxidation plays a role in the turnover of fatty acids in mature plant tissue, especially during senescence. Using radioactively labelled CO_2 the degradation of fatty acids has been estimated at approximately 4% of total fatty acids per day in intact Arabidopsis leaves (Bao *et al.*, 2000). In Arabidopsis KAT2 is required for the timely onset of dark-induced leaf senescence (Castillo and León, 2008). To further analyse this β-oxidation requirement Yang and Ohlrogge (2009) investigated the relationship between timing of natural senescence and disruption of β-oxidation in Arabidopsis. However, they observed that *acx1 acx2, lacs6 lacs7* and *kat2* mutations had almost no effect on the rate of fatty acid breakdown during natural leaf senescence. Indisputably, fatty acid breakdown in senescent leaves is far slower than the rate of fatty acid and TAG degradation in germinating seedlings (Fulda *et al.*, 2004; Germain *et al.*, 2001; Yang and Ohlrogge, 2009). Therefore, the slower rate of degradation during senescence compared to that during germination may allow redundant enzymes to compensate (Yang and Ohlrogge, 2009). *ACX3* and *ACX4* are expressed in senescent leaves at higher levels than in young leaves so they may play a role in complementing *acx1 acx2* (Froman *et al.*, 2000; Hayashi *et al.*, 1999). The alternate thiolase isoform *KAT5* can partially rescue the seedling establishment phenotype when over-expressed in the *kat2* mutant (Germain *et al.*, 2001) and may compensate for the absence of *KAT2* during senescence in the *kat2* mutant (Yang and Ohlrogge, 2009).

Yang and Ohlrogge (2009) also conducted a survey of natural senescence and changes to lipid content in *Brachypodium distachyon*, a model for cereal plants, and switchgrass (*Panicum virgatum*), a potential energy crop. Previous evidence using thin-layer chromatography indicated that TAG increases in senescent leaves up to 12% of total lipid content in Arabidopsis (Kaup *et al.*, 2002) but more accurate measurements as determined by gas chromatography (GC) indicate TAG levels do not exceed 0.35% in Arabidopsis and *B. distachyon*, and reached a maximum of 1.23% in switchgrass (Yang and Ohlrogge, 2009).

The role of β-oxidation in energy metabolism in response to dark treatment induced carbon starvation has been demonstrated in the *pxa1* mutant, which develops necrotic lesions during extended darkness and bleaches when returned to the light, and the *kat2* mutant, which displays

a similar but less severe phenotype (Kunz *et al.*, 2009). This leaf necrosis is more severe with longer dark periods and elevated temperatures, and is dependent on complete darkness as opposed to partial covering of individual leaves. Mutants disrupted in jasmonic acid signalling, *opr3* and *delayed dehiscence 2* (*dde2*; disrupted in allene oxide synthase), were unaffected by prolonged darkness so this phenotype is not due to the role of *pxa1* and *kat2* in JA biosynthesis (Kunz *et al.*, 2009).

Free fatty acids, mainly consisting of C16:0, C16:3, C18:2, and C18:3 accumulate during dark-treatment in *pxa1*, while remaining at low levels in wild-type (Kunz *et al.*, 2009). These fatty acids probably originate from plastid lipid as C16:3 is a specific component of this organelle (Ohlrogge *et al.*, 1991), while C18:3(n-3) and C16:3(n-3) constitute major fatty acids in the chloroplast membrane (Mackender and Leech, 1974). TAG and acyl-CoAs also accumulate in *pxa1* during darkness, while only TAG accumulates in wild-type and to a lesser extent than in *pxa1* (Kunz *et al.*, 2009). The fatty acid profile of accumulated TAG consists mostly of C18:2 and C18:3 and is likely to be derived from plastid lipids.

Two "safety valves" which function to prevent the accumulation of free fatty acids in Arabidopsis have been proposed based on analysis of *pxa1*. They are degradation via β-oxidation, which is disrupted in *pxa1*, and incorporation into TAG, which while increased in *pxa1*, does not accumulate at levels high enough to integrate the free fatty acid pool (Kunz *et al.*, 2009). Energy metabolism in *pxa1* is perturbed as the ATP/ADP ratio is strongly decreased compared to wild-type during extended darkness but this phenotype can be rescued by the supply of sucrose (Kunz *et al.*, 2009). Kunz *et al.* (2009) proposed that the decrease in photosynthetic activity in *pxa1* is due to the amphipathic detergent-like properties of free fatty acids which damage Photosystem II and inhibit the photosynthetic electron transport rate (Vernotte *et al.*, 1983). Mutant seedlings are hypersensitive to exogenous α-linolenic acid (ALA), developing severe leaf bleaching, and this is not prevented by concurrently supplying exogenous sucrose (Kunz *et al.*, 2009).

In *pxa1*, transfer from dark to light results in rapid bleaching due to accumulation of the phototoxic chlorophyll breakdown intermediate pheophorbide A (PhA) and disruptions to chloroplast structure (Kunz *et al.*, 2009). Free ALA leads to degradation of chlorophyll and the accumulation of PhA (Lüthy *et al.*, 1986). Toxic PhA is converted into red chlorophyll catabolite by PhA oxygenase (PAO) (Pruzinská *et al.*, 2007; Pružinská *et al.*, 2003; Tanaka *et al.*, 2003). PAO consumes reductive power in the form of ferridoxin provided by either photosynthesis or the oxidative pentose phosphate pathway. Therefore, *pxa1* accumulates PhA due to impaired catabolism of this intermediate following release from the fatty acid damaged

photosystem, making this accumulation a secondary effect not directly related to the function of β-oxidation (Kunz *et al.*, 2009).

Slocombe *et al.* (2009) reported leaf necrosis and accumulation of TAG in the *cts* mutant in response to extended dark treatment. Diacylglycerol acyltransferase 1 (DGAT1) catalyses the last step of TAG synthesis from acyl-CoA and DAG in the Kennedy pathway and mutants disrupted in this pathway accumulate less seed TAG compared to wild-type (Katavic *et al.*, 1995; Poirier *et al.*, 1999). A *cts dgat1* double mutant has a severe vegetative growth phenotype (Slocombe *et al.*, 2009). This suggests that partitioning of free fatty acids into TAG is essential for plant cell function. LEC2, a seed development transcription factor involved in storage product accumulation, was expressed ectopically during senescence in *cts* resulting in an increase in seed oil type species of TAG in senescing tissue. Such results may ultimately inform biotechnology applications for altering β-oxidation and fatty acid synthesis rates in energy crops (Slocombe *et al.*, 2009).

The *fatty acyl-acp thioesterase b* (*fatb*) mutant, disrupted in plastid acyl-ACP thioesterase activity, has increased rates of fatty acid synthesis and β-oxidation (Bonaventure *et al.*, 2003). Saturated fatty acids are 40-50% lower in the *fatb* mutant compared to wild-type, and mutant plants grow slower. While fatty acid synthesis increases 40% in *fatb*, the proportion of fatty acid per unit fresh weight is maintained at wild-type levels, suggesting a corresponding increase in degradation that has since been confirmed in labelling experiments (Bonaventure *et al.*, 2004). Attempts to isolate *fatb* mutants in the background of β-oxidation mutants such as *cts-2*, *pxa1*, or *kat2*, resulted in embryo lethal phenotypes, confirming the importance of regulating fatty acid breakdown and synthesis (Slocombe *et al.*, 2009).

1.5 Response of peroxisomes and β-oxidation to environment and stress

1.5.1 Clofibrate, salt and drought

Clofibrate (CFB) is a hypolipidemic drug which induces peroxisome proliferation and β-oxidation enzymes (Reddy and Chu, 1996). In Arabidopsis CFB treated plant leaves accumulate *KAT2* transcript and promote peroxisome proliferation (Castillo and León, 2008). Additionally, CFB activates JA-dependent and independent wound related signalling in Arabidopsis (Castillo and León, 2008).

Salt and drought induce ABA accumulation, which by regulating gene expression controls stomatal closure, ion and osmotic homeostasis, growth inhibition, and detoxification pathways (Himmelbach *et al.*, 2003; Zhu, 2002). *KAT2*, *PEX1* and *PEX10* are up-regulated by salt and

ABA treatment in wild-type Arabidopsis but not in the *abi1-1* mutant, with salt induction also disrupted in the *jasmonate resistant 1* (*jar1*) mutant (Charlton *et al.*, 2005b). ABI1 is a protein phosphatase, which acts as a negative regulator of ABA signalling and is transiently inactivated by H_2O_2 (Moes *et al.*, 2008), while JAR1 is a jasmonate:amino-acid synthetase, which generates jasmonyl-isoleucine (JA-Ile) conjugates required for jasmonate signalling (Staswick *et al.*, 2002). Therefore, ABA and JA signalling are implicated in the regulation of the peroxisomal salt-stress response.

Salt stress induces peroxisome proliferation (Mitsuya *et al.*, 2010). In rice (*Oryza sativa*), four members of the PEX11 family are up-regulated by salt treatment (Nayidu *et al.*, 2008). In wild-type Arabidopsis seedlings *PEX11e* is up-regulated by salt, but this response is completely blocked in *abi1-1* (Mitsuya *et al.*, 2010). Salt induction of *PEX11e* requires *JAR1* for part of this transcript response to salt treatment. In response to salt, GFP-labelled peroxisomes increase in abundance in root cells, which, in the absence of a mannitol-response, is most likely due to ionic stress not dehydration (Mitsuya *et al.*, 2010). However, in *PEX11e* over-expressing transgenic plants, in which peroxisomes proliferate, no increased salt tolerance in seedlings or mature plants was observed (Mitsuya *et al.*, 2010). The functional role of β-oxidation and peroxisomes in salt stress response is unknown.

1.5.2 UV and light response

PEX2 is a peroxisomal membrane protein that functions in matrix protein import (Subramani, 1998). In Arabidopsis the *reversal of the det phenotype 3* (*ted3*) dominant mutation altering PEX2 function suppresses *de-etiolated 1* (*det1*) as well as partially suppressing *constitutive photomorphogenic 1* (*cop1*), complementing developmental defects and abnormal global gene expression (Hu *et al.*, 2002). DET1 and COP1 are global repressors of photomorphogenesis, with *det1* and *cop1* mutants developing as if light-grown when grown in darkness (Schwechheimer and Deng, 2000). DET1 and COP1 are both nuclear proteins associated with chromatin (Pepper *et al.*, 1994; Schroeder *et al.*, 2002; von Arnim and Deng, 1994). Mutant analysis of *det1* revealed defective peroxisomes with morphological changes, and the β-oxidation phenotypes of sucrose dependency and IBA resistance (Hu *et al.*, 2002). However, peroxisome function was restored by a single copy of the *ted3* gain-of function mutation and by a *TED3* over-expresser (Hu *et al.*, 2002). Segregation analysis indicated that *ted3* homozygotes were embryo lethal, with RNAi knockdown of *TED3* resulting in small plants with reduced fertility (Hu *et al.*, 2002). Gene expression in *det1* is similar to that of a light stressed seedling, but *ted3* complements most of this misregulation apparently by rescuing peroxisome function (Hu *et al.*, 2002).

Light up-regulates *PEX11b* resulting in peroxisome proliferation (Desai and Hu, 2008; Orth *et al.*, 2007). In *PEX11b* RNAi plants, peroxisomes do not divide or proliferate in the presence of white light (Desai and Hu, 2008). Light induction of *PEX11b* expression is strongly decreased in the photoreceptor mutant *phytochrome A* (*phyA*), with a partial but significant decrease also observed in *hy5 homolog* (*hyh*) (Desai and Hu, 2008; Holm *et al.*, 2002). Peroxisome abundance is lower in *phyA* and *hyh* compared to wild-type, with *PEX11b* over-expressers complementing this peroxisome abundance phenotype (Desai and Hu, 2008). HYH interacts with the promoter of *PEX11b* acting as a direct transcription activator in the presence of light.

There exists some evidence that peroxisomal β-oxidation plays a role in the response of plants to UV stress. An acyl-CoA oxidase has been reported to be induced by UV treatment in parsley (*Petroselinum crispum*), implying an integrated response with primary and secondary metabolism to UV adaption (Logemann *et al.*, 2000). UV affects peroxisome structure, promoting elongation but not proliferation in Arabidopsis cell culture (Lingard and Trelease, 2006). Flavonoids are considered to play a role in protection from UV stress by acting as "molecular sunscreens" (Li *et al.*, 1993). KAT5 has been linked to flavonoid biosynthesis based on co-expression with genes of this pathway (Carrie *et al.*, 2007).

In Arabidopsis subgroup 7 of the Repeat 2-Repeat 3-Myeloblastosis (R2R3-MYB) gene family includes three transcription factors: MYB11, MYB12, and MYB111, all of which have functional similarity and similar target gene specificity towards flavonoid biosynthesis genes such as *CHALCONE SYNTHASE* (*CHS*), *CHALCONE ISOMERASE* (*CFI*), *FLAVANONE 3-HYDROXYLASE* (*F3H*) and *FLAVONOL SYNTHASE 1* (*FLS1*) (Mehrtens *et al.*, 2005; Stracke *et al.*, 2007). A *myb11 myb12 myb111* triple mutant does not synthesise flavonoids but can accumulate anthocyanin, with transcriptome analysis revealing down-regulation of *KAT5* along with many genes of the flavonoid biosynthesis pathway (Stracke *et al.*, 2007). This evidence suggests that not only is *KAT5* co-expressed with genes of flavonoid biosynthesis (Carrie *et al.*, 2007), but that it is also co-regulated with this pathway (Stracke *et al.*, 2007).

The bZIP transcriptional regulator ELONGATED HYPOCOTYL 5 (HY5) is linked to *CHS* gene activity and flavonoid accumulation under visible light and UV-B (Ang *et al.*, 1998; Oravecz *et al.*, 2006). *HY5* is developmentally down-regulated after the first few days of seedlings establishment (Hardtke *et al.*, 2000) but is up-regulated in response to UV-B in a *UV RESISTANCE LOCUS8* (*UVR8*) dependent manner (Brown *et al.*, 2005; Oravecz *et al.*, 2006; Ulm *et al.*, 2004). *KAT5* is down-regulated in *uvr8-6* compared to wild-type in response to UV-B treatment (Favory *et al.*, 2009). No UV-B induced accumulation of flavonol glycosides is

observed in *myb11 myb12 myb111* or *hy5*, with these mutants having reduced tolerance to this stress compared to wild-type (Stracke *et al.*, 2010).

1.6 Aims and Approach

The classical understanding of peroxisomal β-oxidation in oil seeds such as Arabidopsis emphasises the functional role of the pathway in storage lipid breakdown during germination. However, as described in this introduction a growing literature has emerged detailing the involvement of β-oxidation in control of germination and dormancy, light signalling and reproductive success. Therefore peroxisomes and β-oxidation are implicated in many and varied stages of plant development and function. Given these diverse and varied functions, a consolidated approach to elucidating these processes using reverse genetics is vital to further our understanding of peroxisome biology.

Knowledge of the protein content of the peroxisome has grown with advances in genomic sequencing, *in silico* prediction of targeting, and proteomic isolation and analysis of Arabidopsis peroxisomes (Eubel *et al.*, 2008; Reumann *et al.*, 2007; Reumann *et al.*, 2004). Estimates from these studies suggest the total peroxisomal proteome in Arabidopsis is approximately 300 proteins.

For the purpose of understanding novel functions of β-oxidation in Arabidopsis, a priority list of uncharacterised genes with links or similarity to known genes of peroxisomal β-oxidation was compiled for analysis using a reverse genetics approach. These uncharacterised genes consist of acyl-activating enzymes, hydratases, oxidoreductases/dehydrogenases and thiolases. Approximately forty SALK, FLAG, GABI-KAT and CSHL T-DNA insertion lines were obtained from stock centres and screened to homozygosity. As such, the aims of the first component of this project were to:

1. Screen null mutants of *Arabidopsis thaliana* genes predicted to participate in peroxisomal β-oxidation for phenotypes previously described in β-oxidation mutants and for novel phenotypes.
2. Characterise the functions of genes experimentally demonstrated to participate in peroxisomal β-oxidation.

The second part/component of this project involved a focused analysis of the thiolase gene family. Arabidopsis has three thiolase genes, and while KAT2 appears to be the dominant thiolase in β-oxidation for many aspects of plant development (Afitlhile *et al.*, 2005; Castillo *et al.*, 2008; Germain *et al.*, 2001; Hayashi *et al.*, 1998), KAT1 and KAT5 may have specialised roles at different stages of the life cycle (Kamada *et al.*, 2003). *KAT5* for example is up-regulated in flowers and siliques. When this project began, detailed analysis of β-oxidation gene

expression in reproductive tissue had not been attempted. *KAT5* is also novel in the thiolase gene family in that it encodes two isoforms, the cytosolic KAT5.1 and peroxisomal KAT5.2 (Carrie *et al.*, 2007). Additionally, *KAT5* is co-expressed and co-regulated with genes of flavonoid biosynthesis (Carrie *et al.*, 2007; Stracke *et al.*, 2007). Conversely, KAT2 is relatively well characterised with demonstrated functions in metabolism of long-chain fatty acids, and precursors of JA and IAA (Afitlhile *et al.*, 2005; Germain *et al.*, 2001; Hayashi *et al.*, 1998). KAT2 also metabolises membrane lipids during dark-induced senescence (Kunz *et al.*, 2009), and is required for full fertility (Footitt *et al.*, 2007a; Footitt *et al.*, 2007b). Therefore the other aims of the project were to complete:

3. Detailed analysis of thiolase gene expression during germination and reproductive tissue development using promoter reporter genes and qRT-PCR.
4. Genetic characterisation of thiolase single and double mutants to determine functional roles of these genes.

Chapter 2: Materials and Methods

2.1 Arabidopsis growth

2.1.1 Arabidopsis growth on sterile media

The surface sterilisation of Arabidopsis seeds was carried out in a laminar flow. To seed pools ranging in weight from approximately 10-50 mg in 1.5 mL microcentrifuge tubes, 1 mL of sterilisation solution (70% (v/v) ethanol, 0.05% (v/v) Triton X-100) was added, which were mixed continuously by inversion for 5 min. Sterilisation solution was removed and seeds were washed with consecutive solutions of 70% (v/v) and 100% (v/v) ethanol. Ethanol was removed from seeds, with any remaining ethanol evaporating at room temperature in a sterile laminar flow. Seeds were scattered on 0.5 x Murashige and Skoog (MS) growth media (0.22% (w/v) MS, 0.07% (w/v) 2-(*N*-morpholino)ethanesulfonic acid (MES) pH 5.8, 0.8% (w/v) agar) supplemented with 1% (w/v) sucrose, hormones or selective herbicide when required. Seeds were imbibed and stratified for 48 h at 4 °C, and grown under continuous light (~100 µE m^{-2} s^{-1}) at 20 °C.

2.1.2 Soil grown Arabidopsis

Arabidopsis seedlings grown for approximately 10-15 d on MS growth media were transferred to soil in pots sitting in a tray. The soil mix used was 2:1 shamrock peat: vermiculite. Rooms were temperature and humidity controlled, at 22 °C and 60% relative humidity. Day length was varied for experiments as required, using either continuous light (24 h light), long-day (16 h light, 8 h dark) or short-day (8 h light, 16 h dark). Trays of plants were watered as required, on average twice a week. Plants grown to maturity were covered in paper bags when siliques began to dry, to prevent cross contamination and aid seed collection. Seed was collected by hand using a sieve to remove extraneous plant material and stored in microcentrifuge tubes at room temperature.

2.1.3 Hydroponic grown Arabidopsis

Hydroponically grown Arabidopsis was germinated on rock wool plugs inside microcentrifuge tubes suspended in a box of nutrient media as described by Gibeaut *et al.* (1997). Rock wool was used, to provide a well aerated rooting environment and prevent hypoxic stress (Gibeaut *et al.*, 1997), with the nutrient media 0.5 x Hoagland solution (2.5 mM $Ca(NO_3)_2$, 2.5 mM KNO_3, 0.5 mM $MgSO_4$, 0.5 mM KH_2PO_4, 40 mM Fe-EDTA, 25 mM H_3BO_3, 2.25 mM $MnCl_2$, 1.9 mM $ZnSO_4$, 0.15 mM $CuSO_4$, and 0.05 mM $(NH_4)_6Mo_7O_{24}$, pH 5.8) as described previously (Heeg *et al.*, 2008).

2.2 DNA methods

2.2.1 Polymerase chain reaction (PCR)

A typical PCR mix consisted of, 1 x buffer compatible with the enzyme used, 1.5 mM $MgCl_2$, 200 µM dNTPs, 0.2 µM primers and 1 unit of Taq polymerase per 25 µL reaction volume. For PCR requiring a high fidelity polymerase the following mix was used, 1 x Phusion HF, 0.5 µM primers, 200 µM dNTPs, and 1 unit of Phusion DNA Polymerase (Finnzymes) in a total reaction volume of 50 µL. Primer sequences are listed in Appendix I Table. PCR was done using an Eppendorf thermal cycler and various programmes, depending on the template, primer and type of PCR. The QIAquick PCR Purification Kit (Qiagen) was used to purify products, or products were separated on agarose TBE gels, as described below, excised and purified using the QIAquick Gel Extraction Kit (Qiagen).

2.2.2 Restriction enzyme digestion and gel purification

Restriction enzyme digestion was done for a minimum of 90 min using at least 1 unit of enzyme for each µg of DNA in a compatible buffer. Digested products were separated on 0.7-1.5% (w/v) agarose in 1 x TBE (40 mM 2-amino-2-hydroxymethyl-1,3-propanediol (Tris) boric acid, 1 mM EDTA, pH 8.0) gels, depending on the size of the fragments. DNA was purified from agarose TBE gels using the QIAquick Gel Extraction Kit (Qiagen).

2.2.3 Ligation

PCR products (3 µL) synthesised with Taq polymerase and its derivatives so that A (adenine) overhangs were present, were inserted into pCR2.1-TOPO (Invitrogen) according to the manufacturer's instructions. Other DNA fragments were inserted into plasmid vectors possessing compatible ends using 1 unit T4 DNA ligase with 2 x Rapid Ligation Buffer (Promega). In order to prevent self-ligation of a plasmid, shrimp alkaline phosphatase (Roche) was used to dephosphorylate the DNA, according to the manufacturer's instructions. For a table of plasmids and strains used in this thesis see Appendix II.

2.2.4 Preparation of competent *E. coli* cells

Chemically competent *E. coli* DH5α (Sambrook *et al.*, 1989) cells were prepared using the method of Inoue *et al*. (1990). Briefly cells were grown with gentle shaking in 300 mL SOB (2% (w/v) tryptone, 0.5% (w/v) yeast extract, 10 mM NaCl, 2.5 mM KCl, 10 mM $MgCl_2$, 10 mM $MgSO_4$) at 18 °C to an OD at 580 nm of 0.2-0.7. The cells were incubated on ice for 10 min and collected at 3,000 x g for 10 min at 4 °C. Cells were resuspended gently in 80 mL ice cold TB buffer (10 mM piperazine-N,N′-bis(2-ethanesulfonic acid) (PIPES), 15 mM $CaCl_2$, 250 mM KCl, 55 mM $MnCl_2$, pH 6.7) and incubated on ice for 10 min. Cells were again harvested at

3,000 x g for 10 min at 4 °C, resuspended gently in 20 mL of ice cold TB supplemented with 7% (v/v) dimethyl sulfoxide (DMSO), and incubated on ice for 10 min. Aliquots of competent cells were snap-frozen in liquid nitrogen and stored at -80 °C.

2.2.5 Transformation of bacterial cells

Chemically competent *E. coli* DH5α cells (50 µL) were transformed by incubation with 3 µL of ligation solution (described in section 2.2.3) for 30 min on ice, then heat shocked at 42 °C in a water bath for 30 s and then incubated on ice for 2 min (Nishimura *et al.*, 1990). Cells were allowed to recover in 800 µL of liquid SOC medium (2% (w/v) tryptone, 0.5% (w/v) yeast extract, 10 mM NaCl, 2.5 mM KCl, 10 mM $MgCl_2$, 10 mM $MgSO_4$, 20 mM glucose) at 37 °C with shaking at 150 rpm for 60 min. Cells were pelleted and resuspended in 200 µL of SOC before being spread on Luria Bertani (LB) medium (1% (w/v) tryptone, 0.5% (w/v) yeast extract, 0.17 M NaCl) containing 2% (w/v) agar and appropriate selective antibiotic, and incubated overnight at 37 °C. When cells were transformed with pCR2.1-based constructs, they were spread on LB medium as above, in the presence of 50 µL of 240 mM isopropyl β-D-1-thiogalactopyranoside (IPTG) and 4 mg mL^{-1} 5-bromo-4-chloro-3-indol-β-D-galactoside (X-Gal), to allow blue/white colony screening of transformed cells containing inserts.

2.2.6 Plasmid isolation

Transformed *E. coli* cells were grown overnight at 37 °C with shaking at 250 rpm in LB medium containing selective antibiotic. Plasmids were purified using the QuickLyse Miniprep Kit (Qiagen), according to the manufacturer's instructions, resulting in the isolation of 100-200 µg mL^{-1} plasmid DNA. DNA was quantified using a ND-1000 UV-Vis Spectrophotometer (NanoDrop Technologies, Wilmington, DE, USA) from the absorbance at 260 nm.

2.2.7 DNA sequencing

Plasmid DNA was sequenced by the Macrogen sequencing service (Korea; http://dna.macrogen.com/eng/) and analysed using DNAstar (http://www.dnastar.com/).

2.2.8 Genomic DNA isolation

2.2.8.1 Tris-salt extraction

To rapidly genotype large numbers of Arabidopsis T-DNA insertion line mutants a quick, but relatively impure and low yielding DNA isolation protocol was used. Arabidopsis seedlings were grown to between 7-10 d old on MS growth media and then arranged in rows and numbered. A single leaf was removed from each seedling with flame-sterilised scissors. Leaf samples were placed in 200 µL microcentrifuge tubes contained TKE solution (0.1 M Tris-HCl

pH 9.5, 1 M KCl, 0.01 M EDTA) and submerged with a sterile 200 µL pipette tip. The tubes were sealed and incubated in a thermal cycler at 95 °C for 10 min, then chilled to 4 °C. After incubation 60 µL sterile water was added, and samples were stored at -20 °C until further processing. Candidate seedlings of desired genotypes were subsequently confirmed using an alternate DNA extraction protocol (described in 2.2.8.2) resulting in higher quality and yield.

2.2.8.2 Isopropanol precipitation extraction

Approximately 100 mg of Arabidopsis leaf tissue from mature plants was collected in a 2 mL microcentrifuge tube, before adding 500 µL of extraction buffer (0.1 M Tris, 0.05 M EDTA, 0.5 M NaCl, 1% (w/v) polyvinylpyrrolidone (PVP)) and ground using a ball mill at maximum speed (30/s) for 3 min. To the sample 66 µL of 10% (w/v) sodium dodecyl sulfate (SDS) was added, mixed gently by inversion, and incubated at 65 °C for 15 min. Samples were centrifuged at maximum speed for 10 min. The supernatant (approximately 550 µL) was removed to a 1.5 mL tube to which 166 µL of 5 M potassium acetate pH 5.8 was added with mixing by inversion. The sample was centrifuged at maximum speed for 15 min, and the supernatant was transferred in to a 1.5 mL tube. 500 µL isopropanol was added and mixed by inversion. Samples were incubated at -20 °C for 30 min to precipitate DNA, before centrifugation at maximum speed for 15 min. The isopropanol was removed and 500 µL of 70% (v/v) ethanol added, and mixed gently by inversion to wash the DNA pellet. Samples were centrifuged at maximum speed for 5 min. The ethanol was removed from the sample and the DNA pellet was air dried at room temperature before suspension of DNA in 50 µL TE buffer. DNA samples were stored at -20 °C until further processing.

2.3 RNA methods

2.3.1 RNA isolation

Total RNA was isolated from approximately 100 mg of tissue using the Aurum Total RNA Mini kit, according to the manufacturer's instructions. RNA quantity and quality was determined using a ND-1000 UV-Vis Spectrophotometer (NanoDrop Technologies, Wilmington, DE, USA) from the absorbance at 260 nm and 280 nm.

2.3.2 Synthesis of complementary DNA (cDNA)

RNA (1 µg) was synthesised into cDNA using an iScript cDNA Synthesis kit (BioRad), according to the manufacturer's instructions.

2.4 *Agrobacterium* transformation of Arabidopsis

2.4.1 Preparation of competent *Agrobacterium* cells

Agrobacterium tumefaciens strain GV3101 (Koncz and Schell, 1986) cultures were grown overnight at 28 °C in LB medium supplemented with 100 µg mL^{-1} rifampicin and 10 µg mL^{-1} gentamycin to an OD at 680 nm of 0.5-1 (Hofgen and Willmitzer, 1988). Cultures were chilled on ice, and then briefly centrifuged at 1500 rpm to remove cell clumps. The suspension of cells was transferred to a centrifuge tube on ice. Cells were centrifuged at 3000 rpm for 6 min at 4 °C, and the resulting pellet was resuspended in 1 mL of ice cold 20 mM $CaCl_2$ per 50 mL of original Agrobacterium culture. 200 µL aliquots of competent Agrobacterium were snap frozen in liquid nitrogen and stored at -80 °C.

2.4.2 Transformation of *Agrobacterium* cells

For transformation of Agrobacterium cells the freeze-thaw method was used (Hofgen and Willmitzer, 1988). 200 µL aliquots of competent Agrobacterium were thawed on ice, before adding 5-10 µL (1 µg) of plasmid. The cells were frozen in liquid nitrogen and then thawed in a 37 °C water bath for 5 min. To each tube of competent cells 1 mL LB medium was added with mixing by pipetting and inversion. Cells were incubated at 28 °C with gentle shaking for 2-4 h to recover. Cells were resuspend in 100 µL LB before being spread on LB medium containing 2% (w/v) agar, 100 µg mL^{-1} rifampicin, 10 µg mL^{-1} gentamycin and 50 µg mL^{-1} kanamycin (or other selective antibiotic), and incubated at 28 °C for 2-3 d.

2.4.3 Arabidopsis floral dip transformation

Arabidopsis was transformed with Agrobacterium using the floral dip method (Clough and Bent, 1998). Healthy flowering Arabidopsis plants were prepared for transformation by removal of the primary bolt and waiting 4-6 d to encourage proliferation of meristems. Before floral dipping, green siliques were removed from plants. Agrobacterium containing the plasmid for transformation were grown overnight in 500 mL LB medium containing 100 µg mL^{-1} rifampicin, 2.5 µg mL^{-1} gentamycin and 50 µg mL^{-1} kanamycin with shaking at 28 °C until reaching an OD at 580 nm of 0.8. Agrobacterium cultures were centrifuged at 5000 rpm for 10 min and then resuspend to an OD at 580 nm of 0.8 in a solution of 5% (w/v) sucrose. Just prior to dipping with the Agrobacterium-sucrose solution, 0.01% (v/v) silwet L-77 was added and mixed gently by inversion. Arabidopsis flowers were dipped into the Agrobacterium solution for 10 s, and the removed and covered with bags for 24-48 h. After incubation the bags were removed and plants were watered. Once siliques from dipped flowers reached maturity, watering was ceased and plants were allowed to dry out.

2.5 Auxin mutant characterisation

2.5.1 Identification of auxin mutants and plant growth

SALK (Alonso *et al.*, 2003), FLAG (Samson *et al.*, 2004), GABI-Kat (Rosso *et al.*, 2003), and CSHL (Sundaresan *et al.*, 1995) T-DNA lines were obtained from stock centres and screened to homozygosity using PCR-based methods to check for the presence of the T-DNA insertion. When available, multiple alleles per gene were ordered to determine if the mutant phenotype was related to the insertion or due to disruption of an unrelated gene. Primer design utilised the T-DNA Express primer design server (http://signal.salk.edu/tdnaprimers.2.html). RT-PCR primers were designed to bound the insertion sites and used to screen each line for the absence of full-length transcript as an indicator that they were transcript knockouts (Table 3.1). For seed germination and growth assays, 0.5 x MS media (Sigma) was buffered with 0.07% (w/v) MES, solidified with 0.8% (w/v) agar and supplemented with 1% (w/v) sucrose and hormones as indicated. Seed were imbibed on plates at 4 °C for 48 h prior to assays. All *in vitro* assays were conducted at 22 °C under continuous white light (~120 μE m^{-2} s^{-1}). All knockout lines were initially screened for root elongation on 1 μM 2,4-DB (as an indicator of resistance). They were also screened for defects in etiolation in the absence of sucrose (as described below).

2.5.2 Mutant characterisation

Knockout lines that displayed resistance to 2,4-DB were further characterised by dose responses to 2,4-DB and IBA. They were grown for 6 d on media supplemented with 1% (w/v) sucrose and 0, 0.5, 1, 2 or 4 μM 2,4-DB or with 0, 5, 10 or 20 μM IBA. In addition, response to active auxins was assayed using media containing 100 nM NAA, 50 nM 2,4-D or 100 nM IAA. IAA and IBA containing plates as well as controls for those experiments were incubated under yellow filters (Lee filter 101) to reduce the photochemical degradation of indole containing compounds (Stasinopoulos and Hangarter, 1990). Lateral root assays were conducted by growing seedlings for 3 d on media containing 0.5 × MS and 1% (w/v) sucrose. Seedlings were then transferred to similar media supplemented either with no hormone, 5 μM IBA or 80 nM NAA and the number of lateral roots was counted 2 and 3 d after transfer. Etiolation was assessed by sowing seeds to 0.5 × MS media containing either 1% (w/v) or no sucrose, exposing them to light for 6 h, then transferring to the dark. Hypocotyl lengths were measured after 4 d dark growth. Digital photographs were taken of assay plates and Image J (Research Services Branch, NIH) was used to measure root and hypocotyl lengths. All root and hypocotyl measurement experiments were conducted at least twice and means were calculated on least 15 seedlings. Single experiments are depicted in the results.

2.6 Fatty acid analysis

For fatty acid analysis a modified version of the protocol described by Browse *et al*. (1986). Plant tissue (approx. 100 mg, or 10 mg for dry seed) was snap-frozen in liquid nitrogen, ground into a fine powder and extracted with 400 μL isopropyl alcohol (containing 0.01% (w/v) BHT (2,6-di-tert-butyl-4-methylphenol) as an antioxidant) at 75 °C for 15 min. 50 μg of C19:0 fatty acid was added as an internal standard to each sample before the extraction. After cooling down to room temperature 600 μL of n-hexane was added to the tube and the mixture sonicated for 5 min. The isopropyl alcohol-hexane mixture was separated from the cell debris and 500 μL was dried under vacuum. The fatty acids in the extract were converted to their methyl esters by heating at 80 °C for 2 h in 300 μL of methanol with 2.0% (v/v) H_2SO_4. After cooling to room temperature and mixing with 300 μL of 0.9% (w/v) NaCl, fatty acid methyl esters were extracted with 300 μL of n-hexane for GC-MS analysis.

GC–MS analysis utilised an Agilent 6890GC coupled with 5795 mass selective detector. The temperature program was: initial temperature 1 min at 70 °C; temperature was then ramped to 76 °C at 1 °C/min, then ramped to 325 °C at 6 °C/min and held at 325 °C for 10 min. The GC capillary column used for analysis was Varian factor 4 (VF-5 ms, 30 M × 0.25 mm ID and 0.25 μm film). Fatty acid peak areas were normalized to that of the internal standard and the weight of starting tissue to yield mg/g fresh weight for each fatty acid.

2.7 GFP localisation

GFP fusions of SDRa and AAE18 were constructed according to a modification of the fluorescent tagging of full-length proteins (FTFLP) method of Tian *et al.* (2004). FTFLP introduces GFP into genomic clones (including native promoters and terminators) in a position corresponding to approximately 10 amino acids from the C-terminus and enables analysis of spatial and temporal localisation of proteins during plant development. The position close to the C terminus largely avoids structural and functional protein domains and preserves both N- and C- terminal targeting sequences and membrane anchoring signals in full-length proteins (Tian *et al.*, 2004). We adapted the method for use in transient expression assays. Thus, GFP was inserted within a stretch of hydrophilic residues close to the C-terminus but this was done using coding sequence alone and driven by 35S promoter.

Enhanced GFP (eGFP) was amplified including adapters as described by Tian *et al*. (2004). The N-terminal portions of SDR and AAE18 were amplified from total cDNA using appropriate 25-mer primers (primers P1 and P2). Oligos P3 and P4, corresponding to the C-terminal 10 amino acids (AAE18) and 13 amino acids (SDRa) plus the stop codon of the protein (i.e. 33–42 nucleotides), were synthesised to comprise a template for direct inclusion in a second round of PCR. For primer sequences see Apendix I. Primers P1 and P4 included adapters to enable

amplification by universal primers. Primers P2 and P3 had adapters that overlapped with those bounding the GFP fragment. Three-template PCR (TT-PCR) thus included three overlapping templates (the P1–P2 bound fragment, GFP and P3–P4 oligo) and used universal primers with attB cloning sequences. Universal primers and adapters are as described in Tian *et al.* (2004). TT-PCR products were cloned into Gateway vector pDONR207 and sequenced to check PCR accuracy. The GFP constructs were then introduced into a pGREEN (Hellens *et al.*, 2000) vector modified for Gateway. We used pGREEN0179 containing CAMV 2x35S promoter and CAMV terminator with the Gateway A cassette inserted between them in the SmaI site of the pGREEN multiple cloning site (Pracharoenwattana *et al.*, 2005). For colocalisation studies pGREEN0049-RFP-SRL (Pracharoenwattana *et al.*, 2005) was used as a peroxisomal marker.

Plasmids were precipitated onto 1 μm gold particles and biolistically transformed into onion epidermal peel as described in Thirkettle-Watts *et al.* (2003). Fluorescence images were obtained using Olympus BX61 epifluorescence microscope with GFP (U-MGFPHQ) and RFP filters (U-MRFPHQ) and manipulated with CellR software.

2.8 Expression analysis

2.8.1 GUS promoter reporter analysis

Thiolase gene promoter activity was assayed *in planta* using the GUS/GFP reporter fusion vector pHGWFS7 (Karimi *et al.*, 2002). Promoter regions including the non-coding sequence and intergenic DNA upstream of the start codon were amplified by PCR with primers including attB sites for Gateway cloning. *KAT1* promoter was approximately 1 kb whereas *KAT2* and *KAT5* were approximately 2 kb. Amplification products were gel purified (QIAGEN) and recombined into pDONR207, which in turn was transformed into DH5α *E. coli* and selected on 10 μg mL^{-1} gentamycin. Plasmids containing the pDONR207 *KAT* promoters were isolated from *E. coli* and sequenced. *KAT* promoters were recombined from pDONR207 into pHGWFS7, and then transformed into *E. coli* selected on 50 μg mL^{-1} spectinomycin. The pHGWFS7 *KAT* promoter vectors were transformed into Agrobacterium and selected for on 100 μg mL^{-1} rifampicin, 10 μg mL^{-1} gentamycin and 50 μg mL^{-1} spectinomycin. Agrobacterium harbouring the pHGWFS7 *KAT* promoter vectors were used to transform Arabidopsis Col-0 plants using floral dip. Transformed Arabidopsis plants were screened to homozygosity over three generations using selection on 25 μg mL^{-1} hygromycin.

Transformed Arabidopsis plants were grown for GUS staining under continuous light conditions to control for diurnal regulation of promoter activity. Seedlings were grown on 0.5 x MS media in the absence of sucrose and, flowers and siliques were removed from 6 week old soil grown plants. GUS staining was done using the protocol described in Arabidopsis: A

Laboratory Manual (Weigel and Glazebrook, 2002). Tissue samples were stored in 90% (v/v) acetone on ice and then fixed at room temperature for 20 min. Samples were washed three times with 0.05 M sodium phosphate buffer (pH 7.2) to remove acetone. Staining buffer (0.05 M sodium phosphate buffer (pH 7.2), 0.2% (v/v) Triton X-100, 2 mM $K_4[Fe(CN)_6]$, 2 mM $K_3[Fe(CN)_6]$ and 5mM X-Gluc in DMSO) was prepared fresh from stock solutions before staining. Staining buffer was added to samples on ice, and then incubated overnight at 37 °C. After incubation, staining buffer was removed, and the stained samples were preserved using an ethanol series of 20%, 35%, 50% and 70% (v/v) ethanol in water with 30 min incubation for each concentration. Stained samples were stored in 70% (v/v) ethanol at 4 °C, before being viewed using an Olympus S2X7 microscope. Photographs of representative samples were taken with an Olympus ColorView IIIu camera and the accompanying analySIS getIT software.

2.8.2 Quantitative RT-PCR

Aerial tissue samples were taken from 5 week old soil grown plants grown under continuous light conditions and root samples were taken from hydroponically grown plants. Approximately 100 mg of Arabidopsis leaves, roots, stems, flowers or siliques were ground into a fine powder with a mortar and pestle pre-cooled with liquid nitrogen. Ground tissue was stored at –80 °C until processing. RNA was isolated using Aurum BioRad kit to manufacturer's specification. RNA quality and quantity was assessed by spectrophotometric analysis of the A260/A280 ratio using an ND-1000 UV-Vis Spectrophotometer (NanoDrop Technologies, Wilmington, DE, USA). RNA was treated with Turbo DNA-free (Ambion) and subsequently converted to cDNA using the iScript cDNA Synthesis Kit (Bio-Rad). Primer pairs for qRT-PCR were designed using Primer3 ((Rozen and Skaletsky, 2000); http://frodo.wi.mit.edu/), and for *KAT1* and *KAT2* were designed across introns. Due to the similarity of the *KAT5.1* and *KAT5.2* sequences, primers were designed in the respective 5' UTRs and therefore could not bound introns. Primer sequences are listed in the Appendix I Table. qRT-PCR was performed on a Roche LC480 using LightCycler 480 SYBR Green I Master (Roche). Cycle conditions were: 95 °C for 10 min; 45 cycles of 95 °C for 20 s, 60 °C for 20 s, and 72 °C for 20s. Melt curve analysis of real-time PCR products was performed to ensure clean amplification. Crossing point values were calculated under high confidence. Three biological replicates per tissue sample were examined, with at least two technical replicates of each real-time PCR. The average crossing point value of two technical replicates was used to calculate expression relative to an internal reference gene adjusted by primer efficiencies. Two reference genes were tested: *ACT2* (At3g18780) and clathrin adaptor complex subunit (*CACS*; At5g46630) identified by Czechowski *et al.* (2005) as a more suitable reference gene for transcript normalisation. For analysis *CACS* used as it was determined to be stabler than *ACT2*; the average relative expression and standard error for the three biological replicates are shown.

2.9 Thiolase (*kat*) mutant characterisation

For characterisation of thiolase gene function the following mutants were used: *kat1*, *kat2-1*, *kat2-2* and *kat5-1* described in Chapter 3, along with *kat2-4* (L*er*, CSHL_GT18614), *kat2-5* (Ws-4, FLAG_307C02), *kat5-2* (Ws-4, FLAG_065D06) and *kat5-3* (Col, SAIL_567_F03). The recently described *kat2-3* allele (Jiang *et al.*, 2011), was not used in this study. Primer design utilised the T-DNA Express primer design server (http://signal.salk.edu/tdnaprimers.2.html). RT-PCR primers were designed to bound the insertion sites and used to screen each line for the absence of full-length transcript as an indicator that they were transcript knockouts. Double mutants described in Chapter 5 were generated from these single mutants by crossing and selection using PCR-based screening for homozygosity of T-DNA insertions. Independent alleles for single and double mutants were used in experiments to ensure that phenotypes observed were the result of disruption to thiolase gene function and not the result of secondary insertions. As the *kat2-1 kat5-2* double mutant is infertile, plants were genotyped from pools of seedlings homozygous for one mutation and heterozygous for the other.

Measurement of resistance to a range of 2,4-DB concentrations and etiolated hypocotyl extension length were conducted as described for Auxin mutant characterisation (Section 2.5.2). Germination frequency was assayed using seed after ripened for at least 8 weeks after harvest from parent plants. Approximately 250 to 300 seeds were scattered on water agar (0.8% (w/v)) media and immediately placed under growth lights with no stratification. Seeds were allotted into 20 groups of 10 seeds and scored for germination every 24 h. This procedure was repeated four times. For pedigree analysis of segregating *kat2-1* and *kat5-2* alleles, seedlings were grown on 0.5 x MS media containing 1% (w/v) sucrose and genotyped after 10 d growth. A Chi square test of deviation from expected segregation ratio was calculated using Excel.

For seed weight and fatty acid analysis, seed was harvested from soil-grown plants under long-day or continuous light conditions. From each plant between 500 and 600 seeds were counted and weighed. For fatty acid analysis, counted and weighed pools of seed (approximately 10 mg) were extracted and measured by GC-MS using the protocol described in fatty acid analysis.

Anthers were removed from Arabidopsis flowers and the pollen stained on microscope slides using the Alexander stain technique (Alexander, 1969). Pollen was covered with a few drops of Alexander stain solution (9.5% (v/v) ethanol, 25% (v/v) glycerol, 2% (v/v) glacial acetic acid, 5% (w/v) phenol, 0.05% (w/v) malachite green, 0.05% (w/v) fuchsin acid, 0.005% (w/v) orange G), and flamed without boiling. An Olympus BX51 microscope was used for visualisation, with the same camera and software described for GUS visualisation.

For flavonoid mutant phenotype characterisation seeds were imbibed for 24 h in water, then stained with 0.25% (w/v) diphenylboric acid 2-aminoethyl ester (DPBA) for 15 min. The seed coat was removed, and embryos were view using an Olympus BX61 epifluorescence microscope with a FITC filter. To assay disruption to the seedling light signalling hypocotyl response, seeds were stratified for 72 h at 4 °C in the dark, and then placed at room temperature under white light for 3 h before another 21 h of dark. Seedlings were then grown for 96 h either in the dark or using red or blue light, after which hypocotyl length was measured.

2.10 Complementation of the *kat2-1 kat5-2* double mutant

KAT5.1 and *KAT5.2* cDNAs were amplified using Phusion high fidelity polymerase from cDNA isolated from mature rosette leaf RNA using the primers (see Appendix I table: *KAT5.1* and *KAT5.2* cDNA primers) and the PCR program (98 °C 30 s; 35 cycles 98 °C 30 s, 55 °C 30 s, 72 °C 90 s; 72 °C 10 m; 4 °C hold). *KAT5.1* and *KAT5.2* cDNAs were PCR purified. As high fidelity polymerase does not add adenine tails required for TOPO cloning, they were added using the following protocol: 30 µL of clean PCR reaction, 250 µM dATP, 1 x Optimized DyNAzyme Buffer, and 1 unit DyNAzyme II DNA polymerase in a total reaction volume of 40 µL, incubated in a thermal cycler at 72 °C for 20 min, with a 4 °C hold. Adenine tailed *KAT5* cDNAs were ligated into the pCR2.1-TOPO vector, and the resulting ligation mix was transformed into TOPO10F' *E. coli* cells with the transformation protocol previously described using 50 µg mL^{-1} kanamycin, X-gal, and IPTG for blue/white colony screening. pCR2.1-KAT5 plasmids were isolated, and the insertions sequenced to confirm correct sequence.

The *KAT5* cDNAs were then introduced into a pGREEN (Hellens *et al.*, 2000) vector modified for overexpression. We used pGREEN0179 containing CAMV 2x35S promoter and CAMV terminator inserted in the SmaI site of the pGREEN multiple cloning site (Pracharoenwattana *et al.*, 2005). We named this modified vector pGREEN0180. As no restriction enzymes sites were available for directional cloning of *KAT5* cDNAs from pCR2.1-KAT5 into pGREEN0180, insertions were subcloned using *Eco*RI. Following restriction enzyme digest of ~1 µg pCR2.1-KAT5.1, pCR2.1-KAT5.2, and pGREEN0180 with *Eco*RI, DNA fragments were gel separated and extracted. The linearised gel extracted pGREEN0180 was SAP dephosphorylated. *KAT5.1* and *KAT5.2* cDNAs were ligated into pGREEN0180 and transformed into DH5α cells, plated on LB with 50 µg mL^{-1} kanamycin. Minipreps of pGREEN0180-KAT5.1 and pGREEN0180-KAT5.2 were isolated, and digested with *Eco*RV and *Bam*HI to confirm insertion orientation. Agrobacterium transformants of pGREEN0180-KAT5.1 and -KAT5.2 were selected with 100 µg mL^{-1} rifampicin, 10 µg mL^{-1} gentamycin and 50 µg mL^{-1} kanamycin.

As the *kat2-1 kat5-2* double mutant is infertile, plants that were transformed by floral dip were heterozygous for either the *kat2-1* or *kat5-2*. Seedlings resistant to 25 µg mL^{-1} hygromycin were assumed to contain the transgene and were genotyped to ensure persistence of the *kat2-1* or *kat5-2* segregating allele in either the heterozygous or homozygous state.

2.11 Analysis of data from publicly available databases

Genevestigator ((Zimmermann *et al.*, 2004); genevestigator.com) was interrogated for publicly available transcriptome data of genes of interest. Similarly the Bio Array Resource for Plant Biology (BAR; available at bar.utoronto.ca), specifically the Arabidopsis EFP Browser (Winter *et al.*, 2007) and Arabidopsis Interactions Viewer (Geisler-Lee *et al.*, 2007) were accessed for experimental transcriptome data and *in silico* predicted interactome data respectively. Gene co-expression was determined using ATTED-II v6 ((Obayashi *et al.*, 2007); atted.jp) which determines co-expression from publicly available transcriptome data.

Promoter sequences were analysed informatically using Athena ((O'Connor *et al.*, 2005); bioinformatics2.wsu.edu/cgi-bin/Athena) and the database of Plant Cis-acting Regulatory DNA Elements (PLACE; (Higo *et al.*, 1999); dna.affrc.go.jp/PLACE/index.html).

Thiolase gene sequences were retrieved from the collection of sequenced plant genomes at Phytozome v6.0 (phytozome.org) and individually submitted sequences from NCBI (ncbi.nlm.nih.gov). Multiple sequence alignment of predicted protein sequences was conducted using the ClustalW2 algorithm (ebi.ac.uk/Tools/msa/clustalw2). Phylogentic tree of this multiple sequence alignment was visualised using the TreeView program ((Page, 1996); available at taxonomy.zoology.gla.ac.uk/rod/treeview.html).

Chapter 3: Identification of two Arabidopsis genes encoding a peroxisomal oxidoreductase-like protein and an acyl-CoA synthetase-like protein that are required for responses to pro-auxins

The following chapter is a published research article, reproduced as published except for references and methods, which are included in the respective sections of this thesis.

Plant Mol Biol. 2009 Mar;69(5):503-15. Epub 2008 Nov 29.

3.1 Introduction

Plant peroxisomes play a central role in energy metabolism. They house β-oxidation reactions that metabolise fatty acids to produce energy and work in concert with mitochondria and chloroplasts in photorespiration. Nevertheless, peroxisomal function is relatively poorly characterised. Proteome studies (Reumann *et al.*, 2007) in combination with *in silico* predictions (Kamada *et al.*, 2003; Reumann *et al.*, 2004) indicate that plant peroxisomes may contain up to 300 proteins. The subcellular localisation of many of these remains unconfirmed. Of those that have been localised to peroxisomes and functionally characterised, the majority are involved in β-oxidation (Baker *et al.*, 2006; Goepfert and Poirier, 2007). Other proteins contribute to protein import, photorespiration, or oxidation of specific substrates in reactions that evolve oxygen radicals (Baker and Sparkes, 2005; Reumann *et al.*, 2004; Reumann and Weber, 2006).

In Arabidopsis, up to 70 proteins are predicted to have similarity to core or auxiliary β-oxidation enzymes (Reumann *et al.*, 2004). The core β-oxidation pathway metabolises saturated long chain fatty acids to supply energy during seed germination and seedling establishment. The pathway includes five steps (Baker *et al.*, 2006): (1) CoA activation by acyl-activating enzymes/long chain acyl-CoA synthetases (LACS6 and LACS7); (2) oxidation by acyl-CoA oxidases (ACX1-4), (3) hydration by enoyl-CoA hydratase/isomerase; (4) oxidation by a dehydrogenase (steps 3 and 4 mediated by multifunctional proteins AIM1 and MFP2); (5) thiolytic cleavage of acetyl-CoA and release of an acyl-CoA shortened by 2C (catalysed by a 3-ketoacyl-CoA thiolase (KAT1, 2 or 5). Citrate synthase then utilizes acetyl-CoA and oxaloacetate in synthesis of citrate (Baker *et al.*, 2006). Other substrates, such as unsaturated fatty acids and hormone precursors may be metabolised by a variety of auxiliary enzymes before being fed into the pathway at various points. Alternatively, depending on the substrates, different isoforms may substitute for core enzymes' activities (Baker *et al.*, 2006; Goepfert and Poirier, 2007). For example the jasmonic acid (JA) precursor 3-oxo-2-(2'-pentenyl)-cyclopentane-1-octanoic acid (OPC:8) is activated by 4-courmate-CoA ligase (4-CL)-like enzymes (Kienow *et al.*, 2008; Schneider *et al.*, 2005) before entering β-oxidation and indole-3-butyric acid (IBA) is initially oxidized preferentially by IBR3 and ACX3 (Zolman *et al.*, 2007).

Classic indicators of defects in β-oxidation include dependence on exogenously supplied carbon sources, such as sucrose, for seedling establishment and resistance to pro-auxins such as 2,4-dichlorophenoxybutyric acid (2,4-DB) and IBA. In wild-type plants, biologically inactive 2,4-DB is metabolized by one cycle of β-oxidation to the active auxin 2,4-dichlorophenoxyacetic acid (2,4-D). Similarly, IBA is metabolised by a cycle of β-oxidation to indole-3-acetic acid (IAA). Primary root elongation is inhibited by both 2,4-D and IAA.

B-oxidation mutants display root elongation on 2,4-DB and IBA, but not on 2,4-D and IAA (Baker *et al.*, 2006). In this study a reverse genetic approach was used to elucidate roles for auxiliary enzymes of β-oxidation. Uncharacterised, putatively peroxisomal acyl-activating enzymes, hydratases, dehydrogenases and thiolases were screened for sucrose dependence and 2,4-DB resistance. Using these assays, two new proteins were identified with roles in β-oxidation, including the first acyl-activating enzyme required for auxin response.

3.2 Results

3.2.1 Isolation of 2,4-DB resistant mutants

Genes encoding predicted peroxisomal proteins with similarity to known β-oxidation proteins were selected for reverse genetic analysis. These included uncharacterised acyl-activating enzymes, hydratases, dehydrogenases/oxidoreductases and thiolases (Table 3.1). Homozygous mutants were isolated from one ethyl methanesulfonate (EMS) mutagenesis (*kat2-2*) and 37 T-DNA lines representing 20 genes. Of the T-DNA lines, RT-PCR confirmed 23 lines from 17 genes to be lacking full-length transcripts (Table 3.1; Figure 3.1). The transcript knockout lines so obtained are listed in Table 3.1 by their allelic designations. *kat2-2* is a new Col-0 EMS mutant for this gene originally identified in a screen for sucrose dependent mutants (Eastmond, 2006). *kat2-2* was backcrossed twice and sequenced, revealing the lesion to be S140F (TCT→ TTT), a change that presumably affects protein topology near the catalytic Cys138 residue (see (Sundaramoorthy *et al.*, 2006)). *kat2-1* is in Ws-4 background (Germain *et al.*, 2001).

Mutants listed in Table 3.1 were screened for resistance to pro-auxins 2,4-DB and IBA. Screening of homozygous lines on 1 μM 2,4-DB yielded two new 2,4-DB resistant mutants, *sdra* and *aae18*. (Figure 3.2). SDRa is a short chain dehydrogenase/reductase family protein and AAE18 an acyl-activating enzyme (acyl-CoA synthetase) family protein. When screened on 10 μM IBA, the two *sdra* alleles were resistant to IBA, but all three *aae18* alleles were sensitive (Figure 3.2). No further new IBA resistant mutants were revealed amongst the lines listed in Table 3.1. A new mutant allele of *CHY1*, *chy1-4*, was also characterised. It is similar to previously characterised strong alleles of *CHY1*, which are highly resistant to pro-auxins (Lange *et al.*, 2004; Zolman *et al.*, 2001a; Zolman *et al.*, 2001b). Similarly, *ibr3-9* was obtained and characterised, to be used as a partially resistant control (see Zolman *et al.*, 2007). Both of the *sdra* alleles and two of the *aae18* alleles were subsequently characterised in detail, for auxin response and other characteristics.

Table 3.1. T-DNA lines obtained for the study. The assignment of an allelic designation indicates lines for which RNA was absent in homozygotes (except *kat2-2* which is an EMS-derived line). The nomenclature follows Shockey *et al.* (2003) for acyl-activating enzyme (AAE) proteins and Reumann *et al.* (2007) for the hydratase/ isomerase (ECHI) and short chain dehydrogenase/ reductase (SDR) proteins. Peroxisome targeting signals (PTS) were obtained from Reumann *et al.* (2004). HO = homozygous mutant.

Gene	PTS	Line	Allele	Ecotype	Reference/notes
Acyl-activating enzymes					
AAE1 (At1g20560)	-SKL	SALK_041152	*aae1-1*	Col	
AAE5 (At5g16370)	-SRM	SALK_009731	*aae5-1*	Col	
AAE7/ACN1 (At3g16910)	-SRL	SALK_123943		Col	Transcript present in HO
		SALK_133808		Col	Transcript present in HO
AAE12 (At1g65890)	-SRL	GABI_751B10	*aae12-1*	Col	
AAE17 (At5g23050)	-SKL	SALK_025667	*aae17-1*	Col	
		SAIL_83_E04		Col	Transcript present in HO
		FLAG_290G07		Ws-4	Transcript present in HO
AAE18 (At1g55320)	-SRI	SALK_002180	*aae18-1*	Col	
		SALK_019869	*aae18-2*	Col	
		SAIL_445_F06	*aae18-3*	Col	
Putative AAE/BZO1 (At1g65880)	-SRL	SALK_094196	*bzo1-4*	Col	Benzoyl-CoA ligase (Kliebenstein *et al*. 2007)
		GABI_565B09	*bzo1-5*	Col	
Hydratases					
ECHIa/E-COAH-2 (At4g16210)	-SKL	SALK_004620	*echia-1*	Col	
		SALK_024138	*echia-2*	Col	
ECHIb/PECI2 (At4g14430)	-PKL	FLAG_412H03		Ws-4	No insertion in At4g14430
ECHIc/PECI1 (At1g65520)	-SKL	SALK_036386	*echic-1*	Col	
		SAIL_520_D11		Col	Transcript present in HO
		SAIL_100_C05		Col	Transcript present in HO
ECHId/DHNS (At1g60550)	RL(X_5)HL	SAIL_1303_605		Col	Transcript present in HO; Unlikely to be peroxisomal (Kim *et al*. 2008)
MFP2 (At3g06860)	-SRL	SALK_098016	*mfp2-2*	Col	Rylott *et al*. (2006)
Oxidoreductases					
SDRa (At4g05530)	-SRL	SALK_010364	*sdra-1*	Col	
		CSHL_ET10416	*sdra-2*	Ler	
		SALK_042943		Col	Ambiguous genotyping
		SALK_042934		Col	Ambiguous genotyping
SDRb/DECR (At3g12800)	-SKL	SALK_122758	*decr-1*	Col	
		SALK_013922		Col	Transcript present in HO
NQR (AT1g49670)	-SRL	SALK_116822	*nqr-1*	Col	
		SALK_123841	*nqr-2*	Col	
		SALK_014601		Col	Transcript present in HO

Table 3.1 ctd.

Gene	PTS	Line	Allele	Ecotype	Reference/notes
Thiolases					
KAT2 (At2g33150)	RQ(X_5)HL	T-DNA	*kat2-1*	Ws-4	Germain *et al*. (2001)
		EMS (S140F)	*kat2-2*	Col	
KAT1 (At1g04710)	RQ(X_5)HL	FLAG_589G05	*kat1-1*	Ws-4	
		SALK_013834		Col	Transcript present in HO
KAT5 (At5g48880)	RQ(X_5)HL	CSHL_ET5406	*kat5-1*	Ler	
		SALK_144464		Col	Transcript present in HO
Other					
IBR3 (At3g06810)	-SKL	SALK_033467	*ibr3-9*	Col	Zolman *et al*. (2007)
CHY1 (At5g65940)	-AKL	SALK_025417C	*chy1-4*	Col	

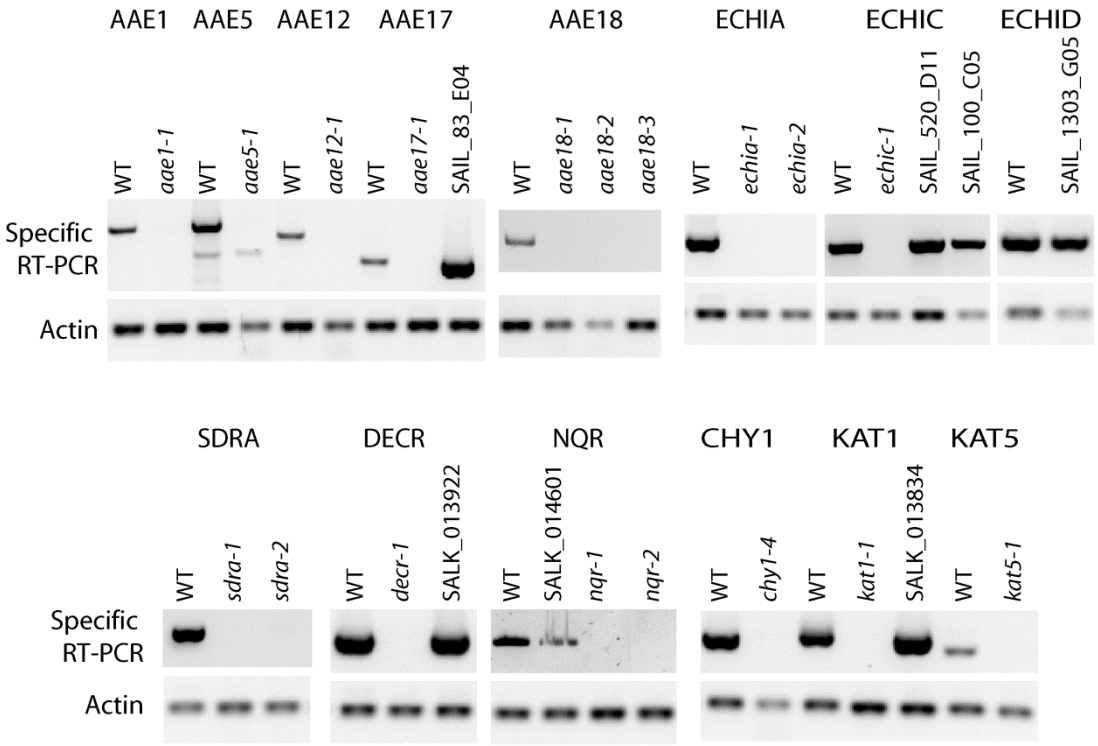

Figure 3.1. RT-PCRs of new T-DNA lines reported in this study.

RNA was isolated using Biorad Aurum RNA isolation kit. RT utilised Biorad iScript. Where insertions interrupted putative transcripts, primers were designed to anneal to transcribed sequences bounding the insertion sites. In cases of insertions in UTRs, 300-400bp, amplicons were designed using primer3. RT-PCR of *ACTIN2* was used as a control. Lines are assumed to be knockouts if transcript was absent; knockouts are indicated by allelic designation if transcript was absent and by their name if transcript remained in the line. AGIs, and a full list of alleles and T-DNA names can be found in Table 3.1.

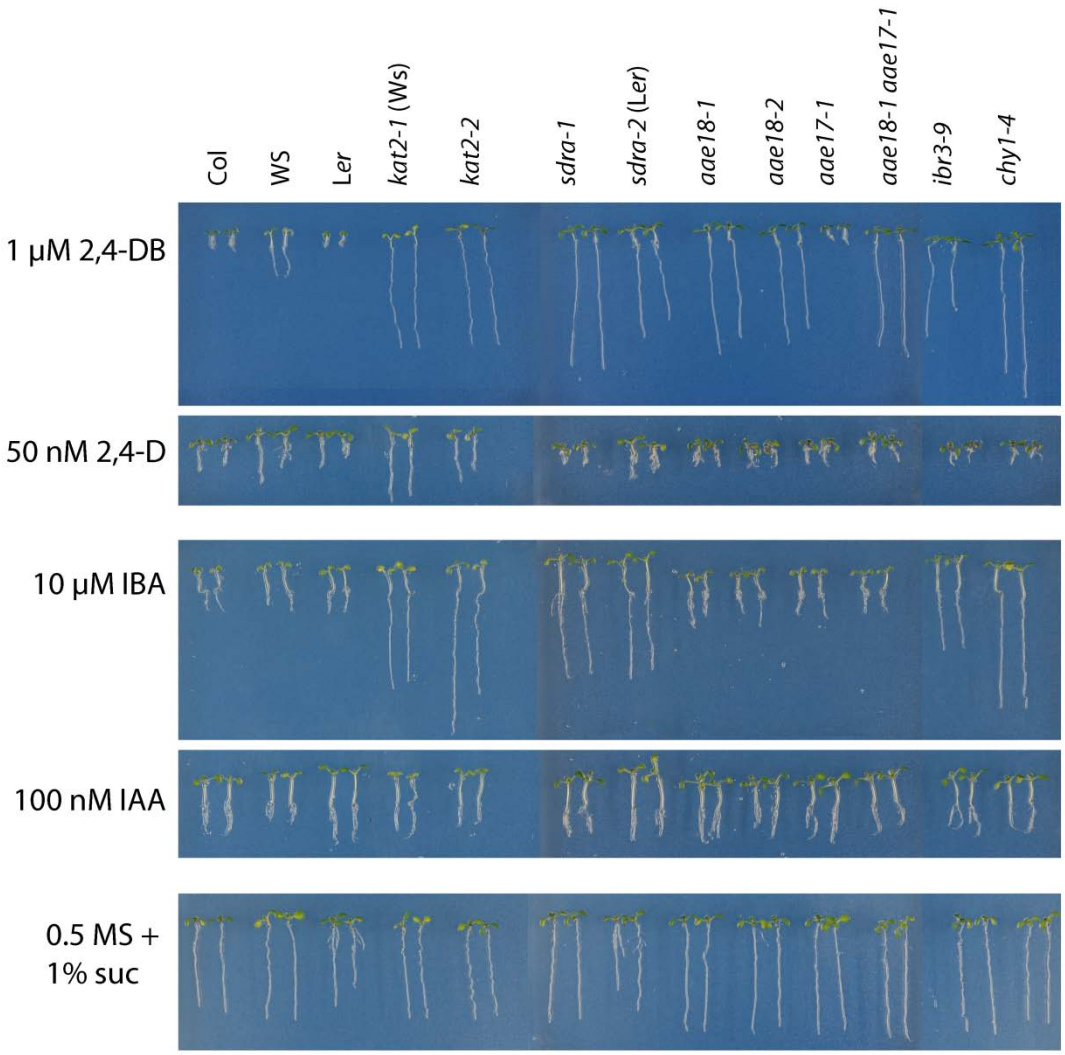

Figure 3.2. Auxin phenotypes of mutant lines.

Plants were grown for 5 d on half strength MS supplemented with 1% sucrose and the indicated hormones.

3.2.2 *sdra* and *aae18* are resistant only to pro-auxins

The new 2,4-DB resistant lines were characterised for dose responses to 2,4-DB. On increasing concentrations of 2,4-DB, *aae18* and *sdra* appeared to be as resistant for root elongation as *chy1* up to 1 μM 2,4-DB, but were less resistant above this concentration (Figure 3.3A). *aae18-1*, *aae18-2* and *sdra-1* were more resistant to 2,4-DB than *ibr3-9*. The *sdra-2* mutant is in L*er* background and shows similar trends but both the L*er* wild-type and *sdra-2* are apparently more sensitive to 2,4-DB than Col-0 and *sdra-1* and are thus presented separately (Figure 3.3B). Both *kat2-1* and *kat2-2* appear to be as resistant as *chy1-4* to 2,4-DB (Figure 3.3C). The *kat2* alleles were more resistant to higher than lower concentrations of IBA and 2,4-DB (Figure 3.3C, F). This was previously noted by Lange *et al*. (2004) for *kat2* grown on 2,4-DB, but there is no obvious explanation for this phenomenon. Neither of the *kat2* alleles germinated on 4 μM 2,4-DB. Lethality of *kat2-1* at high concentrations of 2,4-DB was not previously reported (Lange *et al*., 2004).

When grown on IBA, *chy1-4*, *ibr3-9*, *kat2-1* and *kat2-2* all displayed resistance consistent with that reported in previous studies (Figure 3.2). Compared to growth on media lacking hormone, root elongation of all lines (mutant and wild-type) was markedly inhibited by 5 μM IBA (Figure 3.3D–F). This response is at variance with previous reports for *ibr3* and *chy1* where root growth inhibition was less severe in response to 5 μM IBA (Zolman *et al*., 2007). Similarly, the greater inhibition of root elongation at 5 μM compared to 10 μM IBA for the stronger mutants (*chy1-4* and *kat2-2*) was not reported earlier (c.f. Zolman *et al*., 2001a; Zolman *et al*., 2007). These two discrepancies are most likely due to different media and growth conditions of the studies. In accordance with Zolman *et al.* (2007), *ibr3-9* was less severe in its response to IBA than *chy1-4* (Figure 3.3D). In this study, *kat2* mutants were at least as resistant as *chy1-4* (Figure 3.3F). The *sdra-1* mutant appeared to be almost as resistant to IBA as *chy1-4* at all concentrations tested and was more resistant than *ibr3-9* to IBA (Figure 3.3D). *sdra-2* displayed a similar trend of high resistance with its difference to *sdra-1* most likely attributable to the accession differences of the alleles (Figure 3.3E). Interestingly, all three *aae18* alleles behaved like wild type in their IBA response (Figure. 3.2, 3.3D; *aae18-3* not shown).

sdra, *aae18*, *kat2*, *chy1* and *ibr3* respond normally to the active auxins IAA, 2,4-D and NAA (Figures 3.2, 3.4) indicating there is no general block to auxin signaling. When grown on 100 nM IAA, 50 nM 2,4-D or 100 nM NAA, all genotypes showed inhibition of root length comparable to their respective wild types. Ws-4 (and mutants in Ws-4 background) had a low level of natural resistance to 2,4-D and 2,4-DB compared to Col-0 and L*er* (Figures 3.2, 3.4). The resistance of Ws-4 to low concentration of 2,4-DB has been previously reported (Lange et

al. 2004). Interestingly though, both *kat2-1* (Ws-4) and *kat2-2* (Col-0) appeared to be somewhat resistant to 2,4-D (Figure 3.4).

To further characterise their auxin response, all 2,4-DB-resistant mutants were assessed for their capacity to produce lateral roots. Seeds were germinated and grown for 3 d on medium containing 1% (w/v) sucrose, then plants were transferred to medium containing hormones for 2 d. With the exception of *kat2*, all mutants produced numbers of lateral roots comparable to their wild types when grown on media without added hormone. Both *kat2* mutants produced less lateral roots under these conditions than their wild types (Figure 3.5). This was also the case for *kat2* grown for differing durations on sucrose up to 8 d in total (data not shown).

IBA stimulated lateral root formation considerably in wild type controls as well as in *aae18*. In contrast, *sdra-1*, *sdra-2*, *kat2-1*, *kat2-2*, *chy1-4* and *ibr3-9* all produced fewer lateral roots on IBA than their respective wild types (Figure 3.5). Marked increases in the number of lateral roots were observed in all cases when the seedlings were transferred to media supplemented with 80 nM 1-naphthaleneacetic acid (NAA), indicating no general block to lateral rooting capacity.

3.2.3 SDRa and AAE18 localise to the peroxisome

GFP fusions with SDRa and AAE18 were constructed by inserting GFP in frame into the coding sequence close to the C-terminus. By this method SDRa-GFP and AAE18-GFP both localised to peroxisomes when compared to a peroxisomal RFP-SRL marker (Figure 3.6). SDRa possesses a C-terminal-SRL and AAE18 a C-terminal-SRI. These are both canonical plant PTS1 signal peptides (Reumann *et al.*, 2004), consistent with the observation of peroxisomal GFP. SDRa has moreover been identified in the proteome of leaf peroxisomes (Reumann *et al.*, 2007).

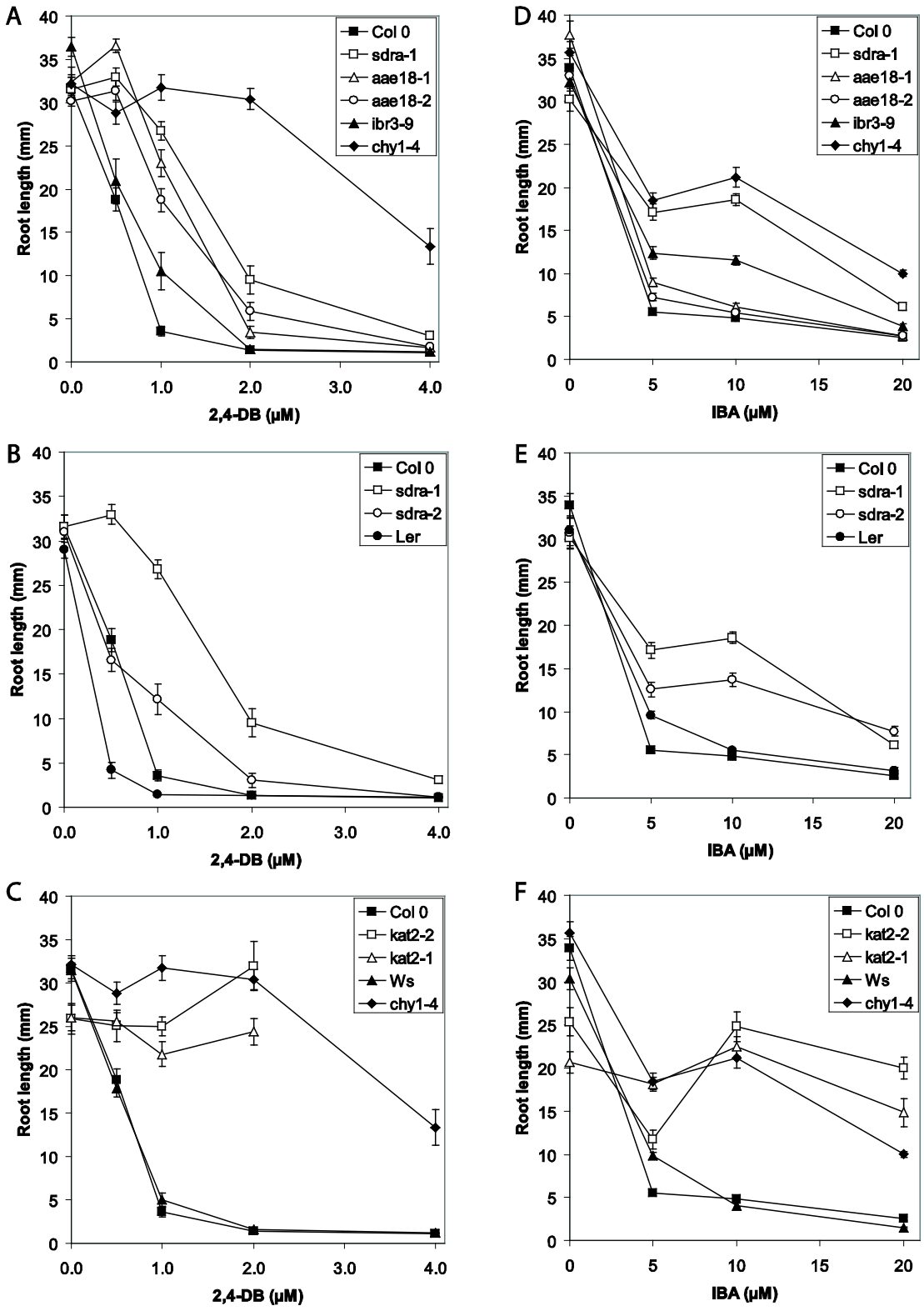

Figure 3.3. Response of mutants to varying concentrations of 2,4-dichlorobutyric acid (2,4-DB) and indole butyric acid (IBA). A-C. Response to 2,4-DB. D-F. Response to IBA. A, D. *sdra-1* and *aae18* mutants. B, E. Comparison of *sdra-1* (Col-0) and *sdra-2* (L*er*) and their respective wild types. C, F. *kat2-1* and *kat2-2* mutants and their respective wild types (Ws-4 and

Col-0). In A, C, D and F, *chy1-4* and *ibr3-9* are included for comparative purposes. Plants were grown for 6 d in continuous light on half strength MS media supplemented with 1% sucrose and the indicated concentration of 2,4-DB or IBA. Each value represents the mean root length with standard error indicated (n≥15).

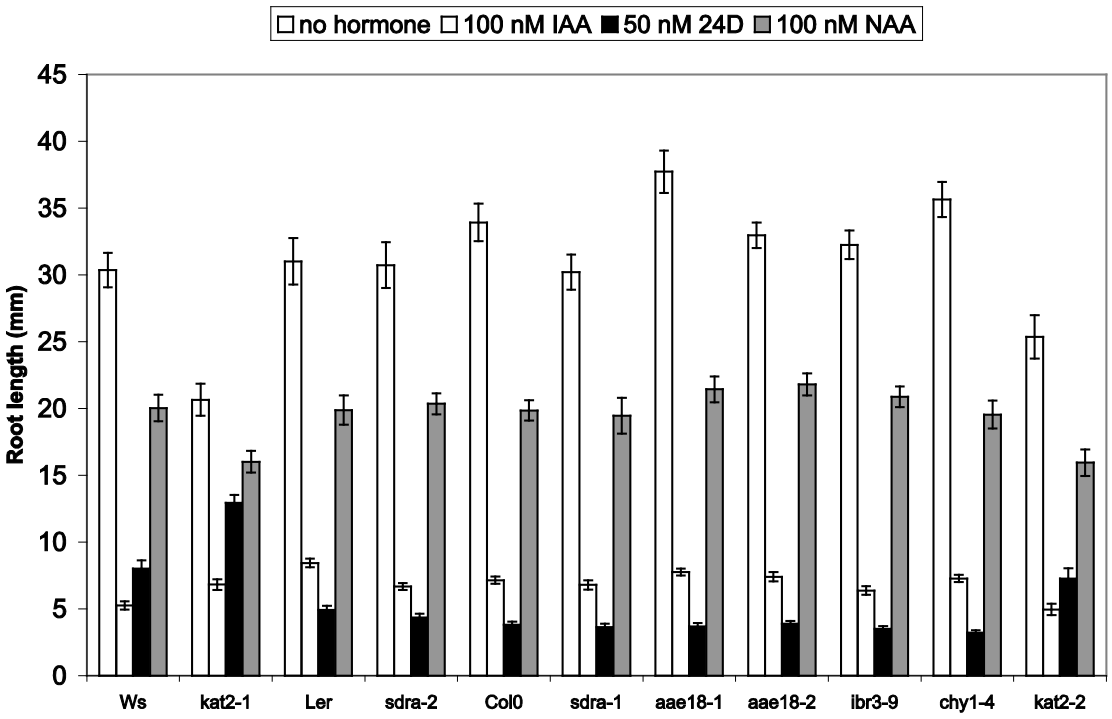

Figure 3.4. Responses of mutants to IAA, 2,4-D and NAA.

Plants were grown for 6 d in continuous light on half strength MS media supplemented with 1% sucrose and the indicated concentration of IAA, 2,4-D or NAA. Each value represents the mean root length with standard error indicated (n≥15).

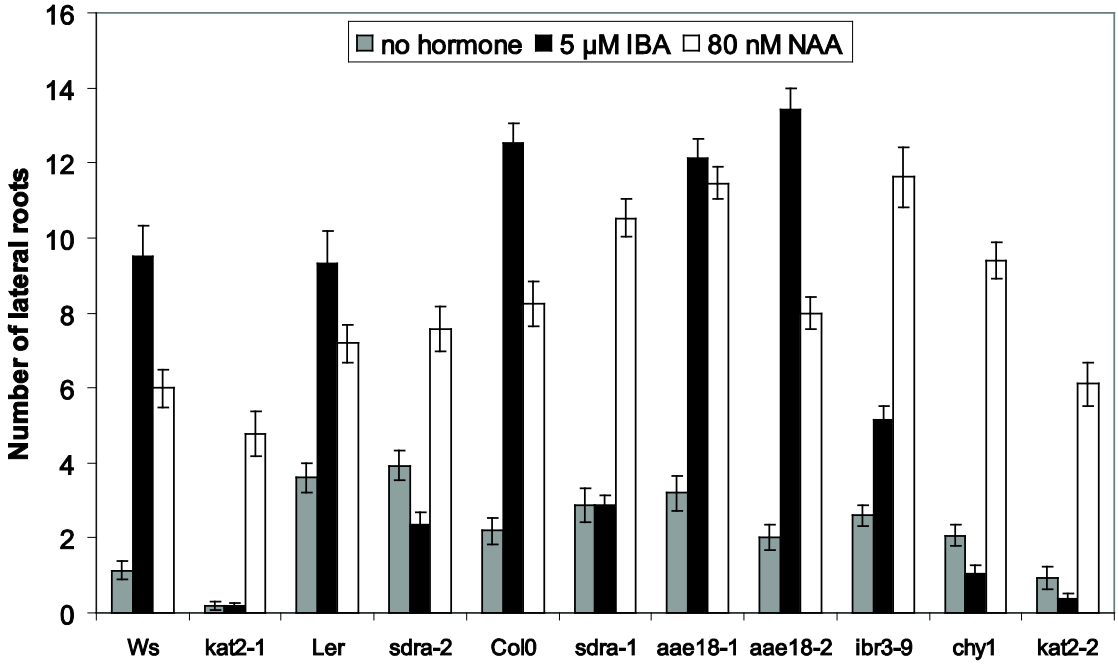

Figure 3.5. Lateral root formation in *sdra* and *aae18* mutants.

Plants were grown for 3 d in continuous light on half strength MS medium supplemented with 1% sucrose, then transferred to similar base media supplemented with the indicated hormones. The number of lateral roots was counted 2 d after transfer. Each value represents the mean number of lateral roots with standard error indicated ($n \geq 15$).

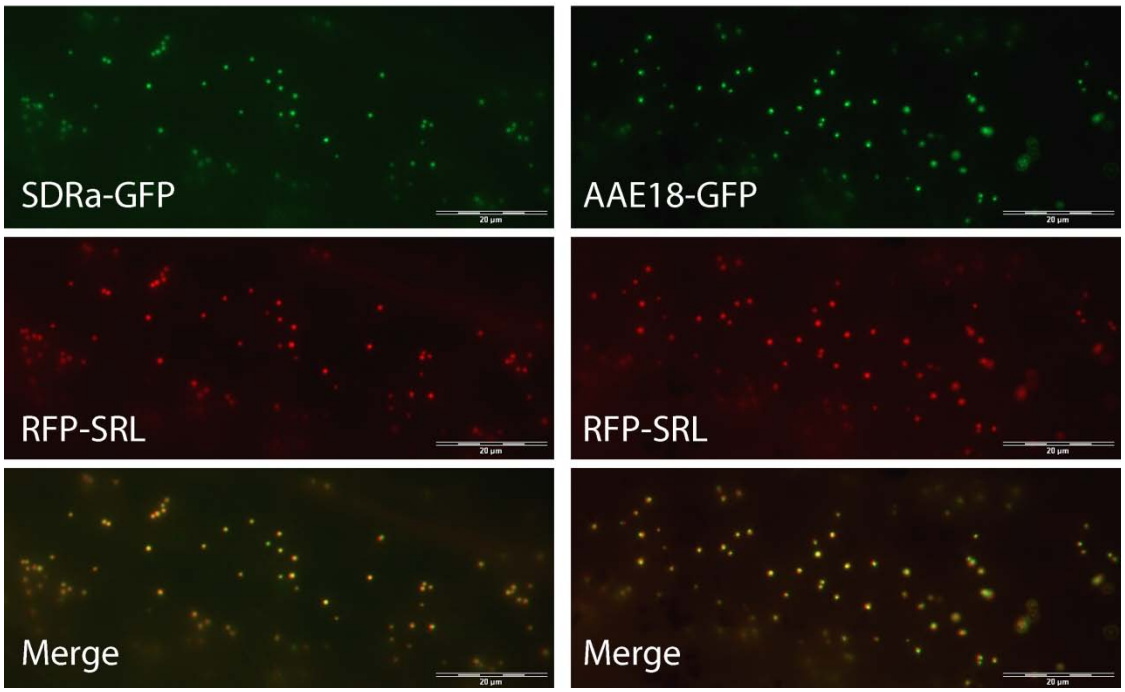

Figure 3.6. *In vitro* targeting of SDRa and AAE18.

GFP was cloned in frame 10-13 amino acid residues upstream from the stop codon in the coding sequence of AAE18 and SDRa. These were co-transformed with the peroxisomal marker RFP-SRL into onion epidermal cells by biolistic bombardment. Localisation of fluorescent proteins was assessed 1 d after transformation by fluorescence microscopy. The length of the scale bar is 20 µm.

3.2.4 *sdra* and *aae18* are not dependent on exogenous sucrose for seedling establishment

To examine whether any of the lines were affected in triacylglycerol (TAG) metabolism, seedlings were grown in the dark on media with or without added sucrose. *sdra* and *aae18* alleles were able to etiolate normally in the absence of sucrose, indicating that TAG metabolism was not affected sufficiently to disrupt seedling germination and growth (Figure 3.7A). As previously describe by Germain *et al.* (2001), neither of the *kat2* alleles emerged from seed coats during this experiment, and *chy1-4* grew poorly without sucrose, as reported previously for *CHY1* mutants (Zolman *et al.*, 2001a; Zolman *et al.*, 2001b). Seedling establishment and early development of *sdra* and *aae18* alleles in the light without exogenously supplied sucrose appeared normal (data not shown).

3.2.5 Fatty acid metabolism in *sdra-1*

Although it is expressed during early seedling establishment (Figure 3.1), further information regarding the expression of the *AAE18* gene is lacking because it is not represented on the Affymetrix genechip ATH1. However, much information regarding the expression of SDRa is available. *SDRa* expression was examined using publicly available microarray data (Schmid *et al.*, 2005). Analysis using Genevestigator V3 (Zimmermann *et al.*, 2004), indicates that *SDRa* is highly expressed throughout the plant life cycle, but is more highly expressed in germinating seeds. During development, similar expression patterns are observed in *SDRa*, *ECH1a*, *ECH1b*, *MFP2*, *ACX2*, *IBR3*, *ACX3*, *ACX4*, *KAT2* and *NQR* (not shown). In line with the apparent co-regulation with β-oxidation genes, *SDRa* also clusters with *NQR* and β-oxidation genes when analysed using ATTED (Obayashi *et al.*, 2007). Many β-oxidation genes are in the top 300 genes co-expressed with *SDRa* including *NQR* (position 1), *MFP2* (5), *IBR3* (79) and *AIM1* (105). Analysis of transcript abundance during the diurnal cycle (Smith *et al.*, 2004) also indicates that in mature leaf tissue, *SDRa* is co-regulated with β-oxidation genes (Figure 3.8).

Despite the apparent link between *SDRa* and β-oxidation genes, no evidence was obtained to show that mobilisation of TAG for seedling growth was impaired in *sdra-1* or *sdra-2* (Figure 3.7A). Nevertheless, the possibility that β-oxidation of specific fatty acids could be impaired was investigated. Total fatty acids were isolated for GC-MS analysis from two d old seedlings, the stage at which TAG breakdown is taking place most rapidly (Germain *et al.*, 2001). The levels of numerous medium- and long-chain fatty-acids were not significantly different in Col-0 and *sdra-1*, including the major TAG fatty acids linoleic acid (C18:2) and eicosenoic acid (C20:1) (Figure 3.7B). In contrast, *kat2-1* contained elevated levels of these fatty acids due to impaired TAG breakdown. These features indicate that fatty acid metabolism in *sdra-1* is

indistinguishable from wild-type, consistent with the hypothesis that SDRa participates preferentially in auxin synthesis.

3.2.6 *aae17 aae18* double knockout remains sensitive to IBA

AAE18 is a member of a large family of acyl-activating enzymes and redundancy of peroxisomal isoform functions has already been demonstrated in the family, with the closely related LACS6 and LACS7 involved in activating TAG-derived fatty acids, but not auxins (Fulda *et al.*, 2004). For this reason we generated a double mutant of AAE18 and AAE17 to examine auxin responses. AAE17 also has a PTS1 (C-terminal SKL). It is the closest relative of AAE18 in the Arabidopsis genome and a good candidate for double mutant analysis. The *aae17-1 aae18-1* double mutant was no more resistant to 2,4-DB than *aae18-1* (Figure 3.9A), normally sensitive to IBA (Figure 3.9B) and mature auxins (Figure 3.9C), produced normal numbers of lateral roots when stimulated by IBA and NAA (Figure 3.9D), and was not dependent on sucrose for etiolation (Figure 3.9E).

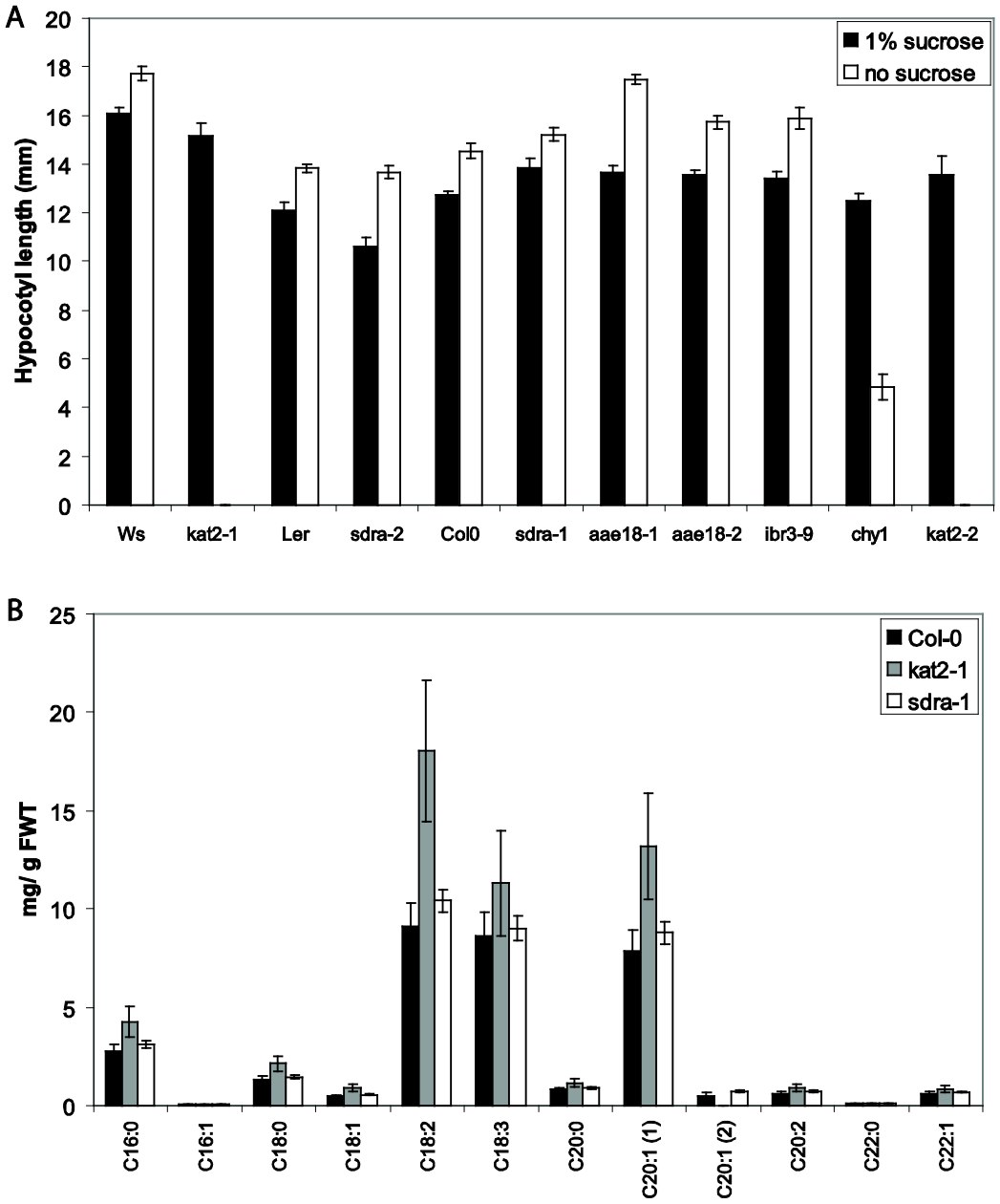

Figure 3.7. TAG metabolism is normal in *sdra* and *aae18*

A. Etiolation of *sdra* and *aae18* is normal in the absence of sucrose. Plants were germinated and grown for 4 d in the dark on half strength MS medium with or without supplement of 1% sucrose. B. Fatty acid analysis of wild-type, *kat2-1* and *sdra-1* mutants. Fatty acids were extracted from seedlings grown for 2 d on half strength MS medium supplemented with 1% sucrose, and then identified and quantified using GC-MS.

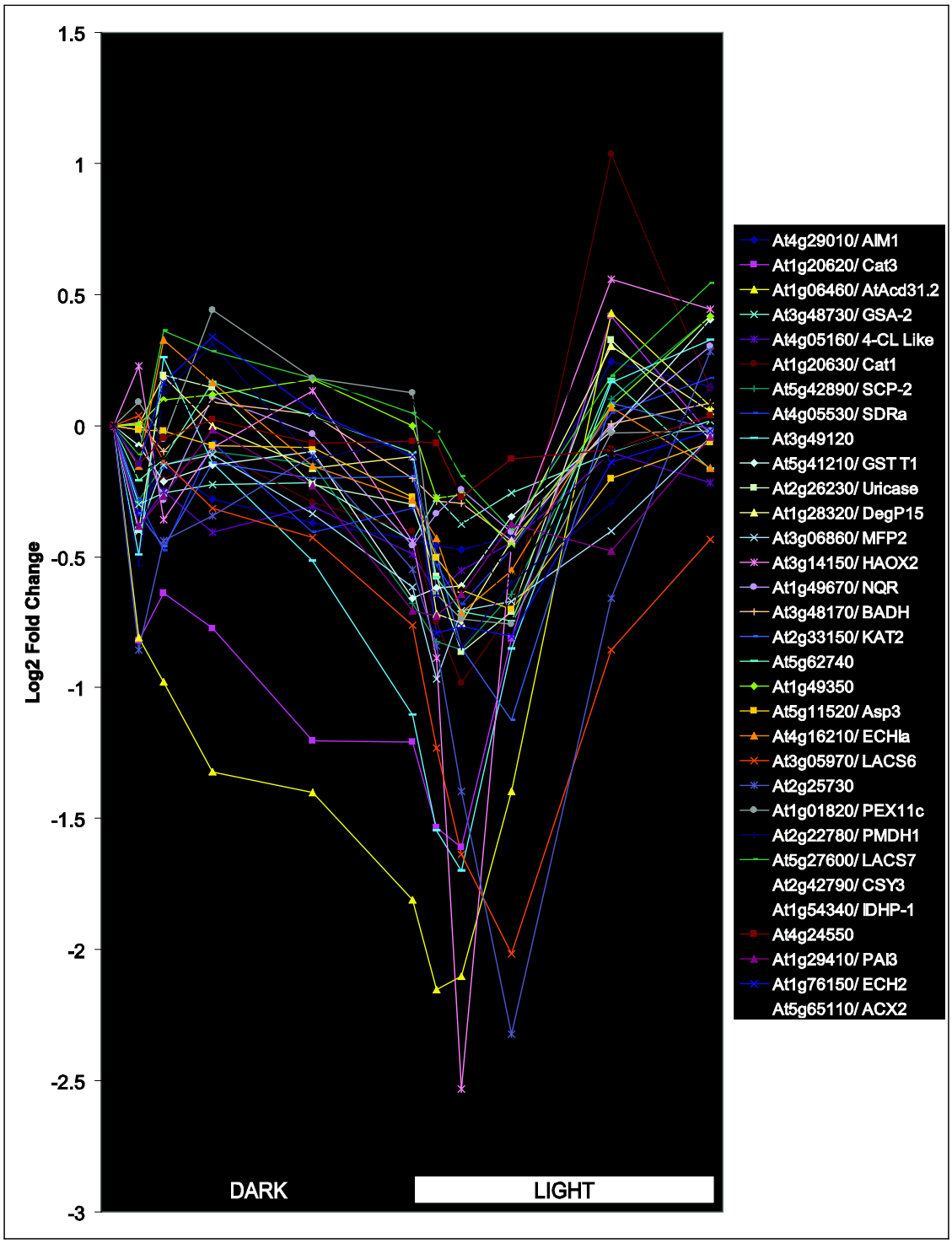

Figure 3.8. SDRa expression correlates with β-oxidation genes during the diurnal cycle.

Many β-oxidation genes are co-ordinately down-regulated during the light period. Core β-oxidation genes (*LACS6*, *LACS7*, *ACX2*, *MFP2*, *AIM1*, *KAT2*, *PMDH1*) and transcripts of some putative auxiliary genes (e.g. *CSY3*, *ECH1a*, *ECH2*, *SCP-2*) experience a maximum during the

dark period and reduced expression in the light. *SDRa* follows a similar pattern. There are rapid changes in transcript levels upon transition from light to dark and dark to light. For many of these genes, there is also an increase in expression during the light period similar to that seen for starch-degrading enzymes (Smith *et al.*, 2004) that may be anticipatory of a dark phase where net energy reserves are consumed.

Putative PTS1- and PTS2-encoding transcripts (identified using ARAPEROX, Reumann *et al.*, 2004) and from other peroxisomal, non-PTS containing genes were identified in the transcriptome data from Smith *et al.* (2004). These 254 transcripts were further filtered to remove those for which the maximum normalised signal across the 11 time points was less than 50. The signal data for the remaining 158 transcripts were $\log_2$ transformed, then normalised against their time 0 values to obtain $\log_2$ fold changes through the diurnal cycle. This matrix was analysed with the CAST algorithm of TMEV (http://www.tm4.org/mev.html) using Pearson correlation coefficient and a threshold of 0.8. The cluster containing *SDRa* is depicted. *ACX2* did not cluster in this group, but is superimposed for comparison.

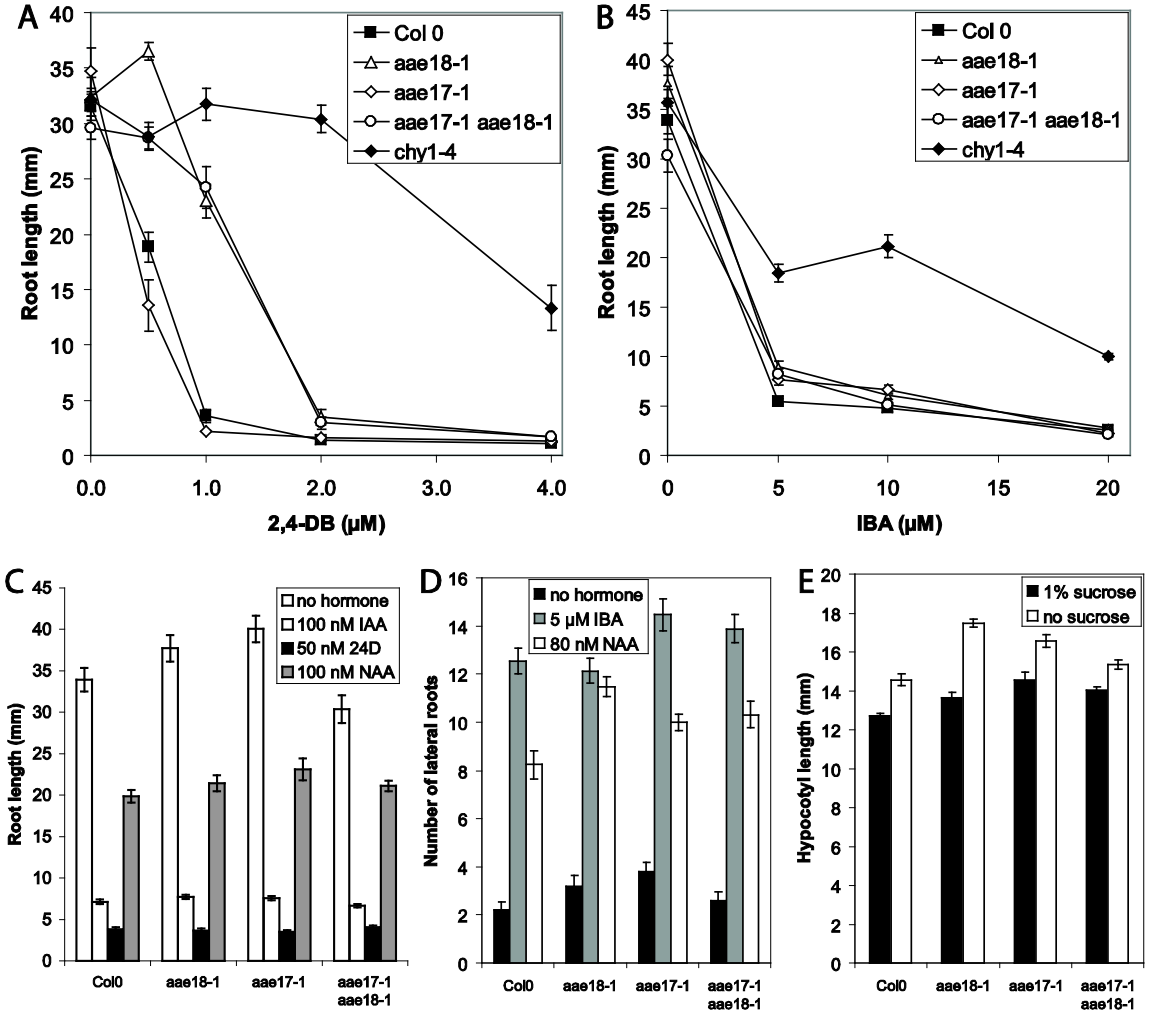

Figure 3.9. *aae17* does not contribute to metabolism of pro-auxins.

A–C. Root length of *aae17*, *aae18* and *aae17 aae18* double mutants grown on different auxin containing media. Root lengths of *aae17-1* and *aae17-1 aae18-1* double mutants were not significantly different to wild-type and *aae18-1* respectively when grown on different concentrations of 2,4-DB (A) and IBA (B), but responded normally to IAA, 2,4 D and NAA (C). D. Lateral root initiation in response to IBA and NAA. E. *aae17-1*, *aae18-1* and *aae17-1 aae18-1* are not dependent on sucrose for hypocotyl elongation.

3.3 Discussion

3.3.1 A model for IBA and 2,4-DB metabolism

The metabolism in peroxisomes of pro-auxins IBA and 2,4-DB to the biologically active forms IAA and 2,4-DB has been used extensively in screening for peroxisomal mutants with reduced capacity for β-oxidation (Baker *et al.*, 2006; Hayashi *et al.*, 1998; Woodward and Bartel, 2005). However, some of the enzymes involved remain to be elucidated. In this work a systematic screen of available T-DNA lines for peroxisomal genes with predicted roles in β-oxidation was employed. Two PTS1-containing, peroxisome-targeted proteins were identified that are proposed to act as, firstly, an acyl-CoA synthetase (acyl-activating enzyme 18, AAE18) that activates 2,4-DB, and, secondly, an oxidoreductase (SDRa) that oxidises 3-hydroxyacyl-CoA derivatives of both 2,4-DB and IBA. Knockouts for *SDRa* and *AAE18* were shown to be compromised in their ability to respond to pro-auxins but were not dependent on sucrose for seedling establishment. They are thus potentially members of the class of β-oxidation genes that have as their primary function hormone metabolism rather than energy provision (Zolman *et al.*, 2000).

Based on the mutant phenotypes reported here and in other studies, we were able to elaborate pathways for β-oxidation of 2,4-DB and IBA (Figure 3.10). By this model 2,4-DB is activated by AAE18. It is subsequently oxidized by IBR3 (Zolman *et al.*, 2007), possibly in conjunction with ACX3 and ACX4, mutants of which are also partially resistant to 2,4-DB (Rylott *et al.*, 2003; Zolman *et al.*, 2000). AIM1 likely contributes the hydratrase/isomerase activity after which SDRa oxidises the 3-hydroxyacyl-CoA derivative. The thiolase activity is provided primarily by KAT2 (Germain *et al.*, 2001; Hayashi *et al.*, 1998). Ultimately, the products of β-oxidation must be released from CoA, a step that could be catalysed by one of the several thioesterases predicted to be targeted to peroxisomes (Reumann *et al.*, 2004). We propose that the oxidation of IBA proceeds via a similar pathway (Figure 3.10), except that enzymes that might activate IBA remain unknown. In addition to IBR3 and ACX3, the first oxidative step in the β-oxidation of IBA may be catalysed by ACX1 and ACX2, mutants of which are resistant to IBA (Adham *et al.*, 2005). Alternatively, *acx1* and *acx2* mutants may cause sequestration of the peroxisomal CoA supply and indirectly yield IBA-resistance (Adham *et al.*, 2005).

It is likely that AIM1 is the major hydratase/isomerase in 2,4-DB and IBA oxidation because the *aim1* mutant is the only hydratase/isomerase containing protein identified to date that is 2,4-DB and IBA resistant (see Richmond and Bleecker, 1999; Zolman *et al.*, 2000). In contrast, *mfp2* is sensitive to 2,4-DB (Rylott *et al.*, 2006) and IBA (data not shown), as are the

ECHI (enoyl-CoA hydratase/isomerase) knockouts examined. Nevertheless, AIM1 may still act with other hydratase/isomerase proteins and it would be instructive to make double mutants with the various *ECHI* genes that were individually sensitive to these hormone precursors. The double knockout *aim1 mfp2* is embryo lethal and thus not testable in this manner (Rylott *et al.*, 2006).

Although AIM1 is at least a trifunctional protein containing epimerase/hydratase and dehydrogenase domains, we propose that that SDRa contributes the bulk of dehydrogenase activity in the oxidation of pro-auxins (rather than AIM1). For example, *sdra-1* is almost as resistant to IBA as *kat2* and is markedly more resistant than *ibr3*, consistent with evidence that IBR3 and ACX3 are partially redundant during the initial oxidative step (Zolman *et al.*, 2007). Similarly, *sdra-1* has a stronger 2,4-DB phenotype than *ibr3*. These observations do not rule out contribution of another dehydrogenase activity at this step. Future studies might examine this by partially complementing *aim1* with truncated protein variants containing either the hydratase/isomerase or the dehydrogenase domains.

KAT2 is likely to be the major thiolase in the pathway as other thiolase mutants (*kat1* and *kat5*) are as sensitive as wild-type to IBA and 2,4-DB. The *kat2* mutant was as resistant to IBA and 2,4-DB as *chy1* (Figures 3.2 and 3.3) in which thiolase activity generally is inhibited by accumulation of the toxic intermediate methacrylyl-CoA (Lange *et al.*, 2004; Zolman *et al.*, 2001a). It was observed that *kat2* had a slightly shorter root (Figure 3.3) and grew fewer lateral roots (Figure 3.5) than wild-type on sucrose medium (without hormones). One possible explanation for this is that *kat2* was delayed in development due to the severe β-oxidation lesion. Alternatively, a block in the conversion of endogenous IBA to IAA may inhibit lateral root initiation. This has previously been suggested to explain the similar phenotype of peroxisomal ABC transporter (*pxa1*) mutants (Zolman *et al.*, 2001b).

Arguably, SDRa fills the role as an oxidoreductase during IBA and 2,4-DB metabolism. This is based on the phenotypes of IBA and 2,4-DB mutants. A possible alternative function of SDRa is that it might constitute the as yet unidentified 3-hydroxy-isobutyrate dehydrogenase (HIBDH) that immediately follows the 3-hydroxy-isobutyryl CoA-hydrolase (HIB-CoAH) encoded by CHY1 (Taylor *et al.*, 2004). The auxin-phenotypes observed in *sdra* could potentially phenocopy those of *chy1* if there was feedback inhibition of CHY1 due to buildup of the 3-hydroxy-isobutyrate in *sdra*. We view this as unlikely, however, because TAG breakdown in *sdra* is unaffected, indicating that the lesion is specific to auxin metabolism and not fatty acid β-oxidation.

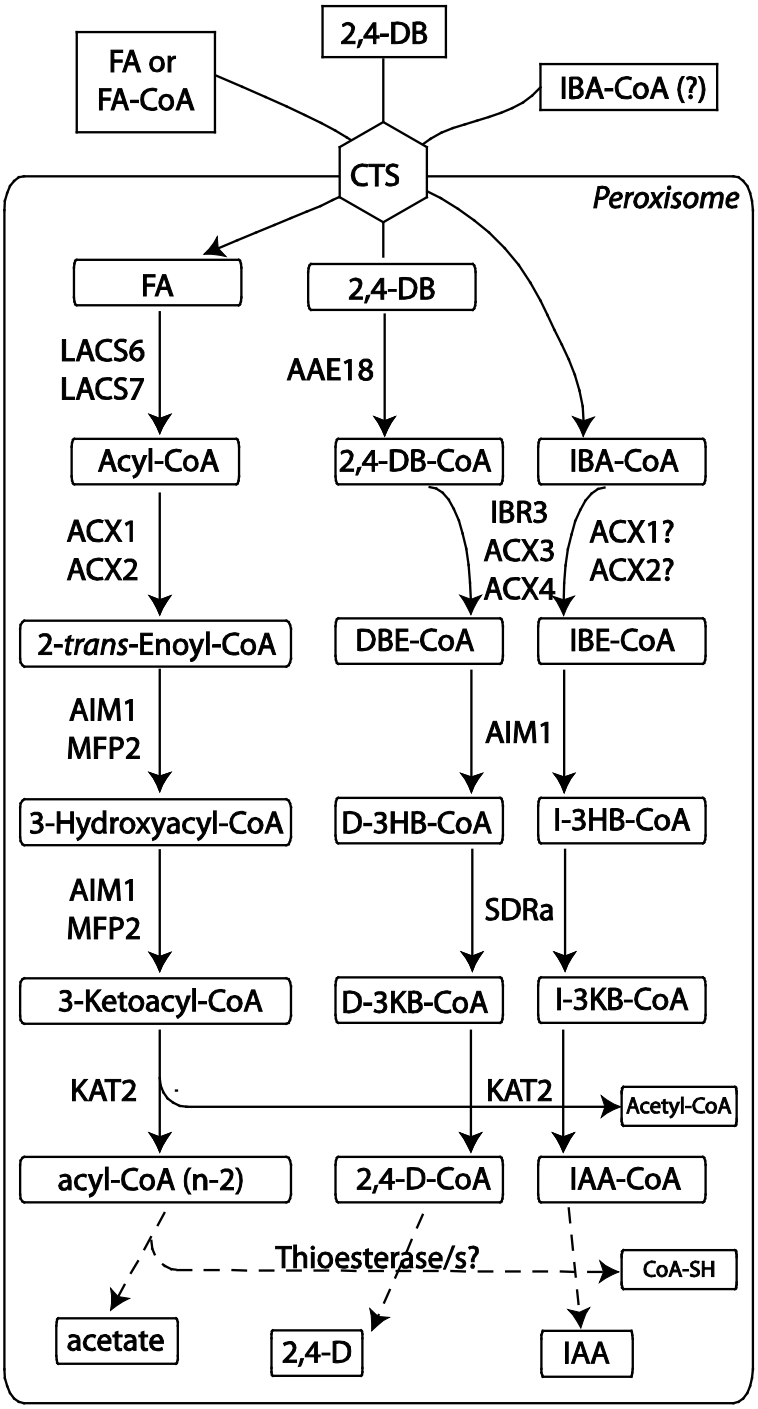

Figure 3.10. Model for β-oxidation of 2,4-DB and IBA.

This model is compiled based on mutant phenotypes and other data and includes the two new genes presented in this work (*SDRa* and *AAE18*). Fatty acid β-oxidation is presented for comparison and to highlight differences between it and the auxin pathways. (Abbreviations: IBE-CoA = indole butenoyl-CoA; I-3HB-CoA = indole-3-hydroxybutenyl-CoA; I-3KB-CoA = indole-3-keto-butenyl-CoA; DBE-CoA = 2,4-dichlorobutenoyl-CoA; D-3HB-CoA = 2,4-dichloro-3-ydroxybutenyl-CoA; D-3KB-CoA = 2,4-dichloro-keto-butenyl-CoA)

3.3.2 Endogenous role of AAE18

Metabolic mutants published to date that are 2,4-DB resistant have for the most part also been resistant to IBA (Woodward and Bartel, 2005; Zolman *et al.*, 2007). Exceptions are the *acx2* mutant and *acx1 acx2* double knockout that are resistant only to IBA (Adham *et al.*, 2005). *aae18* is the first mutant found to be resistant only to 2,4-DB. This indicates either that IBA is not a substrate of AAE18, or that there is genetic redundancy for the activation of IBA. A double knockout of *aae18* with *aae17*, the closest relative of AAE18 (Shockey *et al.*, 2003) was generated and shown also to be sensitive to IBA (Figure 3.9). Thus, it is unlikely that either AAE18 or AAE17 have a role in β-oxidation of IBA. This raises the questions of if, how and where IBA is activated.

There are 63 members of the AAE superfamily (Shockey *et al.*, 2003), 17 of which have a PTS (Reumann *et al.*, 2004). The peroxisome-targeted AAE proteins do not present as good candidates to be an IBA activating enzyme. None of the AAE mutants we tested were IBA resistant, the *lacs6 lacs7* double mutant is sensitive to pro-auxins (Fulda *et al.*, 2004), AAE7 can activate acetate and butyrate (Shockey *et al.*, 2003; Turner *et al.*, 2005), AAE11 can activate medium chain length fatty acids (C6–C8) (Shockey *et al.*, 2003), and BZO1 is a benzoyl-CoA ligase in the pathway of benzoyloxyglucosinolate synthesis (Kliebenstein *et al.*, 2007). Additionally, a systematic *in vitro* substrate screen of the peroxisomal 4CL-like proteins indicated that they could not utilise IBA as a substrate (Kienow *et al.*, 2008). An alternative possibility is that IBA-CoA may be synthesised in the cytosol and imported to the peroxisome by the ABC transporter CTS/PXA1/PED1. CTS imports acyl-CoAs (Footitt *et al.*, 2002; Fulda *et al.*, 2004; Zolman *et al.*, 2001b) and also potentially imports some unesterified substrates (e.g. OPDA during JA biosynthesis (Kienow *et al.*, 2008; Theodoulou *et al.*, 2005)). Possible extra-peroxisomal activation enzymes include the 19 member JAR1/GH3 sub-family of AAE enzymes, some of which are able to conjugate JA (JAR1), SA and IAA (one gene), or IAA (six genes) to amino acids or other compounds (Shockey *et al.*, 2003; Staswick *et al.*, 2005; Staswick *et al.*, 2002).

What is the natural substrate for AAE18? No clues can be garnered through microarray data as *AAE18* is not represented on the ATH1 chip, and it does not respond significantly in the CATMA arrays (http://www.catma.org/). We can look to compounds that are structurally similar to 2,4-DB. One compound with similarity to 2,4-DB, *trans*-cinnamic acid, is potentially metabolised in peroxisomes to benzoic acid during salicylic acid synthesis (Wildermuth, 2006). However, this may be difficult to dissect genetically because it has been previously shown that direct synthesis of SA via isochorismate synthase accounts for the vast majority of defence

related SA synthesis, and a variety of alternative routes (including β-oxidation) probably contribute only to basal SA levels (Wildermuth, 2006; Wildermuth *et al.*, 2001).

3.3.3 Concluding remarks

Recent *in silico* and proteome studies (Reumann *et al.*, 2007; Reumann *et al.*, 2004) have highlighted the dominance of fatty acid β-oxidation in peroxisome function, with perhaps 30% of the peroxisome proteins involved in such metabolism. Here we have screened mutants in 13 uncharacterised putatively peroxisomal genes, but found none that affect seedling growth (and by implication, TAG metabolism) or other visual aspects of plant growth and development (data not shown). We have identified two new proteins that potentially contribute to auxin metabolism, including the first example of a mutant resistant to 2,4-DB but normally responsive to IBA. This indicates that it may be possible to genetically engineer resistance to pro-auxin herbicides without compromising the normal functions of endogenous auxins.

Chapter 4: Sequence and expression analysis of Arabidopsis thiolase genes and promoters

4.1 Introduction

Germination and seedling establishment of oilseed species such as *Arabidopsis thaliana* require β-oxidation to degrade seed storage lipid, which provides the energetic input that drives this stage of development. Genes involved in lipid mobilisation, including β-oxidation, the glyoxylate cycle and gluconeogenesis are expressed co-ordinately during Arabidopsis seed germination, with transcript levels and enzyme activities peaking at 48 h after the commencement of germination (Rylott *et al.*, 2001). Of the three Arabidopsis 3-ketoacyl-thiolase (KAT) genes, expression of *KAT2* is dominant during this stage of the life cycle, with transcript levels far more abundant than *KAT1* and *KAT5* (Germain *et al.*, 2001; Kamada *et al.*, 2003). Genes of lipid mobilisation decline in expression level in the late stages of seedling establishment, a process associated with peroxisome content remodelling as peroxisome function changes at later stages of developmental (Kamada *et al.*, 2003; Lingard *et al.*, 2009; Rylott *et al.*, 2001). However, this is not the only stage of plant development for which peroxisomal β-oxidation has an important functional role. β-oxidation is a significant pathway for the synthesis of many fatty acid-based hormones in plants (Creelman and Mullet, 1995; Woodward and Bartel, 2005), and is required for the turn-over of fatty acids in plant cells during development and senescence (Yang and Ohlrogge, 2009).

In a comprehensive analysis of peroxisome gene expression, Kamada *et al.* (2003) identified 286 candidate genes with predicted or confirmed peroxisome targeting of their respective gene products, and constructed a peroxisomal-specific DNA microarray. Peroxisomal gene expression was surveyed in seedlings, cotyledons, leaves, stems, flowers, siliques and roots, with analysis of this data determining that core peroxisomal functions in Arabidopsis were β-oxidation, H_2O_2 degradation, branched-chain amino acid breakdown, glycolate metabolism, and a large class of genes with unknown function. Peroxisome gene expression was differentiated in an organ-specific manner, with *KAT2* specifically expressed highly in glyoxysomes. *KAT1* and *KAT2* transcript were present constitutively throughout the organs analysed while *KAT5* had flower- and silique-specific expression. Based on clustering analysis of peroxisome gene transcripts, Kamada *et al.* (2003) classified different organ-specific specialised peroxisome types into the categories of glyoxysomes, cotyledonary peroxisomes, leaf peroxisomes, root peroxisomes and unspecialised peroxisomes.

Using an alternative approach, Charlton *et al.* (2005a) made reporter constructs using the promoters of *PEROXIN1* (*PEX1*), *KAT2*, and *MALATE SYNTHASE* (*MLS*). These were selected as representative genes of peroxisome biogenesis, β-oxidation, and the glyoxylate cycle respectively. These genes were not coordinately expressed: *MLS* had a more restricted pattern of expression than *PEX1* and *KAT2*, which were expressed constitutively (Charlton *et al.*, 2005a). Previous to this study, induction of β-oxidation was detected in senescing barley (*Hordeum*

vulgare) leaves (Wanner *et al.*, 1991), and KAT and MS protein were determined to be up-regulated in senescing cotyledons of pumpkin (*Cucurbita* sp. Kurokawa Amakuri) (Kato *et al.*, 1996). However, of the three genes analysed by Charlton *et al.* (2005a) only *KAT2* was up-regulated in response to dark-induced senescence in Arabidopsis. In *Saccharomyces cerevisiae*, β-oxidation genes are regulated by the transcription factors Oaf1p and Pip2p in response to fatty acids (Karpichev *et al.*, 1997; Karpichev and Small, 1998). However, in plants, as β-oxidation plays multiple roles in different organs and during varying stages of development, components of the pathway may be regulated by a variety of mechanisms. For example peroxisomes proliferate in the light (Desai and Hu, 2008), and the hormones abscisic acid (ABA) and gibberellic acid (GA) appear to have some regulatory role during lipid mobilisation in germinating seedlings (Penfield *et al.*, 2006; Penfield *et al.*, 2004).

In Arabidopsis, *KAT2* and *ACYL-OXIDASE 1* (*ACX1*) transcripts both accumulate in response to wounding and dehydration (Castillo *et al.*, 2004). Wounding induces *KAT2* and *ACX1* expression locally and systemically, while *KAT5* is only induced systemically dependent on the JA receptor gene *CORONATINE INSENSITIVE 1* (*COI1*). Exogenous application of JA results in up-regulation of *ACX1* and *KAT5* expression, while ABA up-regulates *ACX1* and *KAT2* (Castillo *et al.*, 2004). During natural and dark-induced senescence *KAT2* expression is induced, while no change is observed for *KAT1* and *KAT5* transcript levels (Castillo and León, 2008). These results suggest that a range of hormones may differentially regulate *KAT* genes.

The three *KAT* genes of Arabidopsis were annotated *KAT1* (At1g04710), *KAT2* (At2g33150) and *KAT5* (At5g48880) based on the chromosome on which they were located (Germain *et al.*, 2001). Subsequent analysis has determined that while both *KAT1* and *KAT2* encode single peroxisome targeted proteins, *KAT5* encodes the cytosolic KAT5.1 and peroxisomal KAT5.2 isoforms (Carrie *et al.*, 2007). The *KAT5.2* transcript differs from *KAT5.1* in the 5' region, with an additional exon encoding a peroxisome targeting signal type 2 (PTS2), and alternate transcription and translation start sites (Carrie *et al.*, 2007). While *KAT2* co-expresses with genes of β-oxidation, *KAT5* instead clusters in co-expression analysis with genes of flavonoid biosynthesis (Carrie *et al.*, 2007). A role for β-oxidation in flavonoid biosynthesis is suggested by down-regulation of flavonoid biosynthesis genes in germinating *cts* seeds, and a corresponding reduction of flavonoids in germinating *cts* and *kat2* seed embryos, with this phenotype complemented by the supply of exogenous sucrose (Carrera *et al.*, 2007). Additionally, in parsley (*Petroselinum crispum*) cells ACX and the flavonoid biosynthesis gene chalcone synthase (CHS) are induced by UV-B irradiation, suggesting interaction between primary and secondary metabolism to regulate the metabolic response to UV-B stress (Logemann *et al.*, 2000).

The functional importance of β-oxidation in reproductive tissue has been demonstrated biochemically (Arai *et al.*, 2002; Baud *et al.*, 2002), as well as by the disruption to reproductive success observed in numerous Arabidopsis β-oxidation mutants (Footitt *et al.*, 2007b; Richmond and Bleecker, 1999; Rylott *et al.*, 2006; Rylott *et al.*, 2003). *ACX1* expression in floral tissue has been studied in great detail using promoter reporter fusions, with strong expression detected in ovaries and pollen grains (Schilmiller *et al.*, 2007). As described previously, expression of the Arabidopsis *KAT* genes has been detected in reproductive tissue (Kamada *et al.*, 2003), but detailed analysis has not been attempted, and nor have *KAT5.1* and *KAT5.2* transcript expression patterns been distinguished. The purpose of the work described in this chapter was to conduct a detailed analysis of thiolase gene expression in Arabidopsis using qualitative and quantitative techniques such as promoter reporters and quantitative RT-PCR.

In the post-genomic age following sequencing of the Arabidopsis genome there has been an explosion of publicly available global transcriptome data of a variety of tissues grown under different conditions (Arabidopsis Genome Initiative, 2000; Schmid *et al.*, 2005; Winter *et al.*, 2007; Zimmermann *et al.*, 2004). Our understanding of peroxisomal protein content has improved due to advances in *in silico* analysis and proteomics of a variety of Arabidopsis tissues (Eubel *et al.*, 2008; Reumann *et al.*, 2007; Reumann *et al.*, 2004). Additionally, sequence data from other plant species is rapidly increasing, allowing analysis of peroxisome genes in other lineages and comparison of gene families across species. The work described in this chapter takes advantage of this progress to assist in the analysis of thiolase gene sequences and expression.

4.2 Results

4.2.1 The plant thiolase gene family: KAT5 dual localisation is conserved in Brassicales

Plant thiolase protein sequences were retrieved from Phytozome v7 (phytozome.org) database of sequenced plant genomes and from NCBI (ncbi.nlm.nih.gov) to investigate the evolutionary history of the plant thiolase gene family. *Arabidopsis thaliana* has 3 thiolase genes encoding 4 transcripts, *KAT1* (At1g04710), *KAT2* (At2g33150), *KAT5.1* (At5g48880.1) and *KAT5.2* (At5g48880.2). Three of these protein sequences contain an N-terminal PTS2, KAT5.1 however does not and has been confirmed by GFP tagging to be localised to the cytosol (Carrie *et al.*, 2007). An investigation of the plant thiolase gene family was conducted to determine if the dual targeting of KAT5 to the cytosol and peroxisome was novel to *Arabidopsis thaliana*, or if evidence for this could be found in other plants.

An amino acid multiple sequence alignment represented as a phylogram tree indicates that the thiolase gene family is present throughout the plant kingdom (Figure 4.1). Analysis of these thiolase protein sequences indicates the presence of PTS2 in all of them, suggesting conservation of targeting to the peroxisome. The conservation of peroxisomal thiolases throughout the plant kingdom including algae, moss, monocotyledons and dicotyledons implies an essential role in plant development and function. Orthologs of *A. thailana* KAT1, KAT2 and KAT5 are found in the closely related *Arabidopsis lyrata*. The *A. thaliana* KAT1 and KAT2 are more closely related to each other than to KAT5. KAT1 does not appear to have any orthologs other than in *A. lyrata*, suggesting it may be a duplication of KAT2 peculiar to the *Arabidopsis* lineage. Part of the genomic region adjacent to *KAT1* and *KAT2* displays synteny; the genes At2g33110 and At2g33120 neighbouring *KAT2* align with At1g04760 and At1g04750 neighbouring *KAT1* (synteny.cnr.berkeley.edu/CoGe/), suggesting genomic duplication. KAT2 has closely related orthologs in *Brassica napus* and *Thellungia halophila*, as well as more distantly related orthologs in *Carica papaya*, *Populus trichocarpa*, *Ricinus communis* and *Oryza sativa* (Figure 4.1).

A. thaliana KAT1, *KAT2* and *KAT5* genes have orthologs in *A. lyrata*, which show a high level of conservation at the genomic sequence level (88%, 90%, and 90% identity, respectively) and exon-intron structure. Additionally the *KAT5* ortholog has alternate start codons, suggesting KAT5.1 and KAT5.2 isoforms are present in *A. lyrata*. By latest estimates, these two species separated approximately 13 million years ago (Mya) (Beilstein *et al.*, 2010), so it would appear that alternate transcripts of *KAT5* have been maintained in the genome for at least this long. While *T. halophila* and *B. napus* are closely related to *A. thaliana*, sequence alignment indicates that these species have KAT2, but not KAT1 or KAT5 orthologs. However, the *T. halophila* and *B. napus* thiolase sequences in Figure 4.1 were not retrieved from Phytozome, but instead are mRNA derived sequences retrieved using BLAST.

Although not found in Phytozome, *B. napus KAT5.1* and *KAT5.2* ortholog ESTs were identified using BLAST search of the Green plant GenBank experimental cDNA/EST database (arabidopsis.org/Blast/) (Figure 4.2). Consensus *Bn*KAT5.1 and *Bn*KAT5.2 sequences were deduced from four (EE471427.1, EV056068.1, EV041699.1, and EV041016.1), and three (EV020238.1, EV046148.1, and EV120853.1) overlapping ESTs, respectively. The *Bn*KAT5.1 and *Bn*KAT5.2 sequences are identical except for the 5' region, which contains the UTR of *Bn*KAT5.1 and the UTR and coding sequence of *Bn*KAT5.2. The presence of in frame stop codons upstream of the *BnKAT5.1* and *BnKAT5.2* start codons suggests that the ORF does not extend further into the 5' UTR sequence and that an additional upstream exon encoding a PTS2 is not absent due to a failure to extend to the far 5' UTR.

A KAT5 homologue is conserved in *C. papaya* with 76% identity at the coding sequence nucleotide level, and 75% identity and 88% similarity at the protein amino acid level. Intron-exon number and structure is conserved at the nucleotide level (Figure 4.3). *C. papaya* KAT5 has two alternate start codons similar to that in *A. thaliana* suggesting dual localisation to the cytosol and peroxisome. KAT5 from *A. thaliana, A. lyrata, C. papaya* and *B. napus* have a predicted PTS2 after the first methionine (Figure 4.4). The high degree of similarity following the secondary methionine (associated with KAT5.1) and the lack of an obvious targeting signal suggests cytosolic localisation of these peptides, based on the previous experimental evidence from *A. thaliana* (Carrie *et al.*, 2007).

BLAST search for *C. papaya* ESTs at the Plant GDB database (www.plantgdb.org/CpGDB/cgi-bin/blastGDB.pl) using the *CpKAT5* sequence resulted in three hits with 99-100% identity (EX266413, 1027 bp; EX273034, 905 bp; EX283228, 707 bp), which appear to be derived from the same coding sequence. This suggests that the *CpKAT5* gene is expressed, but unfortunately none of these three sequences extend to the 5' UTR to determine if the sequence expressed is similar to *KAT5.1* or *KAT5.2*. No cDNAs were identified from the collection.

This implies that the most distant relative to *A. thaliana* with a putative cytosolic localised KAT5 ortholog with evidence of expression is *B. napus*. Current estimates place the separation of *Arabidopsis* from the genus *Brassica*, including *B. napus*, at approximately 43 Mya (Beilstein *et al.*, 2010). The more distantly related *C. papaya* may also have a KAT5 ortholog, but evidence for the expression of a cytosolic isoform is absent from publicly available EST and cDNA databases. Therefore dual localisation of KAT5 orthologs is plausibly conserved in the order Brassicales of which *A. thaliana, B. napus* and *C. papaya* are members.

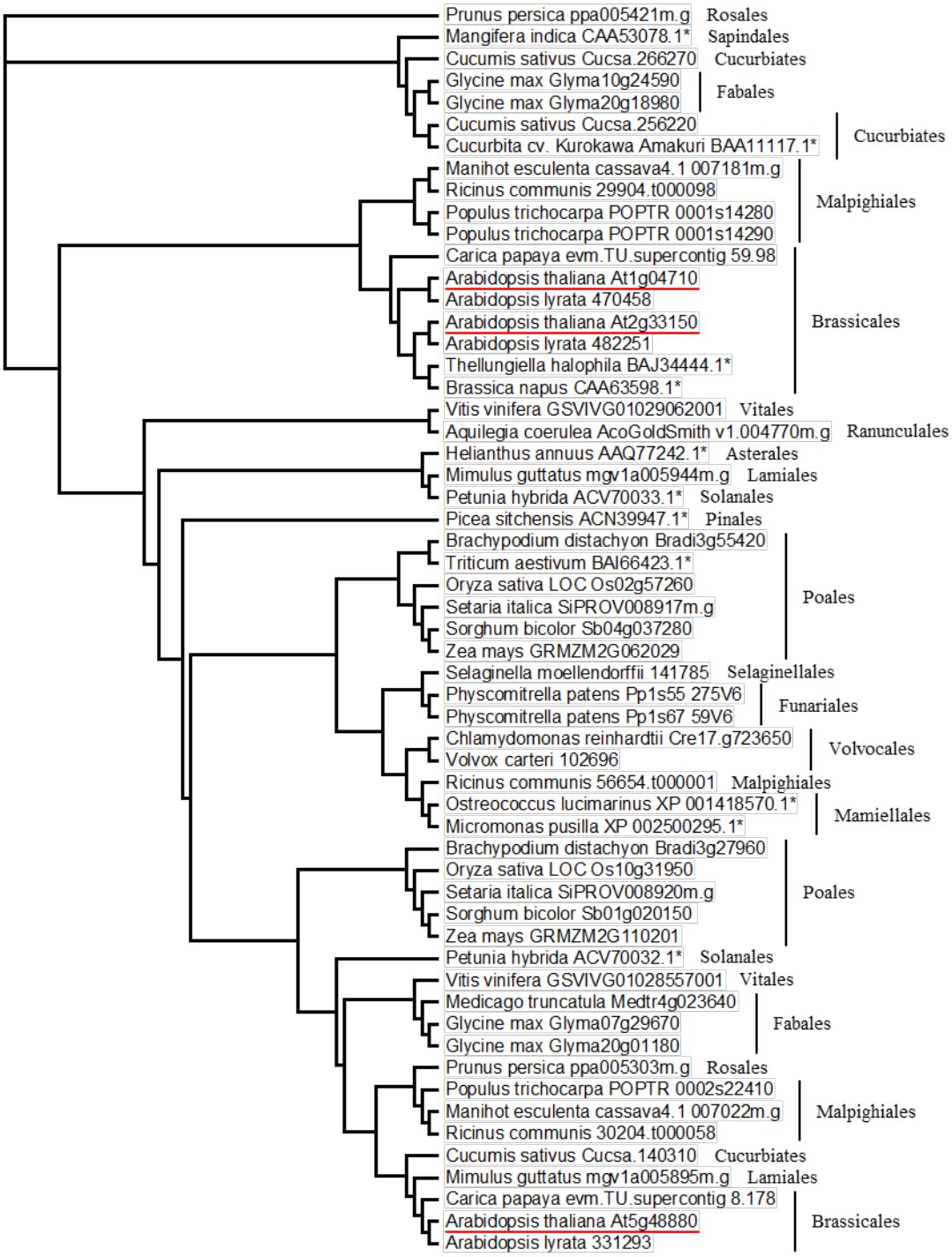

Figure 4.1. Phylogenetic tree of the plant thiolase family proteins.

Sequences were retrieved from Phytozome and NCBI. A multiple sequence alignment was constructed using the ClustalW2 algorithm and represented in a phylogram format using Treeview. *Arabidopsis thaliana KAT1* (At1g04710), *KAT2* (At2g33150) and *KAT5* (At5g48880) are underlined in red. Sequences retrieved from NCBI are marked with asterisk. Taxonomic order of the species is annotated to the right.

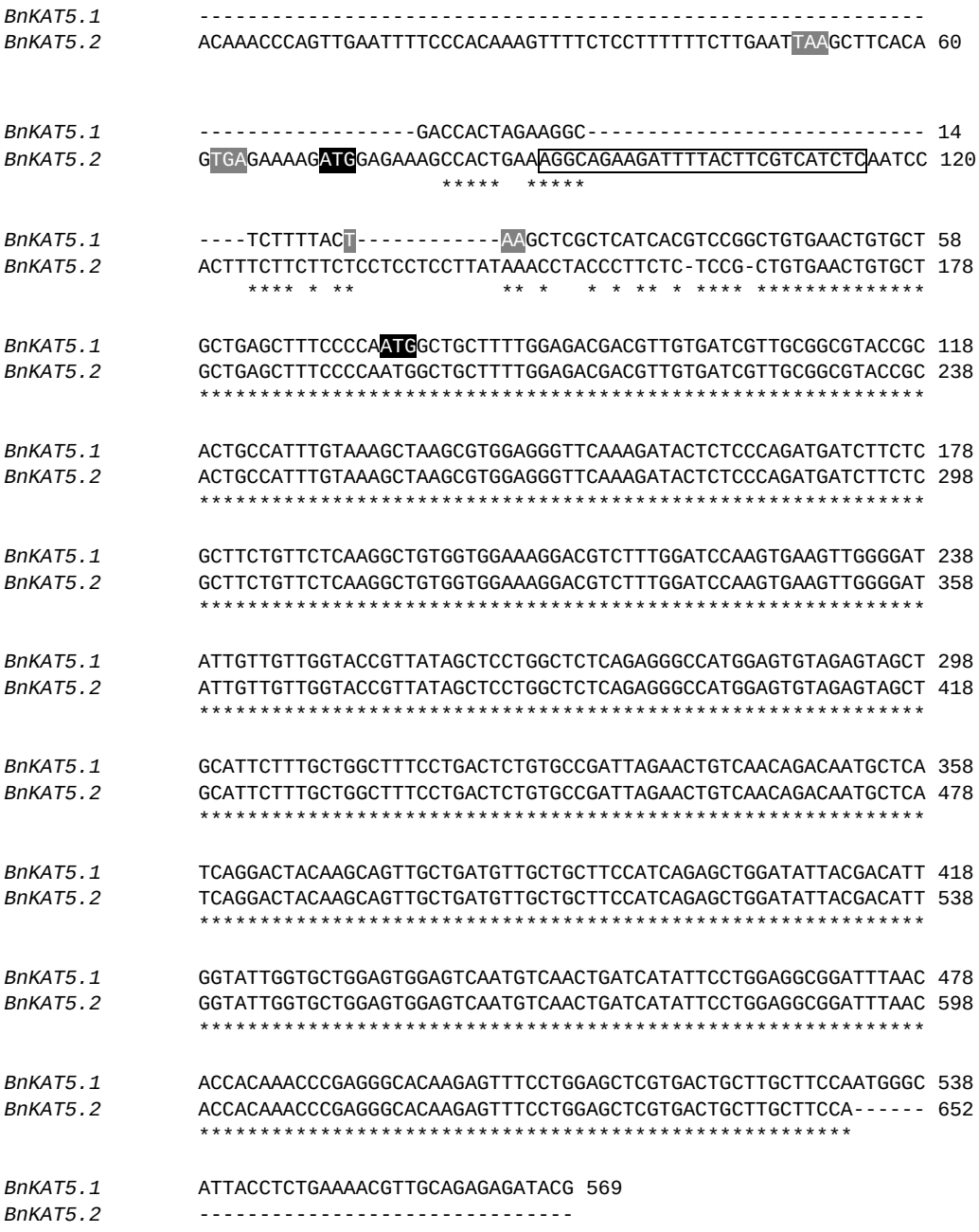

Figure 4.2. Nucleotide sequence alignment of *BnKAT5.1* and *BnKAT5.2* EST consensus sequences.

Consensus sequences were aligned with ClustalW2 algorithm. *BnKAT5.1* and *BnKAT5.2* show sequence identity throughout shared regions except for the 5' end, differing in the 1st exon of *BnKAT5.2* (which encodes a PTS2) and the 5' UTR of *BnKAT5.1*. Start codons are highlighted in black, with upstream in-frame stop codons in grey and *BnKAT5.2* sequence encoding PTS2 outlined in black.


AtKAT.2 ATGGAGAGAGCTATGGAAAGACAAAAGATATTGCTTCGTCATCTCAATCCAG------TT 54
CpKAT.2 ATGGAGAAAGCACTTAACAGAAATAGAATTCTGCTTCATCACTTAAACCCCACCTCCTTT 60
AtKAT.2 TCTTCTTCTAATTCTTCT-CTTAAAC-----ATGAACCTTCTCTTCTGTCTCCTGTGAAT 108
CpKAT.2 TCTTCTTCTTCTTCTTCTTCTCAAACCCACGATGAATCTGCTCCTATCTTTGCTTCAAAT 120
AtKAT.2 TGTGTTTCTGAAGTTT---CCCCA---------ATGGCTGCTTTTGGAGATGACATTGTG 156
CpKAT.2 TGTGCTGCTGGAGATAGTGCTGCATATCAACGGATGGCTGCTTTTGGAGATGATATTGTG 180
AtKAT.2 ATTGTAGCGGCATATCGTACCGCCATTTGCAAAGCGAGACGTGGAGGTTTCAAAGACACT 216
CpKAT.2 ATTGTCGCTGCATGCCGCACTGCCATTTGCAAGGCCAGGCGTGGAGGTTTCAAGGATACC 240
AtKAT.2 CTTCCTGATGATCTTCTTGCTTCTGTTCTTAAGGCTGTAGTGGAAAGAACATCTTTGGAT 276
CpKAT.2 TTAGCTGATGACCTGCTTGCTGCTGTTCTCAAGGCACTGATAGACAAAACAGCATTGAAC 300
AtKAT.2 CCAAGTGAAGTTGGTGATATCGTTGTTGGTACCGTGATAGCGCCTGGTTCTCAGAGAGCA 336
CpKAT.2 CCAAGTGAAGTTGGGGATATAGTGGTTGGTACAGTTTTGGCGCCGGGTTCAGAGAGAGCA 360
AtKAT.2 ATGGAGTGTAGAGTTGCAGCTTATTTTGCTGGTTTTCCTGACTCCGTGCCAGTTAGAACT 396
CpKAT.2 ATGGAGTGTAGGATGGCAGCATTCTATGCTGGTTTCCCTGATAAGGTGCCCGTTAGAACT 420
AtKAT.2 GTCAATAGACAATGCTCATCAGGACTACAAGCAGTTGCTGATGTTGCTGCTTCCATTAGA 456
CpKAT.2 GTCAATAGGCAGTGTTCATCTGGCCTACAGGCAGTTGCTGATGTCGCTGCTTCTATCAAA 480
AtKAT.2 GCTGGTTATTACGACATTGGTATTGGTGCTGGAGTGGAATCAATGTCAACTGATCATATT 516
CpKAT.2 GCAGGATATTATGACATCGGCATTGCAGCTGGAGTGGAGTCGATGACTGTGGATGGTACC 540
AtKAT.2 CCTGGAGGCGGCTTTCATGGCTCTAATCCAAGAGCACAGGATTTCCCAAAAGCCCGTGAT 576
CpKAT.2 GGTAGTGGCAAGTTTCGCCATATTAATCCAAAAACAGAGAGTTTTGCCCAAGCTCGAGAT 600
AtKAT.2 TGTTTGCTTCCAATGGGAATTACTTCTGAAAACGTTGCAGAAAGGTTCGGTGTCACAAGA 636
CpKAT.2 TGTCTTCTTCCTATGGGAATTACTTCTGAAATTGTTGCAGAGCGATATGGAGTGACAAGA 660
AtKAT.2 GAAGAGCAAGATATGGCTGCGGTGGAGTCTCACAAACGCGCTGCAGCTGCAATCGCGTCT 696
CpKAT.2 CAAGAACAAGATCAGGCTGCTGTTGAATCTCATAGGCGTGCATCTGCTGCAACAGCTTCC 720
ATKAT.2 GGTAAACTCAAGGATGAAATCATTCCTGTTGCTACTAAGATTGTGGACCCTGAGACTAAA 756
CpKAT.2 GGTAAATTCGAAGATGAAATTATCCCTGTTTCAACTAAGATTTTAGACCCTCAAACTGGG 780
AtKAT.2 GCAGAGAAGGCAATCGTCGTATCTGTTGATGACGGTGTACGTCCAAACTCAAACATGGCA 816
CpKAT.2 GAAGAGAAATTAGTCTCCATTTCTGTTGACGATGGAATCCGACCAAACACAAACATGATA 840
AtKAT.2 GATTTGGCAAAGCTGAAGACTGTCTTTAAACAGAACGGTTCCACCACAGCTGGCAATGCT 876
CpKAT.2 GATCTTGCAAAACTTAAACCCGCATTCAAAAATGATGGAAGCACCACAGCTGGCAACGCT 900
AtKAT.2 AGTCAGATCAGTGATGGTGCTGGAGCAGTACTGCTAATGAAGAGAAGTTTGGCTATGAAG 936
CpKAT.2 AGCCAGGTGAGCGATGGTGCTGGAGCAGTCCTCCTCATGAAAAGAAGTTTGGCAATGAAG 960
AtKAT.2 AAGGGACTTCCCATTCTTGGAGTATTCAGGAGTTTTGCTGTTACTGGTGTGGAACCATCT 996
CpKAT.2 AGAGGACTTCCAATTCTTGGTGTCTTCAGGAGTTTCGCTGCTGTTGGTGTGGATCCTTCT 1020
AtKAT.2 GTAATGGGTATTGGTCCAGCTGTTGCCATTCCCGCTGCAACTAAGCTCGCAGGGCTCAAC 1056
CpKAT.2 GTTATGGGCATAGGTCCATCTGTTGCTATTCCAGCTGCAGTTAAGTCTGCTGGTCTTGAG 1080

```
AtKAT.2         GTCAGCGATATTGATCTATTCGAGATCAATGAGGCATTTGCATCTCAGTATGTGTACTCT 1116
CpKAT.2         CTTGATAACATTGACATCTTTGAGATTAACGAGGCGTTTGCTTCACAGTTTGTATATTGC 1140
                 *     * *****  * ** ***** ** ***** ***** ** **** *** ** *

AtKAT.2         TGCAAGAAGTTAGAGCTGGATATGGAAAAGGTCAATGTTAATGGAGGAGCCATTGCTATT 1176
CpKAT.2         TGTAAAAAACTGGAGCTTGATCCAGAAAAAGTCAATGTTAATGGAGGTGCTATCGCTCTT 1200
                ** ** **  * ***** ***   ***** ***************** ** ** *** **

AtKAT.2         GGCCATCCCCTGGGTGCTACAGGAGCTCGATGTGTTGCGACATTGTTGCACGAGATGAAG 1236
CpKAT.2         GGGCATCCTCTGGGTGCTACAGGTGCTCGTTGTGTTGCAACTCTACTGCATGAGATGAAA 1260
                ** ***** ************** ***** ******** **  *  **** ********

AtKAT.2         CGGAGAGGAAAAGATTGCCGCTTTGGAGTAATCTCAATGTGCATAGGCACTGGAATGGGA 1296
CpKAT.2         CGTCGTGGAAGGGATTGCCGTTTTGGAGTCATTTCAATGTGCATAGGTTCGGGAATGGGT 1320
                **  * ****  ******** ******** ** **************  * ********

AtKAT.2         GCTGCAGCTGTTTTTGAGAGGGGAGACTCTGTTGATAACTTGTCCAACGCTCGTGTGGCT 1356
CpKAT.2         GCCGCCGCTGTTCTTGAAAGAGGCGACTGCACTGATGAATTAAGTAATGCTCGACCCGTC 1380
                ** ** ****** **** ** ** ****    **** * **    ** *****    *

AtKAT.2         AACGGGGATAGTCATTAG 1374
CpKAT.2         AAC---------CATTAA 1389
                    ***         *****
```

Figure 4.3. Nucleotide sequence alignment of *AtKAT5.2* and CpKAT5.2 coding sequence.

The *Arabidopsis thaliana KAT5.2* and predicted *Carica papaya* orthologous gene sequences were retrieved from Phytozome, and aligned with ClustalW2. Exon-intron structure as predicted by Phytozome is annotated by alternately underlining and not underlining the predicted exons. Intron sequences are not shown The alternate start codons of *KAT5.1* and *KAT5.2* are highlighted in black.

```
AtKAT5.2        MERAMERQKILLRHLN----PVSSSNSSLKHEPSLLSPVNCVS----EVSPMAAFGDDIV 52
AlKAT5.2        MEKAVERQKILLRHLN----PISSTNSSLNHEPSLFSLVNCAS----EVSPMAAFGDDIV 52
BnKAT5.2        MEKATERQKILLRHLN----PLSS--SPPPYKPTLLSAVNCAA----ELSPMAAFGDDVV 50
CpKAT5.2        MEKALNRNRILLHHLNPTSFSSSSSSSQTHDESAPIFASNCAAGDSAAYQRMAAFGDDIV 60
                **:* :*::***:***    . **  *    :.: :   **.:      . *******:*

AtKAT5.2        IVAAYRTAICKARRGGFKDTLPDDLLASVLKAVVERTSLDPSEVGDIVVGTVIAPGSQRA 112
AlKAT5.2        IVAAYRTAICKARRGGFKDTLPDDLLASVLKAVVERTSLDPSEVGDIVVGTVIAPGSQRA 112
BnKAT5.2        IVAAYRTAICKAKRGGFKDTLPDDLLASVLKAVVERTSLDPSEVGDIVVGTVIAPGSQRA 110
CpKAT5.2        IVAACRTAICKARRGGFKDTLADDLLAAVLKALIDKTALNPSEVGDIVVGTVLAPGSERA 120
                **** *******:********.*****:****::::*:*:************:****:**

AtKAT5.2        MECRVAAYFAGFPDSVPVRTVNRQCSSGLQAVADVAASIRAGYYDIGIGAGVESMSTDHI 172
AlKAT5.2        MECRVAAYFAGFPDTVPVRTVNRQCSSGLQAVADVAASIRAGYYDIGIGAGVESMSTDHI 172
BnKAT5.2        MECRVAAFFAGFPDSVPIRTVNRQCSSGLQAVADVAASIRAGYYDIGIGAGVESMSTDHI 170
CpKAT5.2        MECRMAAFYAGFPDKVPVRTVNRQCSSGLQAVADVAASIKAGYYDIGIAAGVESMTVDGT 180
                ****:**::*****.**:*********************:********.******:.*

AtKAT5.2        PGGGFHGSNPRAQDFPKARDCLLPMGITSENVAERFGVTREEQDMAAVESHKRAAAAIAS 232
AlKAT5.2        PGGGFHASNPRAQDFPKARDCLLPMGITSENVAERFGVTREEQDMAAVESHKRAAAAITS 232
BnKAT5.2        PGGGFNTTNPRAQEFPGARDCLLP---------------------------------- 194
CpKAT5.2        GSGKFRHINPKTESFAQARDCLLPMGITSEIVAERYGVTRQEQDQAAVESHRRASAATAS 240
                 .* *.  **:::.*. *******

AtKAT5.2        GKLKDEIIPVATKIVDPETKAEKAIVVSVDDGVRPNSNMADLAKLKTVFKQNGSTTAGNA 292
AlKAT5.2        GKLKDEIIPVATKIVDPETKAEKAIVVSVDDGVRPNSNLADLAKLKTVFKQNGSTTAGNA 292
BnKAT5.2        ------------------------------------------------------------
CpKAT5.2        GKFEDEIIPVSTKILDPQTGEEKLVSISVDDGIRPNTNMIDLAKLKPAFKNDGSTTAGNA 300

AtKAT5.2        SQISDGAGAVLLMKRSLAMKKGLPILGVFRSFAVTGVEPSVMGIGPAVAIPAATKLAGLN 352
AlKAT5.2        SQISDGAGAVLLMKRSLAMKKGLPILGVFRSFAVTGVDPSVMGIGPAVAIPAATKLAGLN 352
BnKAT5.2        ------------------------------------------------------------
CpKAT5.2        SQVSDGAGAVLLMKRSLAMKRGLPILGVFRSFAAVGVDPSVMGIGPSVAIPAAVKSAGLE 360

AtKAT5.2        VSDIDLFEINEAFASQYVYSCKKLELDMEKVNVNGGAIAIGHPLGATGARCVATLLHEMK 412
AlKAT5.2        VSDIDLFEINEAFASQYVYCCKKLELDMEKVNVNGGAIAIGHPLGATGARCVATLLHEMK 412
BnKAT5.2        ------------------------------------------------------------
CpKAT5.2        LDNIDIFEINEAFASQFVYCCKKLELDPEKVNVNGGAIALGHPLGATGARCVATLLHEMK 420

AtKAT5.2        RRGKDCRFGVISMCIGTGMGAAAVFERGDSVDNLSNARVANGDSH 457
AlKAT5.2        RRGKDCRFGVISMCIGTGMGAAAVFERGDSVDNLSNARVANGDDH 457
BnKAT5.2        -------------------------------------------
CpKAT5.2        RRGRDCRFGVISMCIGSGMGAAAVLERGDCTDELSNARPVNH--- 462
```

Figure 4.4. Amino acid sequence alignment of *KAT5.2* orthologous sequences.

The *Arabidopsis thaliana*, *Arabidopsis lyrata*, *Carica papaya* and *Brassica napus* KAT5.2 amino acid sequences were aligned with ClustalW2. The alternate initial methionines of *KAT5.1* and *KAT5.2* are highlighted in black, with the PTS2 outlined in black.

4.2.2 Analysis of Arabidopsis thiolase gene promoters

4.2.2.1 Experimental analysis using promoter-GUS reporter fusions

Promoter sequences were amplified by PCR from wild-type Col-0 genomic DNA. Amplified promoter fragments extended approximately 2 kb upstream of the start codons (*KAT2*, 2156 bp; *KAT5.1*, 2151 bp; *KAT5.2*, 2125 bp) or until the adjacent gene (*KAT1*, 1010 bp), (Figure 4.5). They were cloned using Gateway technology into pDONR207. The constructs were sequenced and then the promoter fragments were inserted into the GUS/GFP fusion promoter reporter plasmid pHGWFS7 (Karimi *et al.*, 2002). Wild-type Col-0 plants were transformed with this construct, and selected to homozygosity of the T-DNA in the T3 generation, using hygromycin resistance as a selective marker. *KAT5.1-GUS* here includes the first exon and 5' UTR of *KAT5.2* and thus includes the full putative promoter that might drive independent transcription of cytosolic *KAT5.1* (Figure 4.5).

As a result, 11 *KAT1-GUS*, 9 *KAT2-GUS*, 10 *KAT5.1-GUS*, and 10 *KAT5.2-GUS* independent transformants were obtained and screened for GUS activity. Lines giving GUS staining patterens representative of the group were selected for more detailed analysis. GUS promoter analysis of seedlings from 2 to 6 d post-stratification suggested low levels of expression for *KAT1-GUS* and *KAT5.2-GUS*, with higher levels for *KAT2-GUS* and *KAT5.1-GUS* (Figure 4.6). In *KAT1-GUS* lines, activity was nearly absent but some GUS staining was observed in the root tip. *KAT2-GUS* is expressed strongly in the cotyledons and hypocotyls, as well as the root tip, with this activity diminishing significantly by 4 d. *KAT5.1-GUS* expression was strong in the cotyledons, hypocotyl and root at 2 d, receding rapidly from the outer edges of the cotyledons to be absent almost entirely by 4 d. Expression in the root remained consistently strong for the 5 d analysed, but was absent from the root tip. Activity was observed in the new leaves forming at the meristem. *KAT5.2-GUS* had lower expression levels with some staining of the base of the hypocotyl and also just above the root tip during the first 3 d of germination. Seedlings grown for 16 d on MS media were also stained for promoter activity (Figure 4.7). Promoter activity was again absent in *KAT1-GUS* lines (Figure 4.7A). *KAT2-GUS* and *KAT5.1-GUS* were expressed in the roots, petioles and new leaves of the rosette meristem (Figure 4.7B-C). *KAT5.2-GUS* promoter activity was limited to petioles (Figure 4.7D).

In flowers, again the *KAT1-GUS* promoter expression was absent at all stages, with only faint staining observed in the immature anthers of young buds in some of the lines (Figure 4.8). *KAT2-GUS* expression increased as flowers mature, and was first observed at early stages in young anthers and petals. As the flowers mature strong staining was observed in the anther filament and petals as well as the tip of the gynoecium and developing ovules. The strongest activity of the *KAT5.1-GUS* promoter was observed in young anthers, but was not present at

later stages of flower development. *KAT5.2-GUS* promoter activity was also higher at earlier stages in petals, and largely absent at later stages. In some *KAT5.2-GUS* lines promoter activity was observed in the anther filament (not shown). Promoter analysis in silique tissue indicated activity in the developing ovules for *KAT2-GUS*, *KAT5.1-GUS* and *KAT5.2-GUS*, with promoter activity absent for the *KAT1-GUS* lines (Figure 4.9).

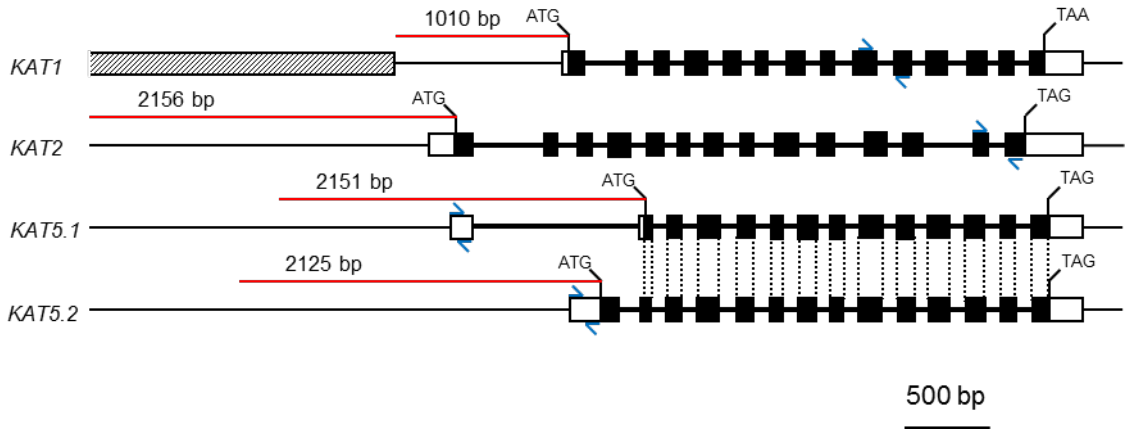

Figure 4.5. Thiolase gene structure and promoter regions used for reporter analysis.

The promoter region upstream of the gene start codon used for reporter analysis is indicated by the red line. Black boxes are exons, and white boxes are untranslated regions. The adjacent gene upstream of the *KAT1* gene is indicated by the grey shaded box. Exonic coding regions shared between the *KAT5.1* and *KAT5.2* genes are indicated by the dotted black lines. The location on the *KAT* gene where qRT-PCR primers used in Figure 4.10 anneal is annotated with blue arrows.

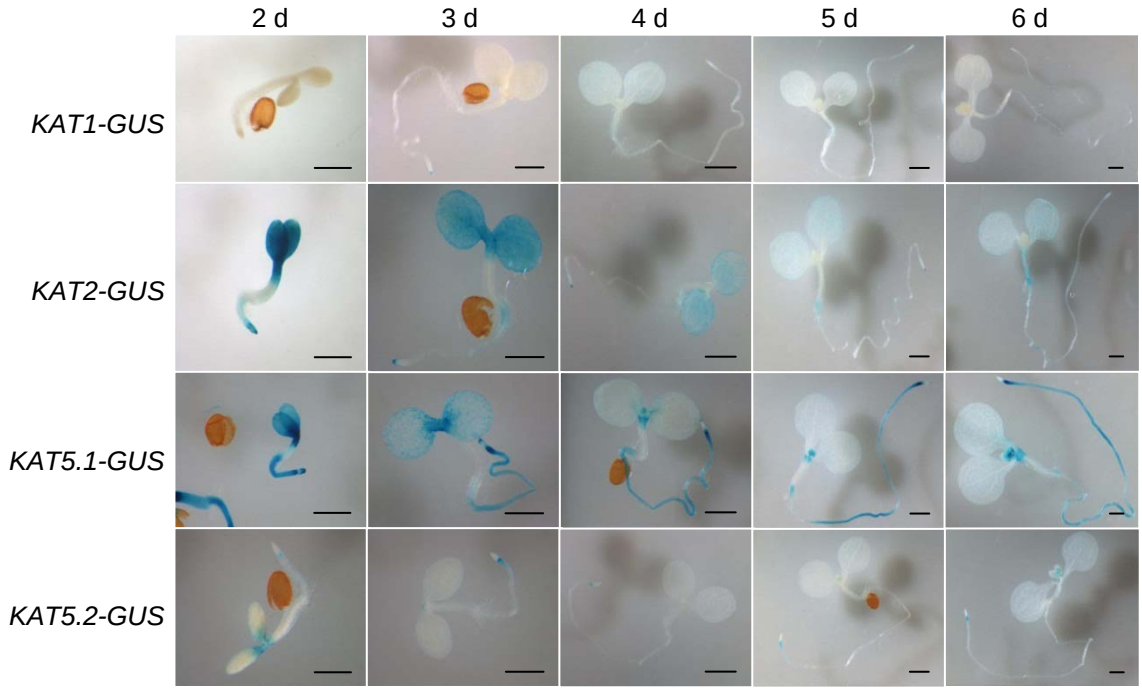

Figure 4.6. Activity of thiolase promoter reporters visualised using GUS during germination and seedling establishment.

Seedlings expressing thiolase promoter-GUS reporter constructs were grown from 2 to 6 d post-stratification on 0.5 x MS media, and stained for GUS activity. The length of the scale bar is 0.5 mm.

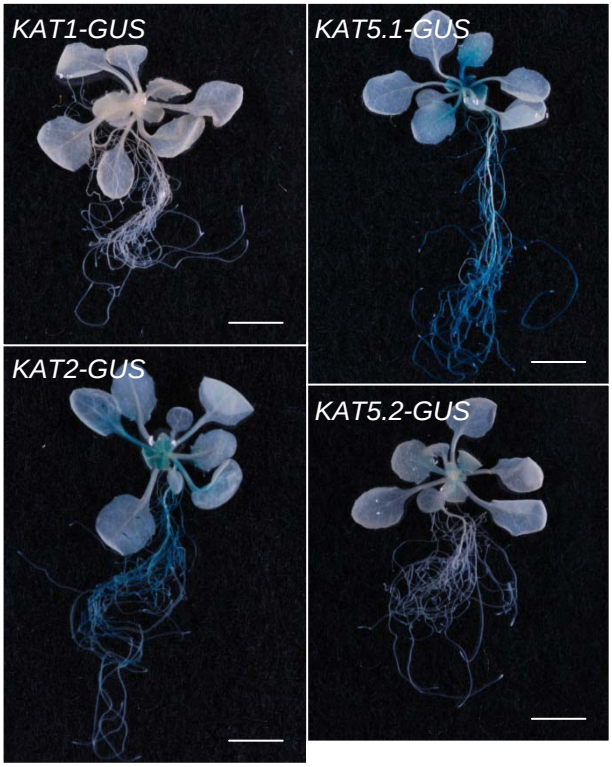

Figure 4.7. Activity of thiolase promoter reporters visualised using GUS in 16 d old seedlings.

Seedlings expressing thiolase promoter-GUS reporter constructs, *KAT1-GUS*, *KAT2-GUS*, *KAT5.1-GUS*, and *KAT5.2-GUS*, were grown for 16 d post-stratification on 0.5 x MS media, and stained for GUS activity. The length of the scale bar is 5 mm.

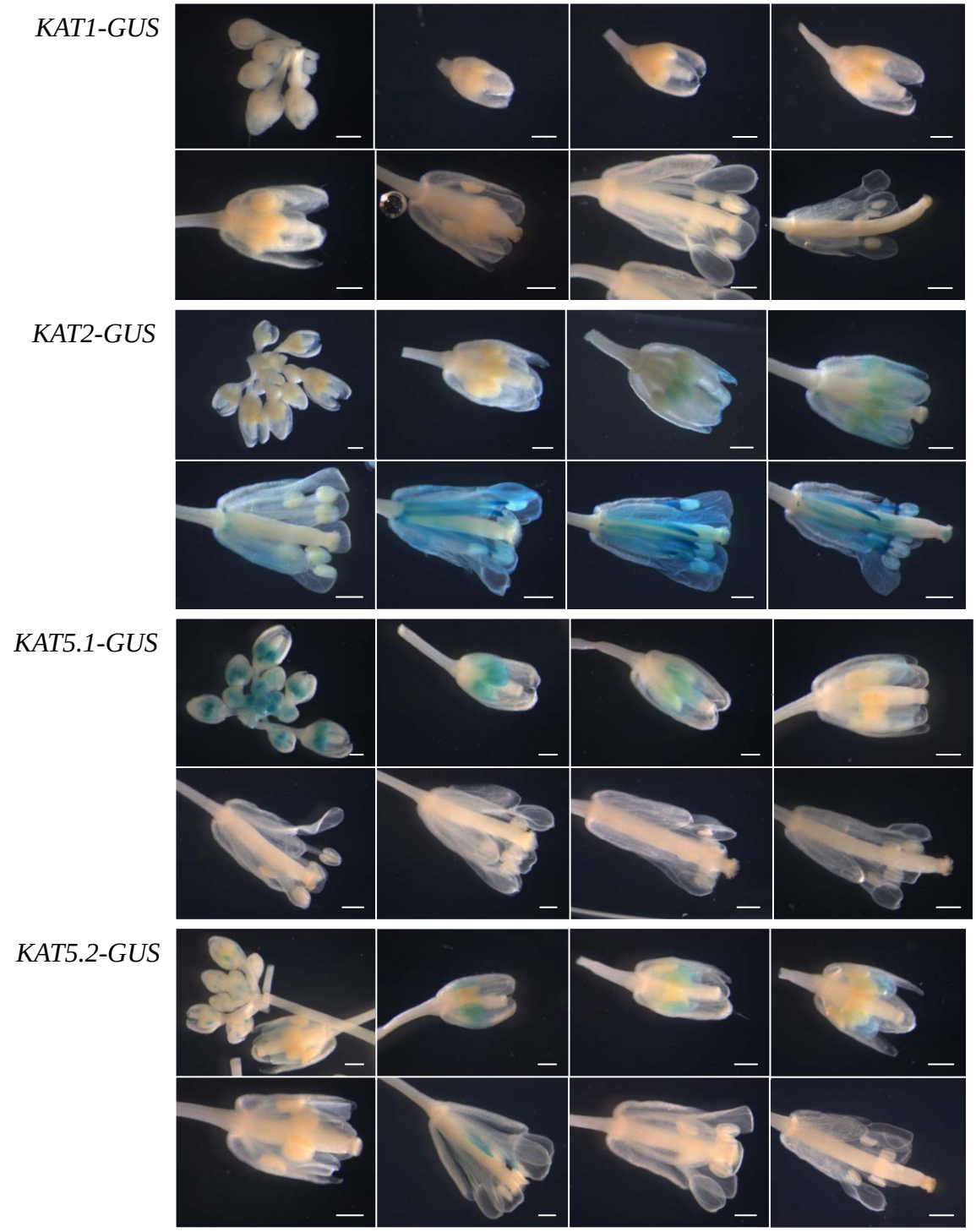

Figure 4.8. Thiolase promoter reporter activity visualised using GUS in flowers.

Flowers were removed from soil-grown Arabidopsis thiolase promoter-GUS reporter plants at various stages of development, and stained for GUS activity. The length of the scale bar is 0.5 mm.

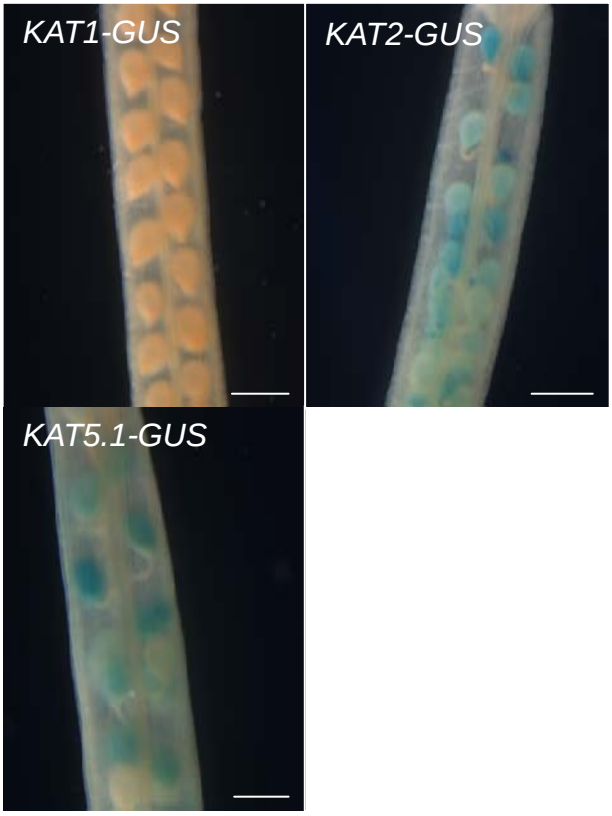

Figure 4.9. Thiolase promoter reporter activity visualised using GUS in siliques.

Thiolase promoter reporter plants, *KAT1-GUS*, *KAT2-GUS*, *KAT5.1-GUS*, and *KAT5.2-GUS*, were grown in soil. Siliques were removed and stained for GUS activity. The length of the scale bar is 0.5 mm.

4.2.2.2 Bioinformatic analysis of gene promoters

4.2.2.2.1 Athena analysis of thiolase and β-oxidation gene promoters

The presence of promoter elements in the thiolase genes was analysed bioinformatically using Athena ((O'Connor *et al.*, 2005); bioinformatics2.wsu.edu/Athena/), which searches for elements upstream of the gene's predicted transcription start site (Table 4.1). The region analysed was from 2 kb upstream of the transcription start site, or until reaching an adjacent gene in the case of *KAT1*. Athena also does not differentiate between *KAT5.1* and *KAT5.2*, analysing from the transcription start site of *KAT5.1*, 1064 bp and 818 bp upstream of the respective start codons of *KAT5.1* and *KAT5.2* (Figure 4.5).

There appears to be fewer predicted elements in the *KAT1* promoter compared to *KAT2* and *KAT5*. This may be partly because a shorter 989 bp region was analysed due to the close proximity of *KAT1* to the adjacent gene At1g04700. However, accounting for the size of the promoter region analysed, the thiolase genes have 9.1, 21.5 and 17 elements per kb for *KAT1*, *KAT2* and *KAT5* respectively. Fewer promoter elements upstream of the *KAT1* gene may be the reason for the low promoter activity observed in the GUS reporter system. The *KAT1* promoter has: putative MYB (MACCWAMC) and MYB4 (AMCWAMC) binding site motifs related to flower development and phenylpropanoid biosynthesis (Sablowski *et al.*, 1994; Zhao *et al.*, 2007); BoxII (GGTTAA) a light-responsive element (Green *et al.*, 1988); a hexamer (CCGTCG) meristem-specific element (Chaubet *et al.*, 1996); MYB1AT (WAACCA) related to ABA-response and dehydration (Abe *et al.*, 2003); and W-box (TTGACY) involved in pathogen-response (Rushton *et al.*, 1996).

The *KAT2* promoter contains the most predicted elements of the three thiolase genes. ABRE-like (BACGTGKM) (Yamaguchi-Shinozaki and Shinozaki, 2005), AtMYC2 (CACATG) (Abe *et al.*, 1997), MYB1AT (WAACCA) (Abe *et al.*, 2003), MYB2AT (TAACTG) (Urao *et al.*, 1993), and MYCATERD1 (CATGTG) (Simpson *et al.*, 2003) suggest a role for *KAT2* in ABA and dehydration-stress response. There are many light responsive elements including: CACGTG motif (Staiger *et al.*, 1989); GATA (AAGATAAGATT) (Gidoni *et al.*, 1989); I-box (GATAAG) (Giuliano *et al.*, 1988); BoxII (GGTTAA) (Green *et al.*, 1988); GBF1/2/3 BS (CCACGTGG) (McKendree *et al.*, 1990); and T-box (ACTTTG) (Chan *et al.*, 2001). Other putative elements identified include: W-box (TTGACY) related to pathogen-response (Rushton *et al.*, 1996); GA induced GAREAT (TAACAAR) (Ogawa *et al.*, 2003); embryogenesis related CARGCW8GAT (CWWWWWWWWG) (Perry *et al.*, 1996); and Evening Element (EE) promoter motif (AAAATATCT), associated with evening-specific timing of gene expression (Harmer *et al.*, 2000).

The *KAT5* promoter contains fewer putative elements than *KAT2*, but more than *KAT1*. The promoter contains: the ABA- and dehydration-responsive elements ATMYC2 BS in RD22 (CACATG) (Abe *et al.*, 1997); MYCATERD1 (CATGTG) (Simpson *et al.*, 2003); MYB1AT (WAACCA) (Abe *et al.*, 2003) and MYB2AT (TAACTG) (Urao *et al.*, 1993). It also contains: the pathogen responsive W-box (TTGACY) (Rushton *et al.*, 1996) and MYB1LEPR (GTTAGTT) (Chakravarthy *et al.*, 2003) elements; GA responsive GAREAT (TAACAAR) (Ogawa *et al.*, 2003); and embryogenesis-related CARGCW8GAT (CWWWWWWWWG) (Perry *et al.*, 1996). Again many light responsive were identified, including: T-box (ACTTTG) (Chan *et al.*, 2001); I-box (GATAAG) (Giuliano *et al.*, 1988); Gap-box (CAAATGAA) (Conley *et al.*, 1994). Additionally, the specific UV-responsive motifs MYB3 (TAACTAAC) (Jin *et al.*, 2000) and MYB4 (AMCWAMC) (Zhao *et al.*, 2007) were identified.

Promoter elements significantly enriched ($p<0.05$) in β-oxidation genes than in the Arabidopsis genome (Table 4.2) include: I-box motif; LTRE promoter motif (ACCGACA), a low temperature responsive element (Hughes and Dunn, 1996); ATHB6 binding site motif (CAATTATTA), associated with ABA signalling (Himmelbach *et al.*, 2002); AG binding site motif (TTDCCWWWWWWGGHAA) and the related motif AGL3 binding site (TTWCYAWWWWTRGWAA), associated with developmental control of expression. AGL3 is expressed in above-ground organs but not roots in contrast to related AGL1 and 2 which are flower-specific (Huang *et al.*, 1995). I-box was found in a large range of promoters for the β-oxidation subset and the Arabidopsis genome, 76% and 65% respectively. LTRE was identified in the promoters of *AIM1* (At4g29010), *CTS* (At4g39850), *AACT1* (At5g47720), and *AACT2* (At5g48230). ATHB6 binding site motif is present in the promoters of *ACX6* (At1g06310), *AIM1* (At4g29010), *LACS7* (At5g27600), and *AACT2* (At5g48230). The AG and AGL3 binding site motifs are only found in the *ACX4* (At3g51840) promoter. There appears to be no enriched transcription factor motifs based on the distribution of identified elements that could be a master-regulator of core β-oxidation gene expression during germination and seedling establishment.

A common factor or element responsible for the peaking of β-oxidation gene expression during the dark period of the circadian cycle is also not apparent from the Athena analysis. One candidate, EE (Harmer *et al.*, 2000), appears to be only present in the promoters of a limited number of circadian-regulated genes. An EE promoter motif has been identified and characterised in the *CAT3* gene promoter, and found to be essential for circadian regulation of expression, with transcript peaking in the evening (Michael and McClung, 2002). Circadian regulation of core β-oxidation genes with co-expression peaking during the dark period has previously been noted for *LACS6*, *LACS7*, *ACX2*, *MFP2*, *AIM1*, *KAT2* and *PMDH1* (Chapter 3). However, in an analysis of 21 β-oxidation genes using Athena the Evening Element promoter

motif was identified only in the promoters of *KAT2*, *CSY2* (At3g58750), *PMDH1* (At2g22780) and *CTS* (At4g39850), suggesting the presence of alternative promoter motifs responsible for the diurnal regulation of transcripts. CIRCADIAN CLOCK ASSOCIATED 1 (CCA1) binding site (AAAAAATCT) is another motif candidate associated with circadian regulation of gene expression (Alabadí *et al.*, 2001; Wang *et al.*, 1997). CCA1 binding site motifs were identified in *ACX3* (At1g06290), *ACX6* (At1g06310), *CSY3* (At2g42790), *LACS6* (At3g05970), *ACX4* (At3g51840), *CTS* (At4g39850), *PMDH2* (At5g09660), *LACS7* (At5g27600), *AACT2* (At5g48230), and *ACX2* (At5g65110). Although the EE and CCA1 promoter binding motifs differ by only a single base pair, it has been shown that modification of the *CAT3* gene promoter EE motif to a CCA1 motif results in the peak time of expression to shift from evening to morning (Michael and McClung, 2002).

Table 4.1. Athena analysis of thiolase gene promoter elements. Prediction of *KAT1*, *KAT2* and *KAT5* gene promoter elements were made using Athena which analyses genomic sequence upstream of predicted transcription start sites. The region analysed was 2 kb, not including genomic regions encoding adjacent genes as in the case of *KAT1* promoter. Athena does not differentiate between *KAT5.1* and *KAT5.2* using the transcription start site of *KAT5.1*, 635 bp upstream of the *KAT5.2* transcription start site.

Transcription Factor/Motif Name	**Element core sequence**	**Number of elements**			**Function**
		KAT1	KAT2	KAT5	
ABRE-like binding site motif	BACGTGKM		1		ABA, dehydration, salt, cold
AtMYC2 BS in RD22	CACATG		1	1	ABA, dehydration
CACGTGMOTIF	CACGTG		2		light, UV, flavonoid
EveningElement motif	AAAATATCT		1		evening-specific
GATA Motif	AAGATAAGATT		2		light
Gap-box Motif	CAAATGAA			1	light
Ibox promoter motif	GATAAG		6	2	light
MYB binding site promoter	MACCWAMC	1	1		flower-specific, phenylpropanoid
MYB1LEPR	GTTAGTT			1	pathogen, ethylene
MYB3 binding site motif	TAACTAAC			1	UV, phenylpropanoid
MYCATERD1	CATGTG		1	1	dehydration
TATA-box Motif	TATAAA	1	5	3	
ARF binding site motif	TGTCTC			2	auxin
BoxII promoter motif	GGTTAA	1	3		light
CARGCW8GAT	CWWWWWWWWG		4	6	embryogenesis
GAREAT	TAACAAR		4	2	GA
GBF1/2/3 BS in ADH1	CCACGTGG		2		light
Hexamer promoter motif	CCGTCG	1			meristem-specific
LEAFYATAG	CCAATGT		1		floral meristem-specific
MYB1AT	WAACCA	2	3	4	ABA, dehydration
MYB2AT	TAACTG		1	1	dehydration, salt
MYB4 binding site motif	AMCWAMC	2	1	4	UV, phenylpropanoid
T-box promoter motif	ACTTTG		3	3	light
W-box promoter motif	TTGACY	1	1	2	pathogen

Table 4.2. Athena analysis of β-oxidation gene promoter elements. Athena was used to predict promoter elements common to genes of β-oxidation, returning the frequency of promoter elements in the β-oxidation gene subset and the complete Arabidopsis genome, calculating the p-value of presence in the subset compared to the complete genome. The subset of β-oxidation genes used: *KAT1 (*At1g04710), *KAT2 (*At2g33150), *KAT5 (*At5g48880), *AACT1 (*At5g47720), *AACT2 (*At5g48230), *LACS6 (*At3g05970), *LACS7 (*At5g27600), *ACX1 (*At4g16760), *ACX2 (*At5g65110), *ACX3 (*At1g06290), *ACX4 (*At3g51840), *ACX5 (*At2g35690), *ACX6 (*At1g06310), *MFP2 (*At3g06860), *AIM1 (*At4g29010), *CSY1 (*At3g58740), *CSY2 (*At3g58750), *CSY3 (*At2g42790), *PMDH1 (*At2g22780), *PMDH2 (*At5g09660), and *CTS (*At4g39850).

Transcription Factor/ Motif Name	**prom's bound in subset**		**prom's bound in genome**		**p-value**
TATA-box Motif	85%	18	93%	28195	0.381
MYB1AT	80%	17	97%	29394	0.584
Ibox promoter motif	76%	16	65%	19685	0.002
W-box promoter motif	76%	16	88%	26630	0.303
CARGCW8GAT	76%	16	79%	23795	0.178
MYB4 binding site motif	76%	16	93%	28080	0.487
GAREAT	57%	12	77%	23321	0.663
T-box promoter motif	52%	11	80%	24250	0.763
MYB2AT	52%	11	50%	15041	0.053
MYCATERD1	47%	10	59%	17951	0.337
AtMYC2 BS in RD22	47%	10	59%	17951	0.337
CCA1 binding site motif	47%	10	44%	13377	0.108
ARF binding site motif	42%	9	65%	19629	0.516
BoxII promoter motif	33%	7	65%	19737	0.941
ABRE-like binding site motif	33%	7	32%	9695	0.234
MYB binding site promoter	28%	6	50%	15133	0.759
DRE core motif	28%	6	39%	11874	0.465
SV40 core promoter motif	23%	5	38%	11669	0.529
LEAFYATAG	23%	5	21%	6458	0.109
CACGTGMOTIF	23%	5	23%	7182	0.338
L1-box promoter motif	23%	5	25%	7796	0.415
ACGTABREMOTIFA2OSEM	19%	4	22%	6806	0.504
MYB1LEPR	19%	4	29%	8957	0.682
GADOWNAT	19%	4	13%	4115	0.179
LTRE promoter motif	19%	4	9%	2932	0.039
EveningElement promoter motif	19%	4	11%	3422	0.126
Gap-box Motif	19%	4	19%	5888	0.3
ATHB6 binding site motif	19%	4	6%	1933	0.024
RAV1-B binding site motif	14%	3	29%	8914	0.553
Hexamer promoter motif	14%	3	21%	6520	0.405
AtMYB2 BS in RD22	9%	2	23%	6920	0.84
AGL2ATCONSENSUS	9%	2	2%	704	0.055
CDA1ATCAB2	9%	2	6%	1825	0.202
GBF1/2/3 BS in ADH1	9%	2	2%	762	0.055
MYB3 binding site motif	9%	2	9%	2842	0.433
RY-repeat promoter motif	9%	2	6%	1928	0.275

Table 4.2 ctd

Transcription Factor/ Motif Name	prom's bound in subset		prom's bound in genome		p-value
ATHB2 binding site motif	9%	2	17%	5370	0.85
CArG promoter motif	9%	2	12%	3819	0.576
UPRMOTIFIAT	4%	1	5%	1504	0.548
ATHB5ATCORE	4%	1	5%	1798	0.601
MYB1 binding site motif	4%	1	14%	4286	0.796
PI promoter motif	4%	1	2%	632	0.216
TGA1 binding site motif	4%	1	5%	1504	0.548
GATA Motif	4%	1	0%	211	0.099
AGATCONSENSUS	4%	1	2%	713	0.289
DREB1A/CBF3	4%	1	13%	4208	0.852
ATHB2ATCONSENSUS	4%	1	2%	696	0.254
AG binding site motif	4%	1	0%	67	0.036
AP1/AG BS in SUP	4%	1	1%	321	0.141
AGL1ATCONSENSUS	4%	1	0%	168	0.085
AGL3 binding site motif	4%	1	0%	84	0.041
UPRE2AT	4%	1	0%	291	0.139
Z-box promoter motif	4%	1	4%	1329	0.525
TELO-box promoter motif	4%	1	16%	4939	0.918

4.2.2.2.2 PLACE analysis of thiolase gene promoters

Due to the limitation of the Athena bioinformatics tool, which only analyses sequence upstream of the transcription start site, analysis of sequence regions immediately upstream of translation start codons was not possible. This limited the promoter region analysed for *KAT1* and *KAT2* as well as preventing differentiation between *KAT5.1* and *KAT5.2*. To analyse promoter region sequences representative of those used in GUS reporter gene experiments, the bioinformatics tool PLACE was used (dna.affrc.go.jp/PLACE/) (Higo *et al.*, 1999). PLACE analysis of the promoter sequences used for GUS analysis confirmed the presence of many of the elements identified by Athena, as well as complementing this data set with additional putative promoter elements.

Differences between the *KAT5.1* and *KAT5.2* promoters used in GUS analysis appear to be minimal. The *KAT5.2* promoter has a few additional elements: ARFAT (Auxin response factor (Ulmasov *et al.*, 1997)); SORLREP2AT (light regulation (Jiao *et al.*, 2005)); and SEBFCONSSTPR10A (defence response (Boyle and Brisson, 2001)). The only element found in *KAT5.1* promoter and not in *KAT5.2* is GCN4OSGLUB1, associated with endosperm specific expression control of rice storage protein glutelin gene: *GluB-1* (Washida *et al.*, 1999). This element is also associated with *KAT2*. However, it is unclear how these promoter elements explain the higher expression observed for *KAT5.1* compared to *KAT5.2*, as well as that of *KAT2*. Potentially other unknown elements or factors explain the increased promoter activity in *KAT5.1* compared to *KAT5.2*, or there is regulation post-transcription. For example there may be additional regulation by elements in the intronic regions of the unspliced mRNA, particularly since alternative transcripts are transcribed from the *KAT5* gene.

Motifs associated with flavonoid biosynthesis genes were identified in the promoter regions for *KAT5.1* and *KAT5.2* by PLACE, which were not identified by Athena. There are two regions in the promoter with homology to the Box L element first characterised in the carrot (*Daucus carota*) *PAL1* gene, which is bound by the transcriptional activator DcMYB1 in response to elicitor treatment and UV-B irradiation (Maeda *et al.*, 2005). This Box L element is similar to the MYBPZM, a core consensus maize P (myb homolog) binding site, which controls red pigmentation of kernel pericarp, cob and floral organs (Grotewold *et al.*, 1994). The carrot Box L and maize MYBPZM elements also show homology to the Box L element identified in the promoter of parsley *PAL* genes, essential but not sufficient for elicitor- and light-responsive activation of *PAL* gene expression (Logemann *et al.*, 1995).

Another region contains an element that has homology to the Box II/G box site found in the parsley *CHS* promoter required for light regulation (Block *et al.*, 1990; Terzaghi and Cashmore, 1995). Box II is the binding site of Common Plant regulatory Factor (CPRF) -1, -2, -3, and -4, a

family of bZIP class transcription factors involved in light-mediated induction of the parsley *CHS* gene (Sprenger-Haussels and Weisshaar, 2000; Weisshaar *et al.*, 1991). This element also has a role in germinating seeds via transcriptional regulation of ABI-3 and ABA- responsive genes including RD29B and R29A (Nakashima *et al.*, 2006). One motif identified by PLACE and not Athena in the *KAT2*, *KAT5.1*, and *KAT5.2* promoters is the TGACGT motif, found in black gram (*Vigna mungo*) α-amylase gene promoter and required for high level expression in cotyledons of germinating seeds (Yamauchi, 2001).

The putative elements identified by Athena and PLACE suggest numerous possible mechanisms for developmental, stress-response and environmental controls of thiolase genes. In particular the identification of promoter motifs characterised from flavonoid biosynthesis genes in the *KAT5* promoter provides a mechanism of co-expression and co-regulation of *KAT5* with genes of this pathway. However, further experiments are required to empirically verify the response of *KAT* genes and requirement for putative promoter motifs/elements. There appears to be no enriched transcription factor motifs based on the distribution of identified elements that could be a master-regulator of core β-oxidation gene expression during germination and seedling establishment. Perhaps a new type of element awaits discovery. In *S. cerevisiae* β-oxidation genes are regulated by the Oaf1p and Oaf2p transcription factors (see discussion).

4.2.3 Quantitative analysis of thiolase gene expression

Expression analysis using qRT-PCR provides quantitative information of transcript levels (Figure 4.10). The expression level of *KAT2* appears to be much higher than the other thiolase genes, an order of magnitude greater. *KAT1* transcript is present in range of tissues at low levels including leaves, flowers, root, silique, and stem. *KAT2* transcript is present in the leaves, flower, silique, root, and stem, with expression to much higher levels in naturally senescing leaves. Transcript of *KAT5.2* is expressed at constitutively low levels in most plant tissues, with much higher levels of expression in flowers and siliques suggesting a more important role in reproductive tissue. Of the tissues measured, *KAT5.1* is expressed exclusively in the flowers and siliques. Induction of *KAT2* transcript in senescing leaves has previously been observed during dark-induced and natural senescence of Arabidopsis (Castillo and León, 2008). No up-regulation was observed for *KAT1*, *KAT5.1* or *KAT5.2* in naturally senescing leaves compared to green leaves in this study.

Arabidopsis thiolase gene expression from publicly available data was analysed to compare to the results from qualitative and quantitative expression analysis described in this chapter. *KAT1*, *KAT2* and *KAT5* were represented using the Genevestigator development plot (Figure 4.11) and anatomy charts (Figure 4.12) (Zimmermann *et al.*, 2004). *KAT1* is constitutively low while the closely related *KAT2* is expressed at a high level, especially during seed germination

and development at the two ends of plant development. *KAT5* displays an expression level between that of *KAT1* and *KAT2*, with the highest expression during seed development. From the anatomy chart it appears that the only tissue in which *KAT5* expression exceeds that of *KAT2* is in seed testa. This data would suggest that *KAT2* is the dominant thiolase in the vast majority of plant tissues.

The BAR eFP browser (Winter *et al.*, 2007) data broadly agrees with the experimental data from promoter analysis and qRT-PCR (Figure 4.13). Again, it is apparent that *KAT2* levels dwarf that of *KAT1* and *KAT5* with expression highest in germinating seeds and senescent leaf (Figure 4.13A). *KAT5* is high in naturally senescent leaf, flowers and siliques. *KAT1* is low for a range of tissues at different stages. Flower specific data shows low expression for *KAT1*, high for *KAT2*, and moderate for *KAT5* (Figure 4.13B). *KAT2* expression is high in all of the floral organs assayed. *KAT5* is high in petals, stamen and carpels, while *KAT1* is highest in pollen. Comparing flower stages of development *KAT1* transcript remains low, *KAT2* increases with development and *KAT5* remains constant (Figure 4.13C). A similar pattern is observed in siliques with a more dramatic decrease in *KAT5* activity with developing seed maturity (Figure 4.13D). Initially *KAT2* and *KAT5* transcript levels appear to be comparable; however, *KAT2* transcript abundance increases several-fold. Collectively, these observations suggest a role for both KAT2 and KAT5 in fertility, in both flowers and siliques.

Analysis with ATTED (Obayashi *et al.*, 2007) confirmed that *KAT5* is co-expressed with flavonoid genes, with direct links in the co-expression cluster to *CHALCONE FLAVANONE ISOMERASE* (*CFI*; At3g55120), *FLAVONOL SYNTHASE* (*FLS1*; At5g08640), and *4-COUMARATE:COA LIGASE 3* (*4CL3*; At1g65060) (Figure 4.14A). This was previously noted by Carrie *et al.* (2007) using BAR Expression Angler. Flavonoids act as molecular 'sun screens' to protect plants from UV damage. UV-B irradiation results in the induction of *KAT5* and genes of flavonoid biosynthesis including *CHALCONE SYNTHASE* (*CHS*; At5g12930), *FLS1* (At5g08640), *CFI* (At3g55120), and flavanone 3-hydroxylase (*F3H*; At3g51240), with expression peaking in roots at 3 h after UV-B exposure (Figure 4.14B).

Many of the enzymes involved in flavonoid biosynthesis have been demonstrated experimentally to interact with each other on the cytosolic face of the endoplasmic reticulum (Hrazdina and Wagner, 1985; Winkel-Shirley, 1999). To determine if an *in silico* prediction could be made for interaction partners of KAT5 that may be associated with this flavonoid biosynthesis complex, the Arabidopsis interaction viewer was interrogated (Geisler-Lee *et al.*, 2007). This identified 22 candidate proteins, five of which had a high interolog (interacting orthologs) confidence value (>10). These five candidates are O-Glycosyl hydrolase family 17 protein (At4g29360), 6-&1-fructan exohydrolase (6&1-FEH; At5g11920), phototropin 1

(PHOT1; At3g45780), poly(A) binding protein3 (PABN3; At5g10350) and calcium-dependent protein kinase 31 (CPK31; At4g04695). None of the predicted interaction partners have an obvious or direct role in flavonoid biosynthesis.

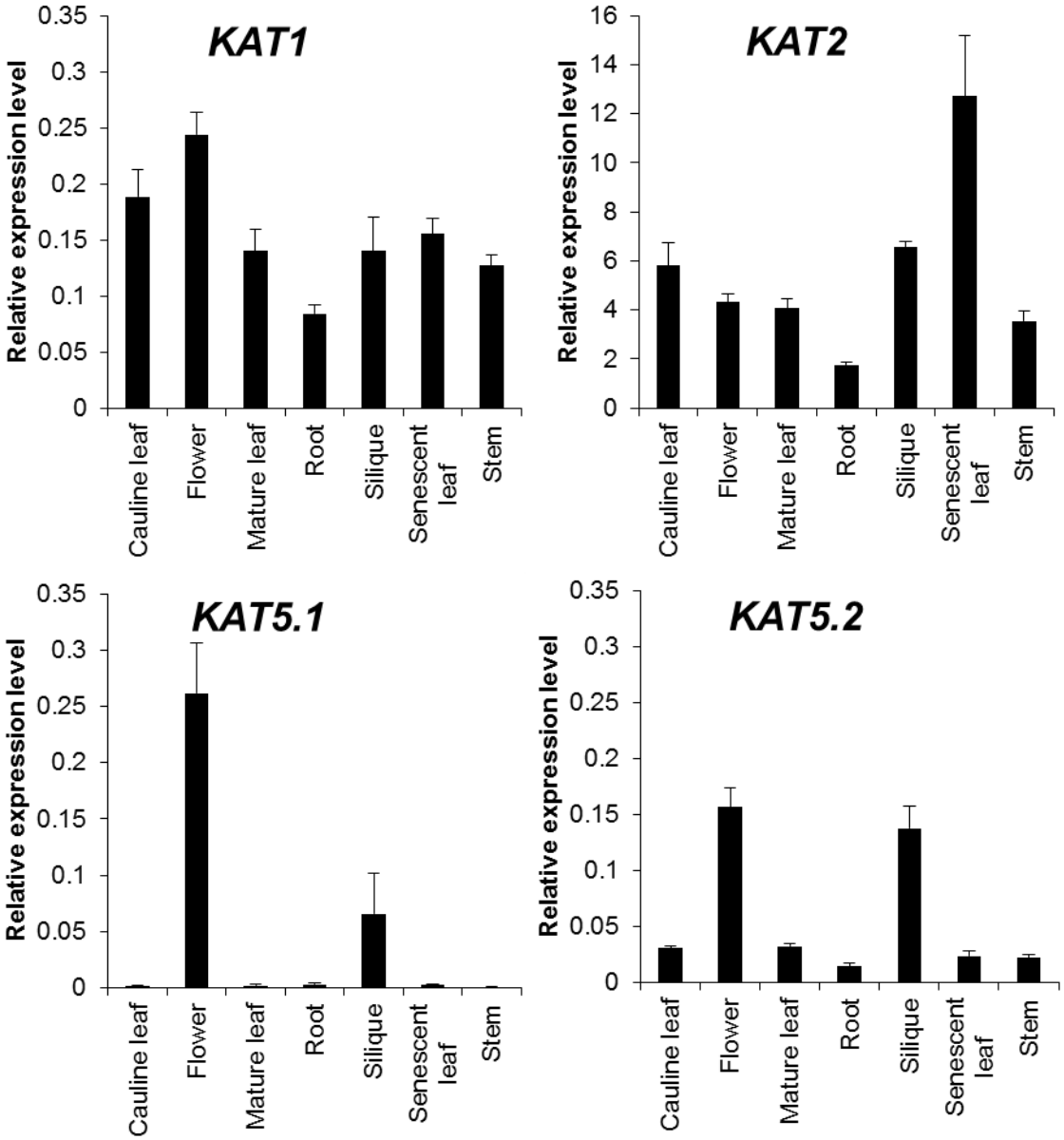

Figure 4.10. Quantitative RT-PCR of thiolase genes in different Arabidopsis organs.

Using qRT-PCR, the abundance of *KAT1*, *KAT2*, *KAT5.1* and *KAT5.2* transcripts was measured and normalised to the reference gene (*CACS*) transcript levels. Transcript was measured in cauline leaf, flower, mature leaf, root, silique, senescent leaf and stem. All charts use the same scale on the y-axis, except for *KAT2*. Error bars represent standard error from the mean (n=4).

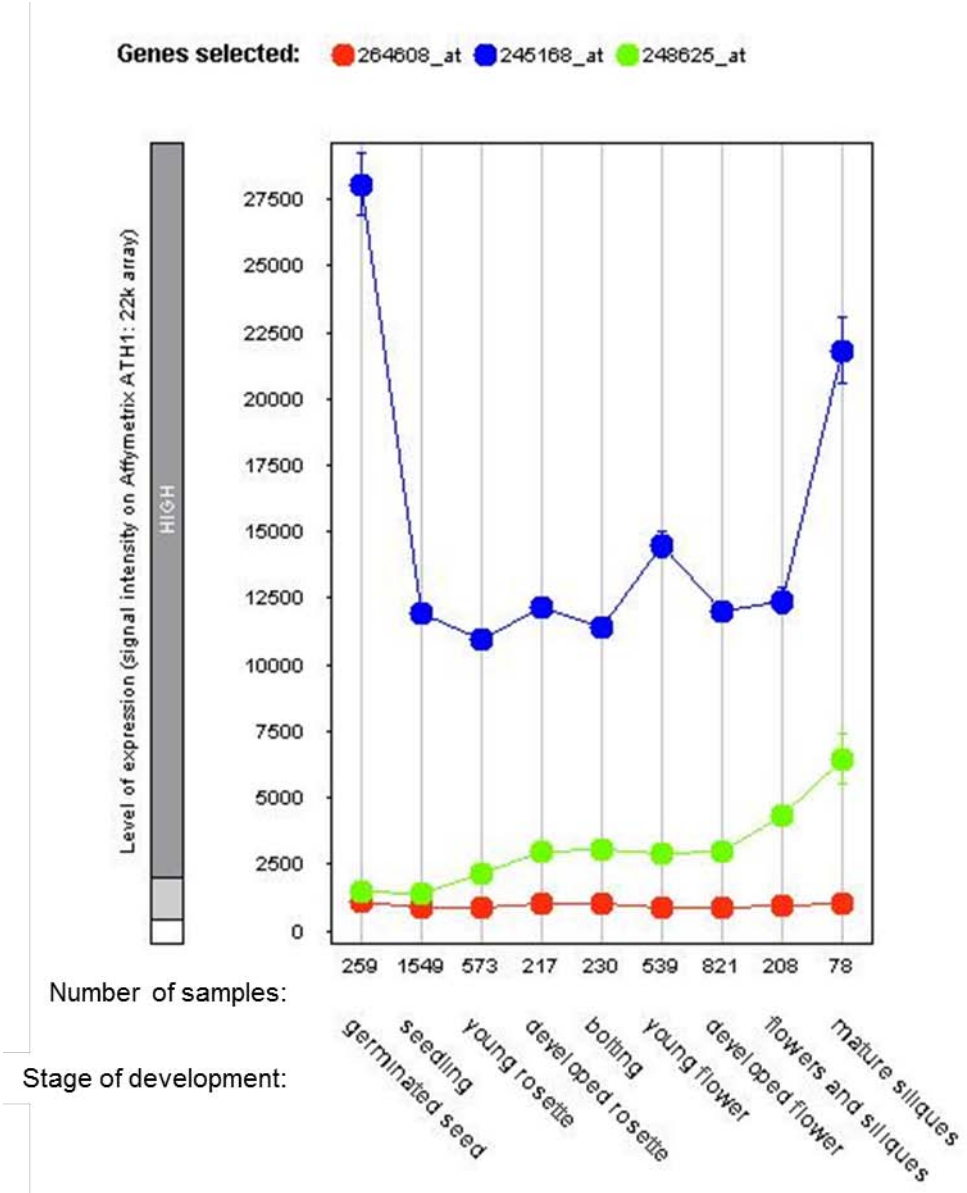

Figure 4.11. Genevestigator analysis of thiolase gene expression in Arabidopsis by developmental stage.

KAT1 (264608_at), *KAT2* (245168_at) and *KAT5* (248625_at) gene expression across the Arabidopsis life cycle as determined and represented by Genevestigator using publicly available microarray data.

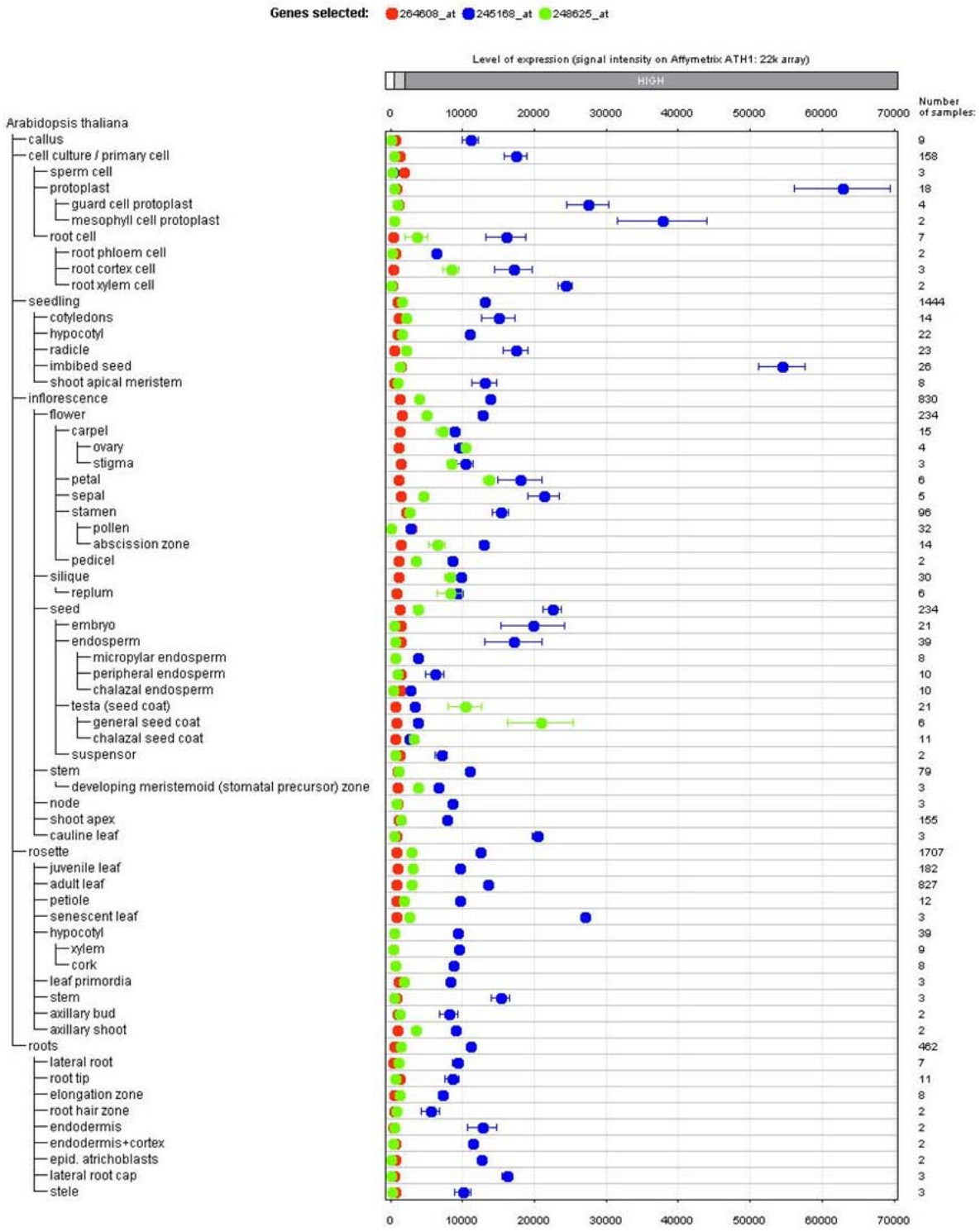

Figure 4.12. Genevestigator analysis of thiolase gene expression in Arabidopsis by anatomy.

KAT1 (264608_at), *KAT2* (245168_at) and *KAT5* (248625_at) gene expression across different Arabidopsis tissues and organs as determined and represented by Genevestigator using publicly available microarray data.

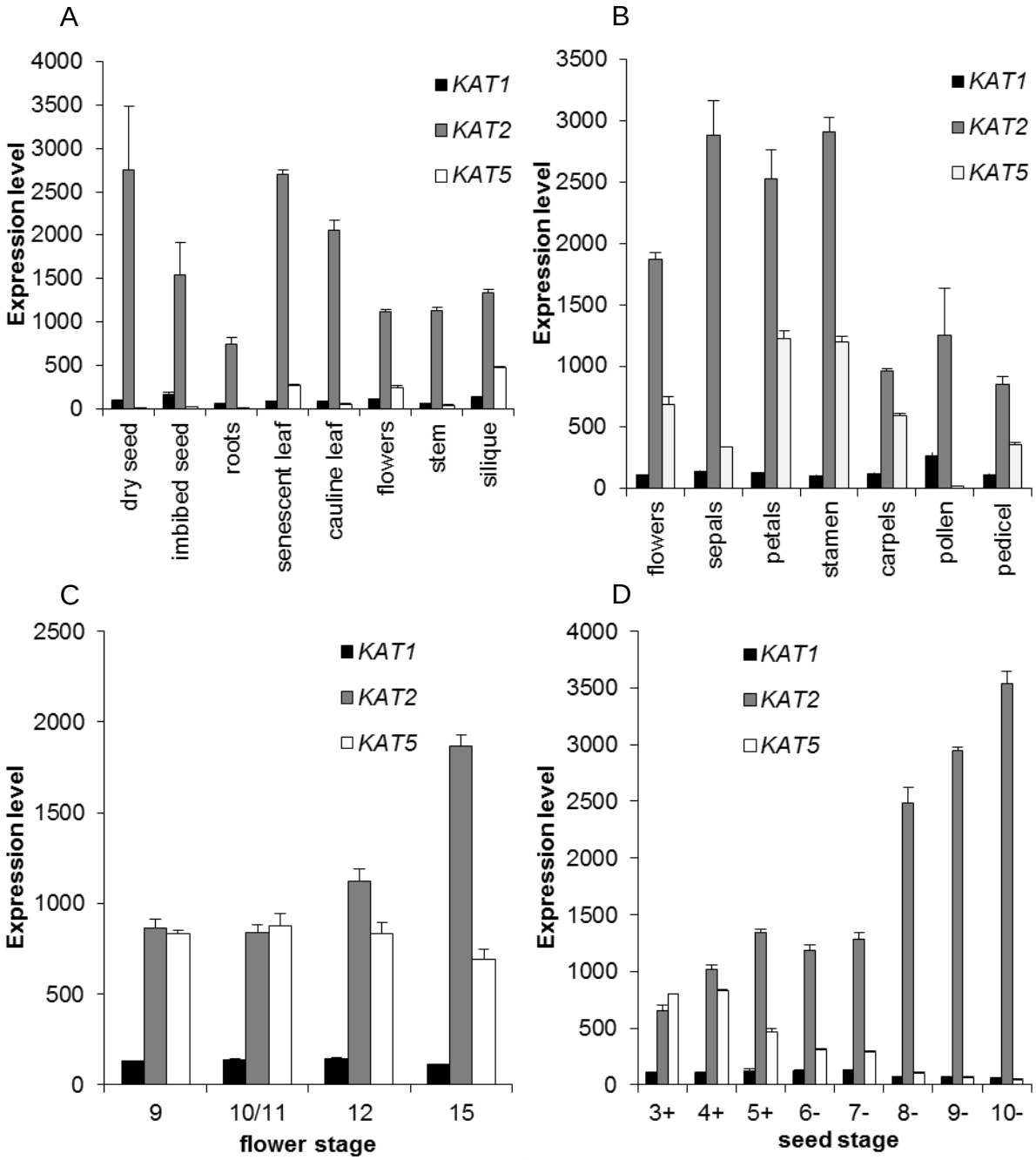

Figure 4.13. Thiolase gene expression in a range of tissue types.

Publicly available data was retrieved from the BAR Arabidopsis eFP browser. A. Development stages across the life cycle. B. Different floral organs. C. Whole flowers at different stages of development. D. Seeds at different stages of development with (+) and without (-) surrounding silique tissue. Error bars represent standard deviation from the mean.

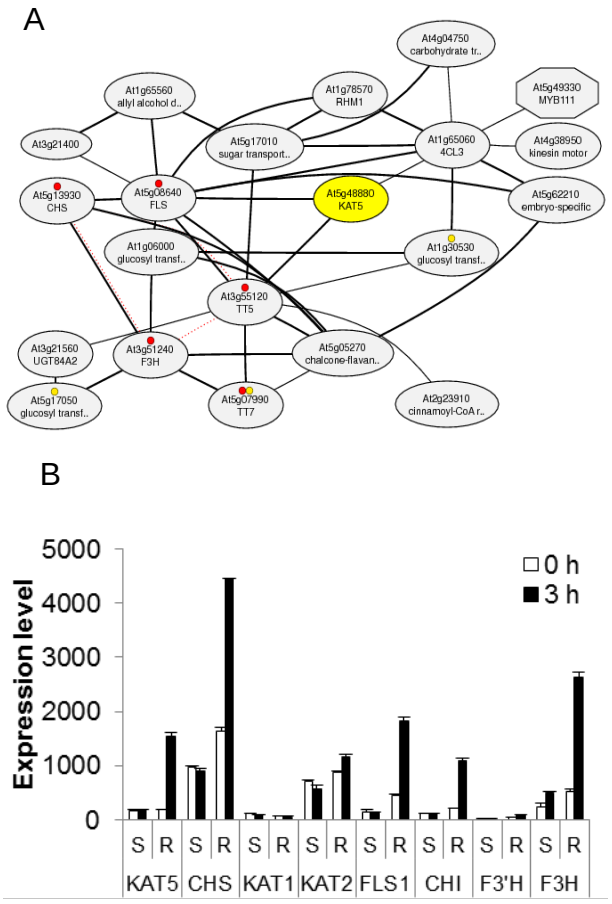

Figure 4.14. Co-expression of *KAT5* with flavonoid biosynthesis genes and up-regulation by UV-B irradiation.

A. Analysis of *KAT5* co-expression using ATTEDII clusters this gene within a network of genes related to flavonoid biosynthesis. B. Data retrieved from BAR Arabidopsis EFP Browser shows up-regulation of KAT5 and flavonoid biosynthesis genes in root, but not shoot tissue 3 h post UV-B irradiation.

4.3 Discussion

4.3.1 Overview of thiolase gene analysis

The constitutive but low expression of *KAT1* in a range of tissues as determined by quantitative and qualitative techniques, suggests the *KAT1* gene does not play an essential role in *Arabidopsis thaliana* growth and development. Based on multiple sequence alignment, KAT1 is closely related to KAT2, and may be the result of recent gene duplication as suggested by genomic synteny between *A. thaliana* and *A. lyrata*. Moreover, the weak *KAT1* promoter and low expression level appears to relegate KAT1 to a minor role in plant metabolism compared to the dominant Arabidopsis thiolase, KAT2. The expression of *KAT2* is consistently high, with up-regulation of gene expression at three stages of the life cycle: germination and seedling establishment; flower and silique development; and senescence of plant tissues. The expression profile of the two isoforms of *KAT5*, the cytosol-localised KAT5.1 and the peroxisomal KAT5.2, does not appear to be highly divergent, with the transcripts of both isoforms predominately accumulating in the reproductive tissue. However, as determined by qRT-PCR *KAT5.2* expression does appear to be consistently slightly higher than *KAT5.1* expression in all tissues except flowers. The purpose of this novel dual localisation of a thiolase in the cytosol and peroxisome remains unclear. Analysis of genomic and EST sequences suggest that dual localisation is conserved in *Brassica napus*, implying selective pressure to maintain the dual targeting of KAT5 in the order Brassicales. Due to a lack of EST data from *Carica papaya* we were unable to confirm expression of alternate transcripts, but genomic sequence data supports a dual transcript hypothesis in this species, also of the order Brassicales.

Care must be taken when analysing the reporter gene experiments described in this chapter. The exon that encodes the KAT5.2 leader sequence is within the *KAT5.1-GUS* reporter construct (Figure 4.5). Therefore the *KAT5.1-GUS* construct will produce both GUS with the initiator methionine of KAT5.1 and GUS with the PTS2-containing leader of KAT5.2 whereas the *KAT5.2-GUS* construct will only produce GUS with the initiator methionine of KAT5.2. This may explain the darker staining generated by *KAT5.1-GUS* construct in spite of the higher *KAT5.2* transcript levels detected by RT-PCR. For example the GUS protein may be more active in the peroxisome than the cytosol. Targeting of GUS to the secretory system or vacuole results in reduced GUS activity, likely due to N-glycosylation (van Rooijen and Moloney, 1995). However evidence that peroxisomal targeting affects GUS activity similarly is lacking (Volokita, 1991). Alternately the stronger staining in *KAT5.1-GUS* constructs may be due to synthesis of two proteins instead of just one in the case of *KAT5.2-GUS* constructs resulting in a greater quantity of GUS and hence greater activity. To determine where the alternative *KAT5* mRNAs are expressed using reporter analysis it would be necessary to determine the

transcriptional start sites of the two transcripts and then make transcriptional reporters (rather than the translational reporters used in the thesis)

4.3.2 Role of thiolase genes in germinating seedlings

β-oxidation is essential for seedling establishment in the absence of an exogenous source of carbon, as the breakdown of stored seed oil in the form of TAG supplies the energetic demand of the growing seedling before photosynthesis (Beevers, 1979). As the *kat2-1* mutant does not establish in the absence of exogenous sucrose, *KAT2* appears to be the most dominant of the Arabidopsis thiolase genes at the seedling stage of development (Germain *et al.*, 2001). Expression analysis of the thiolase genes in this Chapter confirms this genetic evidence with strong expression from the *KAT2* promoter in the cotyledons, where seed oil is stored and degraded during germination. This promoter activity in the cotyledons is strong at early developmental stages and declines over the first 5 d of germination, corresponding to the near complete degradation of seed storage oil by 5 d post imbibition in Arabidopsis (Germain *et al.*, 2001). Measurement of *KAT2* transcript and protein indicates peaking of expression between 2 and 3 d post imbibition (Germain *et al.*, 2001). Similar observations have been made for the genes *MFP2*, *PXA1*, *ACX1*, *LACS6* and *LACS7* (Eastmond *et al.*, 2000b; Fulda *et al.*, 2004; Fulda *et al.*, 2002). Interestingly, strong promoter activity is also observed for *KAT5.1* at this stage of development, predominately in the hypocotyl and root (Figure 4.6). In Arabidopsis seeds oil is abundant in the hypocotyl and radicle (Li *et al.*, 2006), so there is a potential role for KAT5 is oil breakdown. However, *KAT5.1* promoter activity at later stages of development in the root and new leaves, when seed storage oil levels have declined, is unlikely to contribute to this process.

Currently, our understanding of how the core enzymes of β-oxidation are regulated to break down seed oil during germination in Arabidopsis is limited. In the yeast *Saccharomyces cerevisiae* the transcription factors Oaf1p and Oaf2p form a protein complex that in response to oleate (C18:1) activates expression of the peroxisomal β-oxidation-related genes *POX1* (acyl-CoA oxidase), *FOX2* (hydratase/dehydrogenase), *FOX3* (3-ketoacyl-CoA thiolase), *SPS19* (2,4-dienoyl-CoA reductase), *CTA1* (catalase), *PEX11* (peroxisomal membrane protein), *MDH3* (malate dehydrogenase) and *YCAT* (carnitine acetyltransferase), as well as promoting peroxisome proliferation (Karpichev *et al.*, 1997; Karpichev and Small, 1998). The consensus oleate response element CGGNNNTNA (N9-12) CCG has been identified in *S. cerevisiae* as mediating this oleate activation of expression (Karpichev and Small, 1998). As yet, homologous transcription factors or elements have not been identified or characterised in Arabidopsis, or indeed any other plant. In Arabidopsis, β-oxidative degradation of seed lipid may be regulated by this mechanism and/or by regulators of seed germination. A number of plant elements were

identified in the promoters of the thiolase genes and these may be associated with germination and seed storage breakdown.

During Arabidopsis germination and seedling establishment, gene expression and enzyme activity appears to be co-ordinately regulated for the enzymes of β-oxidation, glyoxylate cycle and gluconeogenesis, raising the possibility of a global regulatory mechanism for genes of lipid reserve mobilisation in transition from heterotrophic to autotrophic growth (Rylott *et al.*, 2001). The TGACGT motif identified in the KAT promoters is responsible for high level expression of α-amylase in black gram (*Vigna mungo*) germinating seed cotyledons (Yamauchi, 2001). As determined in this study, *KAT2* expression in cotyledons is strong (Figure 4.6), corresponding with our understanding of oil breakdown in Arabidopsis. Previously, strong expression of *ACX3* was observed in cotyledons using GUS analysis, as well as the root tip and hypocotyl (Eastmond *et al.*, 2000b). Peroxisomes were first isolated from castor bean endosperm, and are abundant in fatty tissues such as endosperm and cotyledons in oil seeds (Beevers, 1979; Breidenbach and Beevers, 1967). In Arabidopsis cotyledons, direct interaction between peroxisomes and lipid bodies has been observed, suggesting an essential role for β-oxidation in oil body breakdown in this tissue (Hayashi *et al.*, 2001).

Many motifs and transcription factor binding sites related to sugar signalling were identified in thiolase promoters, suggesting the potential regulation of β-oxidation by sucrose derived from seed storage oil via the glyoxylate cycle and gluconeogenesis. In Arabidopsis seeds sucrose is synthesised from catabolised TAG during germination (Pritchard *et al.*, 2002), providing for a possible feedback loop for sugar-repression of β-oxidation activity. There is evidence of sugar repression of β-oxidation and the glyoxylate cycle in higher plants. Glucose starvation of maize (*Zea mays*) root tips induces β-oxidation activity (Dieuaide *et al.*, 1993), and in cucumber (*Cucumis sativus*) cell culture, induction of glyoxylate genes *ISOCITRATE LYASE* (*ICL*) and *MALATE SYNTHASE* (*MLS*) in response to starvation has been observed, with repression of these genes following re-supply of sucrose (Graham *et al.*, 1994). Glucose also inhibits ICL activity during germination in *Brassica napus* seedlings (Finkelstein and Lynch, 2000). In Arabidopsis, the presence of exogenous sucrose reduces the rate of storage lipid breakdown during germination, with this repression enhanced under low nitrogen conditions (Fulda *et al.*, 2004; Martin *et al.*, 2002). However, during Arabidopsis germination the genes of β-oxidation, glyoxylate cycle, and gluconeogenesis were not repressed by exogenous 20 mM sucrose (Rylott *et al.*, 2001).

Regulation of storage lipid mobilisation during germination may potentially occur at the steps of TAG lipolysis, import into the peroxisome, β-oxidation, or the glyoxylate cycle (Dietrich *et al.*, 2008; Martin *et al.*, 2002). The presence of sucrose increases seedling

sensitivity to IBA, suggesting β-oxidation remains active with a decreasing flux of fatty acids being regulated at peroxisome import or another upstream stage (Dietrich *et al.*, 2008). Recently, DAD1-like Seedling Establishment-related Lipase (DSEL; At4g18550) has been determined to be involved in regulation of storage lipid mobilisation (Kim *et al.*, 2011). DSEL is a cytosolic member of the DAD1-like acylhydrolase family with *sn*-1-specific lipase enzyme activity, which when over-expressed disrupts β-oxidation resulting in seedling phenotypes of sucrose-dependence, 2,4-DB resistance, and persistence of oil bodies. Conversely, the *dsel* mutant grows slightly faster with no disruption to β-oxidation, suggesting that by an unknown mechanism DSEL is a negative regulator of seedling establishment by inhibiting breakdown of storage oils (Kim *et al.*, 2011).

There is evidence that β-oxidation genes are transcriptionally controlled by carbon status in later stages of plant development. In Arabidopsis seedlings grown in liquid culture, genes of lipid catabolism are rapidly induced during carbon starvation, but return to previous levels following resupply of carbon in the form of sucrose, with the corresponding reduction in lipid content slowly returning to pre-starved levels (Osuna *et al.*, 2007). Dark-induced starvation of Arabidopsis induces *KAT2* expression, and mutants disrupted in *KAT2* and *PXA1* are less tolerant of this stress than wild-type plants (Castillo and León, 2008; Kunz *et al.*, 2009). However, β-oxidation has a demonstrated role in natural plant senescence as well (Castillo and León, 2008; Yang and Ohlrogge, 2009), so this regulation may be related to regulation of senescence-induced genes. In this study *KAT2* was the only thiolase gene up-regulated in naturally senescing leaves (Figure 4.10).

GA and ABA are well-characterised regulators of germination in plants, with GA promoting and ABA inhibiting germination, but it is unclear to what extent these hormones regulate β-oxidation and storage lipid mobilisation. GA and ABA regulate storage protein and sugar breakdown in cereals and Arabidopsis (Fincher, 1989; Lovegrove and Hooley, 2000). GA up-regulates the expression of α-amylase in wheat (Appleford and Lenton, 1997) and barley endosperm (Gubler *et al.*, 1995), and the expression of cysteine proteinases in rice seeds (Watanabe *et al.*, 1991) and barley endosperm (Rogers *et al.*, 1985). GARE (GA response element) identified in the promoter of barley endosperm *α*-amylase was determined to be necessary and sufficient for GA-responsiveness with repression by ABA (Gubler *et al.*, 1995; Skriver *et al.*, 1991). GARE is bound by GAMYB to activate transcription of α-amylase as well as EII(1-3,1-4)-β-glucanase (Gubler *et al.*, 1995; Gubler *et al.*, 1999). Control of storage protein degradation in barley endosperm appears to be similarly regulated, with the cysteine proteinase EFB-1 induced by GA, an effect that is blocked by ABA addition (Cercós *et al.*, 1999). Additionally, the EFB-1 promoter contains a GARE, which regulates GA induction via the transcriptional activator GAMyb (Cercós *et al.*, 1999).

Transcriptome analysis of Arabidopsis seed germination indicates GARE are present in GA-inducible, GA-repressible, and GA-nonresponsive gene promoters at frequencies of 20%, 18%, and 12% respectively, and so may not serve as a major *cis* element for GA-induced gene expression in germinating Arabidopsis seeds (Ogawa *et al.*, 2003). However, many Arabidopsis β-oxidation gene promoters contain motifs homologous to GAREAT (GARE *Arabidopsis thaliana*), suggesting that similar to storage protein and sugar, lipid mobilisation may be regulated by GA and ABA. *ICL* and *MLS* transcript levels are higher in ABA-insensitive (*vp1*) and ABA-deficient (*vp7* and *vp10*) mutant maize embryos during kernel development compared to wild-type (Paek *et al.*, 1998), and *ICL* expression in cotton (*Gossypium hirsulum*, variety Coker 413) embryo cotyledons during embryogenesis is inhibited by ABA (Ihle and Dure, 1972). GA and ABA respectively promote and inhibit expression of *ICL* and *MLS* in germinating castor beans (*Ricinus communis* L.) (Dommes and Northcote, 1985; Martin and Northcote, 1982; Rodriguez *et al.*, 1987).

In Arabidopsis, ABA inhibits expression of genes of β-oxidation and glyoxylate cycle, *ACX3* and *MLS* respectively, but significant expression still occurs with only partial inhibition of lipid breakdown (Pritchard *et al.*, 2002). Control of lipid breakdown appears to be largely ABA-independent (Pritchard *et al.*, 2002). Reserve mobilisation in the endosperm and embryo requires GA as paclobutrazol inhibits lipid breakdown; ABA inhibits mobilisation in the embryo while the endosperm is insensitive (Penfield *et al.*, 2004). ABA inhibition of lipid breakdown in the embryo is regulated via the embryo-specific gene *ABI4* (Penfield *et al.*, 2006). β-oxidation and glyoxylate cycle steady state transcript levels do not appear to be regulated by exogenous ABA in the endosperm or embryo during germination (Penfield *et al.*, 2006), with the possibility that transcription is already induced in late seed development (Schmid *et al.*, 2005). However, *KAT2* expression is induced in the leaves of 3-4 week old seedlings in response to exogenous ABA, and this induction is abolished in a *wrky40-1* mutant, a transcription factor regulating plant defense (Jiang *et al.*, 2011). GARE is also involved in sugar repression, so there may be interactions between sugar- and GA-signalling (Chen *et al.*, 2006; Morita *et al.*, 1998).

4.3.3 Role of β-oxidation genes and thiolase in flowers and siliques

A role for KAT2 and KAT5 in seed development is suggested by the presence of the embryogenesis-specific element CARGCW8GAT in gene promoters, GUS promoter activity in silique embryos, and strong expression of these genes in siliques as determined by qRT-PCR and publicly available microarray data. There is also genetic evidence for a role in embryogenesis for KAT2 and KAT5 (Footitt *et al.*, 2007a, see also Chapter 5).

The reason for the essential role of β-oxidation in reproductive tissue is unclear, but a requirement for the pathway in fatty-acid turnover and/or hormone synthesis during embryogenesis has been suggested (Footitt *et al.*, 2007a; Footitt *et al.*, 2007b). The identification of Arabidopsis peroxisomal transcripts novel to flower and silique tissue may suggest which functions of β-oxidation are required for flower and seed development. In a global analysis of predicted peroxisomal transcripts in a range of Arabidopsis tissues, Kamada *et al.* (2003) identified three genes that showed specific expression in flowers, acyl-CoA activating enzyme 11 (AAE11; At1g66120), cytochrome P450-like protein (CYP77A4; At5g04660), and putative β-alanine-pyruvate aminotransferase (AGT2 homolog; At2g38400), with only one gene displaying green silique-specific expression, proline-rich APG-like protein (GDSL-lipase/hydrolase; At4g28780). Two other transcripts, while identified to be expressed constitutively, were up-regulated in flowers: *AIM1* and *KAT5*. The functions of these flower-specific genes may provide clues to floral peroxisomal β-oxidation function. AAE11 catalyses the ligase reaction of CoA and a fatty acid with substrate specificity to short carbon chains (C6-C8) (Shockey *et al.*, 2003) and is closely related to the characterised enzyme BZO1 (At1g65880), which has benzoyl-CoA ligase activity and is required for seed benzoyloxyglucosinolates accumulation (Kliebenstein *et al.*, 2007). CYP77A4 is an in-chain hydroxylase, which in a yeast heterologous expression system can catalyse the epoxidation of C18:1, C18:2 and C18:3, and has a putative role in plant-pathogen signalling and defence (Sauveplane *et al.*, 2009). At2g38400 is one of three AGT2 homologs identified in the Arabidopsis genome that are implicated in the photorespiratory pathway, and while it remains unclear what metabolic significance AGT homologues have in this pathway, this gene is unlikely to play a role in β-oxidation (Liepman and Olsen, 2003). AIM1 and KAT5 have demonstrated roles in flower development from evidence in mutant studies (Richmond and Bleecker, 1999, see also Chapter 5).

β-oxidation has been suggested as a potential pathway for the synthesis of benzyol-CoA compounds in flowers (Jarvis *et al.*, 2000; Orlova *et al.*, 2006). While the extent to which BA is synthesised via the alternate β-oxidation and non-β-oxidation pathways has been the subject of debate, labelling experiments indicate that both pathways contribute to the plant benzoic acid pool (Boatright *et al.*, 2004), with flux between the alternate pathways varying dependent on the light and dark period cycle (Orlova *et al.*, 2006). Recently, a thiolase from petunia (*Petunia hybrida* cv. Mitchell), *Ph*KAT1, has been identified as functioning in benzoic acid synthesis, with silencing of this gene resulting in a significant decrease in BA and benzoid compound production (Moerkercke *et al.*, 2009). Additionally, the circadian regulation of *PhKAT1*, with expression up-regulated in the dark period, suggests that the β-oxidation pathway contributes the majority of the BA and benzoids released by petunia flowers in the night (Moerkercke *et al.*, 2009). Volatile benzoid compounds are speculated to function in pollinator

attraction (Stuurman *et al.*, 2004). *PhKAT1* is poorly expressed in seedlings and is unlikely to play a role in seed oil breakdown (Moerkercke *et al.*, 2009). There is strong expression of *PhKAT1* and another thiolase *PhKAT2* in the petals, but only *PhKAT1* is regulated in a circadian fashion. In Arabidopsis, *KAT2* and *KAT5* both have transcript and promoter activity in petals, and there is evidence for circadian regulation of *KAT2* at least in leaf tissue (Chapter 3). Moerkercke *et al.* (2009) identify *Ph*KAT1 as an ortholog of Arabidopsis KAT5 based on homology, but KAT2 is also potentially a candidate based on gene expression pattern. However, the extent and importance of flower benzenoid compounds in Arabidopsis is unknown, so it may not be an ideal system for studying synthesis of these compounds.

Kamada *et al.* (2003) identified the silique-specific transcript At4g28780, a GDSL-motif lipase that has a putative role in cutin polymerisation, which occurs on the extracellular surface of epidermal cells (Panikashvili *et al.*, 2010). Cuticular wax formation is essential for the proper development of plant aerial organs, with disruption of this synthesis pathway in reproductive tissue resulting in altered petal and silique morphology as well as fusion of seeds (Panikashvili *et al.*, 2007). The development of cuticular wax is also important for the separation of the seed embryo outer surface and the endosperm. At4g28780 has 63% similarity at the protein level to AgaSGNH, which is involved in cutin formation in the youngest zones of *Agave americana* leaves (Reina *et al.*, 2007). This may suggest a potential role for At4g28780 and β-oxidation pathway in cutin formation contributing to silique morphology. The strong expression of *KAT2* and *KAT5* in silique tissue could implicate these thiolases in any potential β-oxidation-related pathway. Potentially, turnover of fatty acids via β-oxidation could contribute to the flux of substrates entering the elongase reaction, which provides the synthesis of very long chain fatty acids required for wax formation. Cutin monomers are C18 oxygenated fatty acids with similar precursors to the JA pathway; 13-hydroperoxylinolenic acid from lipoxygenase enters the peroxygenase reaction (instead of allene oxide synthase) to generate precursors of cutin monomers (Blée and Schuber, 1993).

Auxin is an important plant hormone with characterised roles in growth and development in many plant tissues (Woodward and Bartel, 2005). Active auxin (IAA) can be synthesised via tryptophan-dependent and –independent pathways, and can also be derived from stored forms, either IAA conjugates (amino acid, sugar or peptide) or IBA. Therefore, alternate metabolic pathways may contribute to the pool of IAA in the cell. IBA undergoes one cycle of β-oxidation and after removal of an acetyl-CoA group is converted to active IAA. It is unknown how much metabolism of IBA to IAA in flowers contributes to organ development. However, levels of IAA have been estimated qualitatively in the separate organs of flowers using the *DR5::GUS* auxin reporter (Aloni *et al.*, 2006). Young floral buds are replete with high levels of conjugated auxin, which can be visualised using immunolocalisation with auxin polyclonal antibodies.

They also have abundant free IAA at the sepal tips. As the floral bud develops, high levels of free IAA accumulate in the stamens. IAA generated in the stamens controls flower development by promoting anther growth and suppressing petal development (Aloni *et al.*, 2006). As stamen IAA levels decrease later in flower development, growth in the petals and stigma becomes more dominant, with large amounts of free IAA accumulating in the stigma. Following fertilisation of the developing embryos, IAA generation is elevated, allowing the establishment of axial polarity.

There is evidence that anther elongation is inhibited in the *cts* and *kat2-1* mutants, and that extension can be promoted by exogenous supply of the synthetic auxin analog NAA (Footitt *et al.*, 2007b). There is also strong genetic evidence that KAT2 is the dominant thiolase in the metabolism of IBA and the synthetic auxin 2,4-DB into IAA and 2,4-D respectively (Germain *et al.*, 2001; Hayashi *et al.*, 1998; Zolman *et al.*, 2000). High *KAT2* promoter activity in anther filaments and in stigmas later in development (Figure 4.8) suggests that KAT2 may have a functional role in the conversion of free IBA into IAA in these tissues. *KAT1* does not appear to be strongly expressed in floral tissue, but there may be some contribution to thiolase activity in pollen as transcriptome data indicates moderate expression of *KAT1* in this tissue.

JA is another plant hormone that is synthesised via β-oxidation, with the precursor OPC:8 going through three cycles of β-oxidation to the active form of JA (Creelman and Mullet, 1995). JA has a demonstrated role in plant fertility, with many mutants disrupted in signalling and metabolism displaying male sterility, which can be rescued by exogenous JA (Park *et al.*, 2002; Sanders *et al.*, 2000). Analysis of *pex6*, *aim1* and *cts* mutants indicates decreased wound-induced JA levels, but levels in flowers have not been analysed (Delker *et al.*, 2007; Theodoulou *et al.*, 2005). The *acx1 acx5* double mutant is deficient in wound-induced JA, and has reduced JA in floral buds resulting in defective pollen development, with fertility restored by supply of exogenous JA (Schilmiller *et al.*, 2007). A mutant disrupted in the *KAT2* gene is deficient in wound-induced JA, but has sufficient thiolase activity to maintain JA levels in unwounded leaves (Afitlhile *et al.*, 2005). Strong expression of *KAT2* and *KAT5* in flowers suggests that in this tissue activity of both thiolases may contribute to JA levels.

Plant reproduction is an energetically costly process, and while carbon is supplied via photosynthetic activity in maternal tissue, the degradation and turnover of fatty acids is also active in embryo tissue (Arai *et al.*, 2002; Baud *et al.*, 2002). There is genetic evidence β-oxidation contributes to ovule respiration via the turnover of fatty acids (Footitt *et al.*, 2007a). Additionally, *in vitro* germination of *kat2-1* and *cts* pollen reveals reduced germination frequency and shorter pollen tube length, but this phenotype can be rescued by exogenous sucrose, suggesting lipid degradation may contribute to the growth of germinating pollen tubes

in vivo (Footitt *et al.*, 2007b). There appears to be a feedback system in the turnover of lipids that controls the level of fatty acid between degradation and synthesis, with impairment of β-oxidation function resulting in disruption of this fine-tuning and pleotropic phenotypic effects (Lin *et al.*, 2004). β-oxidation also has a potentially minor role later in seed development, following the breaking of the trophic connection with maternal tissue (Baud *et al.*, 2002). Once the desiccating seed is a separate entity, β-oxidation of stored oil may provide respiratory substrates, and lipid precursors for membranes or hormones such as JA and IAA.

4.3.4 Co-expression of *KAT5* with flavonoid biosynthesis

Analysis of *KAT5* gene expression places it in a cluster of flavonoid biosynthesis genes, with expression correlation between 0.69 and 0.72 for the genes *CHI* (also known as *TRANSPARENT TESTA5*; *TT5*), *FLS*, and *4CL3*. All three of these genes have demonstrated roles in flavonoid biosynthesis. The *tt5* mutant, disrupted in chalcone isomerase, cannot generate visible anthocyanins or tannins, and has pale yellow-coloured seeds (Winkel-Shirley *et al.*, 1995). In response to UV-B irradiation *tt5* mutant seedlings accumulate less flavonols, and grow more slowly than wild-type (Li *et al.*, 1993). An *fls* mutant was unable to produce the flavonol kaempferol, while remaining unaltered in quercetin content, and has wild-type-like brown coloured seeds, indicating that FLS is not required for testa pigmentation (Wisman *et al.*, 1998). 4CL3 has broad substrate specificity, efficiently converting *p*-coumaric, caffeic and ferulic acids into their CoA esters, with less affinity for 5-hydroxyferulic acid compared to 4CL1 and 4CL2 (Costa *et al.*, 2005).

Additional to the co-expression information, there is evidence of *KAT5* and flavonoid biosynthesis gene co-regulation from experiments with the tissue-specific flavonoid biosynthesis gene transcription-factors MYB11, MYB12 and MYB111 (Stracke *et al.*, 2007). In seedlings, constitutive and UV-B induced expression of *KAT5* and flavonoid biosynthesis gene expression is disrupted in a *myb11 myb12 myb111* triple mutant (Stracke *et al.*, 2010; Stracke *et al.*, 2007). Putative binding sites for transcriptional activation of flavonoid biosynthesis genes have been identified in the promoter of *KAT5* in this study. Analysis of the CHS promoter indicates the presence of a functional MYB recognition element (MRE) required for activation by MYB12 (Mehrtens *et al.*, 2005). MYB12 shows homology to the maize MYB protein *Zm*P (Grotewold *et al.*, 1994), and *Zm*P also activates the MRE (Mehrtens *et al.*, 2005). An element homologous to the binding site of *Zm*P was identified by PLACE in the *KAT5* promoter and is also homologous to the Box L element from carrot and parsley required for UV-B induction of PAL1 (Logemann *et al.*, 1995; Maeda *et al.*, 2005). Mehrtens *et al.* (2005) hypothesise that MRE is bound by R2R3-MYB factors with potential subgroup specificity, so MYB11, MYB12 and MYB111 may all regulate KAT5 via this element.

A role for KAT5 in flavonoid biosynthesis is unclear. Sucrose derived from β-oxidised seed lipid may activate expression of flavonoid biosynthesis genes during germination, with *kat2* and *cts* mutant seeds accumulating less flavonoid in the absence of sucrose (Carrera *et al.*, 2007). However, *KAT5* is expressed mainly in siliques and flowers, where sugars derived from photosynthesis would complement any absence from lipid-derived sources. Transcriptome data indicates that *KAT5* expression is high in seed testa, so KAT5 may play a role in flavonoid accumulation in developing seeds. *KAT5* transcript is up-regulated in response to UV-B irradiation while *KAT1* and *KAT2* are unaffected (Figure 4.14), suggesting KAT5 has a role in flavonoid biosynthesis when the flavonoids function as "molecular sunscreens". KAT5 is also novel amongst Arabidopsis thiolases in having a dual localisation in the cytosol and peroxisome. Cytosolic KAT5.1 may assist in regulation of the cytosolic acetyl-CoA pool required for the secondary metabolism of flavonoid biosynthesis, but a catalytic or biosynthetic role for thiolase is unknown for flavonoids. Many of the enzymes of flavonoid biosynthesis form complexes on the cytosolic face of the endoplasmic reticulum (Winkel-Shirley, 1999); however, *in silico* prediction of KAT5 interaction partners identified none of these flavonoid biosynthesis enzymes. *In silico* prediction of protein interaction has inherent limitations, so experimental work is required to determine interactions (Geisler-Lee *et al.*, 2007).

The UV-responsive and phenylpropanoid gene-specific elements identified in the *KAT5* promoter are supportive of the evidence for co-expression and co-regulation of *KAT5* with genes of flavonoid biosynthesis. Interestingly, motifs associated with UV-response are also found in the gene promoters of *KAT1* and *KAT2* even though expression of these genes is not effected by UV-B irradiation. Light has been discovered to induce peroxisome proliferation in Arabidopsis via the photoreceptor Phytochrome A, the transcription factor HY5 HOMOLOG and the action of the peroxisome biogenesis factor PEROXIN11b, which promotes peroxisome fission (Desai and Hu, 2008). This may account for the many light-responsive elements found in the thiolase gene promoters. However, the expression of thiolase genes does not appear to be responsive to light (Winter *et al.*, 2007). In fact many of these light-responsive elements appear to be common in Arabidopsis gene promoters with high frequencies for T-box (80%), Ibox (65%), Box II (65%) and Gap-box (19%) elements. Their presence in the promoters of thiolase genes may be to some extent a reflection of their ubiquity.

4.4.5 Concluding remarks

Bioinformatic and expression analysis described in this chapter informed experiments performed in the genetic analysis described in Chapter 5, which is concerned mainly with analysis of *kat2* and *kat5* mutants, and associated double mutants as well as exploring the role of *KAT5* in reproductive tissue and flavonoid biosynthesis.

Chapter 5: Reverse genetics reveals an accession dependent role for peroxisomal thiolase in Arabidopsis fertility

5.1 Introduction

In the β-oxidation cycle, acyl-CoA chains are metabolised into acetyl-CoA, with the acyl-CoA chain shortening by two carbons with each turn of the cycle. Fatty acids are initially imported into peroxisomes by the ABC transporter CTS/PED3/PXA1 for which mutants have been isolated by numerous forward and reverse genetics approaches (Hayashi *et al.*, 1998; Russell *et al.*, 2000; Zolman *et al.*, 2001b). Before the fatty acid is metabolised by the β-oxidation pathway, a CoA group is attached by the action of an acyl-CoA synthetase, a large protein family that includes 17 peroxisomal isoforms exhibiting a range of different substrate specificities (Reumann *et al.*, 2004; Shockey *et al.*, 2003). A family of six acyl-CoA oxidases (ACXs) perform the first oxidase step of β-oxidation, concomitantly generated H_2O_2. A range of substrate specificities have been characterised for ACX enzymes in Arabidopsis for short-, medium- and long-chain acyl-CoAs (Eastmond *et al.*, 2000b; Hooks *et al.*, 1999; Rylott *et al.*, 2003). A multi-functional enzyme MFE catalyses the hydratase and dehydrogenase reaction steps of β-oxidation; in Arabidopsis two isoforms of MFE, AIM1 and MFP2, are expressed at different stages of plant growth (Eastmond and Graham, 2000; Richmond and Bleecker, 1999). A 3-ketoacyl-thiolase (KAT) cleaves an acetyl-CoA from the acyl-CoA chain. The Arabidopsis genome contains the *KAT1* and *KAT2* genes, which encode peroxisomal thiolases, and *KAT5*, which encodes both a cytosolic and a peroxisomal isoforms (Carrie *et al.*, 2007). The acyl-CoA molecule now shortened can return to the oxidase step for another cycle of β-oxidation, or by the action of a thioesterase the CoA group is removed and the molecule exits the pathway (Tilton *et al.*, 2000). The acetyl-CoA released from β-oxidation is metabolised by citrate synthase to form citrate. Citrate enters the glyoxylate cycle and gluconeogenesis or it may translocate to the mitochondria where it serves as a respiratory substrate. β-oxidation contributes to seed storage oil degradation during germination; synthesis of fatty-acid based hormones JA, IAA and BA; and catabolism of lipid membrane fatty-acids during senescence (reviewed in Chapter 1).

The major enzymes of long-chain fatty acid breakdown have been characterised genetically, and have been determined play an essential role in seedling establishment before greening of leaves and photosynthesis can drive growth (Baker *et al.*, 2006). LACS6 and LACS7 are acyl-CoA synthetases with long-chain specificity, and the *lacs6 lacs7* double mutant is dependent on sucrose for seedling establishment (Fulda *et al.*, 2004). Similarly, the *acx1 acx2* double mutant, that lacks the long-chain specific ACX1 and ACX 2 oxidases, is impaired in seedling establishment in the absence of exogenous sucrose (Pinfield-Wells *et al.*, 2005). Interestingly, the short-chain fatty acid oxidase double mutant *acx3 acx4* is embryo lethal (Rylott *et al.*, 2003). MFP2 appears to be the major multifunctional protein during germination and establishment, with AIM1 playing a role with MFP2 later in reproductive tissue (Richmond and Bleecker,

1999; Rylott *et al.*, 2006). At least one functional *MFP2* or *AIM1* gene is required for embryogenesis (Rylott *et al.*, 2006). Of the thiolase genes, only the *KAT2* gene is well characterised (Footitt *et al.*, 2007a; Germain *et al.*, 2001; Hayashi *et al.*, 1998). KAT2 appears to have broad substrate specificity being active on long chain fatty acids, metabolising auxin and JA precursors, and degrading membrane lipids during dark-induced senescence (Afitlhile *et al.*, 2005; Germain *et al.*, 2001; Kunz *et al.*, 2009).

The *ped1* (*peroxisome defective1*) mutant, which is allelic to *kat2*, was isolated in a forward genetics screen for growth on toxic levels of the herbicide 2,4-DB, a synthetic auxin precursor (Hayashi *et al.*, 1998). Seedlings of *ped1* were found to require sucrose for post-germinative growth, and electron microscopy revealed that in 5 d old etiolated cotyledons, peroxisomes were two to three times larger than those of wild-type and contained vesicle-like structures. Subsequently, using reverse genetics the T-DNA insertion line *kat2-1* was isolated (Germain *et al.*, 2001). It was confirmed that disruption to thiolase activity resulted in sucrose dependency, with seedlings not breaking down storage TAG, accumulating long-chain acyl-CoAs, and lipid oil bodies persisting after germination. Microscopy confirmed that enlarged peroxisomes were present in fewer numbers than in wild-type and that they had unusual membrane inclusions. A similar but less dramatic observation also made for plastid and mitochondrial size and abundance (Germain *et al.*, 2001). The peroxisomal vesicle structures were hypothesised to be derived from invagination of the peroxisome membrane in contact with lipid bodies (Hayashi *et al.*, 2001). Over-expression of *KAT5* was found to only partially rescue the *kat2-1* impaired seedling establishment phenotype, suggesting that KAT isozymes had different substrate specificities or inappropriate expression from the 35*S* promoter (Germain *et al.*, 2001).

Wound-activated synthesis of JA is defective in *ped1* and antisense *KAT2* leaves, suggesting impairment of β-oxidation of OPC-8:0 to JA (Afitlhile *et al.*, 2005; Castillo *et al.*, 2004). Mechanical damage of leaves triggers local and systemic induction of *ACX1* and *KAT2*, while *KAT5* is induced only systemically with this response disrupted in the JA perception mutant *coronatine-insensitive 1* (*coi1*) (Castillo *et al.*, 2004). Application of exogenous JA induced *ACX1* and *KAT5*, with ABA inducing *ACX1* and *KAT2* expression.

Subtle phenotypic differences in vegetative and reproductive tissue were observed in *kat2-1* plants compared to wild-type with an increase in rosette leaf area and dry weight, but not leaf number (Footitt *et al.*, 2007a). Global proliferative arrest (GPA) of flowering was delayed, resulting in an increased number of siliques, but not an increase in total silique dry weight. The siliques of *kat2-1* are smaller, with reduced seed number and increased ovule abortion due to a decrease in ovule carbon flow into sugars via gluconeogenesis and respiration (Footitt *et al.*, 2007a). Relative to wild-type, *kat2-1* has reduced percentage of fertilised ovules and increased

percentage of aborted ovules per silique (Footitt *et al.*, 2007b). Flower succinate content is lower in *kat2-1*, and pollen tube germination, frequency and length are reduced in the absence of exogenous sucrose (Footitt *et al.*, 2007b).

KAT2 functions in the degradation of lipid membrane fatty acids during senescence, with extended dark treatment resulting in severe leaf necrosis and rapid bleaching following return to light in *kat2-1*. A similar phenotype was observed in *pxa1*, while wild-type plants remained unaffected (Kunz *et al.*, 2009). However, during natural senescence the degradation of lipids was not impaired in *kat2-1* compared to Ws (Wassilewskija, the wild-type background of this allele) plants, potentially due to genetic redundancy and the slower rate of breakdown (Yang and Ohlrogge, 2009).

While KAT2 appears to be the dominant thiolase at many stages of development, the *kat2* single mutant does not display the severe disruptions in fertility observed in other β-oxidation mutants such as *aim1* or *acx3 acx4* (Richmond and Bleecker, 1999; Rylott *et al.*, 2003). Of the other two thiolase genes (*KAT1* and *KAT5*), *KAT1* has very low expression throughout the plant life cycle while *KAT5* is constitutively expressed in a range of tissues, with a higher level of expression in reproductive tissue (Chapter 4). Interestingly, two different mRNAs are transcribed from the *KAT5* gene; these encode a peroxisomal isoform (KAT5.2) and a cytosolic isoform (KAT5.1). *KAT5* is co-expressed with flavonoid biosynthesis genes (Carrie *et al.*, 2007) and is unique amongst β-oxidation genes in doing so. In this study, reverse genetics was used to investigate the function of *KAT1*, *KAT2* and *KAT5* genes in single and multiple mutant combinations.

5.2 Results

5.2.1 *kat2 kat5* double mutants display accession dependent infertility phenotype

Mutants used in these experiments include *kat1* (Ws-4, FLAG), *kat2-1* (Ws-4, (Germain *et al.*, 2001)), *kat2-2* (Col-0, EMS line), and *kat5-1* (L*er*, CSHL_ET5406) that were described in Chapter 3. Additional mutants used for experiments described in this chapter include *kat2-4* (L*er*, CSHL_GT18164), *kat2-5* (Ws-4, FLAG307_C02), *kat5-2* (Ws-4, FLAG_065D06), and *kat5-3* (Col, SAIL_567_F03). Mutants were screened to homozygosity, and analysed by RT-PCR for the presence of transcript. T-DNA lines were concluded to be knockouts if they lacked full-length transcripts (Table 5.1; Figure 5.1). Unexpectedly *KAT2* transcript levels were reduced in the *kat2-2 kat5-3* double mutant, suggesting the EMS point mutation affects transcript levels as well as conserved amino acid residues.

Table 5.1. Thiolase mutant lines used in this study. In addition to thiolase mutants described in Chapter 3, new T-DNA mutant lines were isolated. The recently described *kat2-3* mutant allele (Jiang *et al.*, 2011) was not used in this study.

Gene	Line	Allele	Accession	Reference/notes
KAT1 (At1g04710)	FLAG_589G05	*kat1-1*	Ws-4	Wiszniewski *et al.* (2009)
KAT2 (At2g33150)	T-DNA	*kat2-1*	Ws-4	Germain *et al.* (2001)
	EMS (S140F)	*kat2-2*	Col-0	Wiszniewski *et al.* (2009)
	SALK_024922	*kat2-3*	Col-0	Not used (Jiang *et al.* 2011)
	CSHL_GT18614	*kat2-4*	L*er*	
	FLAG_307C02	*kat2-5*	Ws-4	
KAT5 (At5g48880)	CSHL_ET5406	*kat5-1*	L*er*	Wiszniewski *et al.* (2009)
	FLAG_065D06	*kat5-2*	Ws-4	
	SAIL_567_F03	*kat5-3*	Col-0	

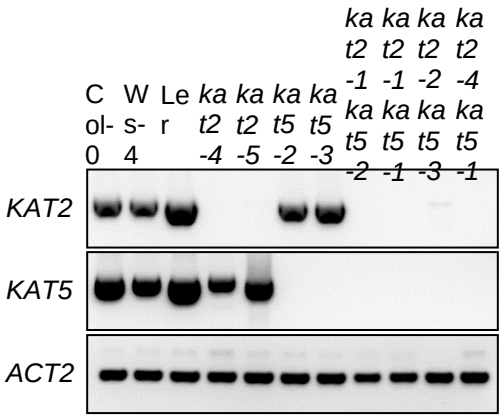

Figure 5.1. RT-PCRs of new thiolase mutant lines reported in this chapter.

RNA was isolated using Biorad Aurum RNA isolation kit. RT utilised Biorad iScript. Where insertions interrupted putative transcripts, primers were designed to anneal to transcribed sequences bounding the insertion sites. RT-PCR of *ACTIN2* was used as a loading control. Lines are assumed to be knockouts if transcript was absent. AGIs, and a full list of alleles and T-DNA names can be found in Table 5.1

Growth of *kat1*, *kat2-1* and *kat5-2* at a gross morphological level is similar to wild-type (Figure 5.2C); however the *kat2-1 kat5-2* double mutant has severe growth defects (Figure 5.2A-C). Double mutant seedlings appear paler than wild-type (Figure 5.2A) suggesting reduced chlorophyll content, a phenotype recently described in the *pex5* mutant (Khan and Zolman, 2010). Double mutant plants are smaller than wild-type and single mutants throughout development, with reduced rosette size and dwarf inflorescences (Figure 5.2A-C). The inflorescences of double mutant plants display a branching phenotype, with unusual internode spacing and anatomy (Figure 5.3A-D). A branching phenotype has previously been observed in *aim1*, which has reduced fertility (Richmond and Bleecker, 1999). The cause of this infertility remains unclear, but Richmond and Bleeker (1999) suggest the accumulation of by-products from unsaturated fatty-acids not metabolised when β-oxidation activity is disrupted may affect fertility.

Developing flowers were malformed, although flowers at later stages of the plant life cycle developed more normally, appearing almost wild-type like (Figure 5.3E-H). These late developing wild-type-like flowers produce a small amount of pollen but the siliques generated by the double mutant were empty. Footitt *et al.* (2007b) demonstrated that *cts* and *kat2-1* pollen has reduced germination frequency, so it is possible the severe disruption to β-oxidation in the double mutant could affect male fertility. However, Alexander staining suggests that double mutant pollen is viable (Figure 5.4), and this pollen has been used to outcross into wild-type Ws-4, so pollen is functional with perhaps only reduced efficiency. Disruption to JA synthesis via β-oxidation can lead to male infertility in mutants such as *acx1 acx5* (Schilmiller *et al.*, 2007), but the application of 100 μM JA failed to restore fertility in *kat2-1 kat5-2*. Attempts to cross wild-type pollen to double mutant flowers which appeared wild-type like were unsuccessful, suggesting a defect to female reproductive tissue.

Confoundingly, double mutants in L*er* and Col backgrounds, *kat2-4 kat5-1* and *kat2-2 kat5-3* respectively, had no obvious phenotype for plant growth and infertility (Figure 5.2D-E). To determine if the abnormal floral phenotype was due to secondary mutations in *kat2-1 kat5-2* background, alternate double mutants were generated using independent alleles. Abnormal flower phenotypes were observed in the alternate double mutants *kat2-5 kat5-2* (Ws-4) and *kat2-1 kat5-1* (a hybrid Ws-4/ L*er* background) (Figure 5.3C-D). Complementation of the *kat2-1 kat5-2* mutant with cytosolic *KAT5.1* and peroxisomal *KAT5.2* cDNAs under the control of the constitutive *35S* promoter resulted in rescue of fertility by *KAT5.2* but not by *KAT5.1* (Figure 5.2C), suggesting the infertility phenotype is due to the disruption of peroxisomal thiolase function. Similarly, complementation by *KAT5.2* rescues the ability of double mutant

seedlings to establish in the absence of exogenous sucrose under dark and light conditions, while *KAT5.1* does not (Figure 5.5).

Figure 5.2. Thiolase mutant growth at various stages of plant development.

A. Ws-4 wild-type (left) and *kat2-1 kat5-2* double mutant (right) on 0.5 x MS with 1% sucrose at 14 d; scale bar, 10 mm. B. Ws-4 and *kat2-1 kat5-2* (inset) in soil at 22 d; scale bar, 15 mm. C. Left to right: Ws-4, *kat1*, *kat2-1*, *kat5-2*, *kat2-1 kat5-2*, *kat2-1 kat5-2 35S:KAT5.1*, and *kat2-1 kat5-2 35S:KAT5.2* in soil at 35 d; scale bar, 60 mm. D. Left to right: L*er*, *kat2-4*, *kat5-1*, and *kat2-4 kat5-1* in soil at 35 d; scale bar, 60 mm. E. Left to right: Col, *kat2-2*, *kat5-3*, and *kat2-2 kat5-3* in soil at 35 d; scale bar, 60 mm. Seedlings on MS media were grown under continuous light conditions; all soil grown plants were under long-day conditions.

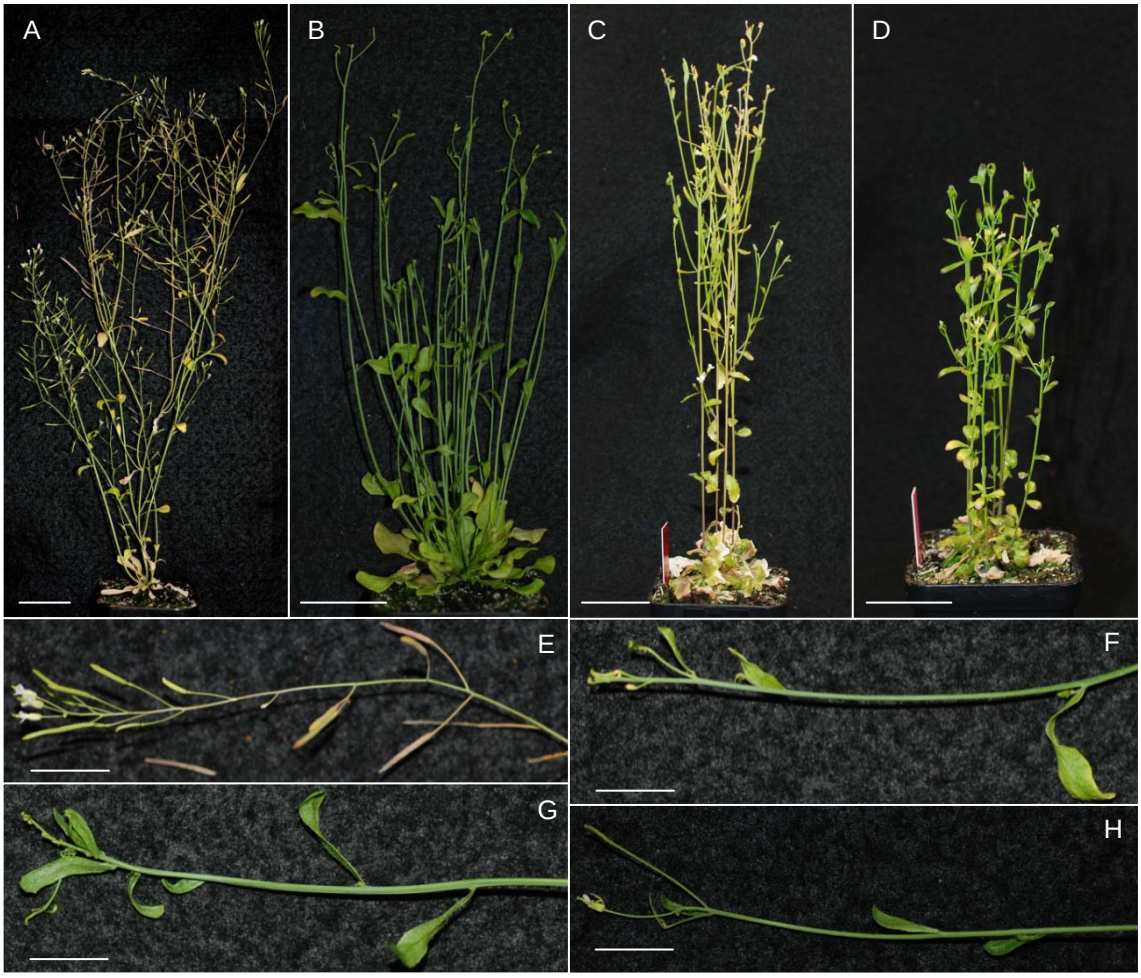

Figure 5.3. Branching, flower and pollen development in the *kat2-1 kat5-2* double mutant.

A, E. Wild-type Ws-4. B-D, F-H. *kat2 kat5* double mutants. Wild-type Ws-4 (A) and *kat2-1 kat5-2* (B) mature plants after 52 d growth in soil, increased branching is observed in the double mutant. *kat2-5 kat5-2* (C) and *kat2-1 kat5-1* (D) mature plants after 85 d growth in soil. Scale bar, 30 mm. Close-up images of 52 d old wild-type Ws-4 (E) and *kat2-1 kat5-2* (F-H) inflorescences at this stage of development show malformation and ectopic positioning of flowers, siliques and cauline leaves in the mutant. Scale bar, 10 mm.

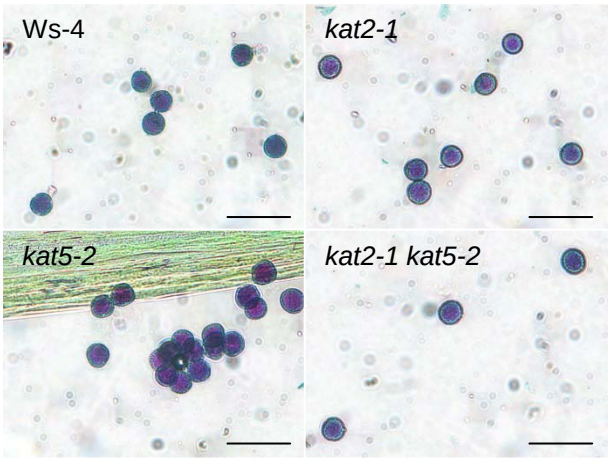

Figure 5.4. Alexander staining of thiolase mutant pollen viability.

Wild-type Ws-4, *kat2-1*, *kat5-2* and *kat2-1 kat5-2* pollen was stained with Alexander solution, and plants were shown to be capable of producing viable pollen. Pollen has purple staining in the cytoplasm indicating viability, the outer exine layer stains green. Scale bar, 50 µm.

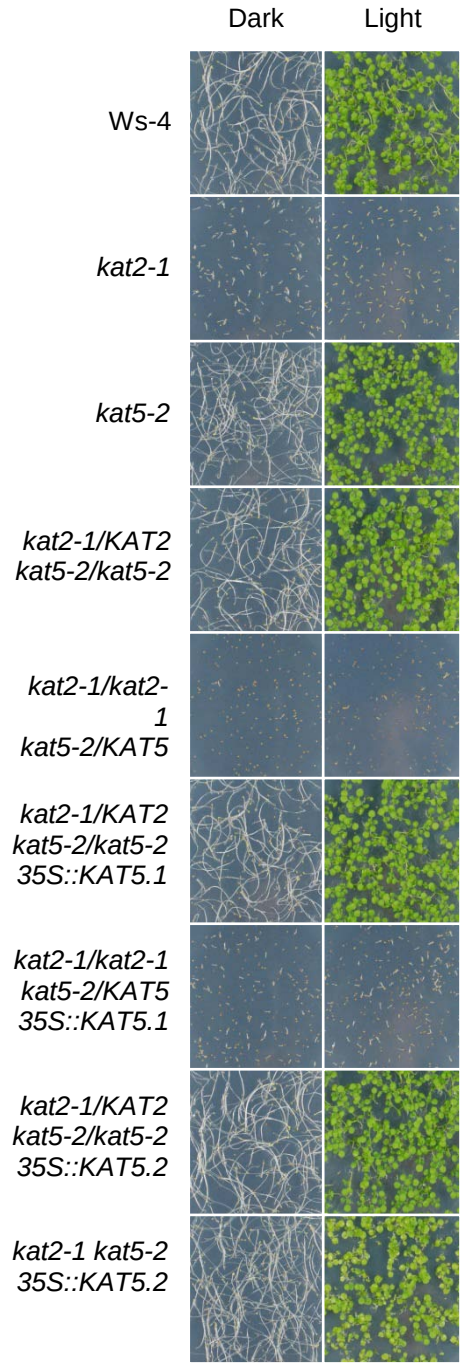

Figure 5.5. Mutant and transgenic seedling establishment under dark and light conditions.

Seedlings were grown on 0.5 x MS containing no sucrose in the dark and light for 8 d. Thiolase mutants in the Ws-4 background including different segregating permutations of *kat2-1* and *kat5-2*, with and without complementation by the *35S:KAT5.1* or *35S:KAT5.2* transgenes. Homozygosity at the *kat2-1* allele inhibits seedling establishment but this phenotype is rescued by complementation with the *35S:KAT5.2* transgene. Scale bar, 20 mm.

5.2.2 KAT2 but not KAT5 is required for seedling establishment in the absence of exogenous sucrose

Impairment of hypocotyl extension of dark grown β-oxidation mutant seedlings in the absence of sucrose has been previously established. As the Ws-background *kat2-1 kat5-2* double mutant is infertile, a segregating population of seed was used for experiments where the parent plant was homozygous for one allele and heterozygous for the other. Sucrose dependency of establishment for *kat2* alleles in Ws-4 and L*er* was confirmed, and this dependency was maintained in the L*er* double mutant (Figure 5.6A). The wild type and all of the mutants in the Ws-4 background had slightly inhibited hypocotyl growth in the sucrose treatment while in the L*er* background sucrose appeared to slightly promote extension (Figure 5.6A). Interestingly, the hypocotyls of *kat2-4* are shorter than those of the *kat2-4 kat5-1* double mutant in the presence of sucrose.

5.2.3 The *kat5* mutation does not enhance 2,4-DB resistance in double mutants

2,4-DB is a synthetic auxin precursor which when metabolised to the active form 2,4-D inhibits seedling root growth. A 2,4-DB concentration curve response for Ws-4 and L*er* mutants and wild-type was conducted to determine thiolase specificity for auxin precursors. For *kat2 kat5* double mutants in the Ws-4 accession, segregating lines were used as described above due to the absence of a fertile *kat2-1 kat5-2* double homozygous mutant. Ws-4 (wild-type), *kat1*, *kat5-2* and *kat1 kat5-2* homozygous mutants, and *kat2-1*/*KAT2 kat5-2*/*kat5-2* were sensitive to 2,4-DB, while *kat2-1* (homozygous) and *kat2-1*/*kat2-1 kat5-2*/*KAT5* were resistant (Figure 5.6B). Segregation of the *kat5-2*/*KAT5* alleles in the *kat2-1* homozygous background did not confer significantly greater resistance to 2,4-DB. L*er* wild-type and *kat5-1* mutant were sensitive to 2,4-DB indicating functional metabolism of this compound (Figure 5.6C). The *kat2-4* and *kat2-4 kat5-1* (L*er*) double mutant was resistant to 2,4-DB at a range of concentrations assayed, with no significant difference in resistance conferred by the presence of the *kat5-1* mutation in the *kat2-4* background.

5.2.4 KAT5 and KAT2 contribute to germination potential in the Ws-4 accession

Reduced germination frequency has previously been described for the β-oxidation mutants *acx1 acx2*, *cts* and *kat2-1* (Pinfield-Wells *et al.*, 2005). To assess the effect of *KAT* single and double mutants on germination potential, matched seed batches were sown to water-agar and placed directly in the light. After 96 h, Ws-4 (wild-type), *kat1*, *kat5-2*, and *kat1 kat5-2* (Ws-4 mutants) had a germination frequency greater than 95% (Figure 5.6D). Disruption of *KAT2* in

Ws-4 background affects germination with frequencies of 85% for *kat2-1*/*KAT2 kat5-2*/*kat5-2*, 70% for *kat2-1* (homozygous), and 50% for *kat2-1*/*kat2-1 kat5-2*/*KAT5* by 96 h. The reduced germination frequency in *kat2-1*/*KAT2 kat5-2*/*kat5-2* seed pool may be due to the segregation of *kat2* from *KAT2*, and/or lower thiolase gene dosage and corresponding activity caused by the absence of *KAT5* in a *kat2* heterozygous or homozygous background. Interestingly a lower germination frequency was observed for the seed pool segregating for the *kat5-2*/*KAT5* allele in the *kat2-1* homozygous mutant background compared to a non-segregating seed pool simply homozygous for *kat2-1*. Following the plateau of seed germination 96 h after imbibition the segregation of the *kat5-2*/*KAT5* allele appears to contribute a 20% reduction in germination frequency in the *kat2-1* homozygous background, with this difference significant at 48 and 72 h ($p<0.05$), as well as the other time points for the duration of the experiment ($p<0.01$). This suggests that while KAT2 is the major thiolase during germination, KAT5 also contributes during this stage of the life cycle in Ws-4.

The germination frequency of L*er* wild-type and *kat5-1* (L*er*) was about 95% frequency by 72 h, while *kat2-4* and *kat2-4 kat5-1* double mutant reached approximately 50% germination by 72 h, plateauing at approximately 50-60% from 144 h (Figure 5.6E). At 240 h, the final time point measured, the germination frequency was maintained at 55-60%. Interestingly, in contrast to the Ws-4 double mutant, the germination frequency for the *kat2-4 kat5-1* double mutant was slightly higher than for the *kat2-4* single mutant at all of the time points measured, with a statistically significant difference at 96 and 120 h ($p<0.05$).

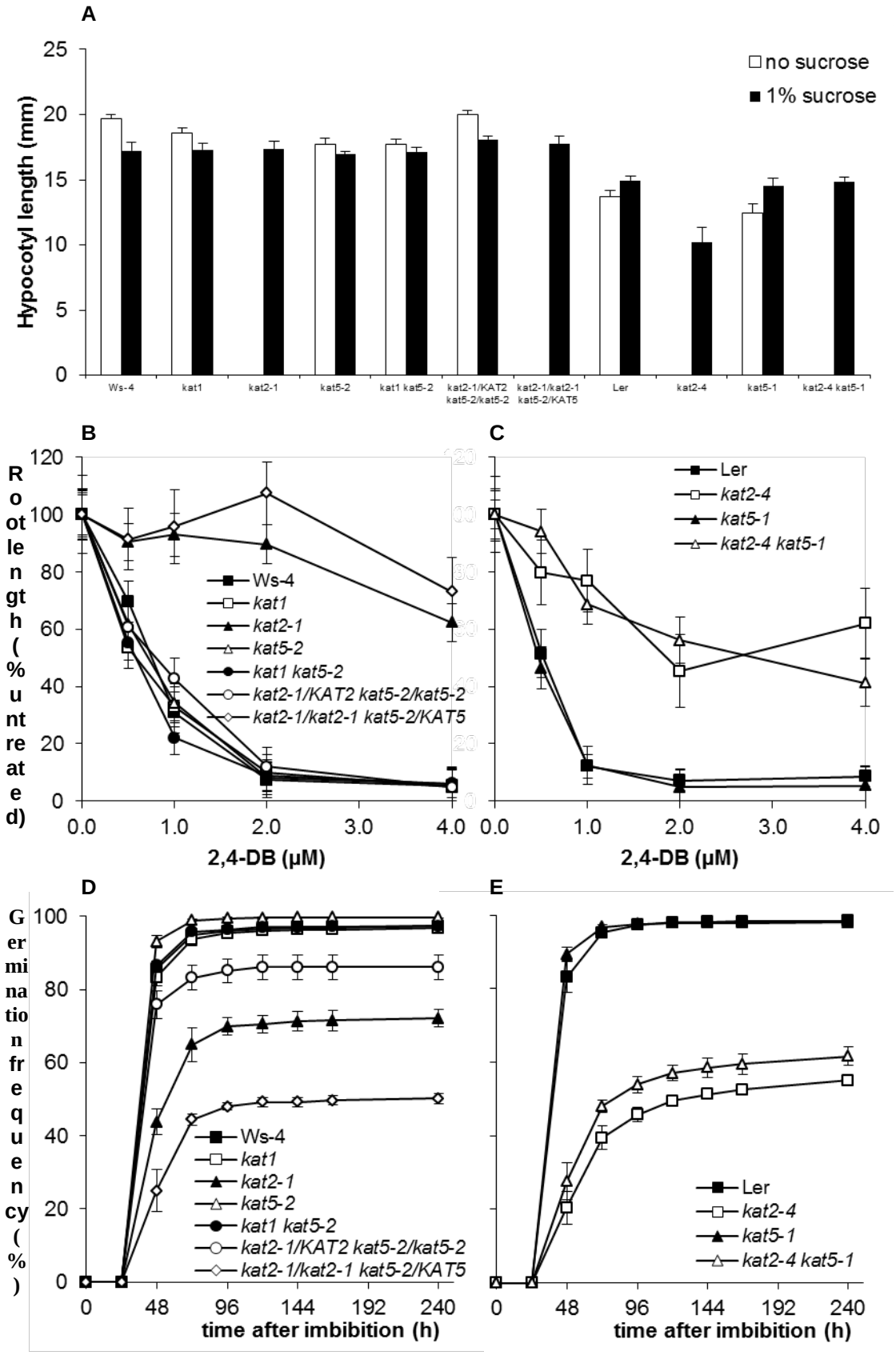
A
Hypocotyl length (mm)
no sucrose
1% sucrose
Ws-4
kat1
kat2-1
kat5-2
kat1 kat5-2
kat2-1/KAT2 kat5-2/kat5-2
kat2-1/kat2-1 kat5-2/KAT5
Ler
kat2-4
kat5-1
kat2-4 kat5-1
B
Root length (% untreated)
2,4-DB (µM)
Ws-4
kat1
kat2-1
kat5-2
kat1 kat5-2
kat2-1/KAT2 kat5-2/kat5-2
kat2-1/kat2-1 kat5-2/KAT5
C
Ler
kat2-4
kat5-1
kat2-4 kat5-1
2,4-DB (µM)
D
Germination frequency (%)
time after imbibition (h)
Ws-4
kat1
kat2-1
kat5-2
kat1 kat5-2
kat2-1/KAT2 kat5-2/kat5-2
kat2-1/kat2-1 kat5-2/KAT5
E
time after imbibition (h)
Ler
kat2-4
kat5-1
kat2-4 kat5-1

Figure 5.6. β-oxidation phenotypes assayed in thiolase mutants.

A. Etiolated hypocotyl extension of thiolase mutants after 4 d on 0.5 x MS media supplemented with or without 1% sucrose (n≥14). B, C. Inhibition of root growth in response to varying concentrations of 2,4-DB of thiolase mutants in the Ws-4 accession (B) and L*er* accession (C) background after 8 d growth (n≥8). D, E. Germination frequency of thiolase mutant after-ripened seed (200 seeds) on water agar in the Ws-4 accession (D) and L*er* accession (E) background from 0 to 240 h post-imbibition (n=4). Segregating pools of seed were used for the *kat2-1 kat5-2* as the double mutant is infertile.

5.2.5 Segregation ratios of *kat2-1* and *kat5-2* in sesquimutants

Segregating pools of Ws-4 seed from *kat2-1 kat5-2* parents, homozygous for one allele but heterozygous for the other (sesquimutants) were analysed using a PCR assay to determine the genotypic segregation ratio at the heterozygous locus (Table 5.2). The seed pool segregating for *kat5-2/KAT5* but homozygous for *kat2-1* did not significantly differ from the expected ratio of 1:2:1 (*KAT5*/*KAT5*: *kat5-2*/*KAT5*: *kat5-2*/*kat5-2*), while the seed pool segregating for *kat2-1/KAT2* but not *kat5-2* did differ significantly ($p<0.01$). In the seed pool segregating for *kat2-1/KAT2*, not only was there a lower proportion of homozygotes than expected, but also heterozygotes were under-represented, as indicated by a ratio of 4:4:1. This may be because double mutant embryos are produced at low frequency or are more likely to abort, as are those that are heterozygous for the *kat2-1/KAT2* allele due to reduced gene dosage. Gametes have only a single copy of each gene so, for example, pollen that is disrupted in the single copies of *KAT2* and *KAT5* may not grow pollen tubes as effectively, impairing fertilisation efficiency. KAT2 function has previously been implicated in pollen germination in the absence of exogenous sucrose *in vitro* (Footitt *et al.*, 2007b), and for ovule respiration (Footitt *et al.*, 2007a) and the additional loss of *KAT5* in either gamete could impact fertility.

5.2.6 Seed weight and oil content is reduced in the *kat2-1* and *kat5-2* single mutants

Seed weight was reduced approximately 10% for both *kat2-1* and *kat5-2* compared to wild-type Ws-4 when parent plants were grown under long-day conditions (Figure 5.7A). Fatty acid degradation for *kat5-2* seedlings 2 to 5 d post-stratification was not significantly different from wild-type Ws-4, as determined by the presence of the TAG marker fatty acid C20:1 (Figure 5.7B). Previously, a slower rate of fatty acid breakdown has been described for *cts*, *lacs6 lacs7*, *acx1 acx2*, and *kat2-1* during germination and seedling establishment (Footitt *et al.*, 2002; Fulda *et al.*, 2004; Germain *et al.*, 2001; Pinfield-Wells *et al.*, 2005).

Seeds collected from *kat2-1* and *kat5-2* mutants grown in long-days had approximately 20% less total fatty acid and TAG marker C20:1 per seed than wild-type (Figure 5.7D). However, on a weight for weight basis total fatty-acid and C20:1 content was the same in both mutants and wild type, indicating that although seed weight was affected it was not due to a shift away from lipid as a major seed storage component (Figure 5.7C). Total and C20:1 fatty acid per seed was significantly reduced in *kat2-1* ($p<0.05$), but not *kat5-2* ($0.05<p<0.10$) (Figure 5.7C). Additionally, a full range of fatty acid species were lower in abundance in the *kat2-1* and *kat5-2* mutant seed (Figure 5.7E). These results are consistent with previously published reports of lower seed lipid in *kat2-1* (Germain *et al.*, 2001). KAT2 and also KAT5 therefore play a role in

seed development. Reduced seed weight has also been reported for *acx1*, *acx1 acx2* and *cts* (Pinfield-Wells *et al.*, 2005), but seed oil content was not assessed in that study.

5.2.7 Flavonoid biosynthesis is not significantly disrupted in *kat5* mutants

KAT5 has been implicated in flavonoid biosynthesis by reports of co-expression, co-regulation and response to UV-B irradiation (Discussed in Chapter 4, see also Carrie *et al.*, 2007; Stracke *et al.*, 2007). However, *kat5* mutant seeds do not display the transparent testa phenotype that is characteristic of flavonoid biosynthesis mutants such as *tt4*, a chalcone synthase EMS mutant from the L*er* background (Chang *et al.*, 1988; Koornneef, 1981) (Figure 5.8A). Staining for flavonoids using a diphenylboric acid 2-aminoethyl ester (DPBA) fluorescence assay revealed no change in *kat5* mutant seedling flavonoid levels, while the *tt4* mutant was disrupted (Figure 5.8B). A functional and phenotypic link of KAT5 to flavonoid biosynthesis remains enigmatic.

Table 5.2. Pedigree analysis of *kat2-1 kat5-2* mutants homozygous at one allele but segregating at the other. Segregating mutant seedlings were genotyped to determine their segregation ratio. Segregation of the *kat2-1* allele differed from expected ratio of 1:2:1 (wild-type: heterozygous: homozygous), but did not at the *kat5-2* allele as determined by Chi square test using Excel. Frequency of seedling genotypes is shown with percentage of total in brackets.

Background	**Segregating mutation**				
mutation	Wild-type	Heterozygous	Homozygous	Total	χ^2 1:2:1 hypothesis
kat2-1	*KAT5*/*KAT5*	*kat5-2*/*KAT5*	*kat5-2*/*kat5-2*		
	28 (30%)	46 (49%)	19 (20%)	93	0.42
kat5-2	*KAT2*/*KAT2*	*kat2-1*/*KAT2*	*kat2-1*/*kat2-1*		
	42 (46%)	40 (44%)	9 (9.9%)	91	3.3×10^{-6}

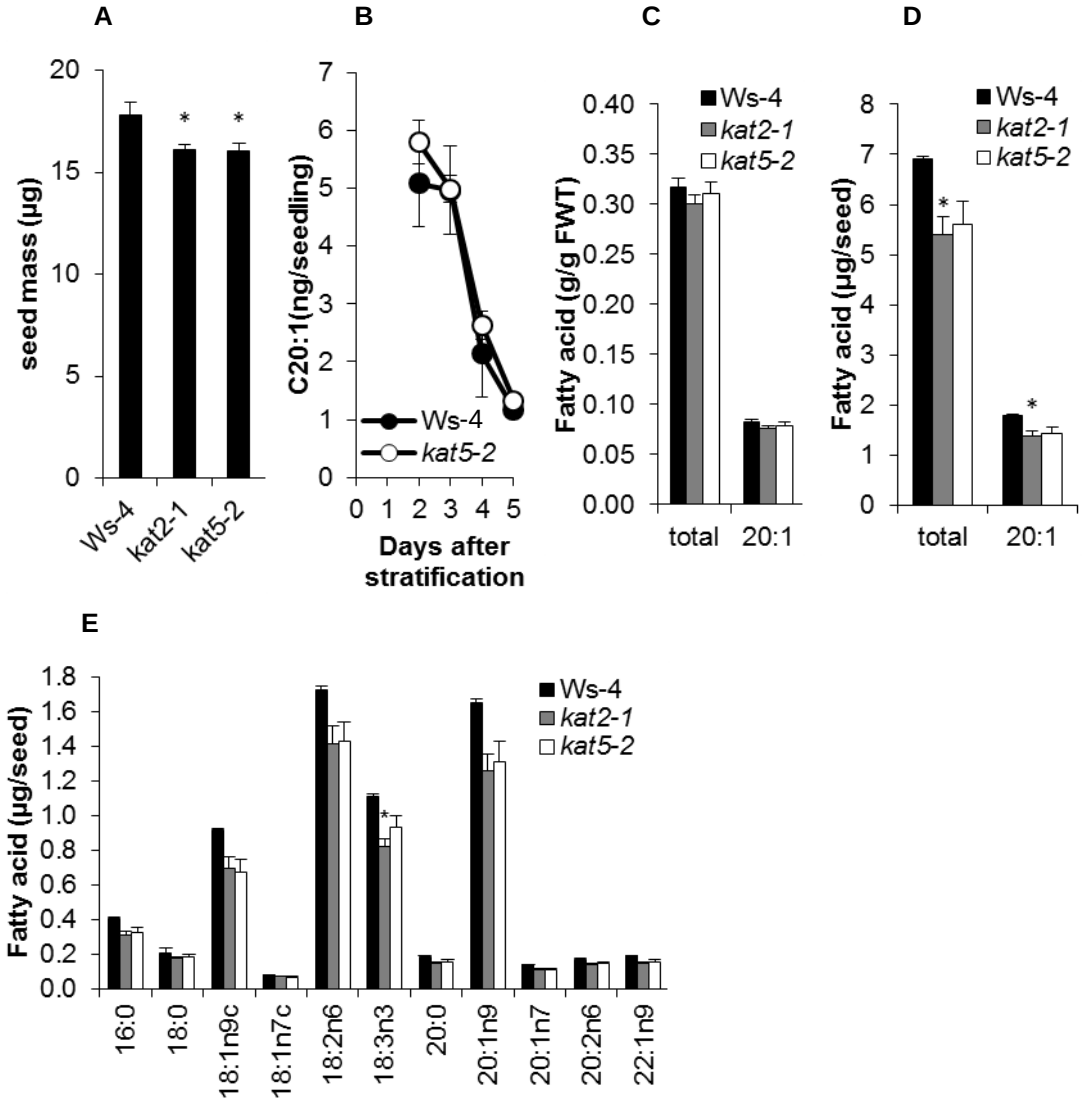

Figure 5.7. Seed weight and fatty acid analysis of *kat2-1* and *kat5-2*.

A. Mean seed weight of pools of 500-600 seeds (n=10). B. Degradation of the TAG lipid marker C20:1 in Ws-4 and *kat5-2* from 2 to 5 d post-stratification (n=4). C, D. Total fatty acid and TAG marker C20:1 content of counted ~10 mg seed pools normalised for (C) seed weight and (D) seed number (n=4). E. Content of individual fatty acid species normalised for seed number (n=4).

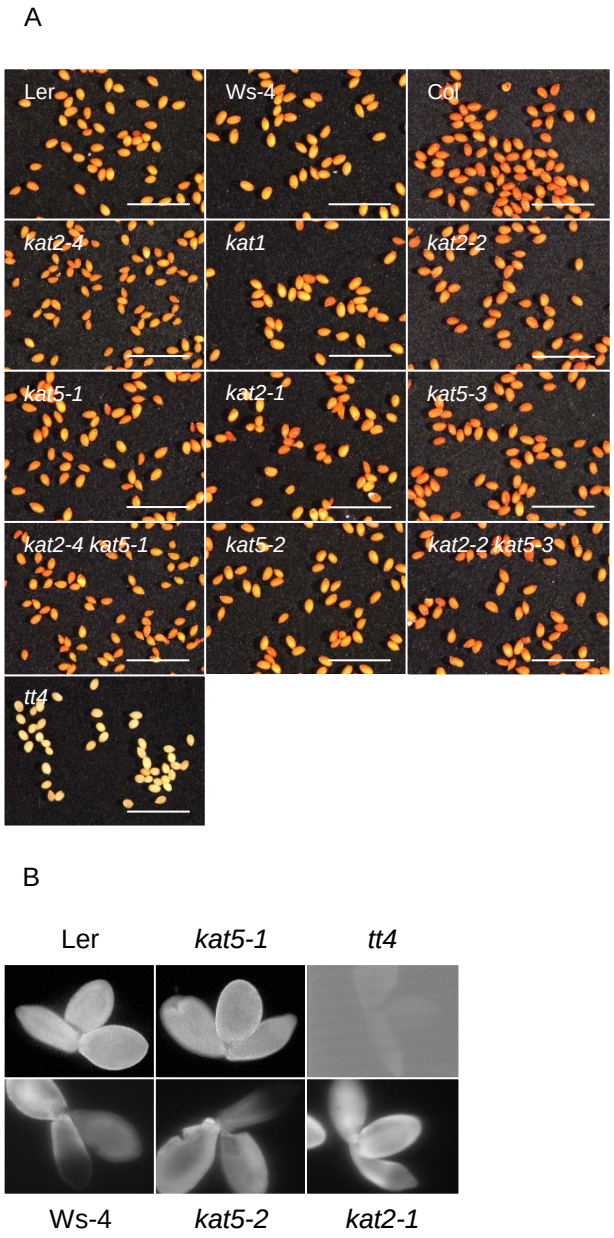

Figure 5.8. Absence of seed-testa flavonoid phenotype in *kat5* mutants.

KAT5 co-expresses and co-regulates with genes of flavonoid biosynthesis. A. However, the transparent seed testa (tt) phenotype observed in *tt4* is not observed in thiolase mutants; scale bar, 2 mm. B. Fluorescent DPBA stain of flavonoids in 24 h imbibed seedlings, testa removed.

5.2.8 Arabidopsis accessions display natural variation in the expression of β-oxidation genes and sequence of the *KAT1* gene

Gene expression analysis of 2 d old seedlings from experiments investigating the glyoxylate cycle mutants *mls* and *icl* (Cornah *et al.*, 2004), were accessed from NASC, and indicated significant difference in the expression of β-oxidation gene expression between Col-0 and Ws-4 accessions. *AACT2*, *LACS7*, *ACX2*, *ACX4*, *MFP2*, *CSY3* and *PMDH1* were lower in Col-0 than Ws-4, while *KAT5*, *ACX1*, *AIM1* and *PMDH2* were higher (Figure 5.9). The largest difference in gene expression was in *KAT5* which was over 4-fold higher in Col-0. Analysis of other growth stages in Arabidopsis was possible using publicly available global expression data generated by Chen *et al.* (2005), which used an older, smaller microarray chip capable of analysing a more limited number of genes than that used by Cornah *et al.* (2004). Additionally these experiments use the Ws-2 accession, which is a similar genotype to Ws-4 (Anastasio *et al.*, 2011). These results indicated that *KAT2* was expressed higher in L*er* and Col-0 compared to Ws-2 (Figure 5.10). *KAT5* expression was highest in flowers and siliques. In flowers KAT5 expression was highest in Col-0, then Ws-2 and L*er*. In young siliques *KAT5* was lower in Col-0 than Ws-2 and L*er*, while in all three accessions expression was similar in older siliques. *KAT1* expression is constitutively low suggesting that it does not play an important role in β-oxidation in any of the three accessions.

Another possibility is that the *KAT1* gene is different at coding sequence level in L*er* and Col-0 compared to Ws-4. Sequencing of the 3,909 bp *KAT1* gene region in these accessions reveals no differences between the L*er* and Col-0 sequence (not shown). However, there are SNPs in the Ws-4 *KAT1* gene sequence in both intron (two SNPs) and exon (five SNPs) sequences (Figure 5.11). No change to intron-exon structure was predicted using the Eukaryotic GeneMark hidden Markov model (http://opal.biology.gatech.edu/GeneMark/eukhmm.cgi; (Lomsadze *et al.*, 2005)). Three of the exon SNPs were at the third bp position of the codon and resulted in silent mutations. However, two of the SNPs were at the second bp position of the codon and result in the mutations L369Q (CTA → CAA) and G433D (GGT → GAT). L369Q is a semi-conserved residue next to an α-helix structure (Pye *et al.*, 2010), while G433D is not a conserved residue (Figure 5.11). Therefore it seems unlikely that these minor changes to Ws-4 KAT1 would result in the dramatic difference in phenotype observed in Ws-4 *kat2-1 kat5-2* mutants, unless L369Q was able to eliminate any last vestige of KAT in *kat2-1 kat5-2*.

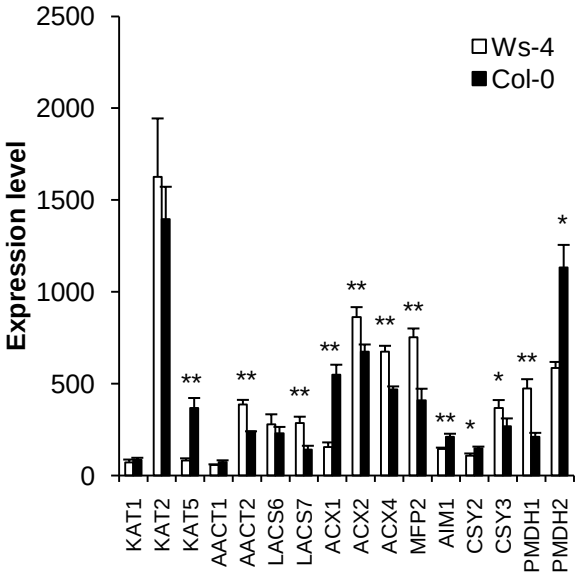

Figure 5.9. β-oxidation gene expression in 2 d old Ws-4 and Col-0 wild-type seedlings.

Publicly available microarray data from Cornah *et al*. (2004) was retrieved from NASC. Statistically significant difference determined by Students t-test (Excel) with $p<0.05$ (*) and $p<0.01$ (**). Mean of 3 biological replicate and standard error is shown.

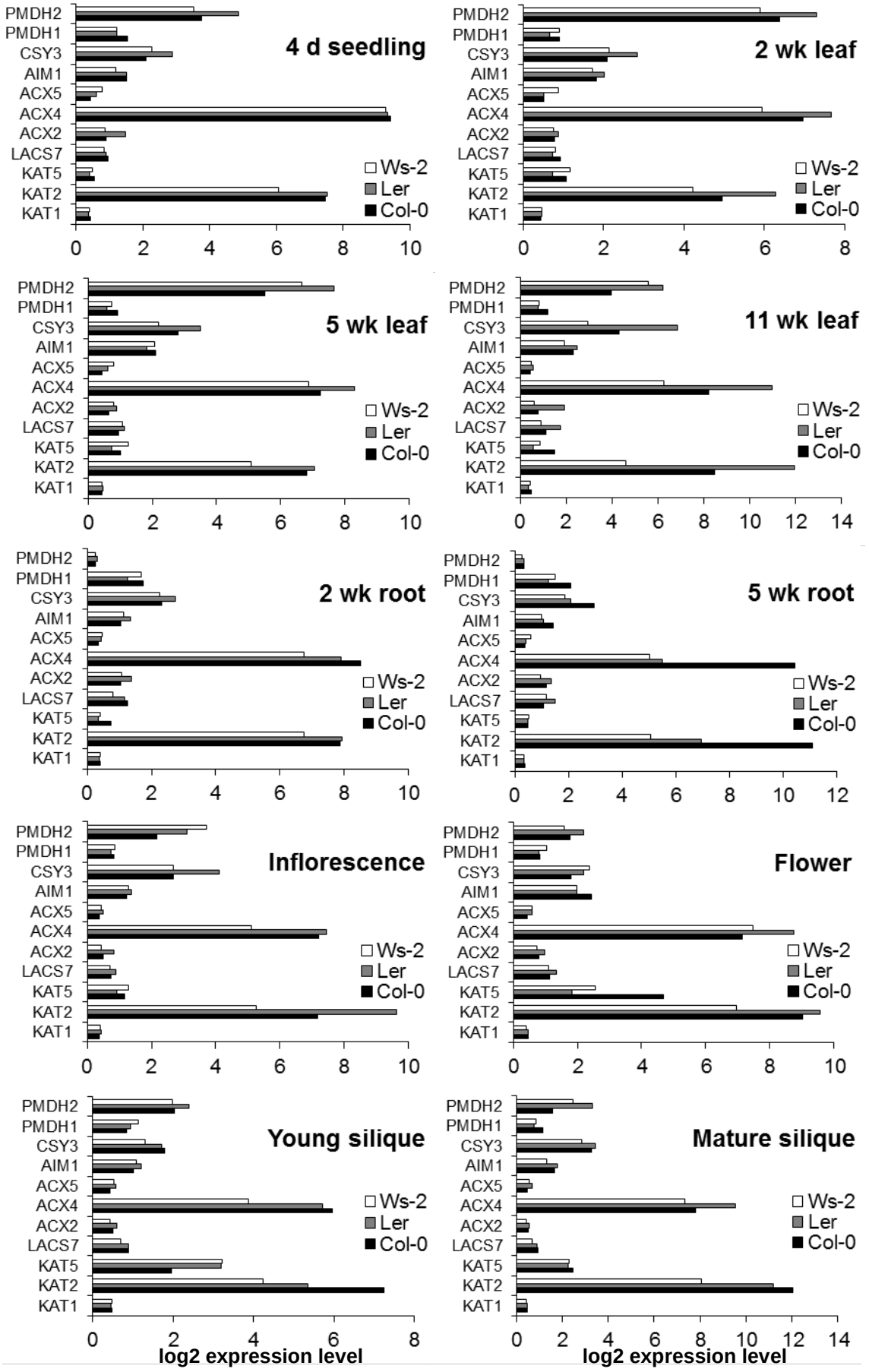
4 d seedling
2 wk leaf
5 wk leaf
11 wk leaf
2 wk root
5 wk root
Inflorescence
Flower
Young silique
Mature silique
PMDH2
PMDH1
CSY3
AIM1
ACX5
ACX4
ACX2
LACS7
KAT5
KAT2
KAT1
Ws-2
Ler
Col-0
log2 expression level

Figure 5.10. β-oxidation gene expression in a range of Ws-2, Col-0 and L*er* wild-type tissues.

Microarray data was provided by Chen *et al*. (2005). Data is derived from small chip so not all β-oxidation genes are present however all three thiolase genes are. No mean or standard error is available for this data as biological independent samples were pooled, resulting in no biological replicates.

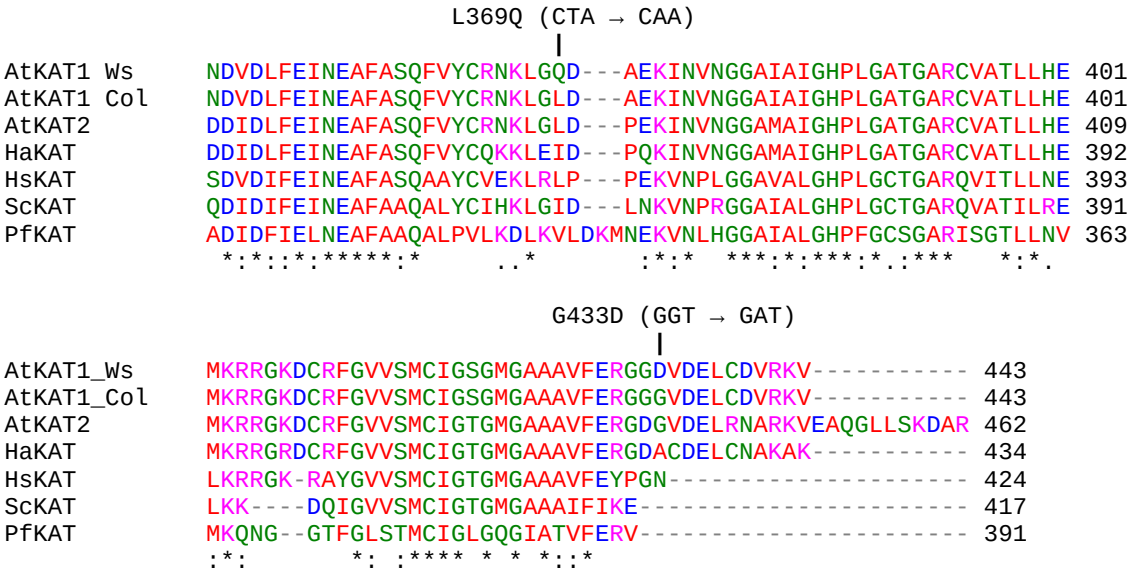

Figure 5.11 Amino-acid sequence alignment of KAT1 sequence region altered in Ws-4.

The amino-acid sequence of KATs from *Arabidopsis thaliana* (AtKAT1 and AtKAT2), *Helianthus annuus* (HaKAT), *Homo sapiens* (HsKAT), *Saccharomyces cerevisiae* (ScKAT), and *Pseudomonas fragi* (PfKAT) were aligned using ClustalW2. Residue colours indicate physicochemical properties: red (small or hydrophobic, including aromatic), blue (acidic), magenta (basic), and green (Hydroxyl, sulfhydryl, or amine). Residue conservations is annotated as follows: asterisk (*) fully conserved, colon (:) strongly similar, and period (.) weakly similar. Residues altered in Ws-4 compared to the Col-0 reference sequence are annotated above the sequence with amino acid and nucleotide codon SNP.

5.3 Discussion

5.3.1 Peroxisomal thiolase activity is required for fertility in Arabidopsis

Peroxisomes are abundant throughout floral tissue and have been observed in Arabidopsis petals, sepals, funiculus, ovules, pistil, young siliques and pollen (Prado *et al.*, 2004; Schilmiller *et al.*, 2007). The expression of *KAT1*, *KAT2*, *KAT5.1* and *KAT5.2* observed using GUS promoter analysis, qRT-PCR and publicly available microarray data indicate an important role for thiolase activity in reproductive tissue (Chapter 4). Some β-oxidation mutants are disrupted in floral structure similar to the *kat2-1 kat5-2* double mutant (Figure 5.3), *aim1* perhaps most severely (Richmond and Bleecker, 1999). However, the *aim1* single mutant is not completely infertile as *kat2-1 kat5-2* appears to be. Ovules with the *kat2-1* or *kat5-2* mutation develop into seed although at a reduced rate as the ratio of homozygotes, heterozygotes and wild-type is not exactly 1:2:1, indicating that a single wild-type copy of one of these genes is sufficient for fertility (Table 5.2). In fact, *kat2-1 kat5-2* pollen is viable and can be successfully crossed to wild-type plants suggesting that the double mutant is not completely male infertile, and that wild-type copies of *KAT2* and *KAT5* in the maternal tissue are sufficient for fertility. Indeed *kat2 kat5* (Ws-4) plants are unable to produce seed and wild-type pollen crossed to mutant flowers does not produce seed. Therefore, KAT2 and KAT5 function in maternal tissue is essential for reproductive success in the Ws-4 accession.

In the Ws-4 background, *kat2 kat5* internode spacing is erratic and secondary inflorescences proliferate but only reach dwarf height (Figure 5.3). Floral organs range in phenotypes from severely malformed to resembling wild-type like flowers. Cauline leaves often develop where flowers would be expected in wild-type plants. In the normal looking flowers of *kat2 kat5* (Ws-4) double mutants, small amounts of pollen are produced late in development. Some other β-oxidation mutants also have flowering phenotypes. Inflorescence branches of *aim1* (Ws-2 background) display a range of phenotypes from small masses of undifferentiated tissue which ceases to develop, to rare floral structures which have normal spiral patterns before terminating (Richmond and Bleecker, 1999). Flower development is characterised by arrest of sepal growth or internal floral organ growth, especially stamens and petals with gynoecium affected less frequently. Pollen development is also impaired. The *ped1 ped3* mutant (L*er*), disrupted in *KAT2* and *CTS*, also has severe developmental defects, with wavy rosette leaves and a dwarf inflorescence that forms sterile, abnormal floral structures (Hayashi *et al.*, 2002).

An increased number of secondary branches proliferate in *aim1* with reduced or no internode elongation (Richmond and Bleecker, 1999), a phenotype often associated with

reduced fertility or sterility (Hensel *et al.*, 1994). Wild-type plants from which developing fruits are surgically removed exhibit a delay in global proliferative arrest (GPA; the coordinate cessation of flower production on all inflorescence branches), and inflorescence meristems continue to proliferate. GPA mediated by communication between inflorescence meristems and developing fruits, is dependent on seed development specifically. The increased secondary branching in *kat2 kat5* (Ws-4) suggests that GPA is delayed in the double mutant. Previous investigation of the *kat2-1* single mutant suggests that GPA is delayed with the disruption of just one thiolase gene, with increased number of flower and siliques observed (Footitt *et al.*, 2007a). The phenotype of the *kat2-1 kat5-2* double mutant would be a more severe representation of impairment to GPA due to greater extent of infertility. Hensel *et al.* (1994) report that from observations in mutants with varying degrees of infertility that the number of seed produced controls the timing and occurrence of proliferative arrest, with a threshold of greater than 30% of wild-type levels of viable seed required for proliferative arrest.

The difference between *aim1* and Ws-2 during vegetative development is greater under short-day conditions compared to long-day (Richmond and Bleecker, 1999). Conversely flowers develop more normally when grown under short-days, while not completely complementing this phenotype. Growth under short-day conditions did not rescue fertility in *kat2 kat5* (Ws-4) double mutants.

In vitro pollen germination in the absence of exogenous sucrose is impaired in *cts* and *kat2*, with reduced germination frequency and shorter pollen tubes (Footitt *et al.*, 2007b). The infertility of Ws-4 *kat2 kat5* is presumably not due solely to impairment of pollen development or fertility as mature plants produce a small amount of viable pollen which can be outcrossed to wild-type plants. Additionally expression of *KAT5.2* from the *35S* promoter successfully complements the fertility phenotype even though this promoter is not expressed in pollen (Wilkinson *et al.*, 1997). A crucial role for β-oxidation in the energy metabolism of the gynoecium is not as obvious as for pollen, since it is probable that sugars would be available from surrounding photosynthetic tissue including the flower sepals.

The embryos of *acx3 acx4* abort early during differentiation and pattern formation in the heart and torpedo stage (Rylott *et al.*, 2003). Embryos of *aim1 mfp2* develop to the heart and globular stages of embryogenesis, aborting in the mid to late-cotyledonary stage of late morphogenesis/early maturation (Rylott *et al.*, 2006). That embryo lethality occurs at different stages suggest that the role of β-oxidation is not in synthesis or degradation of a signalling molecule required during a specific stage of embryo development. Alternately, in different mutants enough β-oxidation activity may be present to allow some further progress in development. Possibly the metabolic cost to the ovule of disruption to β-oxidation impairs

development despite the supply of sugars from parental tissue. Rylott *et al.* (2003) suggest that embryo lethality may be due to the accumulation of toxic levels of acyl-CoA, sequestration of CoA to in the acyl-CoA pool or the disruption of an unknown lipid-based signalling molecule. However, the accumulation of acyl-CoA has been observed in the seedlings of β-oxidation mutants without a resulting toxicity phenotype (Footitt *et al.*, 2002; Germain *et al.*, 2001; Rylott *et al.*, 2003). Moreover, acyl-CoA accumulation in transgenic oilseed rape plants designed to synthesise high levels of medium-chain fatty acids displayed no impairment of embryo development (Eccleston and Ohlrogge, 1998; Larson *et al.*, 2002).

An increase in frequency of embryo abortion has been observed in *kat2-1* compared to wild-type, with a corresponding reduction in seed yield (Footitt *et al.*, 2007a). In labelling experiments, *kat2-1* ovules displayed a reduction in the incorporation of acetate into neutral sugars suggesting disruption of gluconeogenesis. Importantly *kat2-1* ovules but not the ovules of the glyoxylate mutants *mls1* and *icl2* had reduced respiration rates. Footitt *et al.* (2007a) suggested that in reproductive organs the flow of carbon from β-oxidation to glyoxylate cycle to gluconeogenesis is less important as glyoxylate cycle genes are lowly expressed in this tissue (Charlton *et al.*, 2005a; Zimmermann *et al.*, 2004). However, as the expression of citrate synthase is high, citrate rather than succinate, is probably the major respiratory substrate derived from lipid (Footitt *et al.*, 2007a; Pracharoenwattana *et al.*, 2005). Raymond *et al.* (1992) proposed that lipid can be used as a carbon source for respiration from observations in germinating sunflower (*Helianthus annuus*) seeds, with carbon bypassing the glyoxylate cycle to enter the citric acid cycle. Infertility in *kat2 kat5* (Ws-4) may be partly due to a more severe impairment of ovule respiration than that observed in the single *kat2* mutant. Many mutants disrupted in energy metabolism have reduced fertility due to metabolic cost to the plant, for example the mitochondrial malate dehydrogenase mutant in Arabidopsis (Tomaz *et al.*, 2010) or cytoplasmic male sterility in maize (Laughnan and Gabay-Laughnan, 1983).

While some β-oxidation mutants abort at early stages of embryo development, the β-oxidation pathway is also important in seeds that are maturing/desiccating when supply of carbon from the mother plant ceases (Baud *et al.*, 2002). Sucrose from the maternal plant is the major carbon source for both oil and carbohydrate metabolism before breaking of the trophic connection between seed and plant. However, even before the developing seed becomes independent from maternal tissue, β-oxidation is active in turnover of lipids (Arai *et al.*, 2002; Chia *et al.*, 2005). Reduced seed weight has been previously reported in the *acx1-1*, *acx1-1 acx2-1* and *cts-2* mutants (Pinfield-Wells *et al.*, 2005). The seed weight for *kat2-1* and *kat5-2* is reduced and total fatty-acid content, as well as the TAG lipid marker C20:1 is reduced. Lower seed oil content has previously been observed in *kat2-1* (Germain *et al.*, 2001). The *sse1*

peroxisome deficient mutant has reduced rates of fatty-acid synthesis resulting in significantly reduced seed oil acid content, 10-16% of wild-type levels (Lin *et al.*, 2004). It remains unclear what function β-oxidation plays in fatty-acid synthesis, but there is speculation that fatty-acid derived molecules could provide a negative feedback regulating the balance between fatty-acid synthesis and degradation (Lin *et al.*, 2004; Ohlrogge and Jaworski, 1997).

A block in β-oxidation may affect the synthesis or degradation of signalling molecules contributing to infertility. Auxin, JA and BA are signalling molecules which can be synthesised via the β-oxidation pathway (Nyathi and Baker, 2006). JA has an established role in male fertility (Schaller *et al.*, 2000), but the Ws-4 *kat2 kat5* double mutant produces viable, fertile pollen, albeit in smaller quantities than wild-type (Figure 5.4). In the *cts* mutant, flower morphology is wild-type like, but anther filament extension is delayed and fertilisation frequency is reduced similar to JA mutants (Feys *et al.*, 1994; Park *et al.*, 2002; von Malek *et al.*, 2002), but in contrast to these mutants fertility is not rescued by supply of exogenous JA (Footitt *et al.*, 2007b). Similarly, in *kat2-1 kat5-2* exogenous supply of 100 μM JA was unable to restore fertility to flowers.

Disruption to auxin metabolism can affect fertility and shoot branching (Bennett *et al.*, 2006). Auxin can be synthesised via β-oxidation of the precursor IBA to form IAA, and IAA has been determined to play a role in stamen extension (Footitt *et al.*, 2007b). It has also been proposed that reduced anther filament length in *kat2-1* is potentially due to a change in IAA or JA levels (Footitt *et al.*, 2007a). There exists in plants a significant pool of auxin not derived from IBA, in the form of free IAA or IAA conjugated with amino acids, sugars or peptides (Woodward and Bartel, 2005). In *ech2 ibr1 ibr3 ibr10* quadruple mutant has severe defects in IBA conversion, resulting in a 20% reduction to IAA levels in the seedling root tip (Strader *et al.*, 2011). The *ech2 ibr1 ibr3 ibr10* mutant has smaller cotyledons (likely due to decreased cell expansion) and the early leaves develop slower with delayed flowering. However, morphological defects were not observed at maturity with inflorescences similar to wild-type plants. These results suggest that IBA contributes a more significant proportion to free IAA levels in seedlings than in mature plants and therefore, it seems unlikely that in flowers a disruption to the conversion of IBA results in the severe disruption to fertility observed in *kat2-1 kat5-2*.

BA can be synthesised via β-oxidation, with a thiolase in petunia (*Petunia hybridia* cv. Mitchell) recently identified in this role (Moerkercke *et al.*, 2009). However, alternate major pathways for BA synthesis are found in Arabidopsis, notably the non-oxidative and isochorismate pathways (Wildermuth, 2006; Wildermuth *et al.*, 2001). Additionally, it is hypothesised that the BA derived molecules found in petunia do not have a characterised role in

reproductive fertility, but appear to act as volatile compounds which attract pollinators (Moerkercke *et al.*, 2009; Stuurman *et al.*, 2004).

The implication of other novel signalling molecules being synthesised or degraded via β-oxidation has been previously proposed (Baker *et al.*, 2006). It is potentially of interest that the *acx3 acx4* with short-chain specificity displays embryo lethality (Rylott *et al.*, 2003), while *acx1 acx2* with long-chain specificity is fertile (Adham *et al.*, 2005). Recently, a role for KAT2 in the positive regulation of ABA signalling via regulation of ROS homeostasis in plant cells has been suggested (Jiang *et al.*, 2011). Using *kat2-3*, a KAT2 mutant not characterised here, Jiang *et al.* (2011) reported reduced sensitivity to ABA in the mutant and increased sensitivity in seedlings over-expressing *KAT2*. Previously, a link between β-oxidation and ABA in controlling seed dormancy has been revealed in which, by an unknown mechanism, PED3 negatively regulates the transcription factor ABI5, which positively controls PGIP1/PGIP2 regulating pectin degradation, and allowing weakening of the seed coat and germination (Kanai *et al.*, 2010). Jiang *et al.* (2011) attribute the positive regulation of ABA by KAT2, and the converse negative regulation of ABA by PED3 (Kanai *et al.*, 2010), to the different stage of β-oxidation in which these enzymes participate, but this effect requires further study and analysis.

5.3.2 Disruption of β-oxidation results in a defect in vegetative development

The *kat2 kat5* (Ws-4) double mutant has a small rosette and dwarf inflorescence plant growth phenotype. It is unclear if this mature plant phenotype is due to impairment in the generation of signalling molecules and/or energy metabolism. In plants, free fatty acids can be transiently stored in TAG before degradation via β-oxidation. During extended dark treatment, plants catabolise lipids when starch stores are depleted after the end of the regular dark period, but in the *pxa1* mutant amphipathic free fatty acids are not degraded (Kunz *et al.*, 2009). These fatty acids damage chloroplast membranes in *pxa1*, resulting in chlorophyll degradation and accumulation of the phototoxic chlorophyll breakdown intermediate PhA due to a lack of reductive power from photosynthesis or the oxidative pentose phosphate pathway (Kunz *et al.*, 2009). While the accumulation of PhA can be prevented by the supply of carbon in the form of sucrose, *pxa1* is hypersensitive to exogenous α-linolenic acid independent of exogenous sucrose supply, suggesting the phenotype is not solely due to PhA (Kunz *et al.*, 2009).

Fatty acids are not only catabolised during senescence but are continuously turned over during plant growth in a balance between degradation via β-oxidation and synthesis. Estimates of average daily degradation of fatty acids range from 2% (Bonaventure *et al.*, 2004) to 4% (Bao *et al.*, 2000) of total lipid content. Similar rates of degradation are observed during natural

senescence suggesting net loss of lipids during this process is due to a decrease in synthesis rates rather than an increase in breakdown (Yang and Ohlrogge, 2009). While *kat2* is not disrupted in the degradation of fatty acids during natural senescence possibly due to redundancy with other thiolase genes and the slow rate of breakdown (Yang and Ohlrogge, 2009), it does display a phenotype similar to *pxa1* in response to extended to dark treatment including leaf necrosis and accumulation of PhA, albeit less severe (Kunz *et al.*, 2009).

Kunz *et al.* (2009) report chloroplast structural damage and decreased photosynthetic activity before re-exposure of *pxa1* to the light, so disruption of the plant metabolic program is not solely due to the photooxidative effect of PhA, but also free fatty-acid accumulation. With a near complete block in β-oxidation in the Ws *kat2 kat5* mutant, free fatty-acids may accumulate causing damage to the photosystem. During the early stages of development bleaching is observed in mutant seedlings, but bleaching is not evident in mature plants so presumably free fatty-acids do not accumulate to the same extent at this stage of development. A pale seedling phenotype with reduced chlorophyll levels is described in the matrix import protein mutant, *pex5*, which the authors suggest is due to impaired import of photorespiratory enzymes (Khan and Zolman, 2010). However, a role for thiolase in matrix protein import is not obvious, so it seems probable that this effect is due to disruption of β-oxidation.

Other β-oxidation mutants with reduced rosette size phenotypes similar to *kat2 kat5* (Ws) are those with near complete blocks in β-oxidation, such as *ped1 ped3* (Hayashi *et al.*, 2002) and *csy2 csy3* (Pracharoenwattana *et al.*, 2005). Other mutants with blocks in β-oxidation impairing growth during early germination and seedling establishment, such as *acx1 acx2* (Pinfield-Wells *et al.*, 2005), *lacs6 lacs7* (Fulda *et al.*, 2002) or *pmdh1 pmdh2* (Pracharoenwattana *et al.*, 2007), do not have mutant phenotypes at the mature growth stage ostensibly due to redundancy with genes expressed at later stages. Glyoxylate cycle mutants such as *icl* (Eastmond *et al.*, 2000a) and *mls* (Cornah *et al.*, 2004) have no visible mutant phenotype as carbon supply bypasses through citrate instead of succinate, or because β-oxidation of toxic free fatty acids is not disrupted.

5.3.3 Natural variation of β-oxidation gene expression does not explain a divergent role for this pathway in fertility and reproductive success

The infertility phenotype is observed in the Ws-4 double mutants of *kat2-1 kat5-2* and *kat2-5 kat5-2* as well as in the Ws-4 and L*er* hybrid double mutant *kat2-1 kat5-1*. Additionally, the severe mutant phenotype of *kat2-1 kat5-2* (Ws-4) is restored to fertility by complementation with the constitutive expression of peroxisomal *KAT5.2*, but not cytosolic *KAT5.1*, indicating

reproductive impairment is related to peroxisomal thiolase activity. However, curiously no infertility phenotype was observed for the *kat2-4 kat5-1* (L*er*) or *kat2-2 kat5-3* (Col-0) double mutants, although the germination and seedling establishment phenotype observed in the *kat2* single mutants was consistent with that seen in *kat2-1* (Ws-4). This is the first example of accession-dependent natural variation in the β-oxidation pathway or in mutant phenotypes that has been described in the literature. The reason for the differing phenotypic response between the accessions Col-0 and L*er* with the Ws-4 accession remains unclear. β-oxidation mutants with severe infertility phenotypes have been characterised in the Ws accession including changes to floral morphology in *aim1* (Richmond and Bleecker, 1999), and embryo lethality in *acx3 acx4* (Rylott *et al.*, 2003) and *aim1 mfp2* (Rylott *et al.*, 2006), however phenotypes resulting in infertility have also been observed in *csy2 csy3* mutant (Col) (Pracharoenwattana *et al.*, 2005) and *ped1 ped3* (L*er*) mutant (Hayashi *et al.*, 2002).

The genetic background of Ws appears to result in a different effect of delayed flowering on proliferative capacity compared to L*er* from observations of late-flowering mutants (Hensel *et al.*, 1994). In the L*er* background late-flowering mutants displayed only a minor increase in meristem proliferative capacity compared to wild-type, while in the Ws background there was a doubling of proliferative capacity (Hensel *et al.*, 1994). The Col and L*er* accessions both share a common origin from a non-isogenic wild-type strain collected in Gorzów Wielkopolski (also known as Landsberg an der Warthe) in Poland, with the L*er* line derived by X-ray induced mutagenesis from this seed collection (Rédei, 1992). The Col accession was derived from this starting material by Dr Rédei at the University of Missouri, Columbia (Rédei, 1992). The Ws accession originates independently from Belarus (Smyth, 1995), and was adopted by the Arabidopsis community due to greater efficiency in transformation compared to other accessions (Akama *et al.*, 1992; Koornneef and Meinke, 2010). This common origin for Col and L*er* compared to Ws may explain the similar response for these related accessions to disruption of peroxisomal thiolase activity.

A prominent genetic difference in the Ws-0 accession that has previously been described is the 14 bp deletion in the *PHYD* gene, which results in a phyD null phenotype (Aukerman *et al.*, 1997). However, analysis of simple sequence length polymorphisms (Aukerman *et al.*, 1997) and SNPs (Anastasio *et al.*, 2011) indicates Ws-0 is a distinct genotype from Ws-1, Ws-2, Ws-3 and Ws-4. Therefore care must be taken when interpreting results from experiments using the Ws accession for which differences in genotype may have a significant affect.

Potentially the *KAT1* gene in Col and L*er kat2 kat5* may compensate for the loss of function, but not in Ws due to differences in coding or regulatory sequence of *KAT1* in that accession. While the *KAT1* gene region is identical in Col-0 and L*er* there are differences in the

Ws-4 sequence. These SNPs do not result in a change to the predicted exon-intron structure, and most of the exon SNPs result in silent mutations or a mutation in a non-conserved amino acid residues. The SNP resulting in L369Q alters a semi-conserved hydrophobic residue to polar non-charged one, in a region adjacent to an α-helices (Pye *et al.*, 2010). It is unclear if this amino acid residue change would affect the structure of Ws-4 KAT1 protein radically enough to result in the phenotypic difference observed in the double mutants of the different accessions.

Future experiments using the *kat2-1 kat5-1* (Ws-4/Ler hybrid) double mutant could be used to investigate the functionality of Ws-4 KAT1 protein compared to Ler KAT1 protein. It would be expected that the *kat2-1 kat5-1* double mutant population would contain three populations: $KAT1_{Ws\text{-}4}$ homozygous, $KAT1_{Ws\text{-}4}/KAT1_{Ler}$ heterozygous and $KAT1_{Ler}$ homozygous. If *kat2-1 kat5-1* double mutants possessing a $KAT1_{Ler}$ gene were fertile while those homozygous for the $KAT1_{Ws\text{-}4}$ gene were not, this would suggest that the $KAT1_{Ler}$ protein was functional and capable of rescuing the mutant phenotype. However if this is not the case and double mutants possessing a $KAT1_{Ler}$ gene remained infertile it seems unlikely that the accession mutant phenotype difference was related to functional differences in the KAT1 Ws-4 protein due to these SNPs.

Publicly available transcriptome data from Col-0 and Ws-4 seedlings 2 d post-germination indicates differences in the expression level of several β-oxidation genes in these two accessions (Cornah *et al.*, 2004). The greatest difference for a β-oxidation gene appears to be that of *KAT5* which is over 4 times higher in Col-0 than Ws-4 (Figure 5.9). Potentially the redundancy of many β-oxidation genes could result in different isozymes complementing for the loss of function in mutants, due to higher expression in some accessions than others. For the phenotype observed in the Ws *kat2 kat5* double mutant the most likely candidate for compensation in Col and L*er* would be *KAT1*, or potentially the peroxisomal isoform of *AACT1*. However *KAT1* and *AACT1* are not expressed at significantly different levels in Col compared to Ws-4, and remain at very low levels during germination (Cornah *et al.*, 2004).

Publicly available transcriptome data provided by Chen *et al.* (2005) allow for a comparison of expression between reproductive tissue of Ws-2, L*er* and Col-0 (Figure 5.10). The expression of *KAT2* is higher in Col-0 and L*er* than Ws-2 in flowers, and both young and mature siliques. For *KAT5* the pattern is less clear as expression is higher in Col-0 than Ws-2, while L*er* appears generally lower, with no major difference in mature siliques for all three accessions. *KAT1* has constitutively low expression in all three accessions, suggesting that this gene does not play a major role under the conditions measured. For this transcriptome data, pooled samples of multiple plants were used, with no biological replication, making analysis of the statistical significance of the changes in expression not possible. Further experiments analysing expression

of β-oxidation genes in different Arabidopsis accessions, especially in flowers and siliques could potentially be illuminating.

5.3.4 The role of KAT5 in flavonoid metabolism remains unclear

The putative role of KAT5 in flavonoid biosynthesis remains obscure. *KAT5* is co-expressed with flavonoid biosynthesis genes (Carrie *et al.*, 2007) as well as being co-regulated by the transcription factors MYB11, MYB12 and MYB111 which all have high target specificity for several individual genes of this pathway (Stracke *et al.*, 2007). Flavonoids play an essential role in testa pigmentation, with many flavonoid mutants isolated from forward genetic screens due to deficiency in seed coat formation, including the transparent testa (*tt*) and transparent testa glabra (*ttg*) mutants (Debeaujon *et al.*, 2000; Winkel-Shirley *et al.*, 1995). *KAT5* is highly expressed in the seed testa, the only tissue in genevestigator analysis for which *KAT5* expression levels are greater than *KAT2* (Zimmermann *et al.*, 2004). Flavonoid mutant seed colour ranges from yellow (*tt1* to *tt5*, *tt8* and *ttg1*) to pale brown (*tt6*, *tt7* and *tt10*) or grayish brown (*tt9*) (Debeaujon *et al.*, 2000). However, *kat5* mutants have testa pigmentation indistinguishable from wild-type seed of the same genotypic background (Figure 5.8A).

Flavonoids have a functional role as molecular sunscreens in response to UV irradiation with chalcone synthase (*tt4*) and chalcone isomerase (*tt5*) mutants sensitive to exposure (Li *et al.*, 1993). KAT5 and many genes of flavonoid biosynthesis are up-regulated by UV-B treatment (Winter *et al.*, 2007) and this regulation is disrupted in the *myb11 myb12 myb111* triple mutant (Stracke *et al.*, 2010). The induction of *ACX* and *CHS* expression in parsley cells in response to UV irradiation suggests a link between primary and secondary metabolism (Logemann *et al.*, 2000). Peroxisomal β-oxidation and flavonoid biosynthesis have also been linked by the down-regulation of flavonoid genes in the *cts* mutant, with *kat2-1* and *cts* also having reduced embryo flavonoid content during germination in the absence of exogenous sucrose (Carrera *et al.*, 2007). A more general role for peroxisomes in light signalling is suggested by the reversion of the light signalling transcription factor mutant *det1-1* by a dominant *ted3* mutation in the *PEX2* gene (Hu *et al.*, 2002). Additionally, light induced peroxisome proliferation is mediated by the peroxisome biogenesis protein Pex11b, and the *PEX11b* gene is regulated by the far-red light receptor phytochrome A and the bZIP transcription factor HY5 HOMOLOG (Desai and Hu, 2008).

5.3.5 Model of cytosolic and peroxisomal KAT and AACT

In silico analysis of the *KAT2* and *KAT5* promoters resulted in the identification of multiple putative binding sites for transcription factors functionally related to phenylpropanoid and flavonoid metabolism, and response to UV-B irradiation (Chapter 4). There is evidence that

several of the enzymes of phenylpropanoid and flavonoid metabolism including PAL1, C4H, 4CL, CHS, CHI, F3H, and F3'H are localised in complexes on the cytosolic face of the endoplasmic reticulum (Winkel-Shirley, 1999). The peroxisomal thiolases KAT1, KAT2 and KAT5.2 may contribute acetyl-CoA via β-oxidation, which would be converted by acetyl-CoA carboxylase into malonyl-CoA for chalcone synthase in flavonoid biosynthesis (Shorrosh *et al.*, 1994). However, evidence from *Saccharomyces cerevisiae* and Arabidopsis that the peroxisomal membrane is impermeable to acetyl-CoA *in vivo* (Pracharoenwattana *et al.*, 2005; van Roermund *et al.*, 1998), suggests that cytosolic KAT5.1 as a more probable candidate for contribution to flavonoid biosynthesis. Alternately citrate exported from the peroxisome, may provide substrate for ATP-citrate lyase to synthesise cytosolic acetyl-CoA (Fatland *et al.*, 2005). Evidence from knockdown lines indicates that slightly down-regulating expression of *ATP-citrate lyase* (*ACL*) results in severe effect to plant growth and morphology, suggesting that there are no other significant sources of the cytosolic acetyl-CoA pool (Fatland *et al.*, 2005).

Class II thiolases, also known as synthetic thiolases or acetoacetyl-CoA thiolases (AACT), catalyse the reverse reaction to Class I thiolases (3-ketoacyl-CoA thiolase), the Claisen-type condensation of two molecules of acetyl-CoA to form acetoacetyl-CoA. Two genes, *AACT1* (At5g47720) and *AACT2* (At5g48230), encode four cytosolic isoforms AACT1.1, AACT1.2, AACT2.1, and AACT2.2, and one peroxisomal isoform AACT1.3 (Carrie *et al.*, 2007). *AACT2* is widely expressed (Ahumada *et al.*, 2008; Winter *et al.*, 2007), and is co-expressed with genes of the mevalonate (MVA) pathway (Carrie *et al.*, 2007). The MVA pathway synthesises precursors for a variety of plant isoprenoid compounds, including sterols, cytokinins, and ubiquinones that are essential for plant growth and development (Bouvier *et al.*, 2005; Chappell, 1995). *AACT1* is expressed at low levels and does not correlate with isoprenoid biosynthetic genes, with expression mainly restricted to roots and inflorescences (Ahumada *et al.*, 2008; Winter *et al.*, 2007).

Genetic analysis indicates an essential role for AACT2 in isoprenoid metabolism, as the *aact2* mutant has an embryo lethal phenotype, while the *aact1* mutant displayed no growth or development defects (Jin and Nikolau, 2006). AACT1 has no clear metabolic role, but as peroxisomal acetoactetyl-CoA thiolase can also catalyse the reverse degradative reaction (Kanayama *et al.*, 1998), it may participate with KAT1, KAT2 and KAT5.2 in peroxisomal β-oxidation of fatty acids in some tissues (Ahumada *et al.*, 2008).

Kinetic analysis of KAT enzyme activity suggests that this reaction too is reversible, albeit with the reaction equilibrium strongly favouring cleavage of acetyl-CoA (Gilbert *et al.*, 1981). Additionally, KAT activity can be inhibited by acetyl-CoA (Olowe and Schulz, 1980; Wang *et al.*, 1991). KAT5.1 localisation in the cytosol may result in the enzymatic conditions favouring

the synthesis reaction, participating with AACT2 in some reproductive tissues. AACT and KAT could co-ordinately regulate the pools of acetyl-CoA in the peroxisome and cytosol to fine-tune primary metabolism (Figure 5.12). The *KAT5* gene is conserved in the order Brassicales (Chapter 4), which are characterised by the presence of glucosinolates, secondary metabolites involved in plant defence (Fahey *et al.*, 2001). Peroxisomes have been implicated in glucosinolate synthesis as the *bzo1* mutant (At1g65880) was identified in a forward genetics screen for reduced seed benzoyloxyglucosinolate accumulation (Kliebenstein *et al.*, 2007). BZO1 has a predicted PTS1 (Reumann *et al.*, 2004), and benzoyl-CoA ligase activity *in vitro* (Kliebenstein *et al.*, 2007).

However, the results described in this chapter suggest there is significant natural variation in the role of KAT5 at the accession level. These results and the evidence for divergent conservation of *KAT* genes in plants (Chapter 4), demonstrates the metabolic diversity that exists within and between species. Elucidating the implications of natural variation in the β-oxidation pathway for plant primary and potentially secondary metabolism will require further experimentation.

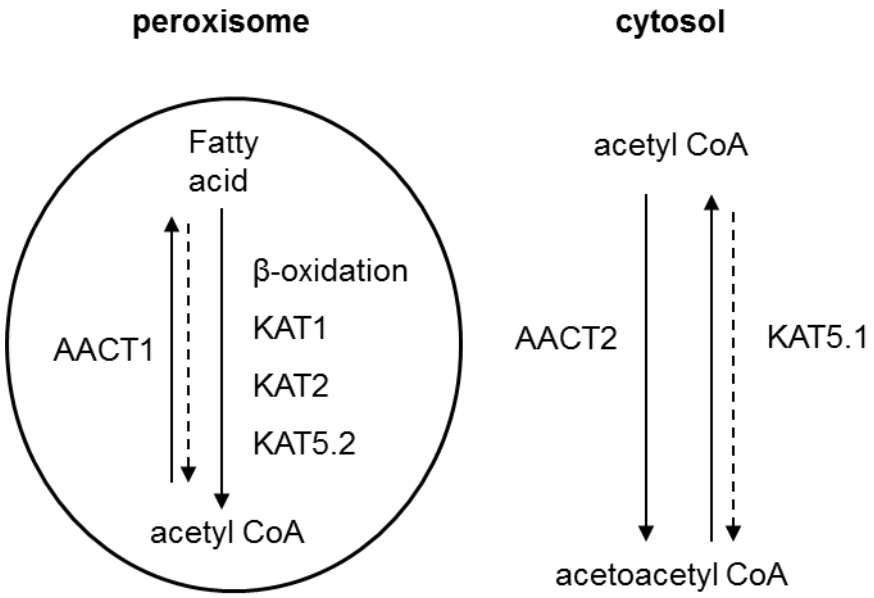

Figure 5.12. Proposed model of degradative and synthetic thiolase enzyme metabolism in peroxisome and cytosol.

KAT1, KAT2, KAT5.2 and AACT1 are all localised in the peroxisome and may contribute to β-oxidation of fatty acids to acetyl-CoA. AACT2 and KAT5.1 are localised in the cytosol. AACT2 catalyses the synthetic reaction that condenses two molecules of acetyl-CoA into one of acetoacetyl-CoA. Biochemical evidence suggests that thiolases may catalyse reaction in both directions depending on stoichiometry.

Chapter 6: General Discussion

6.1 Advancing plant peroxisome biology

At the beginning of this project, many of the core enzymes and associated genes of peroxisomal β-oxidation, especially for long-chain fatty-acid breakdown, had been identified and characterised. There has been a growing literature concerning the component proteins that make up peroxisomes, primarily aided by sequencing of the Arabidopsis genome, which allowed researchers to search for PTS containing proteins encoded in the genomic sequence (Reumann *et al.*, 2004). Attempts to characterise Arabidopsis peroxisomes using proteomic isolation and identification techniques had yielded limited success (Fukao *et al.*, 2003; Fukao *et al.*, 2002). Peroxisome isolation from Arabidopsis proved difficult due to the fragility of the single membrane and contamination from other organelles (Eubel *et al.*, 2008). However, during the latter part of the decade there were significant advances and improvements to proteomics techniques allowing isolation of peroxisomes from leaf tissue (Reumann *et al.*, 2007) and cell culture (Eubel *et al.*, 2008). The combination of preliminary data from Eubel *et al*., another lab in the Centre in Plant Energy Biology at UWA, and the Araperox database allowed us to refine our list of peroxisomal β-oxidation enzymes targeted for characterisation.

So while many of the core enzymes of peroxisomal β-oxidation in Arabidopsis had been characterised, it was unclear what role many of the auxiliary enzymes of β-oxidation served in plant development and function. I used reverse genetics to isolate many mutants disrupted in peroxisomal genes to screen for β-oxidation phenotypes (Chapter 3). I also performed a more detailed characterisation of the Arabidopsis thiolase gene family described in chapters 4 and 5. Another aspect in the initial stages of my project was the characterisation of the peroxisomal glycolate oxidase gene family that is involved in photorespiration. For reasons of succinctness and for flow of this thesis, this glycolate oxidase work has not been covered in the preceding chapters. A submitted manuscript of work, collaborating with other researchers, detailing this characterisation is available in Appendix III. The experimental work described in this thesis, has produced several novel results that have added to the field of peroxisome biology in Arabidopsis.

6.2 Peroxisomal auxin metabolism in Arabidopsis

6.2.1 Identification of auxin metabolism mutants

My work resulted in the identification of two new auxin-precursor resistant mutants (Chapter 3). The *aae18* mutant is the first instance of a β-oxidation mutant resistant to 2,4-DB but not IBA and to date no other β-oxidation mutant has been described with selective resistance to auxin precursors (for review see Strader and Bartel, 2011). This implies that different pathways operate in Arabidopsis for these two auxin precursors. Exclusive 2,4-DB resistance is

an intriguing result considering that 2,4-DB is a synthetic auxin and does not occur endogenously as does IBA (Ludwig-Müller, 2000). 2,4-DB could be analogous to an endogenous compound other than IBA that is also metabolised by β-oxidation. One candidate for a 2,4-DB analogue is *trans*-cinammic acid, which in this model would be activated by AAE18 with CoA for synthesis of benzoic acid via the β-oxidation pathway (Reumann *et al.*, 2004). There is evidence in the literature for differences in 2,4-D and IAA signal transduction. 2,4-D binds with less affinity to the Transport Inhibitor Response 1 (TIR1) auxin receptor than IAA (and also NAA) (Kepinski and Leyser, 2005). Additionally, a small acidic protein (SMAP1), of unknown function, has been identified that mediates 2,4-D but not IAA response (Rahman *et al.*, 2006). Mutants disrupted in SMAP1 function are resistant to 2,4-D but sensitive to IAA, however an alternate putative endogenous ligand for SMAP1 is not suggested by Rahman *et al*. 2006. This implies a partially overlapping pathway of IBA/IAA and 2,4-DB/2,4-D metabolism and signal transduction in Arabidopsis.

The *sdra* mutant that is disrupted in At4g05530, a gene encoding a peroxisomal short-chain dehydrogenase described in chapter 3, was also identified by Zolman *et al.* (2008) via a forward genetic screen and annotated *ibr1*. The *ibr1* mutant is sensitive to IAA and resistant to IBA, but is not sucrose dependent (Zolman *et al.*, 2008). The work described in chapter 3 therefore confirms many of the findings of Zolman *et al.* (2008), with additional experimental data showing GFP-tagged peroxisome targeting and germinating seedling fatty acid analysis. This work has been published in the paper Wiszniewski *et al.* (2009).

6.2.2 Reverse genetics complements the forward genetics approach

Numerous β-oxidation mutants have been identified using forward genetics screens for β-oxidation phenotypes such as sucrose dependence, IBA resistance, and 2,4-DB resistance (Eastmond, 2006; Hayashi *et al.*, 1998; Lange and Graham, 2000; Zolman *et al.*, 2000). The work described in Chapter 3, utilising well-characterised 'classical' β-oxidation phenotypes, and improvements in predictions and empirical data on the peroxisomal proteome, facilitated the use of reverse genetics to identify mutants involved in auxin metabolism. Reverse genetics is advantageous in allowing rapid, targeted isolation of large numbers of mutants available from community collections of T-DNA insertion lines, and screening for these classical phenotypes. This allowed for the relatively fast identification of two genes involved in auxin metabolism, without the need to map the mutations responsible for these phenotypes.

However, there are obvious limitations, as we do not necessarily know all the components of the Arabidopsis peroxisome. Additionally, while coverage of the Arabidopsis genome for T-DNA insertion lines is good, providing a remarkable resource to plant biologists, this coverage is not perfect. For some genes T-DNA insertions lines are not available, and the

presence of a T-DNA insertion is not a guarantee of transcript disruption. For example I was unable to isolate a T-DNA mutant disrupted in the At4g14430 gene encoding an enoyl-CoA hydratase, but a mutant impaired in this genes function, *ibr10*, was identified in a forward genetics screen and shown to have a similar phenotype to *sdra* (Zolman *et al.*, 2008). Large multi-gene families such as the AAE or ECH Arabidopsis families pose significant difficulties for forward or reverse genetic dissection as there may be redundancy between closely related genes. Multiple experimental approaches and strategies will be required for further characterisation of the functions of these genes.

Reverse genetics therefore complements the forward genetics approach that has been used by other researchers. The work described in Chapter 3, demonstrates the viability of using a reverse genetics approach to rapidly and efficiently screen the function of large number of genes. While peroxisomes contain a relatively small number of proteins compared to other organelles in the plant, these techniques can be a useful approach for other researchers attempting to characterise other organelles. The Chloroplast 2010 project is an example of a large-scale reverse genetics attempt to characterise more than 5000 T-DNA mutants associated with chloroplast metabolism, by screening for phenotypes such as changes to leaf fatty acid composition, starch content, and chlorophyll fluorescence (Ajjawi *et al.*, 2010). With sufficient technology and researchers, large-scale reverse genetics can prove a useful tool for understanding organelle biology. However, given limitations to these factors, focusing on smaller systems such as specific enzymatic pathways or smaller organelles is a viable alternative and led the discovery of novel auxin response mutants.

6.2.3 Recent advances in understanding peroxisomal contribution to auxin metabolism

Subsequent to my published work on *sdra* (Wiszniewski *et al.*, 2009), auxin metabolism and β-oxidation has been further characterised by other researchers (for review see Strader and Bartel, 2011). The involvement of IBA to IAA conversion in cell expansion has been demonstrated in an *ibr1 ibr3 ibr10* triple mutant, which has a dramatic reduction to *in planta* conversion of labelled IBA to IAA content in seedlings (Strader *et al.*, 2010). However, despite reduced conversion of IBA to IAA in this triple mutant no change in the free IAA pool was observed. Cell expansion defects in the triple mutant results in a phenotype of shorter root hairs and smaller cotyledons (Strader *et al.*, 2010). This phenotype is even more severe in an *ech2 ibr1 ibr3 ibr10* quadruple mutant, which also has a smaller rosette and later flowering (Strader *et al.*, 2011). Seedlings have less lateral roots, and there is a 20% reduction in free IAA in the seedling root tip as determined by GC-MS (Strader *et al.*, 2011). I described a reduced number of lateral roots in *kat2* mutants (Chapter 3), so this phenotype may be due to lower IAA levels, rather than slower growth due to metabolic block in oil body degradation. Indeed my work

suggests KAT2 is the main peroxisomal thiolase responsible for auxin metabolism as *kat1*, *kat5*, *kat1 kat5* and *kat2 kat5* are not resistant or no more resistant to 2,4-DB than individual *kat2* alleles (Chapter 5). Further experiments using IBA are required to determine if this can be confirmed for endogenous auxins, but initial experiments using single mutants indicate that only *kat2* is resistant to IBA (data not shown).

Notably, while the β-oxidation mutants *pex6*, *acx1 acx2*, *pxa1*, and *chy1* have very low IBA to IAA conversion rates equivalent with the *ibr1 ibr3 ibr10* triple mutant (Strader *et al.*, 2010), these mutants do not have similar fertility phenotypes to the triple mutant (Footitt *et al.*, 2007b; Pinfield-Wells *et al.*, 2005; Zolman and Bartel, 2004; Zolman *et al.*, 2001a). Even in the more severely impaired IBA conversion *ech2 ibr1 ibr3 ibr10* quadruple mutant, infertility is not reported (Strader *et al.*, 2011). This suggests that disruption to auxin metabolism is not the reason reduced fertility is observed in severe β-oxidation mutants, such as *kat2 kat5* (Chapter 5).

6.3 Characterising the Arabidopsis thiolase family

6.3.1 KAT2 is the major peroxisomal thiolase

I attempted characterisation of the Arabidopsis thiolase family, not limited to KAT2 but also investigating the function of KAT1 and KAT5. KAT2 is the major peroxisomal thiolase for many fatty-acids metabolised by β-oxidation, while KAT1 has low constitutive expression and KAT5 has more tissue-specific expression patterns. Using expression and genetic analysis, I discovered that peroxisomal thiolase is essential for fertility; similar to other previously identified severe β-oxidation mutants. However, a novel accession dependent phenotype was also discovered.

KAT2 has a well characterised role in nearly all of the functions of peroxisomal β-oxidation in plant development. *kat2* mutant seedlings do not establish in the absence of an exogenous carbon source, as KAT2 is required for degradation of seed storage lipid during germination (Germain *et al.*, 2001; Hayashi *et al.*, 1998). Oil bodies persist in *kat2* seedlings, and peroxisome, chloroplast, and mitochondria organelle size and abundance is altered (Germain *et al.*, 2001; Hayashi *et al.*, 2001). KAT2 is a major enzyme in auxin metabolism during the conversion of IBA to IAA (Germain *et al.*, 2001; Hayashi *et al.*, 1998; Zolman *et al.*, 2000), and contributes to wound-induced JA levels (Afitlhile *et al.*, 2005). During natural senescence KAT2 is required for the synthesis of JA (Castillo and León, 2008), but is not essential for breakdown of membrane lipids (Yang and Ohlrogge, 2009). However, this appears to be because of the slower rate of degradation during natural senescence, as during dark-induced senescence the block in β-oxidation in the *kat2* mutant results in accumulation of free fatty acids, which disrupt chloroplast function (Kunz *et al.*, 2009).

In contrast far less is known about KAT1 and KAT5, with expression analysis indicating low constitutive expression of *KAT1*, while *KAT5* is up-regulated in siliques and flowers (Kamada *et al.*, 2003). There has been experimental investigation of sub-cellular targeting of the thiolase family in Arabidopsis; GFP-tagged KAT1 and KAT2 localises to peroxisomes while the *KAT5* gene encodes two proteins: cytosolic KAT5.1 and peroxisomal KAT5.2 (Carrie *et al.*, 2007). Additionally, while *KAT2* is co-expressed with genes of β-oxidation as expected, *KAT5* unexpectedly co-expresses with genes of flavonoid biosynthesis (Carrie *et al.*, 2007).

While *KAT5* is co-expressed and co-regulated with flavonoid biosynthesis genes (Carrie *et al.*, 2007; Stracke *et al.*, 2010; Stracke *et al.*, 2007), *kat5* mutants do not display phenotypes typical of disruption to flavonoid biosynthesis: for example, imbibed *kat5* mutant embryos accumulate flavonoids like wild-type. *KAT5* is highly expressed in testa tissue, and many flavonoid mutants have defects to testa colour (Debeaujon *et al.*, 2000), but *kat5* seed testa colour is similar to wild-type. A role for KAT5 in flavonoid biosynthesis is unclear, but potentially KAT5 contributes to biosynthetic rather than the degradative reactions, catalysing the production of acetoacetyl-CoA from acetyl-CoA, as a first step in mevalonate and isoprenoid synthesis.

6.3.2 Thiolase gene function in development

I characterised KAT1, KAT2 and KAT5 transcription and used mutants for functional genetic analysis (Chapters 4 and 5). *KAT1* has low transcript levels, the *KAT1* promoter has low activity and few promoter elements, and a *kat1* mutant had no phenotypes related to IBA or 2,4-DB resistance, sucrose dependence, germination frequency, or mature plant growth and development. Analysis of the plant thiolase family indicated that there were no orthologous genes to *KAT1* other than one found in the *Arabidopsis lyrata* genome. Synteny between genes bordering *KAT2* and *KAT1* indicates that *KAT1* may be recent gene duplication. KAT1 thus does not appear to be an important peroxisomal thiolase for plant function and development.

Promoter analysis indicates that *KAT5* is expressed in hypocotyls and roots of germinating seedlings. *kat5* mutants are not sucrose dependent and fatty-acid analysis during seed germination reveals a profile indistinguishable from wild-type seedlings, implying KAT5 does not contribute to, or is only a very minor player in oil body degradation. Previous observations demonstrate a clear role for KAT2 in this role of TAG breakdown (Germain *et al.*, 2001). However, in the Ws-4 accession the *kat5-2* mutation segregating in the *kat2-1* mutant background resulted in reduced germination frequency (Chapter 5). This genetic and expression evidence indicates that KAT5 may play a role during seed germination in Ws. A role for β-oxidation in seed germination independent of oil breakdown has previously been described for other β-oxidation mutants (Pinfield-Wells *et al.*, 2005; Pracharoenwattana *et al.*, 2005; Russell

et al., 2000). A recent breakthrough indicates that OPDA inhibits germination by acting synergistically with ABA to increase protein levels of ABI5 (Dave *et al.*, 2011). In β-oxidation mutants the accumulation of OPDA not converted to JA during seed development results in reduced germination frequency (Dave *et al.*, 2011). Interestingly, wild-type Ws seeds are more sensitive to inhibition of germination by high concentrations of exogenous OPDA than Col-0 (Dave *et al.*, 2011).

The germination phenotype described in Chapter 5 suggests KAT5 contributes to JA synthesis in some tissues (seeds) or accessions (Ws-4) along with KAT2. Previous experiments have demonstrated that KAT2 contributes primarily to wound-induced JA levels with basal levels persisting at near wild-type levels (Afitlhile *et al.*, 2005). KAT2 is up-regulated locally in response to leaf wounding, while KAT5 is up-regulated systemically, suggesting that KAT2 metabolises the majority of wound-induced JA (Castillo *et al.*, 2004). Perhaps in tissues where KAT2 and KAT5 are both expressed, such as germinating seedlings, flowers and siliques both thiolases contribute to the plant organ JA pool.

JA is required for male fertility, with mutants impaired in JA synthesis or signalling displaying male infertility, which can be rescued by exogenous supply of JA (Park *et al.*, 2002; Schilmiller *et al.*, 2007; Stintzi and Browse, 2000). In Chapter 5 I described the observed impairment of fertility in *kat2 kat5* double mutants of the Ws-4 background. However, this infertility appears not to be due to disruption of JA synthesis as exogenous JA does not restore fertility, *kat2 kat5* pollen is fertile when crossed to wild-type plants, and *35S* expression of peroxisomal *KAT5.2* restores fertility in *kat2-1 kat5-2* despite poor expression from the *35S* promoter in pollen (Wilkinson *et al.*, 1997).

Floral and embryo development defects resulting in varying degrees of infertility in β-oxidation mutants such as *aim1*, *kat2-1*, and *kat2 kat5* (Ws) lead to global proliferative arrest (GPA). In a conference abstract Richmond and Bleeker describe *aim1* crossed with an un-named fatty-acid biosynthesis mutant attenuates the *aim1* phenotype, suggesting accumulation of fatty-acid byproducts from a block in β-oxidation effects plant development (Richmond and Bleecker, 1997). Possibly both forward and reverse genetics could be used to screen for suppressors of GPA inhibition in the *aim1* or *kat2* mutants. However, generating enough *aim1* seed for mutagenesis would present a challenge and the *kat2* GPA phenotype is relatively subtle.

The reason for the importance of β-oxidation in developing embryo fertility is unclear. β-oxidation is active in this tissue contributing to the turn-over of fatty-acids (Arai *et al.*, 2002; Baud *et al.*, 2002). The energetic cost of a block in the breakdown of fatty acids may affect embryo development as is observed in mitochondrial metabolic mutants (Laughnan and Gabay-

Laughnan, 1983). Alternately, the accumulation of free-fatty acids may damage embryo cell membranes similar to the observations of dark-treated *kat2* and *cts* (Kunz *et al.*, 2009). Either a metabolic disruption or toxic byproduct accumulation affecting fertility should inhibit GPA, as male-sterile mutants or simply surgical removal of siliques prevents GPA (Hensel *et al.*, 1994).

6.3.3 Accession dependent infertility in *kat2 kat5*

I made the novel observation that requirement of thiolase for fertility and seed development was dependent on the Arabidopsis accession (Chapter 5). The fertility phenotype was only observed in *kat2 kat5* of the Ws-4 accession, but not in similar double mutants of L*er* and Col background. Currently similar observations do not exist in the literature for other β-oxidation mutants, and in fact severe β-oxidation phenotypes have been described in the Ws-2/Ws-0 (Rylott *et al.*, 2006; Rylott *et al.*, 2003), Col-0 (Pracharoenwattana *et al.*, 2005) and L*er* (Hayashi *et al.*, 2002) accessions. The mature plant and infertility phenotypes were confirmed in alternative allele combinations (*kat2-1 kat5-2* and *kat2-5 kat5-2* both of the Ws-4 background, as well as *kat2-1 kat5-1* a Ws-4/L*er* hybrid) and concluded as caused by the disruption to thiolase activity and β-oxidation in these plants. That is, the observed phenotypes do not appear to be linked to a particular allele. Additionally, the *kat2-1 kat5-2* infertility phenotype was rescued by over-expression of peroxisomal KAT5.2 but not cytosolic KAT5.1, so it is most probable that the infertility phenotype is due to a disruption in peroxisomal thiolase activity.

The difference between Ws-4 and L*er*/Col-0 is difficult to explain. L*er* and Col-0 have a similar origin (Rédei, 1992), so it is perhaps not surprising that mutants in this background have a similar phenotype. There have been reports that Ws mutant plants are more susceptible to inhibition of global proliferative arrest then those in the L*er* background (Hensel *et al.*, 1994), so the phenotypic difference may be due to inherent physiological and genetic differences between Ws and Col/L*er* flowering. There may also be molecular differences directly related to β-oxidation between the different accessions. *KAT1* expression does not appear to be different between Ws, Col and L*er* from publicly available data (Chapter 5). There are differences in the *KAT1* coding sequence between Arabidopsis accessions. Natural variation in gene nucleotide sequences can affect encoded proteins, for example a single nucleotide variation in the 7th intron of *Regulatory Particle 5b* (*RPT5b*) in Ws-4 results in mis-splicing of the transcript and introducing premature stop codon. As a result RPT5b is redundant with RPT5a in Col-0 but not Ws-4, impairing fertility in a *rpt5a* single mutant in Ws-4 but not Col-0 (Gallois *et al.*, 2009; Guyon-Debast *et al.*, 2010).

There are a number of SNPs in the Ws-4 *KAT1* gene sequence but bioinformatically predicted intron-exon splicing is not affected, and many of the mutations are silent or in non-conserved residues. The one semi-conserved residue does not appear to at an important function

site of the KAT1 protein, but this must be determined experimentally and the *kat2-1 kat5-1* (Ws-4/L*er* hybrid) double mutant provides a genetic tool for this experiment. As previously discussed in Section 5.3.3, if double mutants possessing one or two copies of the L*er KAT1* gene were fertile, while mutants homozygous for the Ws-4 *KAT1* gene were not, this would suggest that there exist functional differences in the two proteins. However, if this is not the case then L*er* KAT1 protein is not capable of rescuing the double mutant phenotype. It has also been suggested that the peroxisomal isoform of AACT1 may contribute to β-oxidation as the synthetic reaction catalysed by AACT is reversible (Ahumada *et al.*, 2008). Future experiments measuring thiolase enzyme activity in different tissues of the thiolase mutants could be advantageous in determining the extent of the block to β-oxidation in these mutants.

These experiments also emphasise the importance of taking care when drawing conclusions from observations of β-oxidation mutants in different Arabidopsis accessions. Observations in Ws-4 background mutants may not be typical of other Arabidopsis accessions. The Arabidopsis research community's understanding of Arabidopsis natural variation is growing through omics approaches such as the 1001 Genomes Projects (Weigel and Mott, 2009). Future research will be able to take advantage of these resources to analyse the extent of natural variation at the molecular level, and it's implication for accession phenotype.

6.3.4 Disruption to photosynthesis and photorespiration in *kat2 kat5*?

A pale green phenotype was observed in *kat2-1 kat5-2* seedlings, but not when rescued with *35S:KAT5.2* (Chapter 5). This leaf phenotype has not been previously described in a β-oxidation mutant. Interestingly this phenotype was not observed in older *kat2-1 kat5-2* plants. A pale green leaf phenotype has previously been described for the peroxisome biogenesis mutants *pex6* (Zolman and Bartel, 2004), *pex14* (Hayashi *et al.*, 2000), and *pex5* (Khan and Zolman, 2010), so disruption to peroxisome function can result in this phenotype. The *pex14* mutant has yellow-green leaves and a smaller rosette, but wild-type like growth is recovered under high CO_2 atmospheric conditions, suggesting disruption to the photorespiratory pathway (Hayashi *et al.*, 2000). The import of many peroxisomal photorespiration enzymes requires functional PTS1 import, which is disrupted in *pex14* (Hayashi *et al.*, 2000). Total chlorophyll content is reduced in *pex5* and *pex6* seedling and adult leaves (Khan and Zolman, 2010). However, a role for β-oxidation and thiolase activity in photorespiration is unclear.

In the *pxa1* and *kat2* mutants extended dark-treatment results in accumulation of free fatty-acids, which damage chloroplasts and photosystem II, with leaves developing necrotic lesions (Kunze *et al.*, 2006). Activity from the *KAT2* and *KAT5* promoters was observed during germination, and in young seedlings (Chapter 4). While *kat5* mutants are not disrupted in

storage lipid breakdown (Chapter 5), they may be impaired in the turnover of membrane fatty acids. It is possible that in the *kat2-1 kat5-2* double mutant a more extreme free fatty acid accumulation phenotype is observed, due to turnover of fatty-acids in young fast growing seedlings. Damage to chloroplasts would reduce chlorophyll content, or reduce photosynthesis and increase the flux through photorespiration (Powles, 1984). *pxa1* is hyper-sensitive to exogenous supply of α-linolenic acid (Kunze *et al.*, 2006), so the response of different thiolase mutants and accessions could be informative.

Alternately in *kat2-1* mutant seedlings there have been electron-microscopy observations of changes to peroxisome, mitochondria and chloroplast with an increase in size and decrease in abundance (Germain *et al.*, 2001; Hayashi *et al.*, 2001). Direct interaction between the peroxisome membrane and oil bodies in *ped1* cotyledons results in tubular invaginated structures forming in the peroxisome (Hayashi *et al.*, 2001). The large increase in the size of peroxisomes is possibly due to accumulation of acyl-CoA intermediates due to block in β-oxidation (Germain *et al.*, 2001). Perhaps a more extreme or longer duration effect is observed in *kat2-1 kat5-2* since *KAT5* expression later in development cannot partially complement the phenotype, resulting in impairment of peroxisome matrix protein import.

In cells in which the β-oxidation and photorespiration pathway occur concomitantly in the peroxisome, it is possible that membrane lipid turnover by β-oxidation may produce NADH that would be consumed by the reduction of hydroxypruvute by HPR in the photorespiration pathway (Pracharoenwattana *et al.*, 2007). These two pathways are linked by the enzyme activity of PMDH1 and PMDH2 which contribute NAD/NADH to β-oxidation and photorespiration, but initial experiments observed that a *pmdh1 pmdh2* double mutant grows in air, and does not appear to have a photorespiration phenotype (Pracharoenwattana *et al.*, 2007). However, further experiments revealed subtle defects in photosynthesis and growth rate (Cousins *et al.*, 2008). Accumulation of acyl-CoAs in *kat2 kat5* could inhibit β-oxidation affecting the balance of NADH/NAD levels, and resulting in a photorespiration phenotype. Further experiments would be necessary to examine the pale-leaf phenotype, such as measurement of chlorophyll and free fatty acid levels, trying to recover mutant plants under high CO_2 conditions, and measurement of photoinhibition/photosystem II.

6.4 Concluding remarks, and future directions

In conclusion the work described in this thesis has produced several novel results. This includes the identification of two new auxin precursor resistant mutants one of which has a never before described 2,4-DB but not IBA resistant phenotype. In the thiolase mutants accession dependent infertility and growth defect phenotypes were observed, as well as a pale-green leaf phenotype normally associated with impairment of photorespiration. Future work

could include measurement of thiolase activity in mutants of different accessions, measurement of free fatty-acid levels in mutants, and screening for suppressors of GPA inhibition in *aim1* or *kat2* mutants. The use of genetic tools to investigate whether *KAT1* from L*er* or Col-0 plants is capable of rescuing the double mutant phenotype in Ws-4 plants may be particularly illuminating for investigation of accession differences in thiolase function. While there remain challenges to researchers in this field, this work suggests that further advances and knowledge await the study of peroxisomal function and biology in plants. These advances in our understanding of metabolic function might be most significant in the context of natural variation and fine-tuning of primary and secondary metabolism in different Arabidopsis accessions.

References

Abe, H., Urao, T., Ito, T., Seki, M., Shinozaki, K. and Yamaguchi-Shinozaki, K. (2003) Arabidopsis AtMYC2 (bHLH) and AtMYB2 (MYB) function as transcriptional activators in abscisic acid signaling. *The Plant Cell*, **15**, 63-78.

Abe, H., Yamaguchi-Shinozaki, K., Urao, T., Iwasaki, T., Hosokawa, D. and Shinozaki, K. (1997) Role of Arabidopsis MYC and MYB homologs in drought-and abscisic acid-regulated gene expression. *The Plant Cell*, **9**, 1859-1868.

Adham, A.R., Zolman, B.K., Millius, A. and Bartel, B. (2005) Mutations in Arabidopsis acyl-CoA oxidase genes reveal distinct and overlapping roles in β-oxidation. *The Plant Journal*, **41**, 859-874.

Afitlhile, M., Fukushige, H., Nishimura, M. and Hildebrand, D. (2005) A defect in glyoxysomal fatty acid β-oxidation reduces jasmonic acid accumulation in. *Plant Physiology and Biochemistry*, **43**, 603-609.

Ahumada, I., Cairó, A., Hemmerlin, A., González, V., Pateraki, I., Bach, T.J., Rodríguez-Concepción, M., Campos, N. and Boronat, A. (2008) Characterisation of the gene family encoding acetoacetyl-CoA thiolase in Arabidopsis. *Functional Plant Biology*, **35**, 1100-1111.

Ajjawi, I., Lu, Y., Savage, L.J., Bell, S.M. and Last, R.L. (2010) Large-scale reverse genetics in Arabidopsis: case studies from the Chloroplast 2010 Project. *Plant Physiology*, **152**, 529-540.

Akama, K., Shiraishi, H., Ohta, S., Nakamura, K., Okada, K. and Shimura, Y. (1992) Efficient transformation of Arabidopsis thaliana: comparison of the efficiencies with various organs, plant ecotypes and Agrobacterium strains. *Plant Cell Reports*, **12**, 7-11.

Alabadí, D., Oyama, T., Yanovsky, M.J., Harmon, F.G., Más, P. and Kay, S.A. (2001) Reciprocal regulation between *TOC1* and *LHY*/*CCA1* within the Arabidopsis circadian clock. *Science*, **293**, 880-883.

Alexander, M.P. (1969) Differential staining of aborted and nonaborted pollen. *Stain Technology*, **44**, 117-122.

Allenbach, L. and Poirier, Y. (2000) Analysis of the alternative pathways for the β-oxidation of unsaturated fatty acids using transgenic plants synthesizing polyhydroxyalkanoates in peroxisomes. *Plant Physiology*, **124**, 1159-1168.

Aloni, R., Aloni, E., Langhans, M. and Ullrich, C.I. (2006) Role of auxin in regulating Arabidopsis flower development. *Planta*, **223**, 315-328.

Alonso, J.M., Stepanova, A.N., Leisse, T.J., Kim, C.J., Chen, H., Shinn, P., Stevenson, D.K., Zimmerman, J., Barajas, P., Cheuk, R., Gadrinab, C., Heller, C., Jeske, A., Koesema, E., Meyers, C.C., Parker, H., Prednis, L., Ansari, Y., Choy, N., Deen, H., Geralt, M., Hazari, N., Hom, E., Karnes, M., Mulholland, C., Ndubaku, R., Schmidt, I., Guzman, P., Aguilar-Henonin, L., Schmid, M., Weigel, D., Carter, D.E., Marchand, T., Risseeuw, E., Brogden, D., Zeko, A., Crosby, W.L., Berry, C.C. and Ecker, J.R. (2003) Genome-wide insertional mutagenesis of *Arabidopsis thaliana*. *Science*, **301**, 653-657.

Anastasio, A.E., Platt, A., Horton, M., Grotewold, E., Scholl, R., Borevitz, J.O., Nordborg, M. and Bergelson, J. (2011) Source verification of mis-identified *Arabidopsis thaliana* accessions. *The Plant Journal*, **67**, 554-566.

Ang, L.-H., Chattopadhyay, S., Wei, N., Oyama, T., Okada, K., Batschauer, A. and Deng, X.-W. (1998) Molecular interaction between COP1 and HY5 defines a regulatory switch for light control of Arabidopsis development. *Molecular Cell*, **1**, 213-222.

Appleford, N.E.J. and Lenton, J.R. (1997) Hormonal regulation of α-amylase gene expression in germinating wheat (*Triticum aestivum*) grains. *Physiologia Plantarum*, **100**, 534-542.

Arabidopsis Genome Initiative (2000) Analysis of the genome sequence of the flowering plant *Arabidopsis thaliana*. *Nature*, **408**, 796-815.

Arai, Y., Nakashita, H., Suzuki, Y., Kobayashi, Y., Shimizu, T., Yasuda, M., Doi, Y. and Yamaguchi, I. (2002) Synthesis of a novel class of polyhydroxyalkanoates in Arabidopsis peroxisomes, and their use in monitoring short-chain-length intermediates of β-oxidation. *Plant and Cell Physiology*, **43**, 555-562.

Aukerman, M.J., Hirschfeld, M., Wester, L., Weaver, M., Clack, T., Amasino, R.M. and Sharrock, R.A. (1997) A Deletion in the PHYD Gene of the Arabidopsis

Wassilewskija Ecotype Defines a Role for Phytochrome D in Red/Far-Red Light Sensing. *The Plant Cell Online*, **9**, 1317-1326.

Baker, A., Graham, I.A., Holdsworth, M., Smith, S.M. and Theodoulou, F.L. (2006) Chewing the fat: β-oxidation in signalling and development. *Trends in Plant Science*, **11**, 124-132.

Baker, A. and Sparkes, I.A. (2005) Peroxisome protein import: some answers, more questions. *Current Opinion in Plant Biology*, **8**, 640-647.

Bao, X., Focke, M., Pollard, M. and Ohlrogge, J. (2000) Understanding *in vivo* carbon precursor supply for fatty acid synthesis in leaf tissue. *The Plant Journal*, **22**, 39-50.

Barroso, J.B., Corpas, F.J., Carreras, A., Sandalio, L.M., Valderrama, R., Palma, J., Lupiáñez, J.A. and del Río, L.A. (1999) Localization of nitric-oxide synthase in plant peroxisomes. *Journal of Biological Chemistry*, **274**, 36729-36733.

Baud, S., Boutin, J.-P., Miquel, M., Lepiniec, L. and Rochat, C. (2002) An integrated overview of seed development in *Arabidopsis thaliana* ecotype WS. *Plant Physiology and Biochemistry*, **40**, 151-160.

Beevers, H. (1979) Microbodies in higher plants. *Annual Review of Plant Physiology*, **30**, 159-193.

Behrends, W., Engeland, K. and Kindl, H. (1988) Characterization of two forms of the multifunctional protein acting in fatty acid β-oxidation. *Archives of Biochemistry and Biophysics*, **263**, 161-169.

Beilstein, M.A., Nagalingum, N.S., Clements, M.D., Manchester, S.R. and Mathews, S. (2010) Dated molecular phylogenies indicate a Miocene origin for *Arabidopsis thaliana*. *Proceedings of the National Academy of Sciences*, **107**, 18724-18728.

Bennett, T., Sieberer, T., Willett, B., Booker, J., Luschnig, C. and Leyser, O. (2006) The Arabidopsis MAX pathway controls shoot branching by regulating auxin transport. *Current Biology*, **16**, 553-563.

Bensmihen, S., Rippa, S., Lambert, G., Jublot, D., Pautot, V., Granier, F., Giraudat, J. and Parcy, F. (2002) The homologous ABI5 and EEL transcription factors function antagonistically to fine-tune gene expression during late embryogenesis. *The Plant Cell*, **14**, 1391-1403.

Bernhardt, K., Wilkinson, S., Weber, A.P.M. and Linka, N. (2012) A peroxisomal carrier delivers NAD^+ and contributes to optimal fatty acid degradation during storage oil mobilization. *The Plant Journal*, **69**, 1-13.

Bethke, P.C., Gubler, F., Jacobsen, J.V. and Jones, R.L. (2004) Dormancy of *Arabidopsis* seeds and barley grains can be broken by nitric oxide. *Planta*, **219**, 847-855.

Bethke, P.C., Libourel, I.G.L., Aoyama, N., Chung, Y.-Y., Still, D.W. and Jones, R.L. (2007) The Arabidopsis aleurone layer responds to nitric oxide, gibberellin, and abscisic acid and is sufficient and necessary for seed dormancy. *Plant Physiology*, **143**, 1173-1188.

Bethke, P.C., Libourel, I.G.L. and Jones, R.L. (2006) Nitric oxide reduces seed dormancy in Arabidopsis. *Journal of Experimental Botany*, **57**, 517-526.

Bewley, J.D. and Black, M. (1994) *Seeds: Physiology of Development and Germination* 2 edn.: Springer.

Blée, E. and Schuber, F. (1993) Biosynthesis of cutin monomers: involvement of a lipoxygenase/peroxygenase pathway. *The Plant Journal*, **4**, 113-123.

Block, A., Dangl, J.L., Hahlbrock, K. and Schulze-Lefert, P. (1990) Functional borders, genetic fine structure, and distance requirements of *cis* elements mediating light responsiveness of the parsley chalcone synthase promoter. *Proceedings of the National Academy of Sciences*, **87**, 5387-5391.

Boatright, J., Negre, F., Chen, X., Kish, C.M., Wood, B., Peel, G., Orlova, I., Gang, D., Rhodes, D. and Dudareva, N. (2004) Understanding *in vivo* benzenoid metabolism in Petunia petal tissue. *Plant Physiology*, **135**, 1993-2011.

Bonaventure, G., Bao, X., Ohlrogge, J. and Pollard, M. (2004) Metabolic responses to the reduction in palmitate caused by disruption of the *FATB* gene in Arabidopsis. *Plant Physiology*, **135**, 1269-1279.

Bonaventure, G., Salas, J.J., Pollard, M.R. and Ohlrogge, J.B. (2003) Disruption of the *FATB* gene in Arabidopsis demonstrates an essential role of saturated fatty acids in plant growth. *The Plant Cell*, **15**, 1020-1033.

Bouvier, F., Rahier, A. and Camara, B. (2005) Biogenesis, molecular regulation and function of plant isoprenoids. *Progress in Lipid Research*, **44**, 357-429.

Boyle, B. and Brisson, N. (2001) Repression of the defense gene *PR-10a* by the single-stranded DNA binding protein SEBF. *The Plant Cell*, **13**, 2525-2537.

Breidenbach, R.W. and Beevers, H. (1967) Association of the glyoxylate cycle enzymes in a novel subcellular particle from castor bean endosperm. *Biochemical and Biophysical Research Communications*, **27**, 462-469.

Brown, B.A., Cloix, C., Jiang, G.H., Kaiserli, E., Herzyk, P., Kliebenstein, D.J. and Jenkins, G.I. (2005) A UV-B-specific signaling component orchestrates plant UV protection. *Proceedings of the National Academy of Sciences*, **102**, 18225-18230.

Browse, J., McCourt, P.J. and Somerville, C.R. (1986) Fatty acid composition of leaf lipids determined after combined digestion and fatty acid methyl ester formation from fresh tissue. *Analytical Biochemistry*, **152**, 141-145.

Carles, C., Bies-Etheve, N., Aspart, L., Léon-Kloosterziel, K.M., Koornneef, M., Echeverria, M. and Delseny, M. (2002) Regulation of *Arabidopsis thaliana Em* genes: role of ABI5. *The Plant Journal*, **30**, 373-383.

Carrera, E., Holman, T., Medhurst, A., Peer, W., Schmuths, H., Footitt, S., Theodoulou, F.L. and Holdsworth, M.J. (2007) Gene expression profiling reveals defined functions of the ATP-binding cassette transporter COMATOSE late in phase II of germination. *Plant Physiology*, **143**, 1669-1679.

Carrie, C., Murcha, M.W., Millar, A.H., Smith, S.M. and Whelan, J. (2007) Nine 3-ketoacyl-CoA thiolases (KATs) and acetoacetyl-CoA thiolases (ACATs) encoded by five genes in Arabidopsis thaliana are targeted either to peroxisomes or cytosol but not to mitochondria. *Plant Molecular Biology*, **63**, 97-108.

Castillo, C.M., Martinez, C., Buchala, A., Metraux, J.P. and León, J. (2004) Gene-specific involvement of β-oxidation in wound-activated responses in Arabidopsis. *Plant Physiol*, **135**, 85-94.

Castillo, M.C. and León, J. (2008) Expression of the β-oxidation gene *3-ketoacyl-CoA thiolase 2* (*KAT2*) is required for the timely onset of natural and dark-induced leaf senescence in Arabidopsis. *Journal of Experimental Botany*, **59**, 2171-2179.

Castillo, M.C., Sandalio, L.M., del Río, L.A. and León, J. (2008) Peroxisome proliferation, wound-activated responses and expression of peroxisome-associated genes are cross-regulated but uncoupled in *Arabidopsis thaliana*. *Plant, Cell & Environment*, **31**, 492-505.

Cercós, M., Gómez-Cadenas, A. and Ho, T.-H.D. (1999) Hormonal regulation of a cysteine proteinase gene, *EPB-1*, in barley aleurone layers: *cis*- and *trans*-acting elements involved in the co-ordinated gene expression regulated by gibberellins and abscisic acid. *The Plant Journal*, **19**, 107-118.

Chakravarthy, S., Tuori, R.P., D'Ascenzo, M.D., Fobert, P.R., Després, C. and Martin, G.B. (2003) The tomato transcription factor Pti4 regulates defense-related gene expression via GCC box and non-GCC box *cis* elements. *The Plant Cell*, **15**, 3033-3050.

Chan, C.-S., Guo, L. and Shih, M.-C. (2001) Promoter analysis of the nuclear gene encoding the chloroplast glyceraldehyde-3-phosphate dehydrogenase B subunit of *Arabidopsis thaliana*. *Plant Molecular Biology*, **46**, 131-141.

Chang, C., Bowman, J.L., DeJohn, A.W., Lander, E.S. and Meyerowitz, E.M. (1988) Restriction fragment length polymorphism linkage map for *Arabidopsis thaliana*. *Proceedings of the National Academy of Sciences*, **85**, 6856-6860.

Chappell, J. (1995) Biochemistry and molecular biology of the isoprenoid biosynthetic pathway in plants. *Annual Review of Plant Physiology and Plant Molecular Biology*, **46**, 521-547.

Charlton, W.L., Johnson, B., Graham, I.A. and Baker, A. (2005a) Non-coordinate expression of peroxisome biogenesis, β-oxidation and glyoxylate cycle genes in mature Arabidopsis plants. *Plant Cell Reports*, **23**, 647-653.

Charlton, W.L., Matsui, K., Johnson, B., Graham, I.A., Ohme-Takagi, M. and Baker, A. (2005b) Salt-induced expression of peroxisome-associated genes requires components of the ethylene, jasmonate and abscisic acid signalling pathways. *Plant, Cell & Environment*, **28**, 513-524.

Chaubet, N., Flénet, M., Clément, B., Brignon, P. and Gigot, C. (1996) Identification of *cis*-elements regulating the expression of an Arabidopsis histone H4 gene. *The Plant Journal*, **10**, 425-435.

Chen, P.-W., Chiang, C.-M., Tseng, T.-H. and Yu, S.-M. (2006) Interaction between rice MYBGA and the gibberellin response element controls tissue-specific sugar sensitivity of α-amylase genes. *The Plant Cell*, **18**, 2326-2340.

Chen, W., Chang, S., Hudson, M., Kwan, W.-K., Li, J., Estes, B., Knoll, D., Shi, L. and Zhu, T. (2005) Contribution of transcriptional regulation to natural variations in Arabidopsis. *Genome Biology*, **6**, R32.

Chia, T.Y.P., Pike, M.J. and Rawsthorne, S. (2005) Storage oil breakdown during embryo development of *Brassica napus* (L.). *Journal of Experimental Botany*, **56**, 1285-1296.

Clough, S.J. and Bent, A.F. (1998) Floral dip: a simplified method for Agrobacterium-mediated transformation of *Arabidopsis thaliana*. *The Plant Journal*, **16**, 735-743.

Conley, T.R., Park, S.C., Kwon, H.B., Peng, H.P. and Shih, M.C. (1994) Characterization of *cis*-acting elements in light regulation of the nuclear gene encoding the A subunit of chloroplast isozymes of glyceraldehyde-3-phosphate dehydrogenase from *Arabidopsis thaliana*. *Mol. Cell. Biol.*, **14**, 2525-2533.

Cornah, J.E., Germain, V., Ward, J.L., Beale, M.H. and Smith, S.M. (2004) Lipid utilization, gluconeogenesis, and seedling growth in Arabidopsis mutants lacking the glyoxylate cycle enzyme malate synthase. *Journal of Biological Chemistry*, **279**, 42916-42923.

Corpas, F.J., Barroso, J.B., Carreras, A., Quirós, M., León, A.M., Romero-Puertas, M.C., Esteban, F.J., Valderrama, R., Palma, J.M., Sandalio, L.M., Gómez, M. and del Río, L.A. (2004) Cellular and subcellular localization of endogenous nitric oxide in young and senescent pea plants. *Plant Physiology*, **136**, 2722-2733.

Corpas, F.J., Barroso, J.B. and del Río, L.A. (2001) Peroxisomes as a source of reactive oxygen species and nitric oxide signal molecules in plant cells. *Trends in Plant Science*, **6**, 145-150.

Corpas, F.J., Hayashi, M., Mano, S., Nishimura, M. and Barroso, J.B. (2009) Peroxisomes are required for *in vivo* nitric oxide accumulation in the cytosol following salinity stress of Arabidopsis plants. *Plant Physiology*, **151**, 2083-2094.

Costa, M., Bedgar, D., Moinuddin, S., Kim, K., Cardenas, C., Cochrane, F., Shockey, J., Helms, G., Amakura, Y. and Takahashi, H. (2005) Characterization *in vitro* and *in vivo* of the putative multigene 4-coumarate:CoA ligase network in Arabidopsis: syringyl lignin and sinapate/sinapyl alcohol derivative formation. *Phytochemistry*, **66**, 2072-2091.

Cousins, A.B., Pracharoenwattana, I., Zhou, W., Smith, S.M. and Badger, M.R. (2008) Peroxisomal malate dehydrogenase is not essential for photorespiration in Arabidopsis but its absence causes an increase in the stoichiometry of photorespiratory CO_2 release. *Plant Physiology*, **148**, 786-795.

Crawford, N.M. (2006) Mechanisms for nitric oxide synthesis in plants. *Journal of Experimental Botany*, **57**, 471-478.

Creelman, R.A. and Mullet, J.E. (1995) Jasmonic acid distribution and action in plants: regulation during development and response to biotic and abiotic stress. *Proceedings of the National Academy of Sciences*, **92**, 4114-4119.

Czechowski, T., Stitt, M., Altmann, T., Udvardi, M.K. and Scheible, W.-R. (2005) Genome-wide identification and testing of superior reference genes for transcript normalization in Arabidopsis. *Plant Physiology*, **139**, 5-17.

Dave, A., Hernández, M.L., He, Z., Andriotis, V.M.E., Vaistij, F.E., Larson, T.R. and Graham, I.A. (2011) 12-Oxo-phytodienoic acid accumulation during seed development represses seed germination in Arabidopsis. *The Plant Cell*, **23**, 583-599.

Debeaujon, I., Leon-Kloosterziel, K.M. and Koornneef, M. (2000) Influence of the testa on seed dormancy, germination, and longevity in Arabidopsis. *Plant Physiol*, **122**, 403-414.

Delker, C., Zolman, B.K., Miersch, O. and Wasternack, C. (2007) Jasmonate biosynthesis in *Arabidopsis thaliana* requires peroxisomal β-oxidation enzymes – Additional proof by properties of *pex6* and *aim1*. *Phytochemistry*, **68**, 1642-1650.

Desai, M. and Hu, J. (2008) Light induces peroxisome proliferation in Arabidopsis seedlings through the photoreceptor phytochrome A, the transcription factor HY5 HOMOLOG, and the peroxisomal protein PEROXIN11b. *Plant Physiology*, **146**, 1117-1127.

Dietrich, D., Schmuths, H., Lousa, C.D.M., Baldwin, J.M., Baldwin, S.A., Baker, A., Theodoulou, F.L. and Holdsworth, M.J. (2008) Mutations in the Arabidopsis peroxisomal ABC transporter COMATOSE allow differentiation between multiple functions *in planta*: insights from an allelic series. *Molecular Biology of the Cell*, **20**, 530-543.

Dieuaide, M., Couee, I., Pradet, A. and Raymond, P. (1993) Effects of glucose starvation on the oxidation of fatty acids by maize root tip mitochondria and peroxisomes: evidence for mitochondrial fatty acid β-oxidation and acyl-CoA dehydrogenase activity in a higher plant. *Biochemical Journal*, **296**, 199-207.

Dommes, J. and Northcote, D.H. (1985) The action of exogenous abscisic and gibberellic acids on gene expression in germinating castor beans. *Planta*, **165**, 513-521.

Downie, A.B., Zhang, D., Dirk, L.M.A., Thacker, R.R., Pfeiffer, J.A., Drake, J.L., Levy, A.A., Butterfield, D.A., Buxton, J.W. and Snyder, J.C. (2003) Communication between the maternal testa and the embryo and/or endosperm affect testa attributes in tomato. *Plant Physiology*, **133**, 145-160.

Durner, J., Shah, J. and Klessig, D.F. (1997) Salicylic acid and disease resistance in plants. *Trends in Plant Science*, **2**, 266-274.

Eastmond, P.J. (2006) *SUGAR-DEPENDENT1* encodes a patatin domain triacylglycerol lipase that initiates storage oil breakdown in germinating Arabidopsis seeds. *The Plant Cell*, **18**, 665-675.

Eastmond, P.J., Germain, V., Lange, P.R., Bryce, J.H., Smith, S.M. and Graham, I.A. (2000a) Postgerminative growth and lipid catabolism in oilseeds lacking the glyoxylate cycle. *Proceedings of the National Academy of Sciences*, **97**, 5669-5674.

Eastmond, P.J. and Graham, I.A. (2000) The multifunctional protein AtMFP2 is co-ordinately expressed with other genes of fatty acid beta-oxidation during seed germination in *Arabidopsis thaliana* (L.) Heynh. *Biochemical Society Transactions*, **28**, 95-99.

Eastmond, P.J. and Graham, I.A. (2001) Re-examining the role of the glyoxylate cycle in oilseeds. *Trends in Plant Science*, **6**, 72-78.

Eastmond, P.J., Hooks, M.A., Williams, D., Lange, P., Bechtold, N., Sarrobert, C., Nussaume, L. and Graham, I.A. (2000b) Promoter trapping of a novel medium-chain acyl-CoA oxidase, which is induced transcriptionally during Arabidopsis seed germination. *Journal of Biological Chemistry*, **275**, 34375-34381.

Eccleston, V.S. and Ohlrogge, J.B. (1998) Expression of lauroyl-acyl carrier protein thioesterase in *Brassica napus* seeds induces pathways for both fatty acid oxidation and biosynthesis and implies a set point for triacylglycerol accumulation. *The Plant Cell*, **10**, 613-622.

El-Maarouf-Bouteau, H. and Bailly, C. (2008) Oxidative signaling in seed germination and dormancy. *Plant Signaling and Behavior*, **3**, 175-182.

Emanuelsson, O., Elofsson, A., von Heijne, G. and Cristóbal, S. (2003) *In silico* prediction of the peroxisomal proteome in fungi, plants and animals. *Journal of Molecular Biology*, **330**, 443-456.

Engeland, K. and Kindl, H. (1991) Evidence for a peroxisomal fatty acid β-oxidation involving D-3-hydroxyacyl-CoAs. *European Journal of Biochemistry*, **200**, 171-178.

Eubel, H., Meyer, E.H., Taylor, N.L., Bussell, J.D., O'Toole, N., Heazlewood, J.L., Castleden, I., Small, I.D., Smith, S.M. and Millar, A.H. (2008) Novel proteins, putative membrane transporters, and an integrated metabolic network are revealed by quantitative proteomic analysis of Arabidopsis cell culture peroxisomes. *Plant Physiology*, **148**, 1809-1829.

Fahey, J.W., Zalcmann, A.T. and Talalay, P. (2001) The chemical diversity and distribution of glucosinolates and isothiocyanates among plants. *Phytochemistry*, **56**, 5-51.

Fatland, B.L., Nikolau, B.J. and Wurtele, E.S. (2005) Reverse genetic characterization of cytosolic acetyl-CoA generation by ATP-citrate lyase in Arabidopsis. *The Plant Cell*, **17**, 182-203.

Favory, J.-J., Stec, A., Gruber, H., Rizzini, L., Oravecz, A., Funk, M., Albert, A., Cloix, C., Jenkins, G.I., Oakeley, E.J., Seidlitz, H.K., Nagy, F. and Ulm, R. (2009) Interaction of COP1 and UVR8 regulates UV-B-induced photomorphogenesis and stress acclimation in Arabidopsis. *The EMBO Journal*, **28**, 591-601.

Feys, B., Benedetti, C.E., Penfold, C.N. and Turner, J.G. (1994) Arabidopsis mutants selected for resistance to the phytotoxin coronatine are male sterile, insensitive to methyl jasmonate, and resistant to a bacterial pathogen. *The Plant Cell*, **6**, 751-759.

Fincher, G.B. (1989) Molecular and cellular biology associated with endosperm mobilization in germinating cereal grains. *Annual Review of Plant Physiology and Plant Molecular Biology*, **40**, 305-346.

Finkelstein, R.R. and Lynch, T.J. (2000) Abscisic acid inhibition of radicle emergence but not seedling growth is suppressed by sugars. *Plant Physiology*, **122**, 1179-1186.

Fontaine, O., Huault, C., Pavis, N. and Billard, J.-P. (1994) Dormancy breakage of *Hordeum vulgare* seeds: effects of hydrogen peroxide and scarification on glutathione level and glutathione reductase activity. *Plant physiology and biochemistry*, **32**, 677-683.

Footitt, S., Cornah, J.E., Pracharoenwattana, I., Bryce, J.H. and Smith, S.M. (2007a) The Arabidopsis *3-ketoacyl-CoA thiolase-2* (*kat2-1*) mutant exhibits increased flowering but reduced reproductive success. *Journal of Experimental Botany*, **58**, 2959-2968.

Footitt, S., Dietrich, D., Fait, A., Fernie, A.R., Holdsworth, M.J., Baker, A. and Theodoulou, F.L. (2007b) The COMATOSE ATP-binding cassette transporter is required for full fertility in Arabidopsis. *Plant Physiology*, **144**, 1467-1480.

Footitt, S., Slocombe, S.P., Larner, V., Kurup, S., Wu, Y., Larson, T., Graham, I., Baker, A. and Holdsworth, M. (2002) Control of germination and lipid mobilization by COMATOSE, the Arabidopsis homologue of human ALDP. *The EMBO Journal*, **21**, 2912-2922.

Froman, B.E., Edwards, P.C., Bursch, A.G. and Dehesh, K. (2000) ACX3, a novel medium-chain acyl-coenzyme A oxidase from Arabidopsis. *Plant Physiology*, **123**, 733-742.

Fukao, Y., Hayashi, M., Hara-Nishimura, I. and Nishimura, M. (2003) Novel glyoxysomal protein kinase, GPK1, identified by proteomic analysis of glyoxysomes in etiolated cotyledons of *Arabidopsis thaliana*. *Plant and Cell Physiology*, **44**, 1002-1012.

Fukao, Y., Hayashi, M. and Nishimura, M. (2002) Proteomic analysis of leaf peroxisomal proteins in greening cotyledons of *Arabidopsis thaliana*. *Plant and Cell Physiology*, **43**, 689-696.

Fulda, M., Schnurr, J., Abbadi, A., Heinz, E. and Browse, J. (2004) Peroxisomal acyl-CoA synthetase activity is essential for seedling development in *Arabidopsis thaliana*. *The Plant Cell*, **16**, 394-405.

Fulda, M., Shockey, J., Werber, M., Wolter, F.P. and Heinz, E. (2002) Two long-chain acyl-CoA synthetases from *Arabidopsis thaliana* involved in peroxisomal fatty acid β-oxidation. *The Plant Journal*, **32**, 93-103.

Gallois, J.-L., Guyon-Debast, A., Lécureuil, A., Vezon, D., Carpentier, V., Bonhomme, S. and Guerche, P. (2009) The Arabidopsis proteasome RPT5 subunits are essential for gametophyte development and show accession-dependent redundancy. *The Plant Cell*, **21**, 442-459.

Geisler-Lee, J., O'Toole, N., Ammar, R., Provart, N.J., Millar, A.H. and Geisler, M. (2007) A predicted interactome for Arabidopsis. *Plant Physiology*, **145**, 317-329.

Germain, V., Rylott, E.L., Larson, T.R., Sherson, S.M., Bechtold, N., Carde, J.P., Bryce, J.H., Graham, I.A. and Smith, S.M. (2001) Requirement for 3-ketoacyl-CoA thiolase-2 in peroxisome development, fatty acid β-oxidation and breakdown of triacylglycerol in lipid bodies of Arabidopsis seedlings. *The Plant Journal*, **28**, 1-12.

Gibeaut, D.M., Hulett, J., Cramer, G.R. and Seemann, J.R. (1997) Maximal biomass of *Arabidopsis thaliana* using a simple, low-maintenance hydroponic method and favorable environmental conditions. *Plant Physiology*, **115**, 317-319.

Gidoni, D., Brosio, P., Bond-Nutter, D., Bedbrook, J. and Dunsmuir, P. (1989) Novel *cis*-acting elements in Petunia *Cab* gene promoters. *Molecular and General Genetics*, **215**, 337-344.

Gilbert, H.F., Lennox, B.J., Mossman, C.D. and Carle, W.C. (1981) The relation of acyl transfer to the overall reaction of thiolase I from porcine heart. *Journal of Biological Chemistry*, **256**, 7371-7377.

Giuliano, G., Pichersky, E., Malik, V.S., Timko, M.P., Scolnik, P.A. and Cashmore, A.R. (1988) An evolutionarily conserved protein binding sequence upstream of a plant light-regulated gene. *Proceedings of the National Academy of Sciences*, **85**, 7089-7093.

Goepfert, S., Hiltunen, J.K. and Poirier, Y. (2006) Identification and functional characterization of a monofunctional peroxisomal enoyl-CoA hydratase 2 that participates in the degradation of even *cis*-unsaturated fatty acids in *Arabidopsis thaliana*. *Journal of Biological Chemistry*, **281**, 35894-35903.

Goepfert, S. and Poirier, Y. (2007) β-oxidation in fatty acid degradation and beyond. *Current Opinion in Plant Biology*, **10**, 245-251.

Goepfert, S., Vidoudez, C., Rezzonico, E., Hiltunen, J.K. and Poirier, Y. (2005) Molecular identification and characterization of the Arabidopsis $\Delta^{3,5}$,$\Delta^{2,4}$-dienoyl-coenzyme A isomerase, a peroxisomal enzyme participating in the β-oxidation cycle of unsaturated fatty acids. *Plant Physiology*, **138**, 1947-1956.

Gould, S.G., Keller, G.A. and Subramani, S. (1987) Identification of a peroxisomal targeting signal at the carboxy terminus of firefly luciferase. *The Journal of Cell Biology*, **105**, 2923-2931.

Graham, I.A. (2008) Seed storage oil mobilization. *Annual Review of Plant Biology*, **59**, 115-142.

Graham, I.A., Denby, K.J. and Leaver, C.J. (1994) Carbon catabolite repression regulates glyoxylate cycle gene expression in cucumber. *The Plant Cell*, **6**, 761-772.

Green, P.J., Yong, M.H., Cuozzo, M., Kano-Murakami, Y., Silverstein, P. and Chua, N.H. (1988) Binding site requirements for pea nuclear protein factor GT-1 correlate with sequences required for light-dependent transcriptional activation of the *rbcS-3A* gene. *The EMBO Journal*, **7**, 4035-4044.

Groot, P.H., Scholte, H.R. and Hulsmann, W.C. (1976) Fatty acid activation: specificity, localization, and function. *Advances in Lipid Research*, **14**, 75-126.

Grotewold, E., Drummond, B.J., Bowen, B. and Peterson, T. (1994) The *myb*-homologous *P* gene controls phlobaphene pigmentation in maize floral organs by directly activating a flavonoid biosynthetic gene subset. *Cell*, **76**, 543-553.

Gubler, F., Kalla, R., Roberts, J.K. and Jacobsen, J.V. (1995) Gibberellin-regulated expression of a *myb* gene in barley aleurone cells: evidence for Myb transactivation of a high-pl α-amylase gene promoter. *The Plant Cell*, **7**, 1879-1891.

Gubler, F., Raventos, D., Keys, M., Watts, R., Mundy, J. and Jacobsen, J.V. (1999) Target genes and regulatory domains of the GAMYB transcriptional activator in cereal aleurone. *The Plant Journal*, **17**, 1-9.

Gühnemann-Schäfer, K. and Kindl, H. (1995) The leaf peroxisomal form (MFP IV) of multifunctional protein functioning in fatty-acid β-oxidation. *Planta*, **196**, 642-646.

Guo, F.-Q. and Crawford, N.M. (2005) Arabidopsis nitric oxide synthase1 is targeted to mitochondria and protects against oxidative damage and dark-induced senescence. *The Plant Cell*, **17**, 3436-3450.

Guo, F.-Q., Okamoto, M. and Crawford, N.M. (2003) Identification of a plant nitric oxide synthase gene involved in hormonal signaling. *Science*, **302**, 100-103.

Gurvitz, A., Mursula, A.M., Firzinger, A., Hamilton, B., Kilpelainen, S.H., Hartig, A., Ruis, H., Hiltunen, J.K. and Rottensteiner, H. (1998) Peroxisomal Δ^3-*cis*-Δ^2-*trans*-enoyl-CoA isomerase encoded by *ECI1* is required for growth of the yeast *Saccharomyces cerevisiae* on unsaturated fatty acids. *Journal of Biological Chemistry*, **273**, 31366-31374.

Gurvitz, A., Rottensteiner, H., Kilpelainen, S.H., Hartig, A., Hiltunen, J.K., Binder, M., Dawes, I.W. and Hamilton, B. (1997) The *Saccharomyces cerevisiae* peroxisomal 2,4-dienoyl-CoA reductase is encoded by the oleate-inducible gene *SPS19*. *Journal of Biological Chemistry*, **272**, 22140-22147.

Guyon-Debast, A., Lecureuil, A., Bonhomme, S., Guerche, P. and Gallois, J.-L. (2010) A SNP associated with alternative splicing of *RPT5b* causes unequal redundancy between *RPT5a* and *RPT5b* among *Arabidopsis thaliana* natural variation. *BMC Plant Biology*, **10**, 158.

Hancock, J.T., Neill, S.J. and Wilson, I.D. (2011) Nitric oxide and ABA in the control of plant function. *Plant Science*, **181**, 555-559.

Hardtke, C.S., Gohda, K., Osterlund, M.T., Oyama, T., Okada, K. and Deng, X.W. (2000) HY5 stability and activity in Arabidopsis is regulated by phosphorylation in its COP1 binding domain. *The EMBO Journal*, **19**, 4997-5006.

Harmer, S.L., Hogenesch, J.B., Straume, M., Chang, H.-S., Han, B., Zhu, T., Wang, X., Kreps, J.A. and Kay, S.A. (2000) Orchestrated transcription of key pathways in Arabidopsis by the circadian clock. *Science*, **290**, 2110-2113.

Hayashi, H., De Bellis, L., Ciurli, A., Kondo, M., Hayashi, M. and Nishimura, M. (1999) A novel acyl-CoA oxidase that can oxidize short-chain acyl-CoA in plant peroxisomes. *Journal of Biological Chemistry*, **274**, 12715-12721.

Hayashi, M., Nito, K., Takei-Hoshi, R., Yagi, M., Kondo, M., Suenaga, A., Yamaya, T. and Nishimura, M. (2002) Ped3p is a peroxisomal ATP-binding cassette transporter that might supply substrates for fatty acid β-oxidation. *Plant and Cell Physiology*, **43**, 1-11.

Hayashi, M., Nito, K., Toriyama-Kato, K., Kondo, M., Yamaya, T. and Nishimura, M. (2000) AtPex14p maintains peroxisomal functions by determining protein targeting to three kinds of plant peroxisomes. *The EMBO Journal*, **19**, 5701-5710.

Hayashi, M., Toriyama, K., Kondo, M. and Nishimura, M. (1998) 2,4-Dichlorophenoxybutyric acid-resistant mutants of Arabidopsis have defects in glyoxysomal fatty acid beta-oxidation. *Plant Cell*, **10**, 183-195.

Hayashi, Y., Hayashi, M., Hayashi, H., Hara-Nishimura, I. and Nishimura, M. (2001) Direct interaction between glyoxysomes and lipid bodies in cotyledons of the *Arabidopsis thaliana ped1* mutant. *Protoplasma*, **218**, 83-94.

He, Y., Fukushige, H., Hildebrand, D.F. and Gan, S. (2002) Evidence supporting a role of jasmonic acid in Arabidopsis leaf senescence. *Plant Physiology*, **128**, 876-884.

Heeg, C., Kruse, C., Jost, R., Gutensohn, M., Ruppert, T., Wirtz, M. and Hell, R. (2008) Analysis of the Arabidopsis *O*-acetylserine(thiol)lyase gene family demonstrates compartment-specific differences in the regulation of cysteine synthesis. *The Plant Cell*, **20**, 168-185.

Hellens, R.P., Edwards, E.A., Leyland, N.R., Bean, S. and Mullineaux, P.M. (2000) pGreen: a versatile and flexible binary Ti vector for *Agrobacterium*-mediated plant transformation. *Plant Molecular Biology*, **42**, 819-832.

Hendricks, S.B. and Taylorson, R.B. (1975) Breaking of seed dormancy by catalase inhibition. *Proceedings of the National Academy of Sciences*, **72**, 306-309.

Hensel, L.L., Nelson, M.A., Richmond, T.A. and Bleecker, A.B. (1994) The fate of inflorescence meristems is controlled by developing fruits in Arabidopsis. *Plant Physiology*, **106**, 863-876.

Higo, K., Ugawa, Y., Iwamoto, M. and Korenaga, T. (1999) Plant *cis*-acting regulatory DNA elements (PLACE) database. *Nucleic Acids Research*, **27**, 297-300.

Hills, M.J., Murphy, D.J. and Beevers, H. (1989) Inhibition of neutral lipase from castor bean lipid bodies by coenzyme A (CoA) and oleoyl-CoA. *Plant Physiology*, **89**, 1006-1010.

Hiltunen, J.K., Palosaari, P.M. and Kunau, W.H. (1989) Epimerization of 3-hydroxyacyl-CoA esters in rat liver. Involvement of two 2-enoyl-CoA hydratases. *Journal of Biological Chemistry*, **264**, 13536-13540.

Himmelbach, A., Hoffmann, T., Leube, M., Hohener, B. and Grill, E. (2002) Homeodomain protein ATHB6 is a target of the protein phosphatase ABI1 and regulates hormone responses in Arabidopsis. *The EMBO Journal*, **21**, 3029-3038.

Himmelbach, A., Yang, Y. and Grill, E. (2003) Relay and control of abscisic acid signaling. *Current Opinion in Plant Biology*, **6**, 470-479.

Hofgen, R. and Willmitzer, L. (1988) Storage of competent cells for *Agrobacterium* transformation. *Nucleic Acids Research*, **16**, 9877.

Holdsworth, M.J., Bentsink, L. and Soppe, W.J.J. (2008) Molecular networks regulating Arabidopsis seed maturation, after-ripening, dormancy and germination. *New Phytologist*, **179**, 33-54.

Holm, M., Ma, L.-G., Qu, L.-J. and Deng, X.-W. (2002) Two interacting bZIP proteins are direct targets of COP1-mediated control of light-dependent gene expression in Arabidopsis. *Genes and Development*, **16**, 1247-1259.

Hooks, M.A., Kellas, F. and Graham, I.A. (1999) Long-chain acyl-CoA oxidases of Arabidopsis. *The Plant Journal*, **20**, 1-13.

Hrazdina, G. and Wagner, G.J. (1985) Metabolic pathways as enzyme complexes: evidence for the synthesis of phenylpropanoids and flavonoids on membrane associated enzyme complexes. *Archives of Biochemistry and Biophysics*, **237**, 88-100.

Hu, J., Aguirre, M., Peto, C., Alonso, J., Ecker, J. and Chory, J. (2002) A role for peroxisomes in photomorphogenesis and development of Arabidopsis. *Science*, **297**, 405-409.

Huang, H., Tudor, M., Weiss, C.A., Hu, Y. and Ma, H. (1995) The Arabidopsis MADS-box gene *AGL3* is widely expressed and encodes a sequence-specific DNA-binding protein. *Plant Molecular Biology*, **28**, 549-567.

Hughes, M.A. and Dunn, M.A. (1996) The molecular biology of plant acclimation to low temperature. *Journal of Experimental Botany*, **47**, 291-305.

Ihle, J.N. and Dure, L.S. (1972) The developmental biochemistry of cottonseed embryogenesis and germination. *Journal of Biological Chemistry*, **247**, 5048-5055.

Inoue, H., Nojima, H. and Okayama, H. (1990) High efficiency transformation of *Escherichia coli* with plasmids. *Gene*, **96**, 23-28.

Jarvis, A.P., Schaaf, O. and Oldham, N.J. (2000) 3-hydroxy-3-phenylpropanoic acid is an intermediate in the biosynthesis of benzoic acid and salicylic acid but benzaldehyde is not. *Planta*, **212**, 119-126.

Jiang, T., Zhang, X.-F., Wang, X.-F. and Zhang, D.-P. (2011) Arabidopsis 3-ketoacyl-CoA thiolase-2 (KAT2), an enzyme of fatty acid β-oxidation, is involved in ABA signal transduction. *Plant and Cell Physiology*, **52**, 528-538.

Jiao, Y., Ma, L., Strickland, E. and Deng, X.W. (2005) Conservation and divergence of light-regulated genome expression patterns during seedling development in rice and Arabidopsis. *The Plant Cell*, **17**, 3239-3256.

Jin, H., Cominelli, E., Bailey, P., Parr, A., Mehrtens, F., Jones, J., Tonelli, C., Weisshaar, B. and Martin, C. (2000) Transcriptional repression by AtMYB4 controls production of UV-protecting sunscreens in Arabidopsis. *The EMBO Journal*, **19**, 6150-6161.

Jin, H. and Nikolau, B.J. (2006) Genetic, Biochemical and Physiological Studies Acetyl-CoA Metabolism via Condensation. In *The 17th International Symposium on Plant Lipids* (Benning, C. and Ohlrogge, J. eds). Michigan State University, East Lansing, Michigan: Aardvark Global Publishing Company, pp. 177.

Kamada, T., Nito, K., Hayashi, H., Mano, S., Hayashi, M. and Nishimura, M. (2003) Functional differentiation of peroxisomes revealed by expression profiles of peroxisomal genes in *Arabidopsis thaliana*. *Plant and Cell Physiology*, **44**, 1275-1289.

Kanai, M., Nishimura, M. and Hayashi, M. (2010) A peroxisomal ABC transporter promotes seed germination by inducing pectin degradation under the control of *ABI5*. *The Plant Journal*, **62**, 936-947.

Kanayama, N., Ueda, M., Atomi, H. and Tanaka, A. (1998) Genetic evaluation of physiological functions of thiolase isozymes in the *n*-alkane-assimilating yeast *Candida tropicalis*. *Journal of Bacteriology*, **180**, 690-698.

Kang, J.-H., Wang, L., Giri, A. and Baldwin, I.T. (2006) Silencing threonine deaminase and *JAR4* in *Nicotiana attenuata* impairs jasmonic acid-isoleucine-mediated defenses against *Manduca sexta*. *The Plant Cell*, **18**, 3303-3320.

Karimi, M., Inze, D. and Depicker, A. (2002) GATEWAY vectors for *Agrobacterium*-mediated plant transformation. *Trends in Plant Science*, **7**, 193-195.

Karpichev, I., Luo, Y., Marians, R. and Small, G. (1997) A complex containing two transcription factors regulates peroxisome proliferation and the coordinate induction of β-oxidation enzymes in *Saccharomyces cerevisiae*. *Molecular and Cellular Biology*, **17**, 69-80.

Karpichev, I.V. and Small, G.M. (1998) Global regulatory functions of Oaf1p and Pip2p (Oaf2p), transcription factors that regulate genes encoding peroxisomal proteins in *Saccharomyces cerevisiae*. *Molecular and Cellular Biology*, **18**, 6560-6570.

Katavic, V., Reed, D.W., Taylor, D.C., Giblin, E.M., Barton, D.L., Zou, J., MacKenzie, S.L., Covello, P.S. and Kunst, L. (1995) Alteration of seed fatty acid composition by an ethyl methanesulfonate-induced mutation in *Arabidopsis thaliana* affecting diacylglycerol acyltransferase activity. *Plant Physiology*, **108**, 399-409.

Kato, A., Hayashi, M., Takeuchi, Y. and Nishimura, M. (1996) cDNA cloning and expression of a gene for 3-ketoacyl-CoA thiolase in pumpkin cotyledons. *Plant Molecular Biology*, **31**, 843-852.

Kaup, M.T., Froese, C.D. and Thompson, J.E. (2002) A role for diacylglycerol acyltransferase during leaf senescence. *Plant Physiology*, **129**, 1616-1626.

Ke, J., Behal, R.H., Back, S.L., Nikolau, B.J., Wurtele, E.S. and Oliver, D.J. (2000) The role of pyruvate dehydrogenase and acetyl-Coenzyme A synthetase in fatty acid synthesis in developing Arabidopsis seeds. *Plant Physiology*, **123**, 497-508.

Kepinski, S. and Leyser, O. (2005) The Arabidopsis F-box protein TIR1 is an auxin receptor. *Nature*, **435**, 446-451.

Khan, B.R. and Zolman, B.K. (2010) *pex5* mutants that differentially disrupt PTS1 and PTS2 peroxisomal matrix protein import in Arabidopsis. *Plant Physiology*, **154**, 1602-1615.

Kienow, L., Schneider, K., Bartsch, M., Stuible, H.-P., Weng, H., Miersch, O., Wasternack, C. and Kombrink, E. (2008) Jasmonates meet fatty acids: functional analysis of a new acyl-coenzyme A synthetase family from *Arabidopsis thaliana*. *Journal of Experimental Botany*, **59**, 403-419.

Kim, E.Y., Seo, Y.S. and Kim, W.T. (2011) AtDSEL, an Arabidopsis cytosolic DAD1-like acylhydrolase, is involved in negative regulation of storage oil mobilization during seedling establishment. *Journal of Plant Physiology*, **168**, 1705-1709.

Kliebenstein, D.J., D'Auria, J.C., Behere, A.S., Kim, J.H., Gunderson, K.L., Breen, J.N., Lee, G., Gershenzon, J., Last, R.L. and Jander, G. (2007) Characterization of seed-specific benzoyloxyglucosinolate mutations in *Arabidopsis thaliana*. *The Plant Journal*, **51**, 1062-1076.

Koncz, C. and Schell, J. (1986) The promoter of T_L-DNA gene *5* controls the tissue-specific expression of chimaeric genes carried by a novel type of *Agrobacterium* binary vector. *Molecular and General Genetics*, **204**, 383-396.

Koornneef, M. (1981) The complex syndrome of *ttg* mutants in Arabidopsis. *Arabidopsis Information Service*, **18**, 45-51.

Koornneef, M., Bentsink, L. and Hilhorst, H. (2002) Seed dormancy and germination. *Current Opinion in Plant Biology*, **5**, 33-36.

Koornneef, M. and Meinke, D. (2010) The development of Arabidopsis as a model plant. *The Plant Journal*, **61**, 909-921.

Kunau, W.-H., Dommes, V. and Schulz, H. (1995) β-oxidation of fatty acids in mitochondria, peroxisomes, and bacteria: A century of continued progress. *Progress in Lipid Research*, **34**, 267-342.

Kunz, H.H., Scharnewski, M., Feussner, K., Feussner, I., Flugge, U.I., Fulda, M. and Gierth, M. (2009) The ABC transporter PXA1 and peroxisomal β-oxidation are vital

for metabolism in mature leaves of Arabidopsis during extended darkness. *The Plant Cell*, **21**, 2733-2749.

Kunze, M., Pracharoenwattana, I., Smith, S. and Hartig, A. (2006) A central role for the peroxisomal membrane in glyoxylate cycle function. *Biochimica et Biophysica Acta (BBA) - Molecular Cell Research*, **1763**, 1441-1452.

Lange, P.R., Eastmond, P.J., Madagan, K. and Graham, I.A. (2004) An Arabidopsis mutant disrupted in valine catabolism is also compromised in peroxisomal fatty acid β-oxidation. *FEBS Letters*, **571**, 147-153.

Lange, P.R. and Graham, I. (2000) *Arabidopsis thaliana* mutants disrupted in lipid mobilization. *Biochemical Society Transactions*, **28**, 762-765.

Larson, T.R., Edgell, T., Byrne, J., Dehesh, K. and Graham, I.A. (2002) Acyl-CoA profiles of transgenic plants that accumulate medium-chain fatty acids indicate inefficient storage lipid synthesis in developing oilseeds. *The Plant Journal*, **32**, 519-527.

Laughnan, J.R. and Gabay-Laughnan, S. (1983) Cytoplasmic male sterility in maize. *Annual Review of Genetics*, **17**, 27-48.

Lazarow, P.B. (1981) Assay of peroxisomal β-oxidation of fatty acids. *Methods in Enzymology*, **72**, 315-319.

Leubner-Metzger, G. and Meins, F. (2000) Sense transformation reveals a novel role for class I β-1,3-glucanase in tobacco seed germination. *The Plant Journal*, **23**, 215-221.

Li, J., Ou-Lee, T.M., Raba, R., Amundson, R.G. and Last, R.L. (1993) Arabidopsis flavonoid mutants are hypersensitive to UV-B irradiation. *The Plant Cell*, **5**, 171-179.

Li, Y., Beisson, F., Pollard, M. and Ohlrogge, J. (2006) Oil content of Arabidopsis seeds: The influence of seed anatomy, light and plant-to-plant variation. *Phytochemistry*, **67**, 904-915.

Liepman, A.H. and Olsen, L.J. (2003) Alanine aminotransferase homologs catalyze the glutamate:glyoxylate aminotransferase reaction in peroxisomes of Arabidopsis. *Plant Physiology*, **131**, 215-227.

Lin, Y., Cluette-Brown, J.E. and Goodman, H.M. (2004) The peroxisome deficient Arabidopsis mutant *sse1* exhibits impaired fatty acid synthesis. *Plant Physiology*, **135**, 814-827.

Lin, Y., Sun, L., Nguyen, L.V., Rachubinski, R.A. and Goodman, H.M. (1999) The Pex16p homolog SSE1 and storage organelle formation in Arabidopsis seeds. *Science*, **284**, 328-330.

Lingard, M.J., Monroe-Augustus, M. and Bartel, B. (2009) Peroxisome-associated matrix protein degradation in Arabidopsis. *Proceedings of the National Academy of Sciences*, **106**, 4561-4566.

Lingard, M.J. and Trelease, R.N. (2006) Five Arabidopsis peroxin 11 homologs individually promote peroxisome elongation, duplication or aggregation. *Journal of Cell Science*, **119**, 1961-1972.

Logemann, E., Parniske, M. and Hahlbrock, K. (1995) Modes of expression and common structural features of the complete phenylalanine ammonia-lyase gene family in parsley. *Proceedings of the National Academy of Sciences*, **92**, 5905-5909.

Logemann, E., Tavernaro, A., Schulz, W., Sommssich, I.E. and Hahlbrock, K. (2000) UV light selectively coinduces supply pathways from primary metabolism and flavonoid secondary product formation in parsley. *Proceedings of the National Academy of Sciences*, **97**, 1903-1907.

Lomsadze, A., Ter-Hovhannisyan, V., Chernoff, Y.O. and Borodovsky, M. (2005) Gene identification in novel eukaryotic genomes by self-training algorithm. *Nucleic Acids Research*, **33**, 6494-6506.

Lovegrove, A. and Hooley, R. (2000) Gibberellin and abscisic acid signalling in aleurone. *Trends in Plant Science*, **5**, 102-110.

Ludwig-Müller, J. (2000) Indole-3-butyric acid in plant growth and development. *Plant Growth Regulation*, **32**, 219-230.

Lüthy, B., Matile, P. and Thomas, H. (1986) Properties of linolenic acid-dependent chlorophyll oxidation activity in thylakoid membranes. *Journal of Plant Physiology*, **123**, 169-180.

Mackender, R.O. and Leech, R.M. (1974) The galactolipid, phospholipid, and fatty acid composition of the chloroplast envelope membranes of *Vicia faba*. L. *Plant Physiology*, **53**, 496-502.

Maeda, K., Kimura, S., Demura, T., Takeda, J. and Ozeki, Y. (2005) DcMYB1 acts as a transcriptional activator of the carrot phenylalanine ammonia-lyase gene (*DcPAL1*) in response to elicitor treatment, UV-B irradiation and the dilution effect. *Plant Molecular Biology*, **59**, 739-752.

Martin, C. and Northcote, D.H. (1982) The action of exogenous gibberellic acid on isocitrate lyase - mRNA in germinating castor bean seeds. *Planta*, **154**, 174-183.

Martin, T., Oswald, O. and Graham, I.A. (2002) Arabidopsis seedling growth, storage lipid mobilization, and photosynthetic gene expression are regulated by carbon:nitrogen availability. *Plant Physiology*, **128**, 472-481.

McKendree, W.L., Paul, A.L., DeLisle, A.J. and Ferl, R.J. (1990) In vivo and in vitro characterization of protein interactions with the dyad G-Box of the Arabidopsis *Adh* Gene. *The Plant Cell*, **2**, 207-214.

Mehrtens, F., Kranz, H., Bednarek, P. and Weisshaar, B. (2005) The Arabidopsis transcription factor MYB12 is a flavonol-specific regulator of phenylpropanoid biosynthesis. *Plant Physiology*, **138**, 1083-1096.

Meinhard, M. and Grill, E. (2001) Hydrogen peroxide is a regulator of ABI1, a protein phosphatase 2C from Arabidopsis. *FEBS Letters*, **508**, 443-446.

Mettler, I.J. and Beevers, H. (1980) Oxidation of NADH in glyoxysomes by a malate-aspartate shuttle. *Plant Physiology*, **66**, 555-560.

Michael, T.P. and McClung, C.R. (2002) Phase-specific circadian clock regulatory elements in Arabidopsis. *Plant Physiology*, **130**, 627-638.

Mitchum, M.G., Yamaguchi, S., Hanada, A., Kuwahara, A., Yoshioka, Y., Kato, T., Tabata, S., Kamiya, Y. and Sun, T.-p. (2006) Distinct and overlapping roles of two gibberellin 3-oxidases in Arabidopsis development. *The Plant Journal*, **45**, 804-818.

Mitsuya, S., El-Shami, M., Sparkes, I.A., Charlton, W.L., De Marcos Lousa, C., Johnson, B. and Baker, A. (2010) Salt stress causes peroxisome proliferation, but inducing peroxisome proliferation does not improve NaCl tolerance in *Arabidopsis thaliana*. *PLoS ONE*, **5**, e9408.

Moerkercke, A.V., Schauvinhold, I., Pichersky, E., Haring, M.A. and Schuurink, R.C. (2009) A plant thiolase involved in benzoic acid biosynthesis and volatile benzenoid production. *The Plant Journal*, **60**, 292-302.

Moes, D., Himmelbach, A., Korte, A., Haberer, G. and Grill, E. (2008) Nuclear localization of the mutant protein phosphatase abi1 is required for insensitivity towards ABA responses in Arabidopsis. *The Plant Journal*, **54**, 806-819.

Moreau, M., Lindermayr, C., Durner, J. and Klessig, D.F. (2010) NO synthesis and signaling in plants – where do we stand? *Physiologia Plantarum*, **138**, 372-383.

Morita, A., Umemura, T.-a., Kuroyanagi, M., Futsuhara, Y., Perata, P. and Yamaguchi, J. (1998) Functional dissection of a sugar-repressed α-amylase gene (*RAmy1A*) promoter in rice embryos. *FEBS Letters*, **423**, 81-85.

Müller, K., Hess, B. and Leubner-Metzger, G. (2007) A role for reactive oxygen species in endosperm weakening. In *Seeds: Biology, Development and Ecology* (Adkins, S.W., Ashmore, S.E. and Navie, S.C. eds). Wallingford: CAB International, pp. 287–295.

Müller, K., Linkies, A., Vreeburg, R.A.M., Fry, S.C., Krieger-Liszkay, A. and Leubner-Metzger, G. (2009) *In vivo* cell wall loosening by hydroxyl radicals during cress seed germination and elongation growth. *Plant Physiology*, **150**, 1855-1865.

Nakabayashi, K., Okamoto, M., Koshiba, T., Kamiya, Y. and Nambara, E. (2005) Genome-wide profiling of stored mRNA in *Arabidopsis thaliana* seed germination: epigenetic and genetic regulation of transcription in seed. *The Plant Journal*, **41**, 697-709.

Nakashima, K., Fujita, Y., Katsura, K., Maruyama, K., Narusaka, Y., Seki, M., Shinozaki, K. and Yamaguchi-Shinozaki, K. (2006) Transcriptional regulation of ABI3- and ABA-responsive genes including *RD29B* and *RD29A* in seeds, germinating embryos, and seedlings of Arabidopsis. *Plant Molecular Biology*, **60**, 51-68.

Naredo, M.E.B., Juliano, A.B., Lu, B.R., Guzman, F.D. and Jackson, M.T. (1998) Responses to seed dormancy-breaking treatments in rice species (*Oryza* L.). *Seed Science And Technology*, **26**, 675-689.

Nayidu, N.K., Wang, L., Xie, W., Zhang, C., Fan, C., Lian, X., Zhang, Q. and Xiong, L. (2008) Comprehensive sequence and expression profile analysis of *PEX11* gene family in rice. *Gene*, **412**, 59-70.

Nishimura, A., Morita, M., Nishimura, Y. and Sugino, Y. (1990) A rapid and highly efficient method for preparation of competent *Escherichia coli* cells. *Nucleic Acids Research*, **18**, 6169.

Nito, K., Kamigaki, A., Kondo, M., Hayashi, M. and Nishimura, M. (2007) Functional classification of Arabidopsis peroxisome biogenesis factors proposed from analyses of knockdown mutants. *Plant and Cell Physiology*, **48**, 763-774.

Nyathi, Y. and Baker, A. (2006) Plant peroxisomes as a source of signalling molecules. *Biochimica et Biophysica Acta (BBA) - Molecular Cell Research*, **1763**, 1478-1495.

O'Connor, T.R., Dyreson, C. and Wyrick, J.J. (2005) Athena: a resource for rapid visualization and systematic analysis of Arabidopsis promoter sequences. *Bioinformatics*, **21**, 4411-4413.

Obayashi, T., Kinoshita, K., Nakai, K., Shibaoka, M., Hayashi, S., Saeki, M., Shibata, D., Saito, K. and Ohta, H. (2007) ATTED-II: a database of co-expressed genes and *cis* elements for identifying co-regulated gene groups in Arabidopsis. *Nucleic Acids Research*, **35**, D863-D869.

Ogawa, M., Hanada, A., Yamauchi, Y., Kuwahara, A., Kamiya, Y. and Yamaguchi, S. (2003) Gibberellin biosynthesis and response during Arabidopsis seed germination. *The Plant Cell*, **15**, 1591-1604.

Ohlrogge, J.B., Browse, J. and Somerville, C.R. (1991) The genetics of plant lipids. *Biochimica et Biophysica Acta (BBA) - Lipids and Lipid Metabolism*, **1082**, 1-26.

Ohlrogge, J.B. and Jaworski, J.G. (1997) Regulation of fatty acid synthesis. *Annual Review of Plant Physiology and Plant Molecular Biology*, **48**, 109-136.

Olowe, Y. and Schulz, H. (1980) Regulation of thiolases from pig heart. *European Journal of Biochemistry*, **109**, 425-429.

Olsen, L.J. and Harada, J.J. (1995) Peroxisomes and their assembly in higher plants. *Annual Review of Plant Physiology and Plant Molecular Biology*, **46**, 123-146.

Oravecz, A., Baumann, A., Máté, Z., Brzezinska, A., Molinier, J., Oakeley, E.J., Ádám, É., Schäfer, E., Nagy, F. and Ulm, R. (2006) CONSTITUTIVELY PHOTOMORPHOGENIC1 is required for the UV-B response in Arabidopsis. *The Plant Cell*, **18**, 1975-1990.

Orlova, I., Marshall-Colón, A., Schnepp, J., Wood, B., Varbanova, M., Fridman, E., Blakeslee, J.J., Peer, W.A., Murphy, A.S., Rhodes, D., Pichersky, E. and Dudareva, N. (2006) Reduction of benzenoid synthesis in petunia flowers reveals multiple pathways to benzoic acid and enhancement in auxin transport. *The Plant Cell*, **18**, 3458-3475.

Orth, T., Reumann, S., Zhang, X., Fan, J., Wenzel, D., Quan, S. and Hu, J. (2007) The PEROXIN11 protein family controls peroxisome proliferation in Arabidopsis. *The Plant Cell*, **19**, 333-350.

Osmundsen, H., Bremer, J. and Pedersen, J.I. (1991) Metabolic aspects of peroxisomal β-oxidation. *Biochimica et Biophysica Acta (BBA) - Lipids and Lipid Metabolism*, **1085**, 141-158.

Osuna, D., Usadel, B., Morcuende, R., Gibon, Y., Bläsing, O.E., Höhne, M., Günter, M., Kamlage, B., Trethewey, R., Scheible, W.-R. and Stitt, M. (2007) Temporal responses of transcripts, enzyme activities and metabolites after adding sucrose to carbon-deprived Arabidopsis seedlings. *The Plant Journal*, **49**, 463-491.

Paek, N.C., Lee, B.M., Gyu Bai, D. and Smith, J.D. (1998) Inhibition of germination gene expression by Viviparous-1 and ABA during maize kernel development. *Molecules and Cells*, **8**, 336-342.

Page, R.D.M. (1996) Tree View: An application to display phylogenetic trees on personal computers. *Computer applications in the biosciences*, **12**, 357-358.

Panikashvili, D., Savaldi-Goldstein, S., Mandel, T., Yifhar, T., Franke, R.B., Höfer, R., Schreiber, L., Chory, J. and Aharoni, A. (2007) The Arabidopsis DESPERADO/AtWBC11 transporter is required for cutin and wax secretion. *Plant Physiology*, **145**, 1345-1360.

Panikashvili, D., Shi, J.X., Bocobza, S., Franke, R.B., Schreiber, L. and Aharoni, A. (2010) The Arabidopsis DSO/ABCG11 transporter affects cutin metabolism in reproductive organs and suberin in roots. *Molecular Plant*, **3**, 563-575.

Park, J.-H., Halitschke, R., Kim, H.B., Baldwin, I.T., Feldmann, K.A. and Feyereisen, R. (2002) A knock-out mutation in allene oxide synthase results in male sterility and defective wound signal transduction in Arabidopsis due to a block in jasmonic acid biosynthesis. *The Plant Journal*, **31**, 1-12.

Penfield, S., Li, Y., Gilday, A., Graham, S. and Graham, I.A. (2006) Arabidopsis ABA INSENSITIVE4 regulates lipid mobilization in the embryo and reveals repression of seed germination by the endosperm. *The Plant Cell*, **18**, 1887-1899.

Penfield, S., Rylott, E.L., Gilday, A., Graham, S., Larson, T. and Graham, I. (2004) Reserve mobilization in the Arabidopsis endosperm fuels hypocotyl elongation in the dark, is independent of abscisic acid, and requires *PHOSPHOENOLPYRUVATE CARBOXYKINASE1*. *The Plant Cell*, **16**, 2705-2718.

Pepper, A., Delaney, T., Washburnt, T., Poole, D. and Chory, J. (1994) DET1, a negative regulator of light-mediated development and gene expression in arabidopsis, encodes a novel nuclear-localized protein. *Cell*, **78**, 109-116.

Perry, S.E., Nichols, K.W. and Fernandez, D.E. (1996) The MADS domain protein AGL15 localizes to the nucleus during early stages of seed Development. *The Plant Cell*, **8**, 1977-1989.

Pinfield-Wells, H., Rylott, E.L., Gilday, A.D., Graham, S., Job, K., Larson, T.R. and Graham, I.A. (2005) Sucrose rescues seedling establishment but not germination of Arabidopsis mutants disrupted in peroxisomal fatty acid catabolism. *The Plant Journal*, **43**, 861-872.

Piskurewicz, U., Jikumaru, Y., Kinoshita, N., Nambara, E., Kamiya, Y. and Lopez-Molina, L. (2008) The gibberellic acid signaling repressor RGL2 inhibits Arabidopsis seed germination by stimulating abscisic acid synthesis and ABI5 activity. *The Plant Cell*, **20**, 2729-2745.

Poirier, Y., Ventre, G. and Caldelari, D. (1999) Increased flow of fatty acids toward β-oxidation in developing seeds of Arabidopsis deficient in diacylglycerol acyltransferase activity or synthesizing medium-chain-length fatty acids. *Plant Physiology*, **121**, 1359-1366.

Powles, S.B. (1984) Photoinhibition of photosynthesis induced by visible light. *Annual Review of Plant Physiology*, **35**, 15-44.

Pracharoenwattana, I., Cornah, J.E. and Smith, S.M. (2005) Arabidopsis peroxisomal citrate synthase is required for fatty acid respiration and seed germination. *The Plant Cell*, **17**, 2037-2048.

Pracharoenwattana, I., Cornah, J.E. and Smith, S.M. (2007) Arabidopsis peroxisomal malate dehydrogenase functions in β-oxidation but not in the glyoxylate cycle. *The Plant Journal*, **50**, 381-390.

Pracharoenwattana, I., Zhou, W. and Smith, S.M. (2010) Fatty acid β-oxidation in germinating Arabidopsis seeds is supported by peroxisomal hydroxypyruvate reductase when malate dehydrogenase is absent. *Plant Molecular Biology*, **72**, 101-109.

Prado, A.M., Porterfield, D.M. and Feijó, J.A. (2004) Nitric oxide is involved in growth regulation and re-orientation of pollen tubes. *Development*, **131**, 2707-2714.

Preisig-Müller, R., Gühnemann-Schäfer, K. and Kindl, H. (1994) Domains of the tetrafunctional protein acting in glyoxysomal fatty acid beta-oxidation. Demonstration of epimerase and isomerase activities on a peptide lacking hydratase activity. *Journal of Biological Chemistry*, **269**, 20475-20481.

Pritchard, S.L., Charlton, W.L., Baker, A. and Graham, I.A. (2002) Germination and storage reserve mobilization are regulated independently in Arabidopsis. *The Plant Journal*, **31**, 639-647.

Pruzinská, A., Anders, I., Aubry, S., Schenk, N., Tapernoux-Lüthi, E., Müller, T., Kräutler, B. and Hörtensteiner, S. (2007) *In vivo* participation of red chlorophyll catabolite reductase in chlorophyll breakdown. *The Plant Cell*, **19**, 369-387.

Pružinská, A., Tanner, G., Anders, I., Roca, M. and Hörtensteiner, S. (2003) Chlorophyll breakdown: Pheophorbide a oxygenase is a Rieske-type iron–sulfur protein, encoded by the *accelerated cell death* 1 gene. *Proceedings of the National Academy of Sciences*, **100**, 15259-15264.

Pye, V.E., Christensen, C.E., Dyer, J.H., Arent, S. and Henriksen, A. (2010) Peroxisomal plant 3-ketoacyl-CoA thiolase structure and activity are regulated by a sensitive redox switch. *Journal of Biological Chemistry*, **285**, 24078-24088.

Rahman, A., Nakasone, A., Chhun, T., Ooura, C., Biswas, K.K., Uchimiya, H., Tsurumi, S., Baskin, T.I., Tanaka, A. and Oono, Y. (2006) A small acidic protein 1 (SMAP1) mediates responses of the Arabidopsis root to the synthetic auxin 2,4-dichlorophenoxyacetic acid. *The Plant Journal*, **47**, 788-801.

Raymond, P., Spiteri, A., Dieuaide, M., Gerhardt, B. and Pradet, A. (1992) Peroxisomal β-oxidation of fatty-acids and citrate formation by a particulate fraction from early germinating sunflower seeds. *Plant Physiology and Biochemistry*, **30**, 153-161.

Reddy, J.K. and Chu, R. (1996) Peroxisome proliferator–induced pleiotropic responses: pursuit of a phenomenona. *Annals of the New York Academy of Sciences*, **804**, 176-201.

Rédei, G.P. (1992) A heuristic glance at the past of Arabidopsis genetics. In *Methods in Arabidopsis Research* (Koncz, C., Chua, N.H. and Schell, J. eds). Singapore: World Scientific, pp. 1-15.

Reina, J.J., Guerrero, C. and Heredia, A. (2007) Isolation, characterization, and localization of *AgaSGNH* cDNA: a new SGNH-motif plant hydrolase specific to *Agave americana* L. leaf epidermis. *Journal of Experimental Botany*, **58**, 2717-2731.

Reumann, S. (2004) Specification of the peroxisome targeting signals type 1 and type 2 of plant peroxisomes by bioinformatics analyses. *Plant Physiology*, **135**, 783-800.

Reumann, S., Babujee, L., Ma, C., Wienkoop, S., Siemsen, T., Antonicelli, G.E., Rasche, N., Luder, F., Weckwerth, W. and Jahn, O. (2007) Proteome analysis of Arabidopsis leaf peroxisomes reveals novel targeting peptides, metabolic pathways, and defense mechanisms. *The Plant Cell*, **19**, 3170-3193.

Reumann, S., Ma, C., Lemke, S. and Babujee, L. (2004) AraPerox. A database of putative Arabidopsis proteins from plant peroxisomes. *Plant Physiology*, **136**, 2587-2608.

Reumann, S. and Weber, A.P.M. (2006) Plant peroxisomes respire in the light: Some gaps of the photorespiratory C2 cycle have become filled - Others remain. *Biochimica et Biophysica Acta (BBA) - Molecular Cell Research*, **1763**, 1496-1510.

Richmond, T. and Bleecker, A. (1997) A defect in a fatty acid β-oxidation alters Arabidopsis inflorescence development. In *8th International Conference on Arabidopsis Research*. Madison, WI.: University of Wisconsin Press.

Richmond, T.A. and Bleecker, A.B. (1999) A defect in β-oxidation causes abnormal inflorescence development in Arabidopsis. *The Plant Cell*, **11**, 1911-1924.

Robert, S.S., Singh, S.P., Zhou, X.-R., Petrie, J.R., Blackburn, S.I., Mansour, P.M., Nichols, P.D., Liu, Q. and Green, A.G. (2005) Metabolic engineering of Arabidopsis to produce nutritionally important DHA in seed oil. *Functional Plant Biology*, **32**, 473.

Rodriguez, D., Dommes, J. and Northcote, D.H. (1987) Effect of abscisic and gibberellic acids on malate synthase transcripts in germinating castor bean seeds. *Plant Molecular Biology*, **9**, 227-235.

Rogers, J.C., Dean, D. and Heck, G.R. (1985) Aleurain: a barley thiol protease closely related to mammalian cathepsin H. *Proceedings of the National Academy of Sciences*, **82**, 6512-6516.

Rosso, M.G., Li, Y., Strizhov, N., Reiss, B., Dekker, K. and Weisshaar, B. (2003) An *Arabidopsis thaliana* T-DNA mutagenized population (GABI-Kat) for flanking sequence tag-based reverse genetics. *Plant Molecular Biology*, **53**, 247-259.

Rozen, S. and Skaletsky, H. (2000) Primer3 on the WWW for general users and for biologist programmers. In *Bioinformatics Methods and Protocols: Methods in Molecular Biology* (Misener, S. and Krawetz, S.A. eds): Humana Press, pp. 365-386.

Rushton, P.J., Torres, J.T., Parniske, M., Wernert, P., Hahlbrock, K. and Somssich, I.E. (1996) Interaction of elicitor-induced DNA-binding proteins with elicitor response elements in the promoters of parsley *PR1* genes. *The EMBO Journal*, **15**, 5690-5700.

Russell, L., Larner, V., Kurup, S., Bougourd, S. and Holdsworth, M. (2000) The Arabidopsis COMATOSE locus regulates germination potential. *Development*, **127**, 3759-3767.

Rylott, E.L., Eastmond, P.J., Gilday, A.D., Slocombe, S.P., Larson, T.R., Baker, A. and Graham, I.A. (2006) The *Arabidopsis thaliana* multifunctional protein gene (MFP2) of peroxisomal β-oxidation is essential for seedling establishment. *The Plant Journal*, **45**, 930-941.

Rylott, E.L., Hooks, M.A. and Graham, I.A. (2001) Co-ordinate regulation of genes involved in storage lipid mobilization in Arabidopsis thaliana. *Biochemical Society Transactions*, **29**, 283-287.

Rylott, E.L., Rogers, C.A., Gilday, A.D., Edgell, T., Larson, T.R. and Graham, I.A. (2003) Arabidopsis mutants in short- and medium-chain acyl-CoA oxidase activities accumulate acyl-CoAs and reveal that fatty acid β-oxidation is essential for embryo development. *Journal of Biological Chemistry*, **278**, 21370-21377.

Sablowski, R.W., Moyano, E., Culianez-Macia, F.A., Schuch, W., Martin, C. and Bevan, M. (1994) A flower-specific Myb protein activates transcription of phenylpropanoid biosynthetic genes. *The EMBO Journal*, **13**, 128-137.

Sambrook, J., Fritsch, E.F. and Maniatis, T. (1989) *Molecular Cloning: A Laboratory Manual* New York: Cold Spring Harbour Laboratory Press.

Samson, F., Brunaud, V., Duchêne, S., De Oliveira, Y., Caboche, M., Lecharny, A. and Aubourg, S. (2004) FLAGdb++: a database for the functional analysis of the Arabidopsis genome. *Nucleic Acids Research*, **32**, D347-D350.

Sanders, P.M., Lee, P.Y., Biesgen, C., Boone, J.D., Beals, T.P., Weiler, E.W. and Goldberg, R.B. (2000) The Arabidopsis *DELAYED DEHISCENCE1* gene encodes an enzyme in the jasmonic acid synthesis pathway. *The Plant Cell*, **12**, 1041-1062.

Sauveplane, V., Kandel, S., Kastner, P.-E., Ehlting, J., Compagnon, V., Werck-Reichhart, D. and Pinot, F. (2009) *Arabidopsis thaliana* CYP77A4 is the first cytochrome P450 able to catalyze the epoxidation of free fatty acids in plants. *FEBS Journal*, **276**, 719-735.

Schaller, A. and Stintzi, A. (2009) Enzymes in jasmonate biosynthesis – Structure, function, regulation. *Phytochemistry*, **70**, 1532-1538.

Schaller, F., Biesgen, C., Müssig, C., Altmann, T. and Weiler, E.W. (2000) 12-Oxophytodienoate reductase 3 (OPR3) is the isoenzyme involved in jasmonate biosynthesis. *Planta*, **210**, 979-984.

Schilmiller, A.L., Koo, A.J.K. and Howe, G.A. (2007) Functional diversification of acyl-coenzyme A oxidases in jasmonic acid biosynthesis and action. *Plant Physiology*, **143**, 812-824.

Schmid, M., Davison, T.S., Henz, S.R., Pape, U.J., Demar, M., Vingron, M., Scholkopf, B., Weigel, D. and Lohmann, J.U. (2005) A gene expression map of *Arabidopsis thaliana* development. *Nature Genetics*, **37**, 501-506.

Schneider, K., Kienow, L., Schmelzer, E., Colby, T., Bartsch, M., Miersch, O., Wasternack, C., Kombrink, E. and Stuible, H.P. (2005) A new type of peroxisomal acyl-coenzyme A synthetase from *Arabidopsis thaliana* has the catalytic capacity to activate biosynthetic precursors of jasmonic acid. *Journal of Biological Chemistry*, **280**, 13962-13972.

Schroeder, D.F., Gahrtz, M., Maxwell, B.B., Cook, R.K., Kan, J.M., Alonso, J.M., Ecker, J.R. and Chory, J. (2002) De-etiolated 1 and damaged DNA binding protein 1 interact to regulate Arabidopsis photomorphogenesis. *Current Biology*, **12**, 1462-1472.

Schulz, H. and Kunau, W.-H. (1987) β-oxidation of unsaturated fatty acids: a revised pathway. *Trends in Biochemical Sciences*, **12**, 403-406.

Schwechheimer, C. (2008) Understanding gibberellic acid signaling - are we there yet? *Current Opinion in Plant Biology*, **11**, 9-15.

Schwechheimer, C. and Deng, X.-W. (2000) The COP/DET/FUS proteins - regulators of eukaryotic growth and development. *Seminars in Cell & Developmental Biology*, **11**, 495-503.

Shockey, J.M., Fulda, M. and Browse, J. (2003) Arabidopsis contains a large superfamily of acyl-activating enzymes. Phylogenetic and biochemical analysis reveals a new class of acyl-coenzyme A synthetases. *Plant Physiology*, **132**, 1065-1076.

Shorrosh, B.S., Dixon, R.A. and Ohlrogge, J.B. (1994) Molecular cloning, characterization, and elicitation of acetyl-CoA carboxylase from alfalfa. *Proceedings of the National Academy of Sciences*, **91**, 4323-4327.

Simpson, S.D., Nakashima, K., Narusaka, Y., Seki, M., Shinozaki, K. and Yamaguchi-Shinozaki, K. (2003) Two different novel *cis*-acting elements of *erd1*, a *clpA* homologous Arabidopsis gene function in induction by dehydration stress and dark-induced senescence. *The Plant Journal*, **33**, 259-270.

Skriver, K., Olsen, F.L., Rogers, J.C. and Mundy, J. (1991) *cis*-acting DNA elements responsive to gibberellin and its antagonist abscisic acid. *Proceedings of the National Academy of Sciences*, **88**, 7266-7270.

Slocombe, S.P., Cornah, J., Pinfield-Wells, H., Soady, K., Zhang, Q., Gilday, A., Dyer, J.M. and Graham, I.A. (2009) Oil accumulation in leaves directed by modification of fatty acid breakdown and lipid synthesis pathways. *Plant Biotechnology Journal*, **7**, 694-703.

Smith, S.M., Fulton, D.C., Chia, T., Thorneycroft, D., Chapple, A., Dunstan, H., Hylton, C., Zeeman, S.C. and Smith, A.M. (2004) Diurnal changes in the transcriptome encoding enzymes of starch metabolism provide evidence for both transcriptional and posttranscriptional regulation of starch metabolism in Arabidopsis leaves. *Plant Physiology*, **136**, 2687-2699.

Smyth, D.R. (1995) Flower Development: Origin of the cauliflower. *Current Biology*, **5**, 361-363.

Sparkes, I.A., Brandizzi, F., Slocombe, S.P., El-Shami, M., Hawes, C. and Baker, A. (2003) An Arabidopsis *pex10* null mutant is embryo lethal, implicating peroxisomes in an essential role during plant embryogenesis. *Plant Physiology*, **133**, 1809-1819.

Sprenger-Haussels, M. and Weisshaar, B. (2000) Transactivation properties of parsley proline-rich bZIP transcription factors. *The Plant Journal*, **22**, 1-8.

Staiger, D., Kaulen, H. and Schell, J. (1989) A CACGTG motif of the *Antirrhinum majus* chalcone synthase promoter is recognized by an evolutionarily conserved nuclear protein. *Proceedings of the National Academy of Sciences*, **86**, 6930-6934.

Stasinopoulos, T.C. and Hangarter, R.P. (1990) Preventing photochemistry in culture media by long-pass light filters alters growth of cultured tissues. *Plant Physiology*, **93**, 1365-1369.

Staswick, P.E., Serban, B., Rowe, M., Tiryaki, I., Maldonado, M.T., Maldonado, M.C. and Suza, W. (2005) Characterization of an Arabidopsis enzyme family that conjugates amino acids to indole-3-acetic acid. *The Plant Cell*, **17**, 616-627.

Staswick, P.E., Tiryaki, I. and Rowe, M.L. (2002) Jasmonate response locus *JAR1* and several related Arabidopsis genes encode enzymes of the firefly luciferase superfamily that show activity on jasmonic, salicylic, and indole-3-acetic acids in an assay for adenylation. *The Plant Cell*, **14**, 1405-1415.

Staswick, P.E., Yuen, G.Y. and Lehman, Casey C. (1998) Jasmonate signaling mutants of Arabidopsis are susceptible to the soil fungus *Pythium irregulare*. *The Plant Journal*, **15**, 747-754.

Stintzi, A. and Browse, J. (2000) The Arabidopsis male-sterile mutant, *opr3*, lacks the 12-oxophytodienoic acid reductase required for jasmonate synthesis. *Proceedings of the National Academy of Sciences*, **97**, 10625-10630.

Stracke, R., Favory, J.-J., Gruber, H., Bartelniewoehner, L., Bartels, S., Binkert, M., Funk, M., Weisshaar, B. and Ulm, R. (2010) The Arabidopsis bZIP transcription factor HY5 regulates expression of the *PFG1/MYB12* gene in response to light and ultraviolet-B radiation. *Plant, Cell & Environment*.

Stracke, R., Ishihara, H., Huep, G., Barsch, A., Mehrtens, F., Niehaus, K. and Weisshaar, B. (2007) Differential regulation of closely related R2R3-MYB transcription factors controls flavonol accumulation in different parts of the *Arabidopsis thaliana* seedling. *The Plant Journal*, **50**, 660-677.

Strader, L.C. and Bartel, B. (2011) Transport and metabolism of the endogenous auxin precursor indole-3-butyric acid. *Molecular Plant*, **4**, 477-486.

Strader, L.C., Culler, A.H., Cohen, J.D. and Bartel, B. (2010) Conversion of endogenous indole-3-butyric acid to indole-3-acetic acid drives cell expansion in Arabidopsis seedlings. *Plant Physiology*, **153**, 1577-1586.

Strader, L.C., Wheeler, D.L., Christensen, S.E., Berens, J.C., Cohen, J.D., Rampey, R.A. and Bartel, B. (2011) Multiple facets of Arabidopsis seedling development require indole-3-butyric acid-derived auxin. *The Plant Cell*, **23**, 984-999.

Stuurman, J., Hoballah, M.E., Broger, L., Moore, J., Basten, C. and Kuhlemeier, C. (2004) Dissection of floral pollination syndromes in Petunia. *Genetics*, **168**, 1585-1599.

Subramani, S. (1998) Components involved in peroxisome import, biogenesis, proliferation, turnover, and movement. *Physiological Reviews*, **78**, 171-188.

Sundaramoorthy, R., Micossi, E., Alphey, M.S., Germain, V., Bryce, J.H., Smith, S.M., Leonard, G.A. and Hunter, W.N. (2006) The crystal structure of a plant 3-ketoacyl-CoA thiolase reveals the potential for redox control of peroxisomal fatty acid β-oxidation. *Journal of Molecular Biology*, **359**, 347-357.

Sundaresan, V., Springer, P., Volpe, T., Haward, S., Jones, J.D., Dean, C., Ma, H. and Martienssen, R. (1995) Patterns of gene action in plant development revealed by enhancer trap and gene trap transposable elements. *Genes & Development*, **9**, 1797-1810.

Swinkels, B.W., Gould, S.J., Bodnar, A.G., Rachubinski, R.A. and Subramani, S. (1991) A novel, cleavable peroxisomal targeting signal at the amino-terminus of the rat 3-ketoacyl-CoA thiolase. *The EMBO Journal*, **10**, 3255-3262.

Tanaka, R., Hirashima, M., Satoh, S. and Tanaka, A. (2003) The *Arabidopsis-accelerated cell death* gene *ACD1* is involved in oxygenation of pheophorbide *a*: inhibition of the pheophorbide a oxygenase activity does not lead to the "stay-green" phenotype in Arabidopsis. *Plant and Cell Physiology*, **44**, 1266-1274.

Taylor, N.L., Heazlewood, J.L., Day, D.A. and Millar, A.H. (2004) Lipoic acid-dependent oxidative catabolism of α-keto acids in mitochondria provides evidence for branched-chain amino acid catabolism in Arabidopsis. *Plant Physiology*, **134**, 838-848.

Terzaghi, W.B. and Cashmore, A.R. (1995) Light-regulated transcription. *Annual Review of Plant Physiology and Plant Molecular Biology*, **46**, 445-474.

Theodoulou, F.L., Job, K., Slocombe, S.P., Footitt, S., Holdsworth, M., Baker, A., Larson, T. and Graham, I. (2005) Jasmonic acid levels are reduced in COMATOSE ATP-binding cassette transporter mutants. Implications for transport of jasmonate precursors into peroxisomes. *Plant Physiology*, **137**, 835-840.

Thirkettle-Watts, D., McCabe, T.C., Clifton, R., Moore, C., Finnegan, P.M., Day, D.A. and Whelan, J. (2003) Analysis of the alternative oxidase promoters from soybean. *Plant Physiology*, **133**, 1158-1169.

Tian, G.-W., Mohanty, A., Chary, S.N., Li, S., Paap, B., Drakakaki, G., Kopec, C.D., Li, J., Ehrhardt, D., Jackson, D., Rhee, S.Y., Raikhel, N.V. and Citovsky, V. (2004) High-throughput fluorescent tagging of full-length Arabidopsis gene products *in planta*. *Plant Physiology*, **135**, 25-38.

Tilton, G., Shockey, J. and Browse, J. (2000) Two families of acyl-CoA thioesterases in Arabidopsis. *Biochemical Society Transactions*, **28**, 946-947.

Tomaz, T., Bagard, M., Pracharoenwattana, I., Lindén, P., Lee, C.P., Carroll, A.J., Ströher, E., Smith, S.M., Gardeström, P. and Millar, A.H. (2010) Mitochondrial malate dehydrogenase lowers leaf respiration and alters photorespiration and plant growth in Arabidopsis. *Plant Physiology*, **154**, 1143-1157.

Trelease, R.N. and Doman, D.C. (1984) Mobilization of oil and wax reserves. In *Seed Physiology* (Murray, D.R. ed. New York: Academic Press, pp. 201-245.

Turner, J.E., Greville, K., Murphy, E.C. and Hooks, M.A. (2005) Characterization of Arabidopsis fluoroacetate-resistant mutants reveals the principal mechanism of acetate activation for entry into the glyoxylate cycle. *Journal of Biological Chemistry*, **280**, 2780-2787.

Ulm, R., Baumann, A., Oravecz, A., Máté, Z., Ádám, É., Oakeley, E.J., Schäfer, E. and Nagy, F. (2004) Genome-wide analysis of gene expression reveals function of the bZIP transcription factor HY5 in the UV-B response of Arabidopsis. *Proceedings of the National Academy of Sciences*, **101**, 1397-1402.

Ulmasov, T., Hagen, G. and Guilfoyle, T.J. (1997) ARF1, a transcription factor that binds to auxin response elements. *Science*, **276**, 1865-1868.

Urao, T., Yamaguchi-Shinozaki, K., Urao, S. and Shinozaki, K. (1993) An Arabidopsis myb homolog is induced by dehydration stress and its gene product binds to the conserved MYB recognition sequence. *The Plant Cell*, **5**, 1529-1539.

van Roermund, C.W., Hettema, E.H., Kal, A.J., van den Berg, M., Tabak, H.F. and Wanders, R.J. (1998) Peroxisomal β-oxidation of polyunsaturated fatty acids in *Saccharomyces cerevisiae*: isocitrate dehydrogenase provides NADPH for reduction of double bonds at even positions. *The EMBO Journal*, **17**, 677-687.

van Rooijen, G.J.H. and Moloney, M.M. (1995) Structural requirements of oleosin domains for subcellular targeting to the oil body. *Plant Physiology*, **109**, 1353-1361.

Vernotte, C., Solis, C., Moya, I., Maison, B., Briantais, J.-M., Arrio, B. and Johannin, G. (1983) Multiple effects of linolenic acid addition to pea thylakoids. *Biochimica et Biophysica Acta (BBA) - Bioenergetics*, **725**, 376-383.

Volokita, M. (1991) The carboxy-terminal end of glycolate oxidase directs a foreign protein into tobacco leaf peroxisomes. *The Plant Journal*, **1**, 361-366.

von Arnim, A.G. and Deng, X.-W. (1994) Light inactivation of arabidopsis photomorphogenic repressor COP1 involves a cell-specific regulation of its nucleocytoplasmic partitioning. *Cell*, **79**, 1035-1045.

von Malek, B., van der Graaff, E., Schneitz, K. and Keller, B. (2002) The Arabidopsis male-sterile mutant *dde2-2* is defective in the *ALLENE OXIDE SYNTHASE* gene encoding one of the key enzymes of the jasmonic acid biosynthesis pathway. *Planta*, **216**, 187-192.

Wang, H.-Y., Baxter, C.F. and Schulz, H. (1991) Regulation of fatty acid β-oxidation in rat heart mitochondria. *Archives of Biochemistry and Biophysics*, **289**, 274-280.

Wang, M., van der Meulen, R.M., Visser, K., Van Schaik, H.-P., Van Duijn, B. and de Boer, A.H. (1998) Effects of dormancy-breaking chemicals on ABA levels in barley grain embryos. *Seed Science Research*, **8**, 129-137.

Wang, Z.Y., Kenigsbuch, D., Sun, L., Harel, E., Ong, M.S. and Tobin, E.M. (1997) A Myb-related transcription factor is involved in the phytochrome regulation of an Arabidopsis *Lhcb* gene. *The Plant Cell*, **9**, 491-507.

Wanner, L., Keller, F. and Matile, P. (1991) Metabolism of radiolabelled galactolipids in senescent barley leaves. *Plant Science*, **78**, 199-206.

Washida, H., Wu, C.-Y., Suzuki, A., Yamanouchi, U., Akihama, T., Harada, K. and Takaiwa, F. (1999) Identification of *cis*-regulatory elements required for endosperm expression of the rice storage protein glutelin gene *GluB-1*. *Plant Molecular Biology*, **40**, 1-12.

Watanabe, H., Abe, K., Emori, Y., Hosoyama, H. and Arai, S. (1991) Molecular cloning and gibberellin-induced expression of multiple cysteine proteinases of rice seeds (oryzains). *Journal of Biological Chemistry*, **266**, 16897-16902.

Weber, H. (2002) Fatty acid-derived signals in plants. *Trends in Plant Science*, **7**, 217-224.

Weigel, D. and Glazebrook, J. (2002) *Arabidopsis: A Laboratory Manual* Cold Spring Harbor, New York: Cold Spring Harbor Laboratory Press.

Weigel, D. and Mott, R. (2009) The 1001 Genomes Project for Arabidopsis thaliana. *Genome Biology*, **10**, 107.

Weisshaar, B., Armstrong, G.A., Block, A., da Costa e Silva, O. and Hahlbrock, K. (1991) Light-inducible and constitutively expressed DNA-binding proteins recognizing a plant

promoter element with functional relevance in light responsiveness. *The EMBO Journal*, **10**, 1777-1786.

Wildermuth, M. (2006) Variations on a theme: synthesis and modification of plant benzoic acids. *Current Opinion in Plant Biology*, **9**, 288-296.

Wildermuth, M.C., Dewdney, J., Wu, G. and Ausubel, F.M. (2001) Isochorismate synthase is required to synthesize salicylic acid for plant defence. *Nature*, **414**, 562-565.

Wilkinson, J.E., Twell, D. and Lindsey, K. (1997) Activities of CaMV 35S and *nos* promoters in pollen: implications for field release of transgenic plants. *Journal of Experimental Botany*, **48**, 265-275.

Winkel-Shirley, B. (1999) Evidence for enzyme complexes in the phenylpropanoid and flavonoid pathways. *Physiologia Plantarum*, **107**, 142-149.

Winkel-Shirley, B., Kubasek, W.L., Storz, G., Bruggemann, E., Koornneef, M., Ausubel, F.M. and Goodman, H.M. (1995) Analysis of Arabidopsis mutants deficient in flavonoid biosynthesis. *The Plant Journal*, **8**, 659-671.

Winter, D., Vinegar, B., Nahal, H., Ammar, R., Wilson, G.V. and Provart, N.J. (2007) An "electronic fluorescent pictograph" browser for exploring and analyzing large-scale biological data sets. *PLoS ONE*, **2**, e718.

Wisman, E., Hartmann, U., Sagasser, M., Baumann, E., Palme, K., Hahlbrock, K., Saedler, H. and Weisshaar, B. (1998) Knock-out mutants from an *En-1* mutagenized *Arabidopsis thaliana* population generate phenylpropanoid biosynthesis phenotypes. *Proceedings of the National Academy of Sciences*, **95**, 12432-12437.

Wiszniewski, A., Zhou, W., Smith, S. and Bussell, J. (2009) Identification of two Arabidopsis genes encoding a peroxisomal oxidoreductase-like protein and an acyl-CoA synthetase-like protein that are required for responses to pro-auxins. *Plant Molecular Biology*, **69**, 503-515.

Woodward, A.W. and Bartel, B. (2005) Auxin: regulation, action, and interaction. *Annals of Botany*, **95**, 707-735.

Yamaguchi-Shinozaki, K. and Shinozaki, K. (2005) Organization of *cis*-acting regulatory elements in osmotic- and cold-stress-responsive promoters. *Trends in Plant Science*, **10**, 88-94.

Yamauchi, D. (2001) A TGACGT motif in the′5 -upstream region of α-amylase gene from *Vigna mungo* is a *cis*-element for expression in cotyledons of germinated seeds. *Plant and Cell Physiology*, **42**, 635-641.

Yang, Z. and Ohlrogge, J.B. (2009) Turnover of fatty acids during natural senescence of Arabidopsis, *Brachypodium*, and switchgrass and in Arabidopsis β-oxidation mutants. *Plant Physiology*, **150**, 1981-1989.

Zemojtel, T., Fröhlich, A., Palmieri, M.C., Kolanczyk, M., Mikula, I., Wyrwicz, L.S., Wanker, E.E., Mundlos, S., Vingron, M., Martasek, P. and Durner, J. (2006) Plant nitric oxide synthase: a never-ending story? *Trends in Plant Science*, **11**, 524-525.

Zhao, J., Zhang, W., Zhao, Y., Gong, X., Guo, L., Zhu, G., Wang, X., Gong, Z., Schumaker, K.S. and Guo, Y. (2007) SAD2, an importin β-like protein, is required for UV-B response in Arabidopsis by mediating MYB4 nuclear trafficking. *The Plant Cell*, **19**, 3805-3818.

Zhu, J.-K. (2002) Salt and drought stress signal transduction in plants. *Annual Review of Plant Biology*, **53**, 247-273.

Zimmermann, P., Hirsch-Hoffmann, M., Hennig, L. and Gruissem, W. (2004) GENEVESTIGATOR. Arabidopsis microarray database and analysis toolbox. *Plant Physiology*, **136**, 2621-2632.

Zolman, B.K. and Bartel, B. (2004) An Arabidopsis indole-3-butyric acid-response mutant defective in PEROXIN6, an apparent ATPase implicated in peroxisomal function. *Proceedings of the National Academy of Sciences*, **101**, 1786-1791.

Zolman, B.K., Martinez, N., Millius, A., Adham, A.R. and Bartel, B. (2008) Identification and characterization of Arabidopsis indole-3-butyric acid response mutants defective in novel peroxisomal enzymes. *Genetics*, **180**, 237-251.

Zolman, B.K., Monroe-Augustus, M., Thompson, B., Hawes, J.W., Krukenberg, K.A., Matsuda, S.P.T. and Bartel, B. (2001a) *chy1*, an Arabidopsis mutant with impaired β-

oxidation, is defective in a peroxisomal β-hydroxyisobutyryl-CoA hydrolase. *Journal of Biological Chemistry*, **276**, 31037-31046.

Zolman, B.K., Nyberg, M. and Bartel, B. (2007) IBR3, a novel peroxisomal acyl-CoA dehydrogenase-like protein required for indole-3-butyric acid response. *Plant Molecular Biology*, **64**, 59-72.

Zolman, B.K., Silva, I.D. and Bartel, B. (2001b) The Arabidopsis *pxa1* mutant is defective in an ATP-binding cassette transporter-like protein required for peroxisomal fatty acid β-oxidation. *Plant Physiology*, **127**, 1266-1278.

Zolman, B.K., Yoder, A. and Bartel, B. (2000) Genetic analysis of indole-3-butyric acid responses in *Arabidopsis thaliana* reveals four mutant classes. *Genetics*, **156**, 1323-1337.

Appendices

Appendix I

Gene/Vector	Target	Forward	Reverse
Acyl-activating enzymes			
AAE1 (At1g20560)	SALK_041152 (*aae1-1*)	AGCTAATAAGCTCCTCCGCAC	AATAAAGGTGACAAGGTCCCG
	RT-PCR	same as above	same as above
AAE5 (At5g16370)	SALK_009731 (*aae5-1*)	TTAGGCAGCTCATCCACAAAG	AACAACATCAACACTCGCCTC
	RT-PCR	same as above	same as above
AAE7/ACN1 (At3g16910)	SALK_123943	GACTCTCCCATTGTCACCATG	AGAGCGATTACGAGAAGCATG
	SALK_133808	same as above	same as above
AAE12 (At1g65890)	GABI_751B10 (*aae12-1*)	AAAATGAATGAATGAATGGTTTTAAAC	GAATAAAATCTTGGGCTTGGC
	RT-PCR	ACAAAACAGAACCGGACCAG	TTGGCCTCAGACCTATGACC
AAE17 (At5g23050)	SALK_025667 (*aae17-1*)	AAGTCCCAAAATCGATTCCAC	TTTAAGTCTGTGCCTTGCCTG
	SAIL_83_E04	GCTCTACTGATCCATACAATCTAAATTG	CCTCCAGGATTATCTCCAGAAG
	FLAG_290G07	TCCAATACAGTTTTCCAATACACC	TTTTCTTTCACTTTCATTATGATTCC
	RT-PCR	AGCCTCTAGCTGGGACAACA	CGGAGACGTGGATTCAGATT
AAE18 (At1g55320)	SALK_002180 (*aae18-1*)	GAAGAGCATAGGCGAATTGAG	GTCTGCGATGGAGACAACAA
	SALK_019869 (*aae18-2*)	same as above	same as above
	SAIL_445_F06 (*aae18-3*)	same as above	same as above
	RT-PCR	AAAGAGATGTGGAAGAGCATAGG	CAAGGCTTTATATTCGACTTCGT
Putative AAE/BZO1 (At1g65880)	SALK_094196 (*bzo1-4*)	CTAAAAGGGCTTCATTCGAGG	ATCTTTCCATTCCCGTTTTTG
	GABI_565B09 (*bzo1-5*)	GGGAGTCGAAACAAAAGGTTG	GGGTTAAGTACAGCTCCAGCC
	RT-PCR	CTAAAAGGGCTTCATTCGAGG	ATCTTTCCATTCCCGTTTTTG
Hydratases			
ECHIa/E-COAH-2 (At4g16210)	SALK_004620 (*echia-1*)	TCCTGAAAAGCTCTGAAGATCC	TTTTGTGTTTGAAGGTTTGGG
	SALK_024138 (*echia-2*)	GGTCGATCTTTCTGCTCTGG	GATCCACGTCCGGCTATAAA
	RT-PCR	same as above	same as above
ECHIb/PECI2 (At4g14430)	FLAG_412H03	CACCATTCTCTCCCTTCTCG	CCAAGAATCCCACAAAGCTC
	RT-PCR	same as above	same as above

Gene/Vector	Target	Forward	Reverse
Hydratases (continued)			
ECHIc/PECI1 (At1g65520)	SALK_036386 (*echic-1*)	CAGTGCTACGCACCACACTT	AACACCGTCTAAACCCAACC
	SAIL_520_D11	CCTGGACAGGTCTGTGTAACC	AATCCCCATCTTAACACCCAC
	SAIL_100_C05	CCTCTGCACTGCTAGATAGGG	TCATCGCTAAAATACATCCCG
	RT-PCR	AATCCCCATCTTAACACCCAC	AACACCGTCTAAACCCAACC
ECHId/DHNS (At1g60550)	SAIL_1303_605	ACGTCATTGGGATCAGCATAC	GGTTGTTGCGTAGCTTCAGAG
	RT-PCR	GGCGGTGCATATAAGCAGTT	ATGCTGTTGGAGGAGGACAC
MFP2 (At3g06860)	SALK_098016 (*mfp2-2*)	CCTCCTCAAAAGGATTTCTCG	CAAAGTACCGTTGCTTTGAGG
	RT-PCR	TGACTCGCAAAATCTCAACG	GTTCCACTGAAACGCTGACC
Oxidoreductases			
SDRa (At4g05530)	SALK_010364 (*sdra-1*)	AAGAAGCAAAGTGTGTGGGCA	AAGATTGGAAGGCAAAGTCGC
	CSHL_ET10416 (*sdra-2*)	same as above	same as above
	SALK_042943	TTTTATGTGGCAAGATCAATGC	TTGTTGTTGATTTGTTGTGTGC
	SALK_042934	same as above	same as above
	RT-PCR	AAGAAGCAAAGTGTGTGGGCA	AAGATTGGAAGGCAAAGTCGC
SDRb/DECR (At3g12800)	SALK_122758 (*decr-1*)	CTACCACCATTGTTAGTCCGC	TCAGCGATTTTTGTTTTGAGG
	SALK_013922	CACCGCTTGATGAGTCTCTTC	CAAATTCGGATTTAGATAAAACTTACG
	RT-PCR	GCTGCTGAGGATTTGTCTCC	GAGAGTTGCTTCACCGCTTC
NQR (At1g49670)	SALK_116822 (*nqr-1*)	ATTGGGGGTTTTGAGTGGTAC	GTGTGGTCCAATGGGTAATTG
	SALK_123841 (*nqr-2*)	CCTCAAAGCTTCGAGAAAATG	ATTTCATTTGTCCTGCCTGTG
	SALK_014601	GGTACAGTAAACGCGGATTTG	TCCTTTCTCCTCCGAAAAATC
	RT-PCR	CTGGTTTATCCGCTCTCGTC	TAATCCCGAGGTAAGCATGG

Gene/Vector	Target	Forward	Reverse
Thiolases			
KAT1 (At1g04710)	FLAG_589G05 (*kat1-1*)	ATGTCACCAACTTCACTTGGG	CAGCAGGGAAAAGAAGAAAGC
	SALK_013834	AAATTGCAACGTTCTCCATTG	ACTGTCTTTGGACAAGCAAGC
	RT-PCR	CTCTCTGCCTCAGCTTGCTT	ACTTTCCGGAAGCAGTAGCA
	qPCR	ATGGGATTCGACCTAACACAAC	ATAAGGAGAACAGCTCCAGCAC
	Promoter	*TGCAACGTTCTCCATTGTTG	**TGTTTTCGTTTGATTATTTTGAAGC
KAT2 (At2g33150)	T-DNA (*kat2-1*)	GAGTCCATGACTACCAATCCAATGCC	CCCAAGAGAAGCAAGAGTTGTGGTTG
	EMS (S140F; *kat2-2*)	CTGTACATAGAAGAAACATACCAGGGA	CAGCAACAGCCTGAAGCCCA
	GT18614 (*kat2-4*)	AAGCCCAGATGAGCACTGTC	CTTCTTCGCACAATTACGAGG
	FLAG_307C02 (*kat2-5*)	same as above	same as above
	RT-PCR	GAGTCCATGACTACCAATCCAATGCC	CCCAAGAGAAGCAAGAGTTGTGGTTG
	qPCR	GCCGTTTTGGAGTAGTGTCAA	TCAACTTTCCTTGCGTTGC
	Promoter	*TTTTGCATATCCGCTTGAATC	**TTTTTCCGGCTGATTAAAGATAAA
KAT5 (At5g48880)	CSHL_ET5406 (*kat5-1*)	CCCGGAAAGTTTTTGTCTTTC	ACATTGATTCCACTCCAGCAC
	FLAG_065D06 (*kat5-2*)	CATTGCTCTCTGAGAACCAGG	TCCGATATGAATTCTTGTGGG
	SAIL_567_F03 (*kat5-3*)	TGGTTCTTGAAGATGTCACCG	TAATGGGTATTGGTCCAGCTG
	SALK_144464	TGTGTTTTGTGTAGGCAATGC	TACTCAATGGCAACAACATCG
	RT-PCR	GACTATCCCCGTTAGCCACA	CAGTTGCTGATGTTGCTGCT
	KAT5.1 qPCR	TCGGTTATCTCAACATTTGCAT	CCGACGGATGAATGAGCTA
	KAT5.2 qPCR	TGAGGACCCTGAAGCTCATT	CTTTCCGGGGAAACTGAAAT
	KAT5.1 promoter	*TCTCAAATTCATCACAATGCAG	**TGGGGAAACTTCAGAAACACA
	KAT5.2 promoter	*CCCTTGCAACTTGTCTCCTC	**GATTCTCTCTGTTGCAAACACTTG
	KAT5.1 cDNA	*AATGGCTGCTTTTGGAGATG	**TTCAAGCTCTCTTCGATGTTCTAA
	KAT5.2 cDNA	*TTGCAACAGAGAGAATCATGG	same as above

Gene/Vector	Target	Forward	Reverse
Other genes			
IBR3 (At3g06810)	SALK_033467 (*ibr3-9*)	GCTTCTGTTCTTCTTCGGTCC	TGTATGTTCACCTAAAGCCCG
CHY1 (At5g65940)	SALK_025417C (*chy1-4*)	ACTTCACAGCTTTGCGATCC	GGCCTTGCAACTCATTTTGT
	RT-PCR	same as above	same as above
T-DNA			
FLAG	FLAG pGKB5 LB4	CGTGTGCCAGGTGCCCACGGAATAGT	
	FLAG pGKB5 RB4	TCACGGGTTGGGGTTTCTACAGGAC	
GABI	GABI 8409 LB	ATATTGACCATCATACTCATTGC	
	GABI 3144 RB	GTGGATTGATGTGATATCTCC	
SALK	SALK LBa1	TGGTTCACGTAGTGGGCCATCG	
	SALK LBb1	GCGTGGACCGCTTGCTGCAACT	
SAIL	SAIL pCSA110 LB3	TAGCATCTGAATTTCATAACCAATCTCGATACAC	
CSHL	CSHL DS5-2	CCGTTTTGTATATCCCGTTTCCGT	
	CSHL DS3-2	CGATTACCGTATTTATCCCGTTC	
Cloning			
Gateway	attB1 (*)	GGGGACAAGTTTGTACAAAAAAGCAGGCT	
	attB2 (**)	GGGGACCACTTTGTACAAGAAAGCTGGGT	
Vector primers	M13 forward (-20)	GTAAAACGACGGCCAGT	
	M13 rev	AACAGCTATGACCATG	
	T7 promoter	GTAATACGACTCACTATAG	

Gene/Vector	Target	Forward	Reverse
GFP localisation			
AAE18 (At1g55320)	P1	GCTCGATCCACCTAGGCTATGTGGAAGAGCATAGGCGA	
	P2	AGCTCCACCTCCACCTCCAGGCCGGCCCTTAATCTGATCTCTCAAGACTCTTCTCAG	
	P3	TGCTGGTGCTGCTGCGGCCGCTGGGGCCCAAGAACTACTATCCTTACGAAGTCGAATATAA	
	P4	CGTAGCGAGACCACAGGATTATATTCGACTTCGTAAGGATAGTAGTTCTTG	
SDRa (At4g05530)	P1	GCTCGATCCACCTAGGCTATGGAGAAGAAGCTACCGAGAAG	
	P2	AGCTCCACCTCCACCTCCAGGCCGGCCTCCAGTGATGTAAGAAGAATCATCTGATG	
	P3	TGCTGGTGCTGCTGCGGCCGCTGGGGCCGAAACTTTGGTTGTCGCTGGAGGAATGCCTTCA	
	P4	CGTAGCGAGACCACAGGATTAGAGTCTTGAAGGCATTCCTCCAGCGACAAC	

Appendix II

Strain or Plasmid	Description	Reference
***E. coli* strain**		
DH5α	F$^-$φ80 Δ*lacZ* Δ*M15* Δ(*lacZA-argF*)*U169 deoR recA1 endA1 hsdR17* (r_K^- m_K^-) *phoA supE44* λ$^-$*thi-1 gyrA96 relA1*	Sambrook *et al.*, 1989
Agrobacterium strain		
GV3101	C58C1 rifR	Koncz and Shell, 1986
Plasmid		
pCR2.1	TA-based cloning vector for PCR products with kanR and ampR in bacteria	Invitrogen
pDONR207	Gateway donor vector with gentR in bacteria	Invitrogen
pHGWFS7	GFP-GUS fusion promoter-reporter vector with specR in bacteria and hygR in Arabidopsis	Karimi *et al.*, 2002
pGREEN0049	Plant expression vector with kanR bacteria and Arabidopsis	Hellens *et al.*, 2000
pGREEN0179	Plant expression vector with kanR in bacteria and hygR in Arabidopsis	Hellens *et al.*, 2000
pGREEN0180	pGREEN0179 modified to include a CAMV 2x35S promoter and CAMV terminator with a Gateway A cassette inserted between them in the SmaI site of the MCS	Pracharoenwattana *et al.*, 2005

Appendix III

The genetic dissection of a short term response to low CO_2 demonstrates the potential for peroxide-mediated non-enzymatic decarboxylation of photorespiratory intermediates in the peroxisome

Submitted to Plant Physiology 22 Sep 2011

Running title: Non-Enzymatic decarboxylations during photorespiration

Prof. Steven M. Smith

ARC, Centre of Excellence in Plant Energy Biology, University of Western Australia, 35 Stirling Highway, Crawley, WA 6009, Australia

ssmith@cyllene.uwa.edu.au

Tel: 00-61-(0)8-6488-4403

Fax: 00-61-(0)8-6488-4401

Bioenergetics and Photosynthesis

The genetic dissection of a short term response to low CO_2 demonstrates the potential for peroxide-mediated non-enzymatic decarboxylation of photorespiratory intermediates in the peroxisome

Olivier Keech[1,4], Andrew A. G. Wiszniewski[1], Wenxu Zhou[1], Ricarda Fenske[2], Catherine Colas-des-Francs-Small[1], Lynne Whitehead[3], John D. Bussell[1], Murray R. Badger[3], Steven M. Smith[1*]

[1]Centres of Excellence for Plant Metabolomics and Plant Energy Biology, University of Western Australia, 35 Stirling Highway, Crawley, Western Australia 6009, Australia.

[2]Metabolomics Australia, University of Western Australia, 35 Stirling Highway, Crawley, Western Australia 6009, Australia.

[3]Centre of Excellence in Plant Energy Biology, Research School of Biology, Australian National University, Sullivans Creek Rd, Acton ACT 0200, Australia

[4]Current Address: UPSC, Department of Plant Physiology, Umeå University, S-90187, Umeå, Sweden

*corresponding author

This research was supported by Australian Research Council awards (grants FF0457721 and CE0561495) and the Government of Western Australia Centres of Excellence scheme.

Prof. Steven M. Smith

ARC, Centre of Excellence in Plant Energy Biology, University of Western Australia, 35 Stirling Highway, Crawley, WA 6009, Australia

ssmith@cyllene.uwa.edu.au

Tel: 00-61-(0)8-6488-4403

Fax: 00-61-(0)8-6488-4401

Abstract

Photorespiration is a complex process requiring tight regulation in the flux of metabolites between chloroplasts, peroxisomes and mitochondria. Although the main photorespiratory pathway has been extensively described, there is increasing evidence that our understanding is still incomplete. Here, we employ a series of mutants and treatments to specifically explore the multiple non-enzymatic routes for photorespiratory CO_2 release in Arabidopsis. We show that the photosynthetic CO_2 compensation point and subsequent post-illumination CO_2 burst are increased in a hydroxypyruvate reductase (*hpr1*) mutant, compared to WT. In contrast, a newly characterized glycolate oxidase (*gox1*) mutant has a higher post-illumination burst than the WT, but does not show an increased CO_2 compensation point. This provides evidence that increased CO_2 release leading to higher compensation point depends on peroxisomal metabolism of glycolate. Furthermore, we show that the CO_2 compensation point is increased in a catalase (*cat2*) mutant, consistent with the proposal that decarboxylation can occur by non-enzymatic reaction of intermediates with hydrogen peroxide. Simultaneously blocking hydrogen peroxide breakdown and hydroxypyruvate metabolism in a *hpr1cat2* double mutant showed an even higher CO_2 compensation point than in either single mutant. In contrast, a formate dehydrogenase (*fdh*) mutant was indistinguishable from wild type, discounting a role for mitochondrial FDH during photorespiration. Altogether, our results suggest that when the flux of photorespiratory intermediates through the peroxisome becomes saturating, there is potential for peroxide-mediated CO_2 release. Whether this could provide a beneficial ‘safety valve’ or a deleterious carbon loss under stressful environmental conditions is discussed.

Introduction

Photorespiration is initiated by the oxygenase activity of ribulose 1,5 bisphosphate carboxylase/oxygenase (RubisCO) and significantly influences carbon assimilation in most photosynthetic organisms. It has been estimated to result in a 25 to 50 % reduction in the rate of net CO_2 assimilation in typical C3 plants under ambient CO_2 concentrations (Sharkey, 1988; Roussel and Igamberdiev, 2011). However, photorespiratory fluxes are even higher under hot and dry conditions. The two main reasons for this are, firstly, that RubisCO's kinetic properties are modified with increasing temperature and subsequently favour the oxygenase activity relative to the carboxylase one, and secondly, plants exposed to limited water supply reduce stomatal gas exchange to minimize evaporation, leading to a concomitant decrease in intracellular CO_2 concentration, further favouring oxygenation relative to carboxylation at the RubisCO active site ((Peterhansel et al., 2010) and references therein).

As most crops are C3 plants, bio-engineering photorespiration is one approach to counterbalance the loss of production in a hotter climate and to address the increasing demand for food supply. In a recent study, Kebeish *et al.* (2007) elegantly demonstrated the potential of re-engineering photorespiration. They achieved increased biomass production in *Arabidopsis thaliana* by introducing 3 enzymes (Glycolate DeHydrogenase (GDH), Glyoxylate Carboxy-Ligase (GCL) and Tartronic Semialdehyde Reductase (TSR)) targeted to the chloroplast to create an alternative pathway from glycolate to glycerate, and consequently bypassing the normal photorespiratory pathway. With this alternative pathway, the photorespiratory decarboxylation occurs in the chloroplast where CO_2 can be elevated and re-fixed by RubisCO and there is also a benefit in reduced energy processing costs.

Photorespiration is a complex process requiring a tight regulation in the flux of metabolites between chloroplasts, peroxisomes, mitochondria and cytosol. Any modification of this coupling and flux control may lead to the accumulation of certain intermediates, which could in turn be subjected to enzyme-catalyzed or spontaneous alternative reactions. Several alternative pathways for spontaneous (i.e. non-enzymatic (NE)) decarboxylations during photorespiration are proposed in the literature (reviewed in Fig 1). For instance, in chloroplasts, glycolate resulting from dephosphorylation of the toxic 2-phosphoglycolate could be directly oxidized into glyoxylate via a salicylhydroxamic acid (SHAM)-sensitive glycolate-quinone oxidoreductase (Goyal and Tolbert, 1996). The resulting glyoxylate would further be decarboxylated by either a plastidial pyruvate decarboxylase (Davies and Corbett, 1969) or non-enzymatically by reacting with peroxide (Igamberdiev and Lea, 2002). Alternatively, glycolate could be exported and oxidized into glyoxylate in the mitochondria, where the presence of a GDH (encoded by At5g36580) has been reported by Niessen *et al.* (2007) although its function

as a GDH has recently been challenged by Enqvist *et al.* (2009). Glyoxylate produced in the mitochondrion could either be further oxidatively decarboxylated by reacting with hydrogen peroxide or trans-aminated to glycine (Niessen et al., 2007; Clark et al., 2009). Formate resulting from glyoxylate decarboxylations in chloroplasts or mitochondria could be oxidized by a formate dehydrogenase (FDH) (Colas des Francs-Small et al., 1993; Herman et al., 2002), react with hydrogen peroxide to give H_2O and CO_2 (Halliwell, 1974) or be exported to peroxisomes (Igamberdiev et al., 1999) (Fig 1).

Results obtained with isolated peroxisomes from beet (*Beta vulgaris* L.) (Halliwell and Butt, 1974; Walton and Butt, 1981) and from spinach (*Spinacea oleracea* L.) (Grodzinski, 1978) demonstrated that non-enzymatic decarboxylations could also occur in peroxisomes by peroxidation of either glyoxylate or hydroxypyruvate (Halliwell and Butt, 1974; Grodzinski, 1978; Walton and Butt, 1981). However, as most of these results were obtained from isolated organelles where metabolite exchanges are disturbed, the *in vivo* occurrence and magnitude under various environmental conditions is still uncertain. Furthermore, Wingler *et al.* (1999) reported an accumulation of glyoxylate and formate in glycine decarboxylase (GDC) mutants from barley (*Hordeum vulgare* L.) and *Amaranthus edulis* Speg. The authors proposed an alternative pathway that could partially restore serine production in these mutants. In this alternative pathway, glyoxylate would be non-enzymatically decarboxylated to formate and formate would subsequently be converted sequentially to formyl-THF (TetraHydro-Folate), methenyl-THF and methylene-THF. Finally, the methylene-THF would provide the missing carbon for the production of serine from glycine via the serine hydroxyl-methyl transferase (SHMT). This bypass seems to partially compensate for the lack of GDC activity; however its occurrence in wild type plants is still unknown. Additionally, Cousins *et al.* (2008) noticed that peroxisomal malate dehydrogenase null mutant plants (*pmdh1pmdh2*) had a higher O_2-dependent CO_2 compensation point when compared to the wild type. This implied that, in the *pmdh* plants, either RubisCO specificity had changed or that the rate of CO_2 released per oxygenation was increased. The authors proposed non-enzymatic decarboxylations in the peroxisome to be responsible for this higher compensation point and altered stoichiometry.

In addition to the H_2O_2-linked non-enzymatic decarboxylations discussed above, there is a further untested possibility involving the decarboxylation of hydroxypyruvate in the chloroplast via the actions of transketolase (Fig 1). The fact that glyceraldehyde-3P and hydroxypyruvate can be acted upon irreversibly by a transketolase to produce xylulose-5P is well established although not tested in plants (Kobori et al., 1992; Fiedler et al., 2001). Given that Timm *et al.* (2011) have proposed that hydroxypyuvate can be reduced in the chloroplast via a recently reported hydroxypyruvate reductase (HPR3), such tranketolase-mediated reaction could occur

under certain conditions but might compete with the potential chloroplastic hydroxypyruvate reductase.

In this landscape of possibilities for non-enzymatic decarboxylations, we decided to use the power and utility of Arabidopsis genetics to investigate the probability and the location of these reactions. To do so, we used a panel of photorespiratory mutants to constrain the metabolic flux at strategic steps and we quantified by GC-MS the variations in photorespiratory metabolites when wild type and the different mutants were subjected to a short term exposure to high photorespiratory conditions (i.e. low CO_2). Physiological parameters such as CO_2 compensation point, post illumination burst and maximum rate of CO_2 release were further measured to assess the occurrence of non-enzymatic decarboxylations. Altogether, our results show that alternative decarboxylations occur principally in peroxisomes rather than in chloroplasts or mitochondria. This potential loss of carbon *in vivo* is further discussed with regards to stressful conditions of high temperature and water shortage.

Results

Growth of mutants used in this study

In order to apply constraints at different steps in the photorespiratory pathway, we used the following panel of mutants: *glycolate oxidase1* (*gox1-1* and *gox1-2*; described in the present study), *hydroxypyruvate reductase1* (*hpr1*; (Timm et al., 2008; Pracharoenwattana et al., 2010; Cousins et al., 2011)), *catalase 2* (*cat2-2*; (Queval et al., 2007)), *formate dehydrogenase* (*fdh*, described in present study: Supp Fig 1). We also made double homozygous *hpr1 fdh* and *hpr1 cat2-2* mutants. All these mutants were able to grow in ambient air i.e. 380 ppm CO_2, but the growth of *hpr1*, *cat2-2*, *hpr1 cat2-2* and *hpr1 fdh* plants was slower than the growth of wild type (WT), *fdh* and *gox1-2* plants (Fig 2a, 2b). However, 7 weeks after germination, the slow growth phenotype was less apparent in plants grown in a 12 h light photoperiod than in plants grown in an 8 h light photoperiod (Fig 2a, 2b).

Characterization of gox1 mutants

Glycolate oxidation could potentially lead to non-enzymatic decarboxylations in both the chloroplast and the mitochondrion (Fig 1). In order to assess these possibilities, we hypothesized that any restriction in the photorespiratory flux between glycolate and glyoxylate in the peroxisome would lead to an accumulation of glycolate and could subsequently favour alternative pathways for glycolate conversion in either chloroplast or mitochondrion.

In Arabidopsis, glycolate oxidases are encoded by three independent genes. Only two, *GOX1* (At3g14420) and *GOX2* (At3g14415), are expressed in leaves and are co-expressed with

other photorespiratory genes (eFP Browser (www.arabidopsis.org); (Foyer et al., 2009)). The third gene, *GOX3*: At4g18360, is preferentially expressed in roots and during leaf senescence, which suggests a different metabolic function for this isoform (eFP Browser, www.arabidopsis.org; (Winter et al., 2007)). Located in tandem on the third chromosome, *GOX1* and *GOX2* are only separated by 890bp from stop codon to start codon, which includes about 500bp of untranscribed intergenic region. The two genes share a 92.4% nucleotide identity and the corresponding proteins have 95.1% identity and 97.3% similarity. For this study, we isolated two independent *gox1* knockout mutants, both disrupted by a T-DNA insertion (Fig 3a,b,c).

The two mutants, named *gox1-1* and *gox1-2*, grew normally in ambient air (380 ppm CO_2) and did not exhibit a different visible phenotype when compared to their respective Col-0 WT plants (Fig 3a). Using qRT-PCR, we also checked the abundance of endogenous transcripts under ambient air (380 ppm CO_2) and after short term exposure to low CO_2 (1 h at 100ppm). In WT leaves, under both conditions, the expression of *GOX1* was about 3-fold higher than the expression of *GOX2* and these expression levels did not change under low CO_2 (Fig 3d). Surprisingly, the absence of *GOX1* in *gox1-1* and *gox1-2* mutants did not affect the expression of *GOX2*, even after short term exposure to low CO_2. However, when we quantified by GC-MS the relative amount of glycolate in these plants, we noticed a drastic accumulation of glycolate in the two *gox1* mutants under short term exposure to low CO_2. The pool of glycolate was approximately 30-fold higher than in ambient air (Fig 3e) whereas no such accumulation was seen in the WT. However, despite the accumulation of glycolate, the remaining activity of glycolate oxidase in the *gox-1* mutants due to the presence of GOX2 protein activity was apparently sufficient to sustain the processing of glycolate at near normal rates in the peroxisome albeit at much higher steady-state levels of glycolate substrate under high photorespiratory conditions.

Photorespiratory intermediates under short term exposure to low CO_2

To assess the impact of a short term exposure to low CO_2 on photorespiration, we determined by GC-MS the relative amount of photorespiratory intermediates in plants grown in ambient air and in plants subjected to 100 ppm CO_2 for approximately 1 h (Fig 4). As already mentioned above, *gox1-2* showed a substantial accumulation of glycolate under low CO_2 that was much larger than the other genotypes. However, the rest of the metabolic profile for *gox 1-2* was very similar to the profile for WT. Further, the low CO_2 treatment led to an increase of glyoxylate and glycine in all genotypes when compared to ambient air. Interestingly, we noticed a slight but recurrent accumulation of oxalate in almost all genotypes when plants were subjected to low CO_2, indicating a potential photorespiration-dependent production of oxalate as

suggested in Figure 1. Serine levels appeared more consistent between ambient air and low CO_2 than the other metabolites measured, however, its relative amount was significantly higher in *hpr1* and *hpr1 cat2-2* than in any of the other genotypes tested (Fig 4). The accumulation of serine is likely to be a direct effect of the downstream constriction of the flux through HPR. Altogether, these results confirmed that a short term exposure to low CO_2 triggers an increased flux into photorespiratory intermediates and represents a consistent treatment to establish high photorespiratory conditions.

Compensation point, Post-Illumination Burst and Maximum rate of CO_2 release

In the normal operation of the photorespiratory pathway, it is expected that one CO_2 will be released by glycine decarboxylase for every two glycolate molecules processed. If non-enzymatic decarboxylations occur during photorespiration, they should contribute to an increased stoichiometry of CO_2 release per glycolate produced by RubisCO oxygenation (Cousins et al., 2008; Cousins et al., 2011). As a simple and rather direct estimation of this CO_2 release stoichiometry, we measured 3 physiological parameters: the CO_2 compensation point (Γ), the post-illumination CO_2 burst (PIB) and the corresponding maximum rate of CO_2 release. Four mutant lines had a significantly higher Γ than WT (Fig 5a). The Γ was determined at ambient O_2 concentration (21%) from leaf discs positioned in a closed chamber directly coupled to a membrane inlet mass spectrometer. The average value of Γ for WT was around 50 ppm and a similar value was recorded for *fdh*, *gox1-1* and *gox1-2*. Interestingly, *cat2-2* had a significantly higher Γ of 60 ppm. *hpr1* and *hpr1 fdh* had a Γ value of about 72 ppm, significantly higher than both WT and *cat2-2*. Finally, the Γ of almost 110 ppm that was recorded for the double mutant *hpr1 cat2-2* was the greatest and was significantly different from the Γ measured for all the other genotypes (Fig 5a). This very high value of Γ in *hpr1 cat2-2* demonstrates a synergistic effect of the two mutations on the engagement of extra CO_2 release processes.

Concomitantly, the CO_2 released during the PIB was estimated as the area of PIB peak identified from the change in CO_2 with time following the darkening of the leaf disc (Fig 5b, 5c). With the exception of *fdh*, all genotypes had a significantly higher PIB peak area than the WT, most likely reflecting an accumulation of metabolites in the light that were subsequently decarboxylated in the dark period (Fig 5c). However, the width of the peaks together with the maximum rate of CO_2 release (i.e. peak height) differed significantly between genotypes (Fig 5b, 5d). These differences could reflect the different origins of the metabolites accumulated as well as giving information on the speed of decarboxylation reactions. For instance, the decarboxylations occurring in *cat2-2* and *gox1-2* were very fast with a high peak value, suggesting that they were enzymatically catalyzed. However, the decarboxylations of *hpr1* and *hpr1 cat2-2* (Fig 5a, 5b) appeared slower with a lower peak value and could reflect the

occurrence of a pathway producing glycolate and CO_2 by non-enzymatic reactions instead of reduction of hydroxypyruvate (cf Fig 1).

Discussion

GOX1 is required for short term acclimation to high photorespiratory conditions

We investigated possibilities for pathways alternative to glycine decarboxylase leading to decarboxylations of photorespiratory intermediates. To do so, we used several photorespiratory mutants to constrain the photorespiratory flux and we estimated the potential additional decarboxylations occurring during photorespiration. As reviewed in Figure 1, glycolate would be a node in the photorespiratory metabolism and could lead to alternative decarboxylations primarily originating from the generation of glyoxylate in various cell compartments.

Two recent studies have reported the effect of down-regulation of glycolate oxidase. In the first study, on maize (*Zea mays*), Zelitch *et al.* (2009) showed that GOX1 was essential for survival of the plant in ambient air. The authors proposed glycolate cytotoxicity to be responsible for necrotic lesions and the death of developing seedlings. However, this notion of toxicity remains challenged by older reports where 2P-glycolate and glyoxylate were considered to be the main cytotoxic compounds instead of glycolate (reviewed in Peterhansel *et al.* (2010)). In parallel, Xu *et al.* (2009) reported that an estradiol-inducible *GOX* antisense line in rice had reduced biomass when grown under ambient air. They proposed that GOX exerted negative regulation over photosynthesis notably by repressing RubisCO and RubisCO activases. In the present study, the suppression of *GOX1* in *Arabidopsis thaliana* did not influence the normal growth of the plants. Grown in ambient air, *gox1* and WT were indistinguishable phenotypically from one another and nor did their metabolic profiles differ. However, under short term exposure to low CO_2, WT metabolite profile was similar to that in ambient air, but *gox1* accumulated a high amount of glycolate (Fig 3d, 4). We assume that such a significant increase of glycolic acid in *gox1* mutants under high photorespiratory conditions would result in an accumulation of glycolate in most cell compartments including chloroplasts, peroxisomes and also the cytosol. This accumulation correlated with a significantly higher PIB than in WT but without an increase of the CO_2 compensation point. Presumably, this indicates that the increased accumulation of glycolate in the light contributed to an increase maximum PIB peak height and area, without engaging extra decarboxylation reactions additional to glycine decarboxylase. Altogether, our data support the view that glycolate oxidase activity is more rate-limiting in the *gox1* mutants than in the WT and that glycolate levels are increased as a result. However, increased glycolate does not lead to alternative reactions responsible of additional releases of CO_2. This does not support previous speculations (summarized in Fig 1) on the engagement of alternative non-peroxisomal pathways originating from glycolate metabolism in the chloroplast

and mitochondria that could lead to glyoxylate production and subsequent decarboxylations in those compartments.

Although *GOX1* and *GOX2* are located in tandem on the third chromosome, the transcript level of *GOX1* in ambient air was 3-fold higher than *GOX2*. In addition, after short term exposure to high photorespiratory conditions, we did not observe an induction of *GOX2* despite the large accumulation of glycolate recorded in the *gox1* mutants. In contrast, WT plants barely showed any increase in glycolate, which suggests a prominent role for *GOX1* in maintaining high flux rates of glycolate metabolism occurring under transiently high photorespiratory conditions. This differential expression between the two genes raises some questions about their regulation as well as their potential stress-responsive DNA elements. A survey with Athena (http://www.bioinformatics2.wsu.edu/cgi-bin/Athena/cgi/home.pl, (O'Connor et al., 2005)) revealed a different enrichment in transcription factor motifs between the two assumed gene promoters (results not shown). However, further investigations are needed to assess whether the two *GOX* genes are under control of the same, or two distinct, promoters.

Non-enzymatic decarboxylations occur in vivo in peroxisomes and formate dehydrogenase is not involved in additional decarboxylations

We have shown that alternative non-peroxisomal decarboxylations originating from glycolate are unlikely to occur. Using genetic resources in *Arabidopsis thaliana*, we applied different constraints to the photorespiratory flux through peroxisomes to assess whether NE-decarboxylations could occur *in vivo*. Cousins *et al.* (2008) reported that a *pmdh* null mutant had a higher compensation point than the WT. In parallel, Timm *et al.* (2008) noticed that a peroxisomal *hpr1* mutant also had a higher compensation point than the corresponding WT. Importantly, Cousins *et al.* (2011) further showed that *hpr1* and a *hpr1 pmdh1 pmdh2* triple mutant had higher CO_2 compensation points but this was not due to changes in mitochondrial respiration. The authors showed that values for Γ were similar in WT and *hpr1* lines at low O_2 (10%) and that rates of RubisCO carboxylation were similar between WT and *hpr1* at 10 and 20% O_2. This strongly reinforces our conclusion that the higher Γ measured in *hpr1* is linked to photorespiration. Here, we demonstrate that this higher compensation point is enhanced when coupled to a lower peroxisomal catalase activity as the double mutant *hpr1 cat2-2* had a significantly higher compensation point than *hpr1* and *cat2-2* alone. Moreover, the higher PIB recorded in *hpr1*, *cat2-2* and the double mutant *hpr1 cat2-2* was consistent with an accumulation of metabolites that were further decarboxylated in the dark period. However, the shape of the peaks (Fig 5b) suggested that some of these decarboxylations were not as fast as those occurring in *gox* mutants for instance. Further, the double mutant *hpr1 fdh* was not significantly different from *hpr1* alone in any respect. Altogether, these results provide strong

evidence that, *in vivo*, NE-decarboxylations can occur in the peroxisome when intermediates such as hydroxypyruvate accumulate with H_2O_2. Additionally, we show that formate dehydrogenase is not involved in the process, strengthening the idea that glycolate is not exported to mitochondria for degradation (as proposed in Fig 1).

With regard to the involvement of transketolase-mediated decarboxylation in the chloroplast (Fig 1), the potential for this will be increased when peroxisomal hydroxypyruvate reductase activity is reduced and hydroxypyruvate is routed for processing via the cytosol and chloroplast (Timm et al., 2011). However, the fact that lower peroxisomal catalase activity stimulates extra decarboxylations would argue for a central role for peroxisomal H_2O_2 mediated NE-decarboxylation in increasing the release of CO_2 from each glycolate produced. In addition, Timm *et al.* (2011) found that HPR triple knockouts (peroxisomal, chloroplastic and cytosolic forms of HPR) required high CO_2 for growth and clearly indicates that transketolase in the chloroplast cannot substitute for the processing of hydroxypyruvate by cytosolic or chloroplastic HPR activities back into the Calvin cycle under what would be extreme conditions. Taken together, it appears that chloroplastic transketolase may barely contribute to the processing of hydroxypyruvate. However, its potential remains to be fully assessed.

Importance of photorespiratory non-enzymatic decarboxylations in the field

The experiments conducted here with mutants have demonstrated the significant occurrence of NE-decarboxylations when these mutants are exposed to extreme photorespiratory conditions at the CO_2 compensation point. However, the catalytic efficiencies of hydroxypyruvate reductase, serine-glycine aminotransferase and catalase are such that the probability of NE-decarboxylation of glyoxylate or hydroxypyruvate is expected to be minor under normal ambient conditions, although, being a chemical reaction, it may not be nil. Despite this, NE-decarboxylations would be favored at high temperature or by high oxidative stresses. A recent report showed that heat stress leads to a strong increase of H_2O_2 formation in *Phaseolus vulgaris* L. leaves (Huve et al., 2011). Additionally, under conditions of abiotic stress, increased fatty acid oxidation and jasmonate synthesis can increase peroxisomal H_2O_2 production by acyl CoA oxidase activity (Pinfield-Wells et al., 2005; Baker et al., 2006). Furthermore superoxide, nitric oxide and peroxynitrite are produced in the peroxisome and can inhibit catalase activity (Baker et al., 2006). Iron deficiency and heavy metal toxicity can also lead to significant reductions in leaf catalase activity (Dekock et al., 1960; del Rio et al., 1978; Nenova and Stoyanov, 1995). All the above conditions are likely to favor NE-decarboxylations by increasing the potential for peroxide-mediated reactions with compounds such as hydroxypyruvate and glyoxylate.

As a result of the effects of increasing temperature on both RubisCO kinetics and the NE-decarboxylation reactions, photosynthetic losses caused by photorespiratory-linked decarboxylations will be exacerbated by hotter and drier conditions, which are likely to occur in many agricultural regions of the world (Ainsworth and Ort, 2010). While the temperature effects on RubisCO are relatively well studied, the extent to which NE-decarboxylations might increase under such difficult growing conditions remains a somewhat open and unanswered question. It has been shown that high temperatures induced greater CO_2-compensation point in potato (*Solanum tuberosum* L.) (Wolf et al., 1990) and ivy leaves (*Hedera helix* L.) (Bauer, 1978). Although NE-decarboxylations occurring in the peroxisome can ultimately contribute to carbon loss, the challenge remains to determine the extent to which these losses contribute to photosynthetic inefficiencies at elevated temperatures in the field and whether these losses will increase in the future under high photorespiratory conditions resulting from additional abiotic stress or nutritional deficiency.

Finally, we need to question whether there may be a selective advantage for land plants to have the possibility of non-enzymatic peroxide-mediated decarboxylation reactions in the peroxisome. Currently there is no satisfactory answer to the question of why glycolate metabolism occurs through a peroxide-generating oxidase in the peroxisome rather than by means of a glycolate dehydrogenase in another cellular compartment. The evolution of land plants from algae was accompanied by the switch from glycolate dehydrogenase to glycolate oxidase (Chauvin et al., 2008). Photorespiration itself is speculated to provide a 'safety valve' for photosynthesis so that under conditions of over-reduction of the photosynthetic electron transport chain, reducing equivalents can be removed from the chloroplast in the form of glycolate. The possibility exists that GOX could provide a safety valve for photorespiration such that glycolate oxidation can continue when the cellular NADH/ NAD ratio is high, and that simultaneous H_2O_2 production allows excess photorespiratory intermediates (glyoxylate and hydroxypyruvate) to be oxidized to CO_2 and water without feeding carbon skeletons into NADH-producing mitochondrial respiratory pathways.

Materials and Methods

Plant material and growth conditions

Plants were grown in a controlled environment with a temperature cycle of 22 °C/17 °C, light intensity of 150 µmol m^{-2} s^{-1} and humidity of 60%. Photoperiods were 12 h light /12 h dark or a 8 h light /16 h dark. Seven week-old plants were used throughout the experiments.

Screening of T-DNA insertion lines and isolation of knock-out mutants

Arabidopsis T-DNA insertion lines were identified from the SIGnAL database (http://signal.salk.edu/cgi-bin/tdnaexpress) and except where noted were obtained from the ABRC. Genotyping primers were designed using the T-DNA Express primer design server (http://signal.salk.edu/tdnaprimers.2.html). The *hpr1* mutant (Pracharoenwattana et al., 2010) and the *cat2-2* mutant (Queval et al., 2007) have been described previously.

gox mutants - SAIL_177_G11; (Sessions et al., 2002) and WiscDsLox461-464K16; (Woody et al., 2007) were identified as insertions in GOX1 (At3g14420) and designated as *gox1-1* and *gox1-2* respectively. PCR-based screening was used to identify the lines homozygous for T-DNA insertions. The gene-specific primers gox1-1 were used in combination with the T-DNA left border primer SAIL pCSA110 LB3 (Sessions et al., 2002) (S_Table 1). The gene-specific primers *gox1-2* were used in combination with the T-DNA left border primer WiscDsLox p745 LB 5'- 3' (Woody et al., 2007) (S_Table 1).

fdh - The Arabidopsis *fdh* T-DNA insertion line used in this paper was obtained from the NASC collection (SALK_108751, (Alonso et al., 2003)). The insertion of the T-DNA is located within 511 bases of the third exon (540 base pairs as predicted by AGI-TIGR) of the unique *FDH* gene (At5g14780) (S_Fig 1). We used fdh gene specific primers in combination with SALK T-DNA left border primer NLB (S_Table 1).

RT-PCR and qRT-PCR

Total RNA was isolated from leaves using the RNAeasy kit (Qiagen, Australia), treated with Ambion DNA-*free* kit (Applied Biosystems, Australia) and 1µg of RNA was used to generate cDNA with the SuperScript III kit for RT-PCR (Invitrogen, Australia). Gene specific primers for RT-PCR were used to confirm transcript knockout for *gox1*, *gox2* and *fdh* lines. RT-PCR primers were designed to surround the T-DNA insertion using Primer3 (http://frodo.wi.mit.edu/primer3/). For RT-PCR, PCR was performed for 30 cycles with gene-specific primers, sequences for which are provided in S_Table 2.

qRT-PCR was performed on a LightCycler 480 (Roche Applied Science, Australia). Transcript abundance was calculated relative to the geometrical mean of 3 reference genes (APT1: At5g60390; Clath: At1g27450; eF1α: At5g46630). Primer sequences are provided in S_Table 2.

Metabolic Profiling

Plant tissues (20–30 mg) were snap frozen and pulverized in liquid nitrogen. The enzymes in the tissue were inactivated by heating on a Thermomixer with mixing at 1200 rpm at 75°C for 20 min in 500 µL of extraction solution (methanol:water = 20:3, with adipic acid as internal standard). Cell debris was removed by centrifugation for 3 min at room temperature. For each sample, 100 µL of supernatant was transferred to a new tube and dried using a SpeedVac. The residue was dissolved in 20 µL of pyridine with methoxylamine hydrochloride (20 mg mL^{-1}) and incubated at 65°C for 60 min with shaking at 750 rpm. Metabolites were converted to tert-butyldimethylsilyl derivatives by reacting at 65°C for 60 min with 30 µL of N-methyl-N-(Tert-Butyldimethylsilyl)trifluoroacetamide. The metabolite derivatives were analyzed by GC-MS (Agilent 7890A gas chromatograph coupled with a 5975C inert XL MSD with Triple-Axis Detector). GC-MS data were processed by MSD ChemStation. Metabolite derivatives were identified by comparison of the retention time and mass spectra of authentic standards, and the amount of metabolites was calculated using the extracted ion current signal of a metabolite specific ion. Each metabolite peak was normalized to the adipic acid internal standard and tissue weight.

Low CO_2 experiments

For short-term adaptation to low CO_2, 7 week old plants were transferred into a sealed plastic container with 50 ml CO_2 scrubber (Grace Sodasorb, WR Grace & Co, Chicago, USA). Temperature, oxygen and CO_2 levels were recorded. Plants were individually harvested and snap frozen in liquid nitrogen when CO_2 concentration was about 100 ppm. Control plants were placed in to similar conditions but without the CO_2 scrubber.

Mass Spectrometric Measurements

-Compensation point, Post-Illumination Burst and Max rate of CO_2 release

The exchange of CO_2 was measured from leaf discs (area $1cm^2$) placed into a closed leaf chamber connected to a mass spectrometer (IsoprimeMicromass) as described previously (Cousins et al., 2008). Briefly, after a 2 min dark period, the leaf disc was illuminated (400 µmol quanta m^{-2} s^{-1}) for 10 min, and then darkened for 4 min; this cycle was repeated twice. Compensation point, Post-illumination Burst (PIB) and maximum CO_2 release were consequently determined twice per sample.

Acknowledgements

The authors would like to thank Dr. Graham Noctor for providing *cat2* mutants seeds and Prof. Per Gardeström for critical reading of the manuscript.

Literature Cited

Ainsworth EA, Ort DR (2010) How Do We Improve Crop Production in a Warming World? Plant Physiol **154:** 526-530

Alonso JM, Stepanova AN, Leisse TJ, Kim CJ, Chen HM, Shinn P, Stevenson DK, Zimmerman J, Barajas P, Cheuk R, Gadrinab C, Heller C, Jeske A, Koesema E, Meyers CC, Parker H, Prednis L, Ansari Y, Choy N, Deen H, Geralt M, Hazari N, Hom E, Karnes M, Mulholland C, Ndubaku R, Schmidt I, Guzman P, Aguilar-Henonin L, Schmid M, Weigel D, Carter DE, Marchand T, Risseeuw E, Brogden D, Zeko A, Crosby WL, Berry CC, Ecker JR (2003) Genome-wide Insertional mutagenesis of *Arabidopsis thaliana*. Science **301:** 653-657

Baker A, Graham IA, Holdsworth M, Smith SM, Theodoulou FL (2006) Chewing the fat: β-oxidation in signalling and development. Trends Plant Sci **11:** 124-132

Bauer H (1978) Photosynthesis of Ivy Leaves (*Hedera helix*) after Heat Stress I. CO_2-Gas Exchange and Diffusion Resistances. Physiol Plantarum **44:** 400-406

Chauvin L, Tural B, Moroney JV (2008) *Chlamydomonas reinhardtii* has genes for both glycolate oxidase and glycolate dehydrogenase. *In* JF Allen, E Gantt, JH Golbeck, B Osmond, eds, Photosynthesis. Energy from the Sun. Springer Netherlands, pp 823-827

Clark SM, Di Leo R, Dhanoa PK, Van Cauwenberghe OR, Mullen RT, Shelp BJ (2009) Biochemical characterization, mitochondrial localization, expression, and potential functions for an Arabidopsis γ-aminobutyrate transaminase that utilizes both pyruvate and glyoxylate. J Exp Bot **60:** 1743-1757

Colas des Francs-Small C, Ambard-Bretteville F, Small ID, Remy R (1993) Identification of a major soluble protein in mitochondria from nonphotosynthetic tissues as NAD-dependent formate dehydrogenase. Plant Physiol **102:** 1171-1177

Cousins A, Walker B, Pracharoenwattana I, Smith S, Badger M (2011) Peroxisomal hydroxypyruvate reductase is not essential for photorespiration in Arabidopsis but its absence causes an increase in the stoichiometry of photorespiratory CO_2 release. Photosynth Res **108:** 91-100

Cousins AB, Pracharoenwattana I, Zhou W, Smith SM, Badger MR (2008) Peroxisomal malate dehydrogenase is not essential for photorespiration in Arabidopsis but its absence causes an increase in the stoichiometry of photorespiratory CO_2 release. Plant Physiol **148:** 786-795

Davies DD, Corbett RJ (1969) Glyoxylate decarboxylase activity in higher plants. Phytochemistry **8:** 529-542

Dekock PC, Commisiong K, Farmer VC, Inkson RHE (1960) Interrelationships of catalase, peroxidase, hematin, and chlorophyll. Plant Physiol **35:** 599-604

del Rio L, Gomez M, Yañez J, Leal A, Lopez Gorge J (1978) Iron deficiency in pea plants effect on catalase, peroxidase, chlorophyll and proteins of leaves. Plant Soil **49:** 343-353

Engqvist M, Drincovich MF, Flügge U-I, Maurino VG (2009) Two D-2-hydroxy-acid dehydrogenases in *Arabidopsis thaliana* with catalytic capacities to participate in the last reactions of the methylglyoxal and β-oxidation pathways. J Biol Chem **284:** 25026-25037

Fiedler E, Golbik R, Schneider G, Tittmann K, Neef H, König S, Hübner G (2001) Examination of donor substrate conversion in yeast transketolase. J Biol Chem **276:** 16051-16058

Foyer CH, Bloom AJ, Queval G, Noctor G (2009) Photorespiratory metabolism: genes, mutants, energetics, and redox signaling. Ann Rev Plant Biol **60:** 455-484

Goyal A, Tolbert NE (1996) Association of glycolate oxidation with photosynthetic electron transport in plant and algal chloroplasts. P Natl Acad Sci USA **93:** 3319-3324

Grodzinski B (1978) Glyoxylate decarboxylation during photorespiration. Planta **144:** 31-37

Halliwell B (1974) Oxidation of formate by peroxisomes and mitochondria from spinach leaves. Biochem J **138:** 77-85

Halliwell B, Butt VS (1974) Oxidative decarboxylation of glycolate and glyoxylate by leaf peroxisomes. Biochem J **138:** 217-224

Herman PL, Ramberg H, Baack RD, Markwell J, Osterman JC (2002) Formate dehydrogenase in *Arabidopsis thaliana*: overexpression and subcellular localization in leaves. Plant Sci **163:** 1137-1145

Huve K, Bichele I, Rasulov B, Ninemets U (2011) When it is too hot for photosynthesis: heat-induced instability of photosynthesis in relation to respiratory burst, cell permeability changes and H_2O_2 formation. Plant Cell Environ **34:** 113-126

Igamberdiev AU, Bykova NV, Kleczkowski LA (1999) Origins and metabolism of formate in higher plants. Plant Physiol Biochem **37:** 503-513

Igamberdiev AU, Lea PJ (2002) The role of peroxisomes in the integration of metabolism and evolutionary diversity of photosynthetic organisms. Phytochemistry **60:** 651-674

Kebeish R, Niessen M, Thiruveedhi K, Bari R, Hirsch H-J, Rosenkranz R, Stabler N, Schonfeld B, Kreuzaler F, Peterhansel C (2007) Chloroplastic photorespiratory bypass increases photosynthesis and biomass production in *Arabidopsis thaliana*. Nat Biotech **25:** 593-599

Kobori Y, Myles DC, Whitesides GM (1992) Substrate specificity and carbohydrate synthesis using transketolase. J Org Chem **57:** 5899-5907

Nenova V, Stoyanov I (1995) Physiological and biochemical-changes in young maize plants under iron-deficiency. II: Catalase, peroxidase, and nitrate reductase activities in leaves. J Plant Nutr **18:** 2081-2091

Niessen M, Thiruveedhi K, Rosenkranz R, Kebeish R, Hirsch H-J, Kreuzaler F, Peterhansel C (2007) Mitochondrial glycolate oxidation contributes to photorespiration in higher plants. J Exp Bot **58:** 2709-2715

O'Connor TR, Dyreson C, Wyrick JJ (2005) Athena: a resource for rapid visualization and systematic analysis of Arabidopsis promoter sequences. Bioinformatics **21:** 4411-4413

Peterhansel C, Horst I, Niessen M, Blume C, Kebeish R, Kürkcüoglu S, Kreuzaler F (2010) Photorespiration. The Arabidopsis Book **8:** 1-24

Pinfield-Wells H, Rylott EL, Gilday AD, Graham S, Job K, Larson TR, Graham IA (2005) Sucrose rescues seedling establishment but not germination of Arabidopsis mutants disrupted in peroxisomal fatty acid catabolism. Plant J **43:** 861-872

Pracharoenwattana I, Zhou WX, Smith SM (2010) Fatty acid β-oxidation in germinating Arabidopsis seeds is supported by peroxisomal hydroxypyruvate reductase when malate dehydrogenase is absent. Plant Mol Biol **72:** 101-109

Queval G, Issakidis-Bourguet E, Hoebericht sFA, Vandorpe M, Gakière B, Vanacker H, Miginiac-Maslow M, Van Breusegem F, Noctor G (2007) Conditional oxidative stress responses in the Arabidopsis photorespiratory mutant *cat2* demonstrate that redox state is a key modulator of daylength-dependent gene expression, and define photoperiod as a crucial factor in the regulation of H_2O_2-induced cell death. Plant J **52:** 640-657

Roussel MR, Igamberdiev AU (2011) Dynamics and mechanisms of oscillatory photosynthesis. Biosystems **103:** 230-238

Sessions A, Burke E, Presting G, Aux G, McElver J, Patton D, Dietrich B, Ho P, Bacwaden J, Ko C, Clarke JD, Cotton D, Bullis D, Snell J, Miguel T, Hutchison D, Kimmerly B, Mitzel T, Katagiri F, Glazebrook J, Law M, Goff SA (2002) A high-throughput Arabidopsis reverse genetics system. Plant Cell **14:** 2985-2994

Sharkey TD (1988) Estimating the rate of photorespiration in leaves. Physiol Plantarum **73:** 147-152

Timm S, Florian A, Jahnke K, Nunes-Nesi A, Fernie AR, Bauwe H (2011) The hydroxypyruvate-reducing system in Arabidopsis: multiple enzymes for the same end. Plant Physiol **155:** 694-705

Timm S, Nunes-Nesi A, Pamik T, Morgenthal K, Wienkoop S, Keerberg O, Weckwerth W, Kleczkowski LA, Fernie AR, Bauwe H (2008) A cytosolic pathway for the

conversion of hydroxypyruvate to glycerate during photorespiration in Arabidopsis. Plant Cell **20:** 2848-2859

Walton NJ, Butt VS (1981) Metabolism and decarboxylation of glycolate and serine in leaf peroxisomes. Planta **153:** 225-231

Wingler A, Lea PJ, Leegood RC (1999) Photorespiratory metabolism of glyoxylate and formate in glycine-accumulating mutants of barley and *Amaranthus edulis*. Planta **207:** 518-526

Winter D, Vinegar B, Nahal H, Ammar R, Wilson GV, Provart NJ (2007) An "electronic fluorescent pictograph" browser for exploring and analyzing large-scale biological data sets. PLoS ONE **2:** e718

Wolf S, Olesinski A, Rudich J, Marani A (1990) Effect of high temperature on photosynthesis in potatoes. Ann Bot-London **65:** 179-185

Woody S, Austin-Phillips S, Amasino R, Krysan P (2007) The *WiscDsLox* T-DNA collection: an Arabidopsis community resource generated by using an improved high-throughput T-DNA sequencing pipeline. J Plant Res **120:** 157-165

Xu H, Zhang J, Zeng J, Jiang L, Liu E, Peng C, He Z, Peng X (2009) Inducible antisense suppression of glycolate oxidase reveals its strong regulation over photosynthesis in rice. J Exp Bot **60:** 1799-1809

Zelitch I, Schultes NP, Peterson RB, Brown P, Brutnell TP (2009) High glycolate oxidase activity is required for survival of maize in normal air. Plant Physiol **149:** 195-204

Figure Legends

Figure 1. Possible pathways leading to decarboxylation of photorespiratory intermediates, resulting in a variable stoichiometry of CO_2 release per RubisCO oxygenation reaction. Plain lines represent known and confirm reactions whereas dash lines represent suggested alternative pathways. Question marks (?) refer to side or putative reactions. 1: RubisCO, 2: 2P-glycolate phosphatase, 3: glycolate oxidase, 4: catalase, 5: glutamate:glyoxylate aminotransferase, 6: glycine decarboxylase, 7: serine-hydroxymethyl transferase, 8: serine:glyoxylate aminotransferase, 9: peroxisomal hydroxypyruvate reductase, 10: malate dehydrogenase, 11: glycerate kinase, 12: glutamine synthase, 13: glutamate:oxoglutarate aminotransferase, 14 formate dehydrogenase, 15: 10-formyl-THF synthetase 16: 5,10 methenyl-THF cyclohydrolase, 17: 5,10 methylene-THF dehydrogenase, 18?: SHAM-sensitive glycolate-quinone oxidoreductase, 19?: glycolate dehydrogenase/lactate dehydrogenase, 20: cytosolic hydroxypyruvate reductase, 21: chloroplastic hydroxypyruvate reductase, 22?: transketolase.

Figure 2. Phenotypes of several photorespiratory mutants (A: Col0, B: *gox1-2*, C: *hpr*, D: *cat2-2*, E: *fdh*, F: *hpr cat2-2*, G: *hpr fdh*) 7 weeks after sowing. Plants were grown (a) in 8h light photoperiod and (b) in 12h light photoperiod.

Figure 3. Characterization of the two alleles of *gox1* mutant. For all experiments, plants grown both in ambient air (AA) and submitted to low CO_2 (LC) were analysed. (a) phenotypes of *gox1-1* and *gox1-2* grown in short-day photoperiod, (b) T-DNA insertions: SAIL_177_G11 for *gox1-1* and WiscDsLox461-464K16 for *gox1-2*, (c) transcripts content of *GOX1* and *Actin2* in leaves from Wt, *gox1-1* and *gox1-2* under either ambient air or low CO_2 conditions, (d)

Relative expression of *GOX1* and *GOX2* estimated by qRT-PCR. Results were normalized to the geometrical mean of three reference genes. (e) Relative content of Glycolate per mg fresh weight in mature leaves determined by GC-MS.

Figure 4. Relative abundance of photorespiratory intermediates for several mutants under ambient air or short exposure to low CO_2. White bars = ambient air (380ppm), black bars = low CO_2 (100ppm). Results are mean ± SD of 4 biological replicates (and at least 4 technical replicates for each). Corresponding treatments of each genotype were compared to WT by Student's t-Test (significance level: 1 < 0,05; 2 < 0,01 and 3 < 0,001) for 380ppm and 100ppm conditions, respectively. For each genotype, significant differences between 380ppm and 100ppm conditions were assessed by Student's t-Test (significance level: * < 0,05; ** < 0,01 and *** < 0,001).

Figure 5. Compensation point, post-illumination burst and maximum rate of CO_2 release for several photorespiratory mutants. Compensation point expressed in ppm (a), representative integration of the relative release of CO_2 after switching the light off (b), PIB expressed as peak area (c), maximum rate of CO_2 release in the dark (d). Results are mean ± SD of 3 biological replicates (4 technical replicates for each). All genotypes were compared to WT by Student's t-Test (significance level: * < 0,05; ** < 0,01 and *** < 0,001). (+) *hpr1 cat2-2* was significantly different from *hpr1* (significance level: + < 0,01).

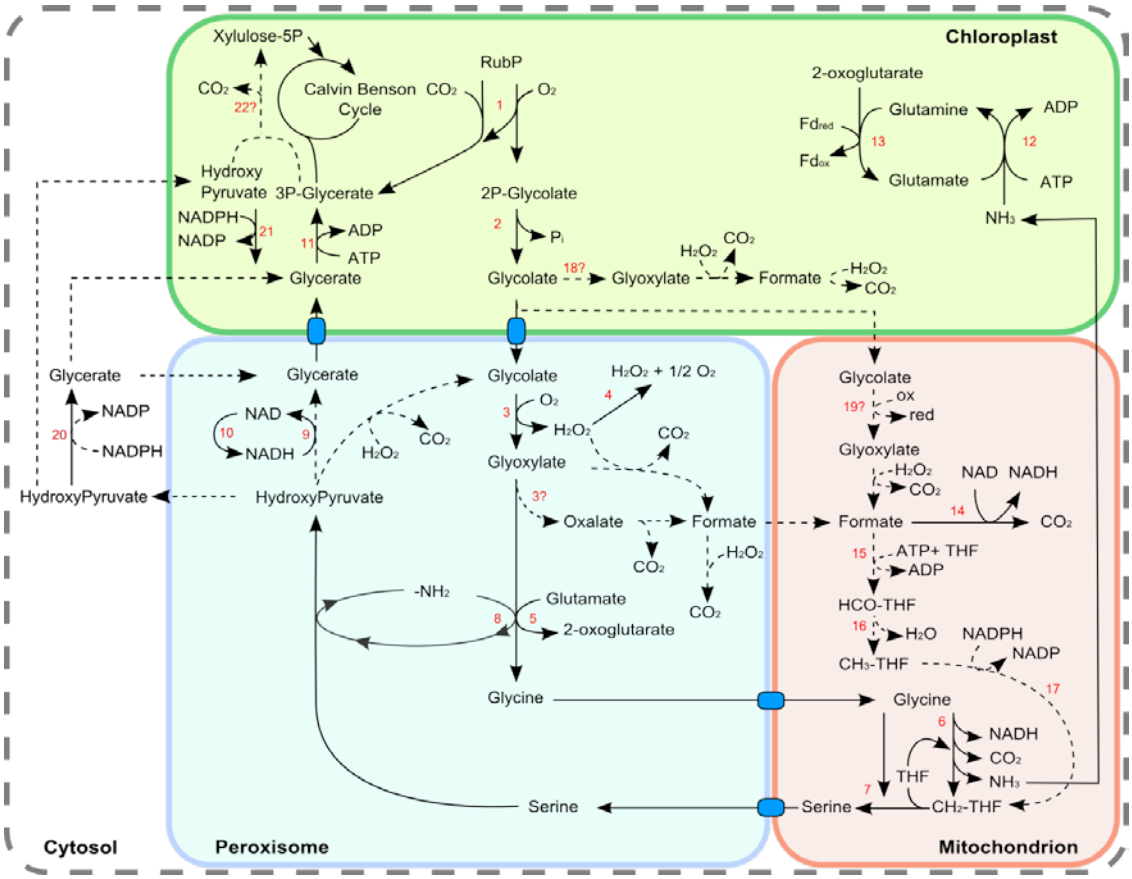

Figure 1. Possible pathways leading to decarboxylation of photorespiratory intermediates, resulting in a variable stoichiometry of CO_2 release per RubisCO oxygenation reaction. Plain lines represent known and confirm reactions whereas dash lines represent suggested alternative pathways. Question marks (?) refer to side or putative reactions. 1: RubisCO, 2: 2P-glycolate phosphatase, 3: glycolate oxidase, 4: catalase, 5: glutamate:glyoxylate aminotransferase, 6: glycine decarboxylase, 7: serine-hydroxymethyl transferase, 8: serine:glyoxylate aminotransferase, 9: peroxisomal hydroxypyruvate reductase, 10: malate dehydrogenase, 11: glycerate kinase, 12: glutamine synthase, 13: glutamate:oxoglutarate aminotransferase, 14 formate dehydrogenase, 15: 10-formyl-THF synthetase 16: 5,10 methenyl-THF cyclohydrolase, 17: 5,10 methylene-THF dehydrogenase, 18?: SHAM-sensitive glycolate-quinone oxidoreductase, 19?: glycolate dehydrogenase/lactate dehydrogenase, 20: cytosolic hydroxypyruvate reductase, 21: chloroplastic hydroxypyruvate reductase, 22?: transketolase.

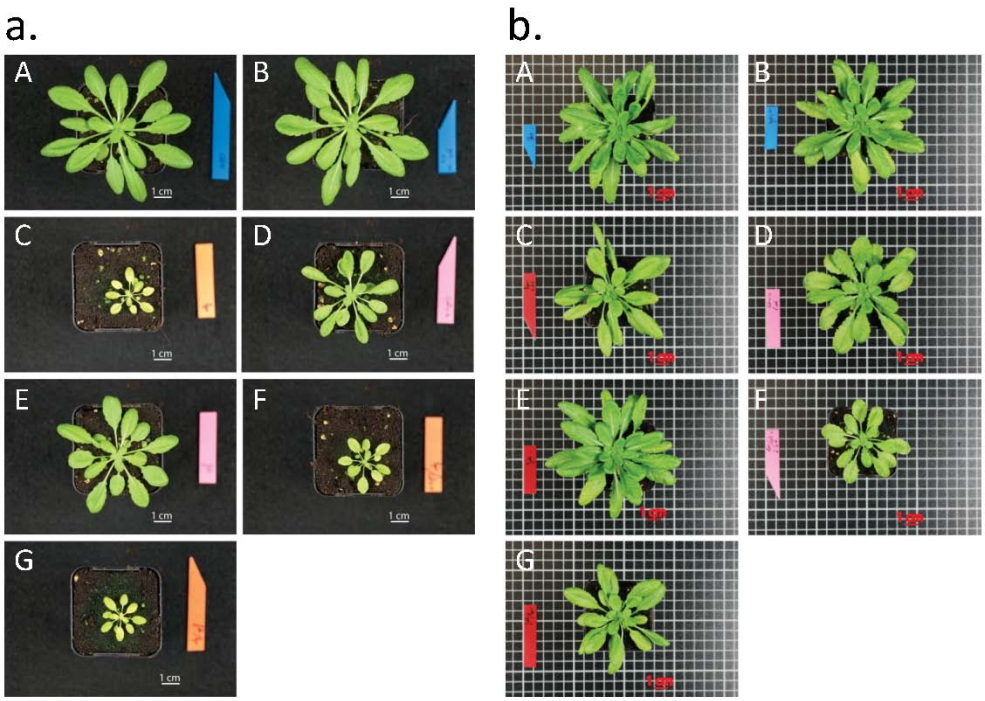

Figure 2. Phenotypes of several photorespiratory mutants (A: Col0, B: *gox1-2*, C: *hpr*, D: *cat2-2*, E: *fdh*, F: *hpr cat2-2*, G: *hpr fdh*) 7 weeks after sowing. Plants were grown (a) in 8h light photoperiod and (b) in 12h light photoperiod.

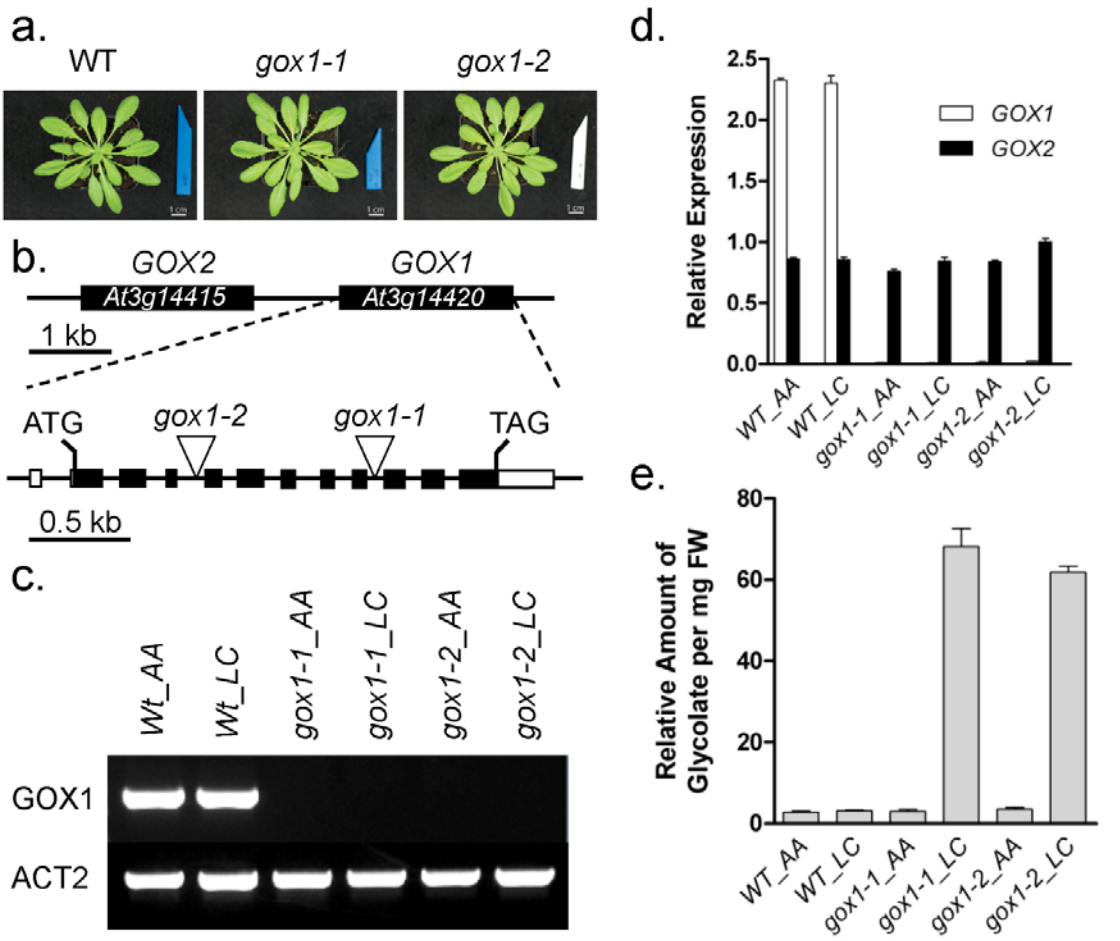

Figure 3. Characterization of the two alleles of *gox1* mutant. For all experiments, plants grown both in ambient air (AA) and submitted to low CO_2 (LC) were analysed. (a) phenotypes of *gox1-1* and *gox1-2* grown in short-day photoperiod, (b) T-DNA insertions: SAIL_177_G11 for *gox1-1* and WiscDsLox461-464K16 for *gox1-2*, (c) transcripts content of *GOX1* and *Actin2* in leaves from Wt, *gox1-1* and *gox1-2* under either ambient air or low CO_2 conditions, (d) Relative expression of *GOX1* and *GOX2* estimated by qRT-PCR. Results were normalized to the geometrical mean of three reference genes. (e) Relative content of Glycolate per mg fresh weight in mature leaves determined by GC-MS.

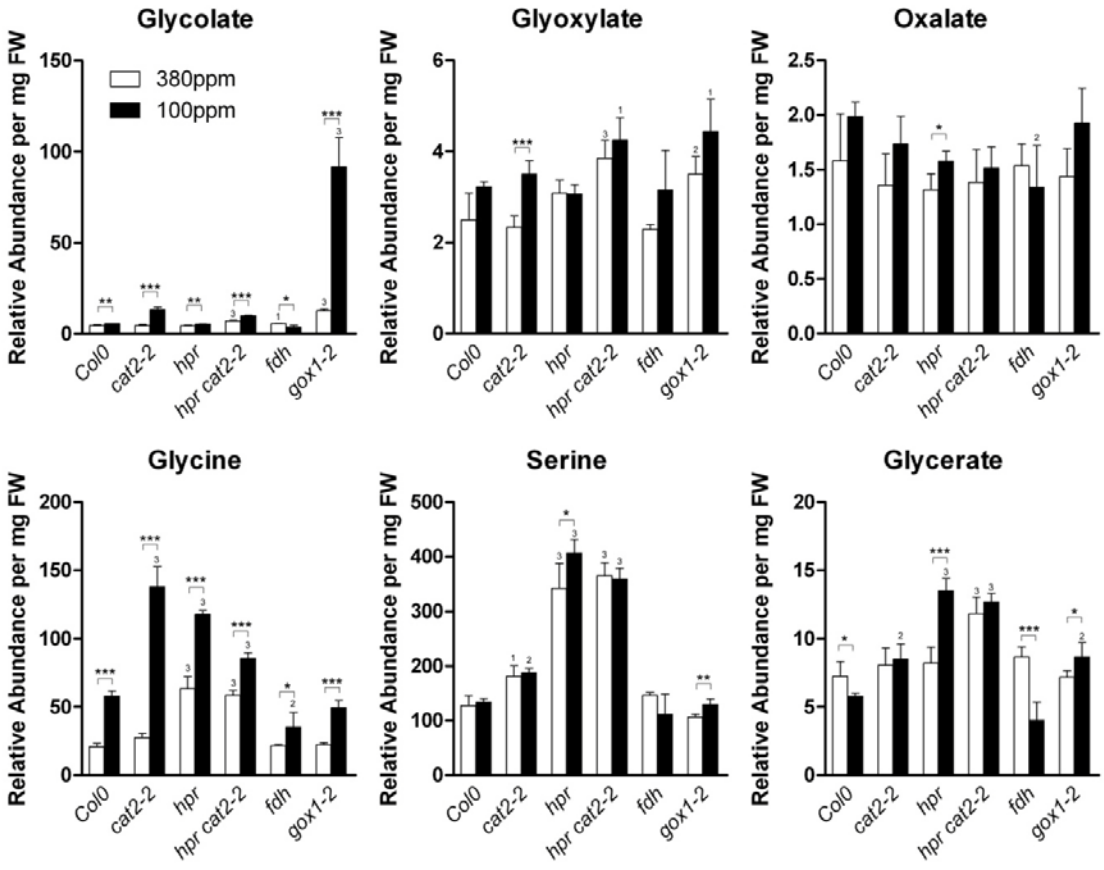

Figure 4. Relative abundance of photorespiratory intermediates for several mutants under ambient air or short exposure to low CO_2. White bars = ambient air (380ppm), black bars = low CO_2 (100ppm). Results are mean ± SD of 4 biological replicates (and at least 4 technical replicates for each). Corresponding treatments of each genotype were compared to WT by Student's t-Test (significance level: 1 < 0,05; 2 < 0,01 and 3 < 0,001) for 380ppm and 100ppm conditions, respectively. For each genotype, significant differences between 380ppm and 100ppm conditions were assessed by Student's t-Test (significance level: * < 0,05; ** < 0,01 and *** < 0,001).

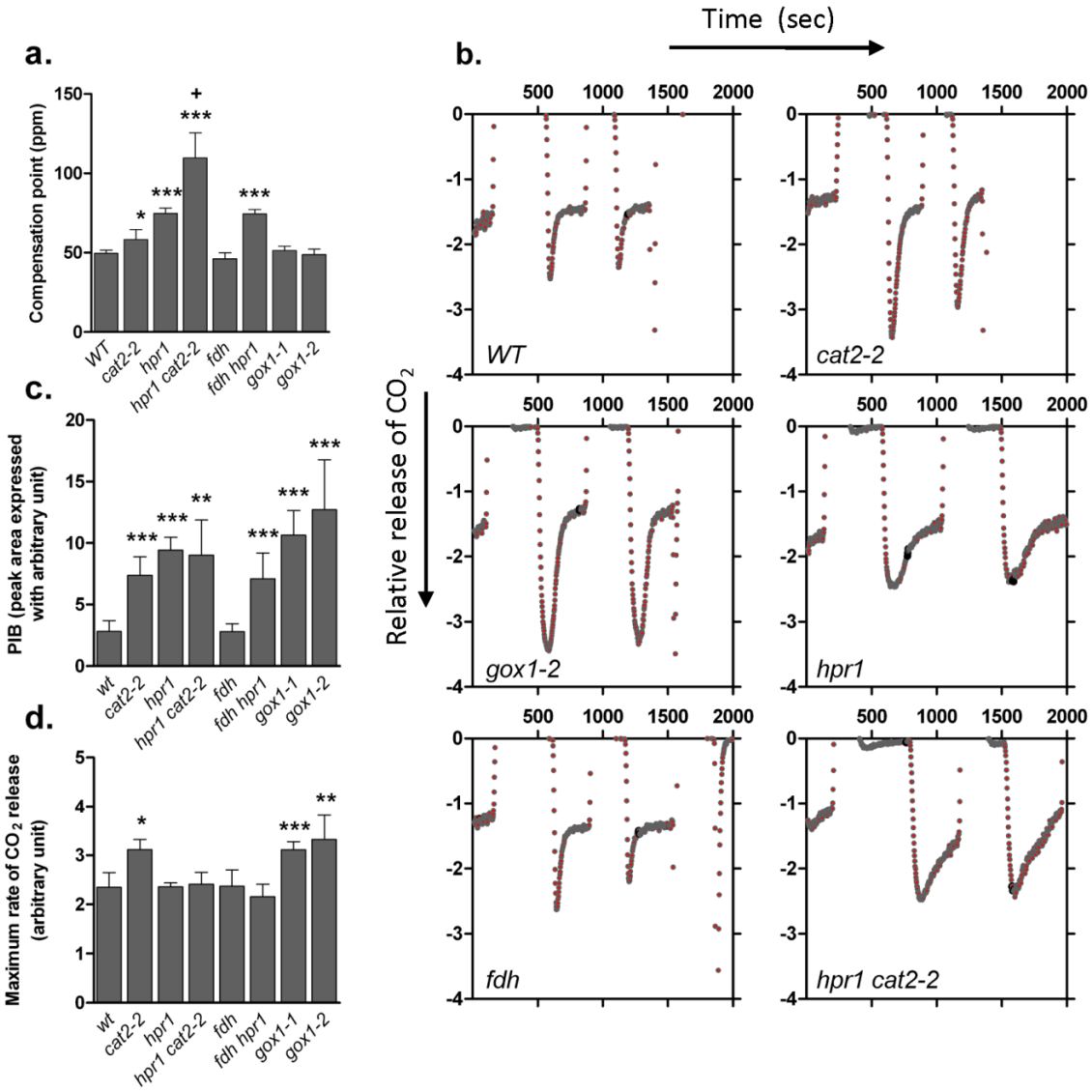

Figure 5. Compensation point, post-illumination burst and maximum rate of CO_2 release for several photorespiratory mutants. Compensation point expressed in ppm (a), representative integration of the relative release of CO_2 after switching the light off (b), PIB expressed as peak area (c), maximum rate of CO_2 release in the dark (d). Results are mean ± SD of 3 biological replicates (4 technical replicates for each). All genotypes were compared to WT by Student's t-Test (significance level: * < 0,05; ** < 0,01 and *** < 0,001). (+) *hpr1 cat2-2* was significantly different from *hpr1* (significance level: + < 0,01).

Supporting Information

S_Figure 1. Molecular characterization of *formate dehydrogenase (fdh)* mutant

S_Table1. Primers for characterization of gox1 mutants.

S_Table2. Primers for RT and qRT-PCR.

S_Fig 1.

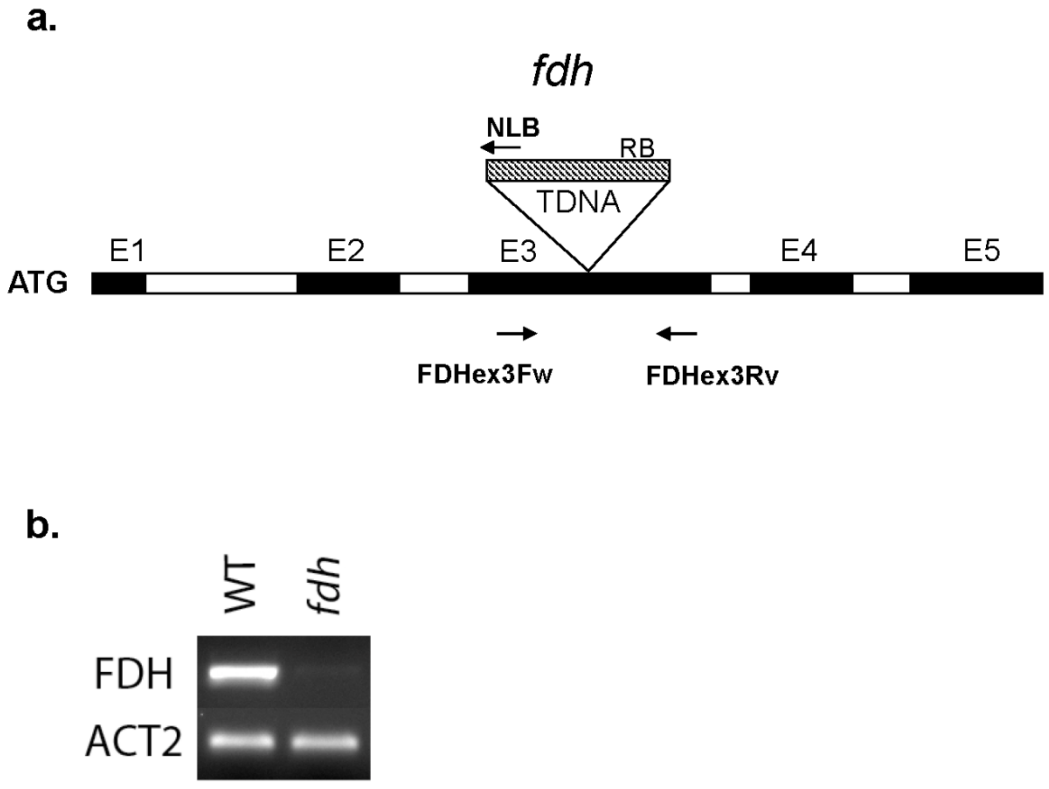

S_Figure 1. Isolation of *formate dehydrogenase (fdh)* mutant. T-DNA insertion (SALK_108751) in the third exon of the *FDH gene (*At5g14780) with corresponding primers (a), RT-PCR comparing wild type (WT) and *fdh* mutant. The *Actin 2* was used as reference *(b).*

Supplemental Table 1. Primers for characterization of *gox1* and *fdh* mutants.

Gene	Mutant	Target	Primer	5' -> 3'
GOX1	*gox1-1*	SAIL_177_G11	LP	TCACAAGAAATTGATCTGTGGG
			RP	GAAGGACTTGACCTCGGAAAG
			SAIL pCSA110 LB3	TAGCATCTGAATTTCATAACCAATCTCGATACAC
	gox1-2	WiscDsLox461-464K16	LP	CAGAAGCTGCCTAAGATGGTG
			RP	TGTCATATTTCAAATGACTTGGC
			WiscDsLox p745 LB	AACGTCCGCAATGTGTTATTAAGTTGTC
FDH	*fdh*	SALK_108751	NLB	GGTGATGGTTCACGTAGTGGGCCATGC
			Ex3-F	GGAAGCAACGTGGTCTCAGT
			Ex3-R	GTCCTTAGGAGCTGGCTGTG

Supplemental Table 2. Primers for RT and qRT-PCR.

Technique	gene	OligoN (5'-3')
RT-PCR		
	hpr1_For	GTTGTTAGCACAAAACCGATGCC
	hpr1_Rev	TCATAGCTTCGAAACAGGC
	cat2-2_For	CCCAGAGGTACCTCTTCTTCTCCCATG
	cat2-2_Rev	TCAGGGAACTTCATCCCATCGC
	GOX1_For	TGACATGACAACCACCGTCT
	GOX1_Rev	CCAAGTGCAAGTGCTTTGAA
qRT-PCR		
	GOX1_For	CTCATTGGCAGCTGAAGGAGAG
	GOX1_Rev	CTTTAGGGACCGACACCCACTC
	GOX2_For	TGCACTAGCTGCTGAAGGAGAA
	GOX2_Rev	ACTGAGTGACCGGCACCCACTT
	MLS_For	ACCCAAAAGCGAATGAGATG
	MLS_Rev	TTTTCCCATGTGACCAGTGA
	ICL_For	GAGTTTGTCCTCGCTTCTGG
	ICL_Rev	GAGCCAAGCCACTGATCTTC
	APT1_For	TTCTCGACACTGAGGCCTTT
	APT1_Rev	ATTTGGCACCAATAGCCAAC
	Clath_For	AGAAAATTCCCAGGGCAAAC
	Clath_Rev	AACGAACTCGCAGACCAGAT
	eF1a_For	TGGTGACGCTGGTATGGTTA
	eF1a_Rev	TCCTTCTTGTCCACGCTCTT